LONDON'S GLOBAL UNIVERSITY

Formulation and Assessment of Taste-masked Electrospun Fibre Mats for Paediatric Drug Delivery

Hend E. Abdelhakim

Thesis submitted in partial fulfilment of the requirements for the degree of Doctor of Philosophy

April 2021

School of Pharmacy
University College London

Declaration of Authorship

I, Hend Abdelhakim, confirm that the work presented in this thesis is my own. This work was conducted at UCL School of Pharmacy between October 2016 and April 2021 under the supervision of Professor Duncan Craig, Professor Catherine Tuleu, Professor Mohan Edirisinghe and Dr Alastair Coupe. Where information has been derived from other sources, I confirm that this has been indicated in the thesis.

Abstract

Since the Paediatric Regulation came into force by the European Medicines Agency in 2007, the drive to formulate age-appropriate dosage forms has been accelerated. The aim of this thesis was to develop new approaches for paediatric formulation design through the optimisation of novel taste-masking and taste-assessment methods. Electrospinning was demonstrated to be a suitable taste-masking technology, producing fibre mats that can be further formulated into easy to swallow oral films.

The electrospinning of Eudragit E PO, a taste-masking polymer, was optimised using Quality by Design principles and in particular Design of Experiment. To further enhance the taste-masking capability of the electrospun mat, co-axial electrospinning was utilised using another taste-masking polymer, Kollicoat Smartseal. The use of both polymers successfully taste-masked chlorpheniramine maleate, a known bitter anti-histamine. This was demonstrated using an electronic biosensor tasting system or E-tongue. The E-tongue was used to assess the bitterness threshold of this model drug but also of other standard bitter drugs for benchmarking. In addition, it was used to taste-assess various formulations which aided in ranking and deselecting formulations.

Electrospun fibre mats can be further processed into a number of different dosage forms for final presentation to the patient. The fibre mats were designed to be presented as an oral film. A water-soluble outer layer was added to the films using multi-axial electrospinning. A human panel was conducted to investigate the mouthfeel and overall acceptability of electrospun PVA films versus solvent-cast PVA films. The electrospun films were found to be as acceptable as the standard solvent-cast films, a very promising result for clinical translation. PVA and PVP were electrospun with the previously optimised polymers using tri-axial and tetra-axial electrospinning. The taste of the multi-axial electrospun fibre mats were assessed and it was found that adding a water-soluble outer layer reduces the taste-masking ability. Thus, it was found that electrospinning of a bitter drug using hydrophobic taste-masking polymers is very promising in the formulation of paediatric oral films.

Impact statement

This PhD aimed to design and manufacture a taste-masked age-appropriate formulation to be used in young children. Electrospinning was employed as the taste-masking manufacturing technology, whereas an electronic tasting system was used to assess the taste of the formulations manufactured.

The potential impact of this research can be summarised as follows. From an academic perspective, this study is the first to use an electronic tongue to taste-assess electrospun fibres. In addition, this is one of the first studies to assess mouthfeel of electrospun films using human taste panels, thus providing a blueprint and precedent for taste-assessment of electrospun fibre mats. Both these studies have been published in peer-reviewed international journals.

The data analysis method for the electronic tasting system was advanced during my PhD, which led to outreach activity in providing taste-assessment for bitter drugs and formulations to external companies. This can be used to further generate commercial activity beyond the PhD, demonstrating impact.

In addition, a database of bitterness profiles, as determined by the E-tongue, of commonly used drugs was compiled. The data obtained from this study will be extremely useful to future researchers working on paediatric formulations of these drugs.

The use of electrospinning as a taste-masking platform is quite novel and although there have been studies in the field, there is still a considerable gap. In this PhD, electrospinning using two taste-masking polymers, Eudragit E PO and Kollicoat Smartseal was thoroughly researched. There are no previous reports in the literature of electrospinning Kollicoat. Using Quality by Design principles, a blueprint was provided for using these two polymers to taste-mask bitter drugs, using chlorpheniramine maleate as a model drug. There are no previous reports of electrospinning Eudragit E PO with chlorpheniramine maleate before. In addition, multi-axial electrospinning was thoroughly researched in order to provide a continuous manufacturing process that will lead to the production of a

pharmaceutically elegant end-product. Co-axial, tri-axial, and tetra-axial electrospinning were all explored to manufacture a taste-masked orodispersible film for use in children. Tetra-axial electrospinning is very niche with only one publication in the literature on the matter, therefore our work has provided knowledge into the research methods of the technique.

These results help to validate the usage of electrospinning as a taste-masking technique. This may encourage future researchers both in academia and industry to use this technique for taste-masking of other drugs which may lead to development of more effectively taste-masked formulations which should help to improve patient adherence to drug regimens, particularly in the paediatric population.

Overall, the clinical impact of this research is evident. If this formulation, or another formulation that either employs the taste-masking principles researched, or the taste-assessment techniques used and developed, were licensed to be used in children, then clinically this will have a positive impact on adherence of medicines and therefore treatment outcomes. Through the involvement of Pfizer Ltd., this formulation has a real potential to reach the bedside, demonstrating real life impact.

Acknowledgements

First and foremost, I would like to thank my supervisor Professor Duncan Craig for believing in me and giving me the opportunity to complete this PhD. His support along the way was invaluable and I believe that if it was not for his continued encouragement this work would not have been possible. His words of wisdom to me are too many to mention here, but the ones that will stick with me forever are “the strongest steel has to go through the hottest fire” and to “always add 50 % extra time to your plan”. Thank you, Duncan, for being a supportive supervisor, encouraging teacher, inspiring manager and amazing friend.

I would like to thank my secondary supervisor Professor Catherine Tuleu for all her guidance in this PhD, especially with regards to conducting a human panel. I was fortunate enough to have the opportunity to work with UCL’s Mechanical Engineering department, where I was supervised by Professor Mohan Edirisinghe, where his support and guidance helped me publish my first paper from this PhD.

My industrial supervisor, Dr Alastair Coupe, was extremely supportive and provided me with the pharmaceutical insight needed to plan the formulation aspect of my project. I really also enjoyed our chats about life whilst having –decaf- coffee. This brings me on nicely to thank my sponsors, Pfizer and the Medical Research Council for funding this PhD project.

B28 became my home away from home in those last four years. I would like to thank the lab members for being amazing colleagues and supportive friends when I needed them. I want to thank Dr Essam Tawfik, Dr Sean Askin, Mr Antony Omita, Dr Fauzi Jalil, Mr Kenneth Ho, Mr Se Hun Chung, Ms Zoe Whiteley, Ms Shorooq Abukhamees, Ms Rawan Fitaihi, Ms Charitini Volitaki, Ms Amal Abdulghani, Ms Beshair Alsaffar, Dr Maryam Parhizkar and Dr Asma Buanz for supporting me in the lab when I needed them, and for sharing plenty of laughs and making life-long memories together.

I would also like to thank Professor Susan Barker, or our lab aunty, who has supported me both in my work and my daily life at the School of Pharmacy, and without her this experience would not have been as amazing as it has been.

I would like to thank all my close friends in supporting me and keeping my spirits up when I needed a boost to keep my momentum, I especially want to thank my best friend Aya Fathy for always being there for me and motivating me to always keep going.

Most importantly, I would like thank my family for the love and support they have provided me with since the day I was born. If it was not for the nurturing environment they gave me, I would not be the person I am today, and I would not have been so lucky to be acquainted with the incredible people I mention here. I would like to especially thank my father, Essam Abdelhakim, who has always been my role model in hard work, perseverance and resilience. My mother, Mervat Elsheashaei, I thank you for being so loving, kind, yet strong, and for the sacrifices you have made so I can get to where I am today. Thank you for always believing in me and telling me to never give up, and that when one door closes another door will be waiting, which was very true for this PhD. I would like to thank my older sister and brother, Reem Abdelhakim and Moamen Abdelhakim for their love and for all the good times we shared and continue to share. I would also like to thank my niece Sofia, the newest member of the family and the one that brings us all together and puts a constant smile on our faces, thank you for making me smile at times where I felt low and giving me the energy to keep going.

Last but not least, I would like to thank my other half, Morad, for his continued encouragement and support. Your support allowed me to thrive and pour my heart back into the PhD, especially during the COVID-19 pandemic and lockdown. Thank you for being an amazing friend and always baking me yummy treats to keep me going.

Table of Contents

List of Figures

List of Tables

List of Abbreviations & Acronyms

AC0	1st generation basic bitterness sensor
AE1	Astringency sensor
AFM	Atomic Force Microscopy
AN0	2nd generation basic bitterness sensor
ANOVA	Analysis of Variance
ASD	Amorphous Solid Dispersion
API	Active Pharmaceutical Ingredient
BATA	Brief Access Taste Aversion
BCS	Biopharmaceutics Classification System
BT0	3rd generation basic bitterness sensor
BPCA	Best Pharmaceuticals for Children Act
C00	Acidic bitterness sensor
CMP	Critical Material Parameters
CP	Centre Point
CPA	Change of membrane Potential caused by Adsorption
CPM	Chlorpheniramine Maleate
CPP	Critical Process Parameters
CQA	Critical Quality Attributes
CRO	Contract Research Organisation
DF	Degrees of Freedom
DMAc	*N,N*-dimethylacetamide
DMSO	Dimethyl Sulfoxide
DoE	Design of Experiment
DSC	Differential Scanning Calorimetry
EPR	Electronic Patient Record

E-EPO	Eudragit E PO
EMA	European Medicine's Agency
EuPFI	European Paediatric Formulation Initiative
FDA	Food and Drug Administration
FTIR	Fourier-transform Infrared
GCP	Good Clinical Practice
GPCR	G Protein–coupled Receptors
GRAS	Generally Regarded As Safe
ICH	International Conference on Harmonisation
IMI	Innovative Medicines Initiative
IV	Intravenous
KCT	Kollicoat Smartseal
MTDSC	Modulated Temperature Differential Scanning Calorimetry
NICE	National Institute for Clinical Excellence
OFAT	One Factor At a Time
PIP	Paediatric Investigation Plan
PSP	Paediatric Study Plan
PDCO	Paediatric Committee
PCA	Principal Component Analysis
PKDL	Polycystic Kidney Disease Like Protein
PREA	Paediatric Research Equity Act
PROP	Propylthiouracil
PTC	Phenylthiocarbamide
PUMA	Paediatric Use Marketing Authorisation
PVA	Polyvinyl Alcohol

PVC	Polyvinyl Chloride
PVP	Polyvinylpyrrolidone
PXRD	Powder X-Ray Diffraction
QbD	Quality by Design
RH	Relative Humidity
RSD	Relative Standard Deviation
STEP	Safety and Toxicity of Excipients for Paediatrics list
SD	Standard Deviation
SEM	Scanning Electron Microscopy
T2R	Type 2 Receptor
TEM	Transition Electron Microscopy
SF	Salivary Flow
T_g	Glass Transition Temperature
TGA	Thermogravimetric Analysis
T_m	Melting Temperature
TPP	Target Product Profile
UV	Ultraviolet
V_r	Reference Electric Potential
V_s	Sample Electric Potential
WHO	World Health Organisation
W/V	Weight in Volume
W/W	Weight in Weight
XRD	X-Ray Diffraction

Scientific Publications and Presentations

International Peer-Reviewed Publications

- *Electrospinning optimization of Eudragit E PO with and without Chlorpheniramine Maleate using a Design of Experiment Approach.* (**2019**) **Hend E. Abdelhakim**, Alastair Coupe, Catherine Tuleu, Mohan Edirisinghe and Duncan Q. M. Craig. **Molecular Pharmaceutics** 16, 6, 2557–2568

- *Human mouthfeel panel investigating the acceptability of electrospun and solvent cast orodispersible films.* (**2020**) **Hend E. Abdelhakim**, Gareth R. Williams, Duncan Q. M. Craig, Mine Orlu and Catherine Tuleu. **International Journal of Pharmaceutics** 585 119532.

- *Development and Evaluation of Feline Tailored Amlodipine Besylate Mini-Tablets Using l-lysine as a Candidate Flavouring Agent* (**2020**) Chinedu S. Ekweremadu, **Hend E. Abdelhakim**, Duncan Q. M. Craig and Susan A. Barker. **Pharmaceutics** 12 (10), 1-13.

- *A Potential Alternative Orodispersible Formulation to Prednisolone Sodium Phosphate Orally Disintegrating Tablets* **(2021)** Essam A. Tawfik, Mariagiovanna Scarpa, **Hend E. Abdelhakim,** Haitham A. Bukhary, Duncan Q.M. Craig, Susan A. Barker and Mine Orlu. **Pharmaceutics** (13) 120.

Oral Communications

Talks

Utilising co-axial electrospinning as a taste-masking technology for paediatric drug delivery. Oral Presentation at UCL School of Pharmacy Research Day; 10th March 2021.

Electrospinning as a taste-masking technology for paediatric drug delivery. Oral Presentation at the *EU-China Symposium on Electrospinning in Drug Delivery, held in London, UK; 28th August 2019.*

Utilising co-axial electrospinning as a taste-masking technology for paediatric drug delivery. Oral presentation at the 3rd European Meeting on Pharmaceutics, Biopharmaceutics, and Pharmaceutical Technology, held in Bologna, Italy; 25th-26th March 2019.

Posters

Abstract accepted for poster presentation to PBP World Meeting Conference, Vienna, March 2020; Event postponed to May 2021 (virtual) due to Covid-19 pandemic.

Mouthfeel evaluation comparison between orally administered electrospun fibre mats and solvent-cast fast-dissolving films.

Co-axially electrospun chlorpheniramine maleate fibres for paediatric drug delivery. Poster presentation at the UCL School of Pharmacy Annual Research Day, held in London, UK; 21 September 2018.

Taste-masked nanofibres for paediatric drug delivery. Poster presentation at the UK China Mini symposium on electrospinning in drug delivery 08 Apr 2018, London, UK.

Taste-assessment of electrospun chlorpheniramine maleate fibres using an electronic taste sensing system. Poster presentation at the SPaeDD-UK Accelerating paediatric formulation development meeting held in London, UK; 28 March 2018.

Taste-masked nanofibres for paediatric drug delivery. Poster presentation at the 11th World Meeting on Pharmaceutics, Biopharmaceutics, and Pharmaceutical Technology, held in Granada, Spain; 19th- 22nd March 2018

Electrospinning Optimisation of Drug-Loaded Eudragit E PO for Paediatric Oral Drug Delivery. Poster presentation at the 2017 AAPS (American Association for Pharmaceutical Scientists) Annual General Meeting and Exposition held in San Diego, California, USA; 11th - 15th November 2017.

Taste-assessment of electrospun chlorpheniramine maleate fibres using an electronic taste sensing system. Poster presentation at the 9th EuPFI (European Paediatric Formulation Initiative) Annual Conference 'Formulating Better Medicines for Children' held in Warsaw, Poland; 20th - 21st September 2017.

Manufacturing optimisation of electrospun Eudragit® E PO for paediatric oral drug delivery. Poster presentation at the 13th ULLA (European University Consortium for Pharmaceutical Sciences) Summer School held in Leuven, Belgium; 08th - 14th July 2017.

Chapter 1

Introduction

1.1 General Introduction

A key challenge in formulating oral medicines for children is to overcome the aversive taste of drugs as well as to improve the patient's ability to swallow the dosage forms. To overcome this challenge, there is a need to develop novel dosage forms that reduce the challenge of swallowing whilst also being taste-masked. One formulation approach that may allow ease of swallowing is the development of fast-dissolving drug delivery systems, such as orally disintegrating films. These films reduce the challenge of swallowing as they disintegrate upon contact with saliva. An obvious disadvantage, however, is the exposure of the active pharmaceutical ingredient (API) to the taste buds on the tongue and in the mouth upon dissolution. Effective taste-masking of the drug will therefore need to be coupled with the disintegration properties of the medication; it is this challenge of coupling the ease of swallowing via rapid disintegration with the ability to mask taste that forms the central theme of this thesis.

1.2 Age-appropriate Formulations

Children are often administered medicines originally designed for adults, with absorption and distribution data historically being extrapolated from adult studies with concomitant risks of under- or over-dosing. Pharmacologically this is unsuitable because children are not merely small adults but are instead are a heterogenous group in their own right. Indeed, infants are not just small children. In addition, there will also be inter-individual differences within each age group, both in terms of bioavailability and formulation acceptability. This means that even a specially formulated paediatric formulation may not be suitable to the various subgroups, thereby influencing acceptability and eventual compliance. Therefore, age-appropriate paediatric formulations need to be designed with each target population in mind [1].

The guideline on clinical investigation of medicinal products in the paediatric population (CPMP/ICH/2711/99) uses the following age groups in relation to developmental stages [1]:

- Preterm newborn infants (<37 weeks gestation)
- Term newborn infants (0 to 27 days)
- Infants and toddlers (1 month to 23 months)
- Children (2 to 11 years)
- Adolescents (12 to 16 or 18 years depending on the region)

Each of these age groups require different formulations to meet their varying needs [2]. Therefore, novel formulations have been developed to target those vulnerable groups. These include small-sized solid oral drug delivery systems (e.g., minitablets and multi-particulates) and orally dispersible products (e.g., orodispersible tablet, orodispersible films and chewable formulations). The cost of manufacturing of these innovative formulations needs to be viable so as to ensure patient access [3].

Importantly, however, the formulation must be acceptable which means that the patient is willing and able to take and the carer to administer the medicines as intended. Palatability is key to acceptability within the paediatric population, and is defined as the overall appreciation of a medicines organoleptic properties, such as its appearance, smell, taste, mouthfeel and aftertaste [4].

1.2.1 Taste

Poor taste of medicines is one of the main adherence barriers in children [5]. A study assessing children's views on taking medicines showed that 63 % of children aged 10 to 18 identified "bad taste of medicines" as an adherence barrier [6]. Certain antibiotics (especially penicillins) are so unpalatable that most children find them unacceptable, and training is required for the child to learn to accept taking the medicine. Poor adherence results in treatment failure, complications, and also drug resistance [7]. An observational study on the palatability of oral prednisolone in children in the UK and Saudi Arabia has found that the taste of the steroids medicine is very poor that it may affect adherence to treatment [8]. Due to the challenge of poor swallowability of conventional solid dosage forms, care-givers often crush or manipulate the dosage form, thereby increasing the bitter intensity of the medicine, as the coating layer has been compromised. Overall, lack of pleasant tasting drug formulations for children may lead to suboptimal treatment outcomes [9].

1.2.2 Swallowing

The age at which children can swallow tablets varies widely. A study investigating 30 children aged 4 to 8 years has shown that 67 % of them were able to swallow a 6 mm tablet, 81 % of them were able to swallow an 8 mm tablet, and 95 % of them were able to swallow 10 mm tablets. The same study has shown that 25 children aged between 9 to 12 years were able to swallow 6 mm and 8 mm tablets 100 % of the time, and for the 10 mm tablets only 96 % of children were able to swallow them [10]. The study also found that repetition and experience were key in successful swallowing of tablets in children, and this notion is shared by other research [11]. In addition, 48 % of the 4 to 8 years group displayed at least one negative facial expression when swallowing the tablets, which shows that although they were able to swallow the tablet, it was not a pleasant experience. Another study by Meltzer *et al.* (2006) found that 91 % of 125 children aged between 6 to 11 years of age were able to successfully swallow a 7 mm placebo tablet [11]. It is accepted that children generally can swallow tablets from the ages of six onwards, but this varies between different children. Moreover, many adults also have difficulty swallowing tablets [12].

1.2.3 Challenges and Current Need

Challenges of effective age-appropriate formulations that offer dosing flexibility, include swallowing, palatability, excipient safety, and involvement of a caregiver. Dosing flexibility is advantageous as it allows the accurate administration of low doses and small volumes across all the age groups. To overcome compliance issues with oral solid medicines, measures such as splitting tablets in half are commonly seen in practice. This is unsuitable because it is incorrect to assume that the drug distribution will be the same in both halves. Undesirable practices also include crushing tablets and opening capsules and sprinkling or mixing with food [13], which can affect their absorption and bioavailability.

All these measures are sometimes examples of unlicensed use of medicines. A large proportion of medicines are given to children in an unlicensed or off-label manner. Off-label describes a medicine being used outside of its product license, as in using a different route of administration, or a different indication, or outside of stated age limits. Unlicensed use medicines include altering the original form of the medicine or importing a medicine that is not licensed in its country of use [14]. Manipulation by the patient or caregiver should always be kept to a minimum as this can introduce error and result in under or over-dosing [15]. A common decision pathway for the unlicensed use of medicines in children is shown in Figure 1.1.

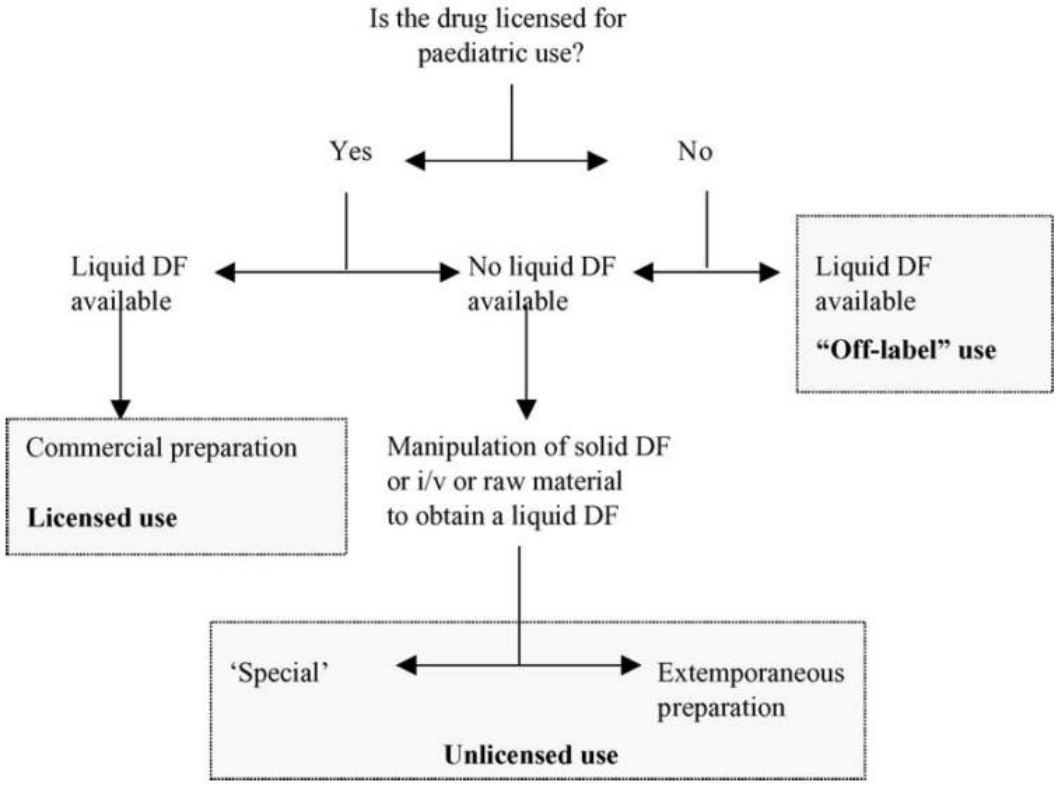

Figure 1.1. Decision pathway for providing oral doses to children for whom whole tablets/capsules are unsuitable (DF: dosage form; i/v: intravenous). Adapted from [14].

The use of unlicensed and off-label medicines in children has implications for the prediction, avoidance, and treatment of adverse drug reactions. The safety data included in the licensed version of the medicine may not be applicable to its off-label or unlicensed use [16]. There is, therefore, a need to manufacture palatable

medicines that are licensed for paediatric use as this will reduce errors caused by the unlicensed use.

1.2.4 Current Formulations

Currently, there are a number of formulations on the market for both adult and paediatric use. Liquid dosage forms generally are easier to swallow, however they are more difficult to taste-mask and have more stability issues. Solid dosage forms on the other hand are easier to manufacture and taste-mask, but they can be harder to swallow by children. Some of the most common formulations' advantages and limitations are summarised in Table 1.1 [3].

Table 1.1. Some of the most common formulations' advantages and limitations. Adapted from [3]**.**

Formulation	Advantage	Limitation
Oral solution and suspension	Increased dose flexibility Ease of swallowing	Stability issues Higher transportation cost Lack of controlled release Palatability Caregiver errors Multi use formulation requires preservative
Elixir		Alcohol levels too high for paediatric administration
Tablet	Ease of manufacturing Low cost Stable Taste-masking	Poor dose flexibility Swallowing difficulties Splitting or crushing tablets
Mini-tablet	Can be swallowed from as young as 6 months	Low maximum dose so multiple tablets often administered Need specialised dispenser

Multiparticulate	Controlled release Taste-masking Dose flexibility	Grittiness / mouthfeel may be an issue Co-administration with food may alter bioavailability
Orodispersible tablet	Likely no water needed No need for swallowing Taste-masking by coating API	Costly manufacturing and packaging Not a flexible dosage form
Orodispersible film	No water needed No need for swallowing Dose flexibility Elegant appearance	Taste-masking Controlled release Limited drug amount Specialised packaging
Chewable formulation	Swallowing aided Water not required	Controlled-release Taste-masking Bioavailability may be altered depending on chewing ability Not a flexible dosage form
Effervescent tablet	Ease of swallowing	High amount of sodium Taste-masking

1.2.5 Development of New Formulations

To address the need for age-appropriate medicines in children, initiatives and regulations have been introduced. Bespoke drug development programs, repurposing medicines or using new technologies such as nanotechnology, are all different approaches for formulating more licensed medicines in children. The use of miniaturized platforms such as mini-tablets or mini-capsules offer an advantage to children, enabling them to swallow with ease; however risks of choking and aspiration needs to be taken into consideration [15].

The World Health Organisation (WHO) has issued a document outlining the Target Product Profile (TPP) of a paediatric formulation [12]. TPPs guide industries to manufacture formulations that possess the most critical attributes of a formulation, resulting in products that responds to the needs of end-users. Properties such as safety, tolerability, palatability and cost of manufacture should all be taken into consideration when formulating a paediatric formulation. In

addition, potential adherence needs to be taken into consideration. Factors that influence adherence include formulation's size, frequency of administration, length of treatment and taste [17].

Policies and regulations (Section 1.2.6) have driven more paediatric clinical trials and therefore more licensed medicines in children. New initiatives are being introduced for involving children in clinical trials, an example is to standardise protocols leading to harmonisation and simplification of the process. Paediatric Good Clinical Practice (GCP) regulations ensure appropriate training for staff involved in paediatric clinical trials [18][19].

In addition, encouraging non-trial data from day-to-day clinicians in hospital wards, can lead to a national research database, as in the case with the national neonatal research database, an Electronic Patient Record (EPR) helping to achieve a "cradle to grave record" [20].

Another important issue in the introduction of new medicines for children is the collaboration of stakeholders, namely: children and their parents, clinicians, clinical networks, pharmaceutical industry & Contract Research Organisations (CRO), regulatory committees, ethics committees, and any other applicable institutions e.g. National Institute for Clinical Excellence (NICE). Figure 1.2 shows how some of these stakeholders are connected.

The lack of age-appropriate formulations can lead to poor compliance and therefore medicine's wastage. Most children's caregivers will in turn manipulate a formulation to improve acceptability, rendering it unlicensed. An unlicensed formulation can affect the solubility of a drug, risking its bioavailability. In an effort to improve treatment outcomes, prescribers resort to specials and off-label medicines which can increase the risk of adverse drug reactions [16]. In order to help tackle these various issues, pharmaceutical companies and academic research facilities need to collaborate to formulate novel dosage forms. In addition, regulations can help accelerate these initiatives and incentivise companies further. In my opinion, this problem is multi-faceted and the solution must, therefore, be interdisciplinary.

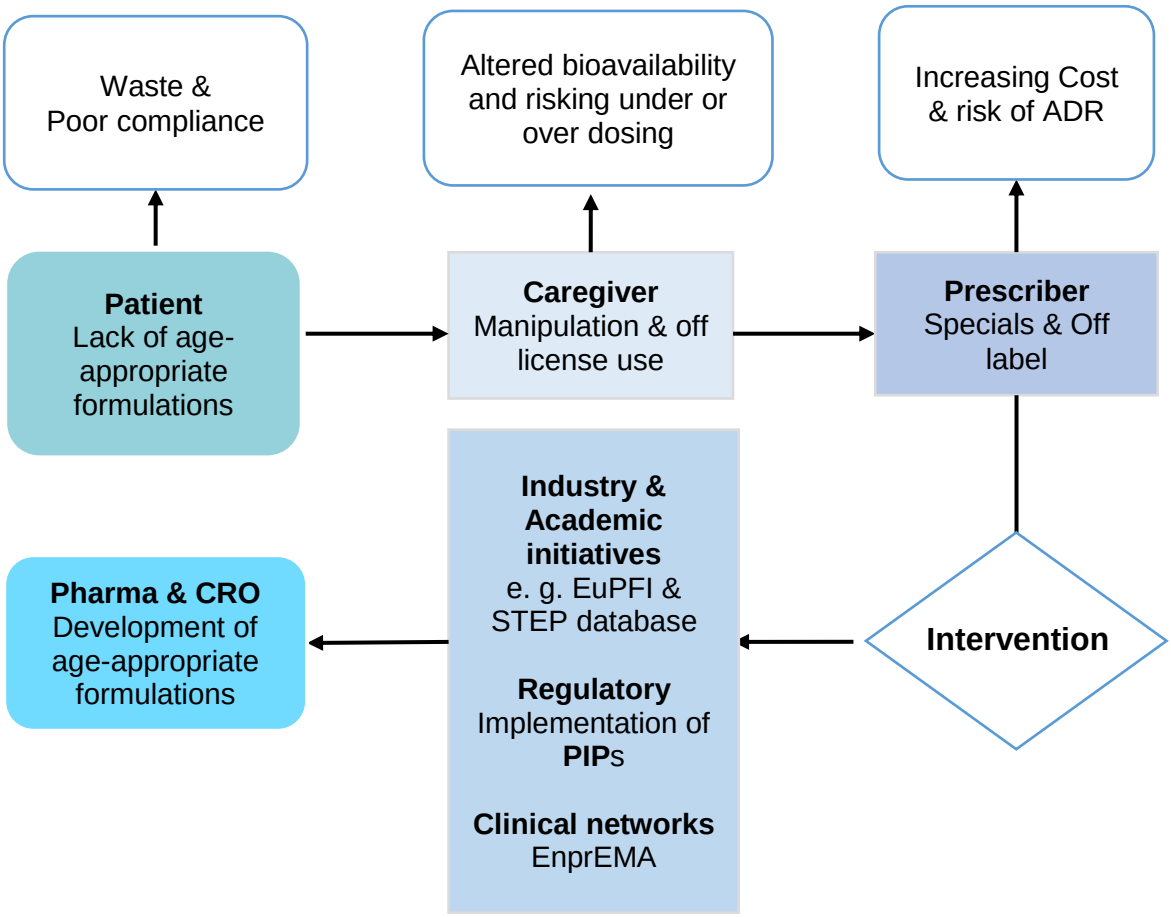

Figure 1.2. The interplay between some of the stakeholders involved in the development of medicines in children.

1.2.6 Regulations

Formulation of paediatric medicines has been limited in the past, with little enforcement from regulatory authorities to encourage further work in this area. Based on the EMA's database, from January 2007 to May 2016 a total of 66 pharmaceutical products were approved for paediatric use, but they were limited to tablets, capsules, solutions and powder sachets [21]. These conventional formulations can present acceptability challenges especially with regards to palatability and swallowing ability. The first regulatory action was brought about by International Conference on Harmonisation (ICH) of Technical Requirements for Registration of Pharmaceuticals for Human Use in 2000 with the adoption of the ICH E11 guideline [18]. This guideline outlined critical issues in paediatric drug development and encouraged timely paediatric drug development; however,

this was not a mandatory guideline, only a recommendation, and therefore had little effect on paediatric submissions.

In the USA, sections of the Food and Drug Administration Amendments Act (FDAAA) regulating appropriate paediatric drug development are:

- Title III or the Paediatric Medical Device Safety and Improvement Act
- Title IV or Paediatric Research Equity Act (PREA)
- Title V or the Best Pharmaceuticals for Children Act (BPCA)

The BPCA introduced Paediatric Written Requests. This a voluntary request to undergo trials to determine if a drug would be applicable for use in the paediatric population. In 2003, PREA mandated Paediatric Study Plans (PSP), which was the next move forward in regulating paediatric dosage forms. These were mandatory for all marketing applications, if the application relates to a new API, formulation, indication, dosing regimen or route of administration. If not applicable to children, a waiver could be granted [22].

In the EU, similar regulations have been implemented. In January 2007, the EU Paediatric Regulation (Reg 1901/ 2006/EU and Reg 1902/2006/EU) was adopted. Its objective was to improve the health of children in Europe by facilitating the development and availability of medicines for children aged 0 to 17 years. One of the aims of the regulation was to reduce the level of off-label use. It also set up in place a system of obligations, rewards and incentives. The regulation obliged companies to agree a Paediatric Investigation Plan (PIP) with the European Medicines Agency (EMA). Similar to the PSP, the PIP aimed at ensuring that the necessary data are gathered through studies in children, to support the availability of authorised medicines for children. The only difference between the US PSP and the EU PIP is that a PIP needs to be submitted by the end of Phase 1 of a clinical trial, whilst a PSP is submitted at the end of Phase 2. A 10-year report was issued detailing the impact the regulation has had. Figure

1.3 shows the number of new paediatric products, indications and posology, before and after the paediatric regulation came into force [23].

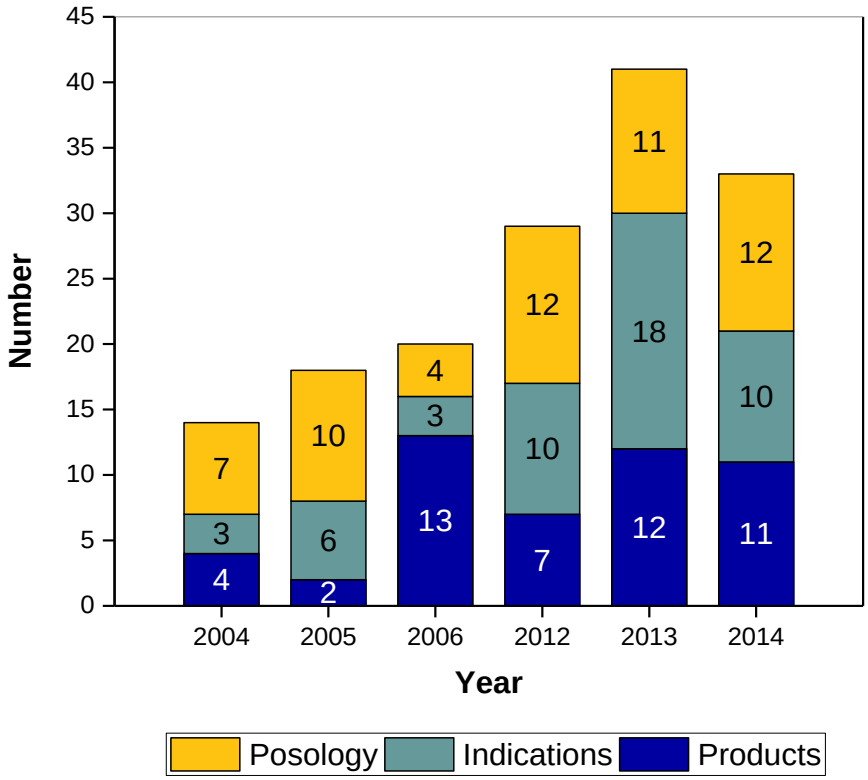

Figure 1.3. A graph showing the number of new paediatric products, indications and posology, before and after the paediatric regulation came into force in 2007. Adapted from [23]**.**

Finally, the Paediatric Use Marketing Authorization (PUMA) is an EU initiative intended to stimulate the development of off-patent products for use in the paediatric population. PUMA guarantees a 10 (8 + 2) year data protection [24].

Patients suffering from rare diseases deserve the same high-quality research and treatment innovation as other patients. The Orphan Drug Regulation governs orphan medicinal products, intended for the diagnosis, prevention, or treatment of serious conditions that affect no more than 5 in 10,000 people. Due to the limited number of patients suffering from rare diseases, the pharmaceutical industry has been reluctant previously to invest in research to develop products in this area [25]. To provide an incentive to manufacturers, if an orphan medicine has a PIP submitted (no waiver granted) with the application, the regulators will

provide ten years of market exclusivity plus two years for paediatric purposes [26].

These regulations have incentivised and mandated the pharmaceutical industry to develop more paediatric medicines; in 2017, 43 marketing authorisations were approved for paediatric dosage forms, improving the availability of paediatric options [22]. Nonetheless, taste-masking remains a formulation challenge for paediatric medicines. Taste is a complex physiological sense and therefore masking it can be a challenging task.

1.3 Taste background

1.3.1 Taste

Flavour is the combined term for the overall appreciation of a substance, including its taste, aroma, feeling factors and texture. Flavour itself is therefore a perception resulting from the various signals from the gustatory, olfactory and trigeminal systems. Since it is a perception, it is inevitably linked to individual behaviour. Since behaviour cannot be measured directly, this complicates the availability of a standard test for taste-assessment [27].

Classically, taste has been classified into five basic qualities: salty, sweet, sour, bitter and umami. Other qualities such as, fatty, metallic, and astringent, may also be considered as basic tastes [28]. Olfaction contributes a large extent to the taste of a substance [29]; when combined with input from the approximately 300 human olfactory receptors, a large variety of flavours can be perceived [30].

Mouthfeel can be a cause of aversiveness of the ingested substance, as in the case with experiencing oral grittiness. Grittiness is increasingly perceived with increasing size of particles, as well as amount. Grittiness is generally considered an unpleasant mouthfeel, and therefore creates another formulation challenge [31]. Other oral sensations include tingling, burn, and cooling. All of those sensations can contribute to the overall palatability of a formulation [32].

1.3.2 Physiology

All the mentioned taste qualities and sensations are experienced by taste buds found on the tongue, the organ responsible for taste. Papillae are found on the surface of the tongue and they contain one or more taste buds which transduce taste. Taste buds are the primary units of the taste system and they are embedded in fungiform, foliate, and circumvallate papillae. Filiform papillae lack taste buds but play an important role in transducing texture, temperature, and pain. The basic structure of the tongue and the taste bud is shown in Figure 1.4 [30]. Taste buds are onion-like structures that can respond to all stimuli as each of them contain between 50 to 100 taste bud cells [33]. There are four types of taste bud cells: type I, type II, type III, and taste cell precursors.

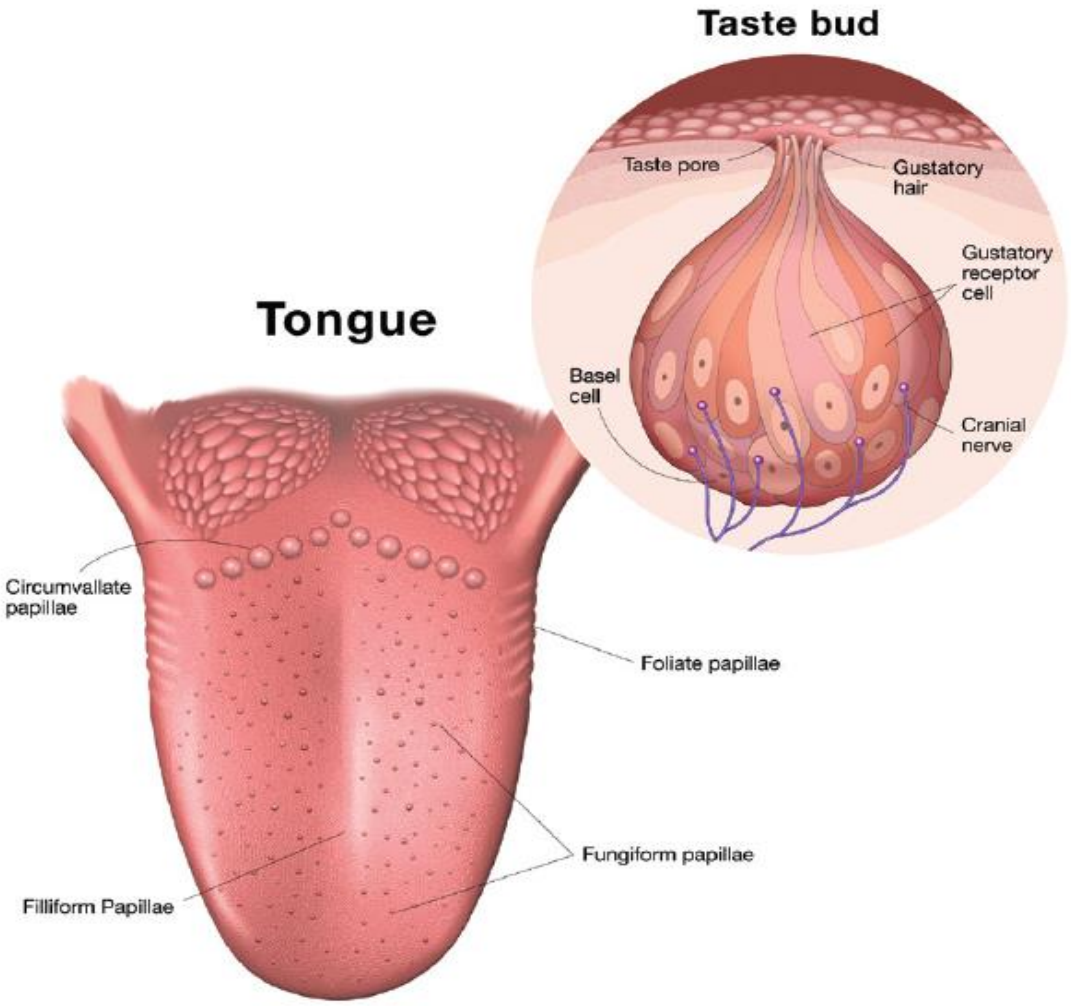

Figure 1.4. The basic structure of the human tongue and taste buds. Adapted from [30]**.**

Figure 1.5 summarises the taste sensing cells and the tastes they detect. Type I cells maintain the structure of the taste buds. Ion exchange channels are expressed on type I cells and are responsible for the perception of salty tastes [34].

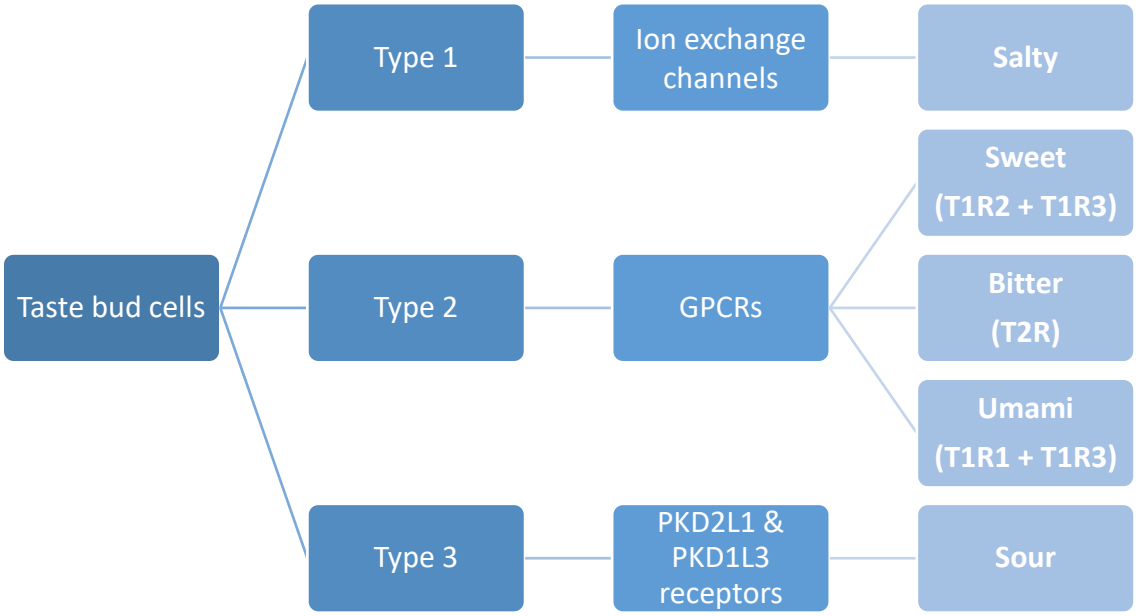

Figure 1.5. A diagram summarising the main type of taste bud cells and the taste qualities they are responsible for detecting.

Type II cells, also known as taste receptor cells, express G protein–coupled receptors (GPCRs), involved in mediating sweet, bitter, and umami taste [27]. Bitter tastes are sensed by GPCR of the type 2 receptors (T2R) family. There are 25 T2Rs in the oral cavity. T2Rs are also expressed extra-orally which suggests the existence of endogenous ligands, however, no known endogenous ligands have been found to date. Bitter compounds activate a number of these receptors at once; no known ligand activates all 25 T2Rs [35].

Umami tastes are sensed by the activation of heterodimeric receptors of T1R1 and T1R3 subunits. Similarly, sweet tastes are sensed by activation of heterodimeric receptors of T1R2 and T1R3 subunits [34].

Taste III cells, or presynaptic cells, express polycystic kidney disease 2-like 1 protein (PKD2L1) and polycystic kidney disease 1-like 3 protein (PKD1L3) channels, which together are involved in perception of sour taste [34].

Taste cell precursors, or as they were previously referred to as type “IV” cells, do not possess obvious taste functions. They are likely to be undifferentiated or immature taste cells; the exact significance of those cells remains to be elucidated [28].

1.3.3 Population Variation

Taste sensitivity varies across individuals. This could be due to a number of factors. The number and distribution of taste buds can affect the intensity of some tastes [36]. Gender differences can play a role. It has been shown that women have more fungiform papillae and more taste buds, and therefore more likely to have more intense taste perceptions [37]. It has also been documented in the literature that hormonal changes can all have varied effects on certain taste perceptions; these include: menstruation [38]; pregnancy [39]; and menopause [40].

Age can affect the perception of taste. A study that compared taste perceptions of young adults (19 to 33 years) to the elderly (60 to 75 years) found that absolute taste perception does not change with ageing, however, intensity decreased with age [41]. It has been suggested that young children perceive bitter tastes more strongly than adults; this therefore can be a limitation of adult human taste panels [42].

Genetics also play a role in taste variation. Across the population, a subset of people would be classified as non-tasters, whom cannot identify the bitterness of the recognised bitter compounds propylthiouracil (PROP) and phenylthiocarbamide (PTC). This phenotype is due to a haplotype involving polymorphisms at 3 amino acid positions in the hT2R38 protein[27]. Similarly, people who perceive these compounds as intensely bitter are classified as

supertasters. Supertasters have more fungiform papillae than the general population and therefore have a lower bitterness threshold [37].

Taste buds are bathed in saliva; the medium responsible for the dissolution of medicines and other compounds, allowing for the perception of flavour. Changes in saliva compositions can vary from individual to another. Saliva is made of 99 % water, electrolytes, enzymes and other proteins. It also consists of food remains, nasal mucosal fluid, and other fluids. At rest, there is a small unstimulated salivary flow (SF), however, 80 % to 90 % of saliva is a result of mechanical, gustatory, olfactory or pharmacological stimulus. SF index is a parameter that classifies saliva produced by both stimulated and unstimulated means, into normal, low, or very low salivation. Normal salivary pH ranges from 6 to 7 and varies in accordance with the SF, from 5.3 (low flow) to 7.8 (peak flow) [43]. Proline-rich proteins found in saliva can bind with bitter-tasting tannins found in some foods, increasing their acceptability [27]. Ironically, those proteins are associated with greater perceptions of PROP bitterness; supertasters have a significantly higher concentration of those proteins in their saliva [44].

One’s preference for certain flavours can also be influenced by culture and experiences. A taste perception study found that detection thresholds for bitterness, sweetness, saltiness and sourness were all lower for Japanese compared to Thai populations. Moreover, Thai populations had a stronger spicy preference which may have resulted in poorer taste sensitivity and perception compared to populations that prefer milder tastes, such as the Japanese [45]. More specifically in dosage form design, market research has shown that bubble gum and grape flavours are preferred in the USA, whereas citrus and red berry flavours are preferred in Europe [46]. Therefore, developing a palatable formulation needs to take into account cultural differences and their own definitions of an acceptable flavour [13].

1.4 Taste Masking

1.4.1 Taste Masking

There are many techniques to taste-mask bitter drugs already in use. An ideal method would be one that does not significantly increase the cost of manufacturing, is tolerated by the patient, and does not change the therapeutic value of the drug [29]. The choice of a taste-masking method will depend on the drug type, route of administration and compatibility of the API with the masking agent [47]. The most conventional techniques used in oral preparations include the addition of sweeteners and flavouring agents. Perhaps flavouring agents would be the first excipients that are suggested when taste enhancement is discussed. Natural flavours include extractions from natural origins, as the name suggests, into various forms such as a juice, tincture, spirit, syrup or oil. Most commonly used flavours include lemon, orange, peppermint, and berries [48]. The choice of flavouring agent usually depends on known popularity of particular flavours amongst a certain age group, drug, or indication association. A US based company, FLAVORx, created customisable flavour-based taste-masking of liquids, crushed tablets, and opened capsules. They provide pharmacies with an optional device that suggests different flavouring agents depending on the drug prescribed, and an associated device fully automates reconstitution and flavouring of the medicine [49]. In addition, the flavouring agents are also available for manual reconstitution and are FDA approved.

Other chemical and physical innovative techniques have been used to taste-mask bitter drugs. Obscuration of taste methods such as the addition of sweeteners would not be suitable for drugs with a high degree of bitterness. This is because sweeteners do not physically coat the bitter tastant, rather it elicits a sweet taste alongside it, thereby reducing the bitterness perceived up to a level. In addition, sweeteners often have a short duration of action, whereas bitter medicines can elicit bitterness after the formulation is swallowed, leaving an unpleasant aftertaste [50]. Furthermore, sugars have been linked to increased dental caries in children, which is why the amount of sugars used in most commonly prescribed children medicines have reduced in recent years. Artificial

sweeteners such as aspartame are also used, but have the same limitations for highly bitter drugs [48].

Another taste obscuration method involves increasing the viscosity of a liquid formulation by adding gums or carbohydrates such as microcrystalline cellulose, decreasing the drugs' contact with the taste buds; this renders the bitter drug inaccessible and therefore taste-masked. The addition of lipids such as surfactants and oils can also increase the viscosity of a formulation [20].

Lowering the pH of a liquid formulation can reduce the bitterness of a medicine effectively, especially in the paediatric population as they have a preference for sour tastes [18]. Modification of the API by the addition of an acid, such as citric acid, raises concerns as it has been linked to dental erosion due to its ability to dissolve the hydroxyapatite of tooth enamel and dentin. Similar to sucrose-sweetened medicines, acid addition will reduce but not completely eliminate bitter tastes of medicines [27]. A further API modifying creating a prodrug which can alter the drug's solubility and therefore its ability to come in contact with taste buds, hence masking the bitterness [29].

A more novel way of taste-masking bitter medicines is to use taste receptor blockers. Until now, 13 bitter taste receptor blockers have been found, and like most ligands, no one antagonist can block all 25 receptors. These bind to taste receptors therefore competitively blocking the receptor from the bitter API [29]. The downside of using a taste blockade mechanism is that the bitter blocker would have to be ingested separately prior to the medicine; compliance issues may be problematic. Another limitation of this technique is the genetic diversity of taste receptors which results in differing taste perceptions, thus it is unlikely that bitter-blockers will have the same effect in every individual [51].

Complex formation using cyclodextrins is another technique used to mask bitter drug molecules. This mechanism works by encapsulating the highly bitter hydrophobic APIs in the cyclodextrin's cavity via hydrogen bonding or van der Waals' forces leading to inclusion complexes [52]. Research by Liu *et al.* (2019) showed successful complexation of donepezil in hydroxypropyl-B-cyclodextrin

that resulted in a taste-masked orodispersible film [53]. A study by Hesari *et al*. (2016) explored the taste-masking of ranitidine via complexation with cellulose derivatives, leading to an orodispersible tablet with rapid disintegration time and an improved taste [54].

Furthermore, ion exchange resins can also be used to form a complex with bitter drugs. Ion exchange resins are high molecular weight water insoluble polymers that have either a basic or an acidic functional group. The complex of the drug with the ion exchange resin does not dissolve at saliva pH and therefore prevents exposure to taste receptors [20]. Drug resin complexes (DRC) are formed due to ion exchange reactions and have been used to taste mask bitter drugs to improve medicine compliance. Fast-disintegrating tablets containing chlorpheniramine maleate were formulated using cation exchange resins. Taste-masked ODF of betahistine with a cation exchange resin was also successfully developed through the use of DRC [55]. Drug molecules are released from the complex by exchanging with appropriately charged ions in the gastro-intestinal tract.

Similar to complex formation, creating a physical barrier can effectively taste-mask bitter drugs intended to be formulated into solid dosage forms. Coating of a core material in a taste-masking insoluble shell prevents the bitter drug from coming in contact with taste buds, but allows release further down in the gastrointestinal tract where it will be released. Microencapsulation is a form of film coating, as the name suggests, on a particle level, that can be incorporated into formulations such as ODTs and chewable tablets [29]. Microencapsulation can be achieved using various techniques including spray drying [48]. Spray-dried microspheres were used to successfully taste-mask famotidine mixed with Eudragit E PO that was further incorporated into ODTs [56]. Microparticles prepared by spray drying cetirizine dihydrochloride with Eudragit E PO were employed as taste-masking vehicles and further processed into ODTs. They were demonstrated to be taste-masked using both *in-vivo* and *in-vitro* evaluations [57].

Another barrier forming strategy is the use of liposome and multiple emulsions. Trapping the drug within the lipid part of a liposome or the oily phase of a w/o/w emulsion would prevent it reaching the taste receptors and hence masks the bitter

taste [29]. A w/o/w emulsion of ibuprofen was prepared for paediatric use [58] with the mention of the drug's bitterness, however, no formal taste-assessment was recorded for the formulation. Taste-masking of chlorpromazine, an antipsychotic drug, has also been reported by multiple emulsions [59].

Solid dispersion methods involve dispersing a solid drug in an inert solid carrier, by physical mixing, co-grinding, or by solvent evaporation method. This includes methods such as hot melt extrusion and electrospinning. Carriers that can be used include various sugar or polymeric carriers, such as Eudragits [60] [20]. Hot melt extrusion has been employed as a taste-masking technique a number of times, resulting in age-appropriate dosage forms of paracetamol [61], theophylline [62] and isoniazid [63].

More recently, innovative techniques such as 3D printing have been utilised to taste-mask bitter APIs. Multi-layered fast-dissolving films containing paracetamol or ibuprofen with a separate taste-masking layer were fabricated by Ehtezazi *et al.* (2018) providing a proof of concept study for the printing of films [64]. Wang *et al.* utilized 3D printing coupled with HME to effectively taste-masked caffeine citrate with Eudragit E PO, resulting in the formulation of donut-shaped tablets that may be more appealing to the paediatric population [65].

Creating a barrier, either on a molecular or physical level, appears to be the most efficient way of effectively taste-masking highly bitter drugs. In this project, electrospinning is utilised to taste mask a bitter drug. This technique allows for full solvent evaporation, and the manufacturing of fibre mats that can be formulated into easy to swallow solid dosage forms. A taste-masked formulation needs to be tested thoroughly through various taste-assessment means to ensure effective taste-masking.

1.4.2 Electrospinning

Solid dispersions have been used as a physical taste-masking method. Various techniques are used to achieve taste-masked amorphous solid dispersions (ASD), including electrospinning. Electrostatic spinning, or electrospinning, is a

nanofabrication technique in which electrostatic forces are used to convert a viscous solution into fibres through solvent evaporation. Using the solvent method, the drug and polymer carriers are dissolved in a solvent system that they are both miscible in, forming a solution. Removal of the solvent via electrospinning results in the formation of amorphous solid dispersions [66]. A wide variety of nanomaterials have been used in medicine to advance treatment. Specifically in the drug delivery field, due to their large surface area to volume ratio, nanomaterials can improve bioavailability, and enhance water solubility [67]. There are a number of different techniques for the manufacturing of nanofibres, and many parameters can be varied to produce the desired end-product.

A basic electrospinning apparatus consists of a syringe pump, forcing a polymer solution through a metal needle that is connected to a conductor, attached to a high voltage generator. The solution is pumped through the needle at a controlled flow rate towards a ground collector plate. The voltage source is connected to both the spinneret and the collector plate [68]. An electrospinning apparatus, (Spraybase®), is shown in Figure 1.6.

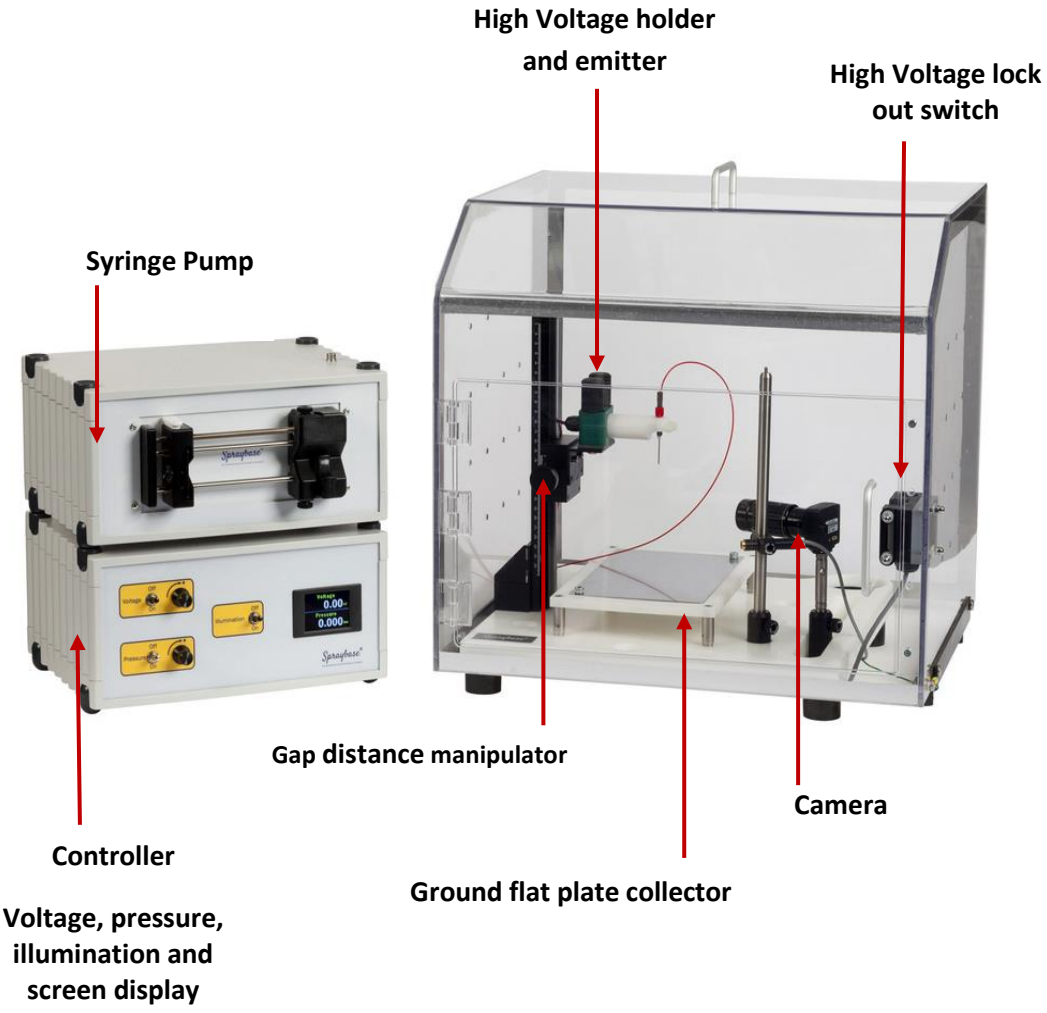

Figure 1.6. A real image of an electrospinning apparatus, Spraybase ®. Adapted from [282].

The high voltage applied overcomes the surface tension between the solution ejected from the spinneret and the surrounding air. When sufficient charge is applied, the dripping solution forms a suspended droplet known as the Taylor cone [69]; this is the critical point at which the fibres begin to form. This mechanism is shown in Figure 1.7. Throughout this process, the solvent evaporates and by the time the jet reaches the oppositely charged collector, the solid structure deposits and the fibre mat is formed. To form a thicker fibre mat, the electrospinning time is increased, or the collector size can be decreased [70].

A stable Taylor cone allows for narrow fibre size distribution. Increased branching will give rise to a high variation in fibre diameter size, and may influence beading.

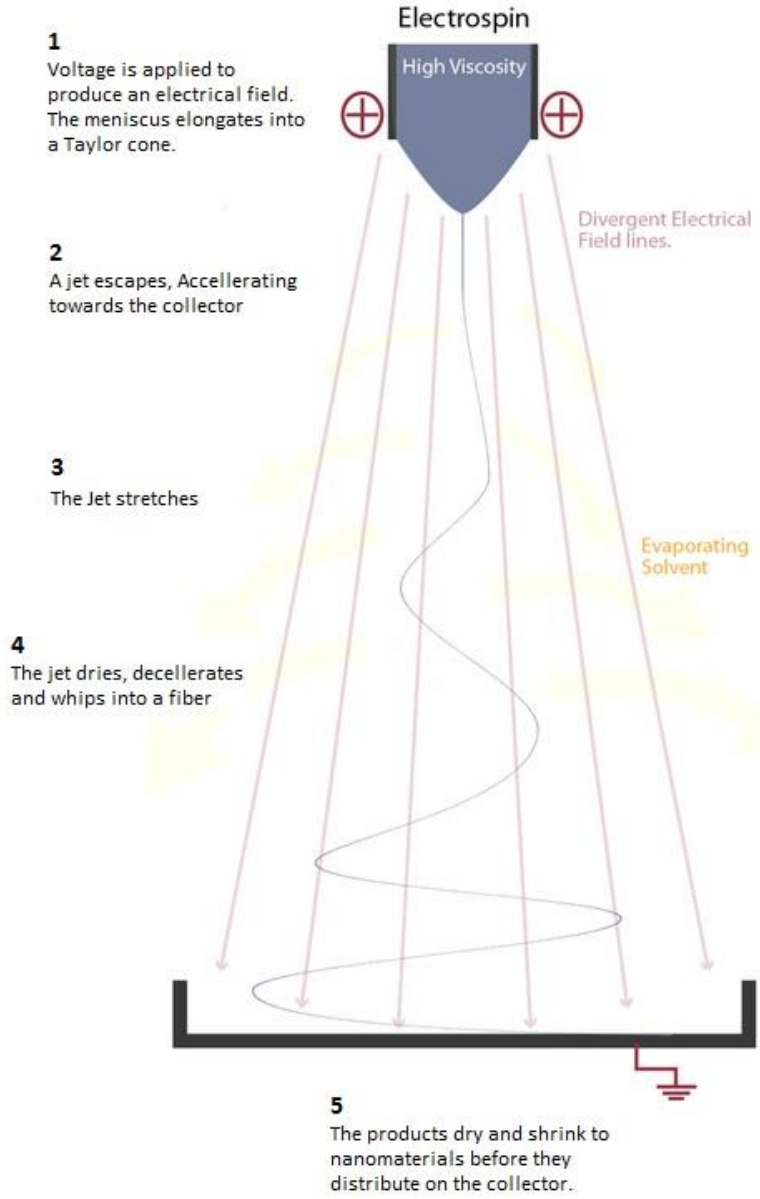

Figure 1.7. Mechanism of solution elongation and nanofibre production in electrospinning. Adapted from [282]**.**

A known defect that can occur in the electrospinning process is the formation of beads. Bead-on-fibres are considered to be defects due to the fact that they reduce the large surface area per volume, which is one of the main advantages of nanofibres [71]. In addition, beading can alter drug release as they can be formed of empty polymer pockets or conversely be reservoirs for APIs. In addition, beading can represent un-evaporated portions of the solution used,

likely due to low viscosity [72]. Thus, controlling beading defects is an essential part of electrospinning optimisation.

This PhD will focus on electrospinning's application in the drug delivery field, especially as a taste-masking platform. The polymer used to create the fibres should match the lipophilic character of the drug chosen so they can dissolve in the same solvent. If this is not possible, the drug can be dissolved in a small amount of a compatible solvent before being added to the polymer solution [69].

Once in the body, the release of the drug from nanofibre matrices is mainly by the mechanisms of desorption from the nanofibre surface, diffusion through the channels and pores of nanofibres or matrix degradation. The drug release kinetics can be modulated by the choice of polymer and through control over the nanofibre diameter, porosity, geometry, and general morphology [69].

1.4.2.1 Effect of Process Parameters

Electrospinning is affected by a number of factors, namely solution, process and environmental factors. Monitoring and changing these parameters can give rise to fibres with a range of morphological and functional properties. If the electrospinning process is not sufficiently optimised, this would give rise to an unstable polymer jet. Rayleigh instability is a phenomenon where a column of liquid ejected is inclined to break up into droplets with smaller individual surface areas. It naturally occurs because surface tension draws the fluid jet into a shape with a minimum surface area for a given area. Therefore, sufficient surface tension is needed to overcome the Rayleigh instability, thereby ensuring the continuous motion of the electrospun jet. This instability usually only occurs at a low applied voltage or when the solution is of a low viscosity that is incapable of reaching a chain entanglement concentration [73]. Nonetheless, the Rayleigh instability is essential for the viability of other techniques such as electrospraying, where individual sprayed particle formation is desirable. Fine-tuning of solution parameters is what differentiates electrospinning and electrospraying.

Once Rayleigh instability is overcome, another instability becomes prevalent. The second instability is known as an axisymmetric instability and it is where the mutual force of the jet's own surface tension, and that applied by the high voltage are in competition. Although this gives rise to a jet and eventually fibre formation, it is interrupted by beading [74]. In this case, the operator needs to re-optimise the process parameter such as increasing the applied voltage or altering the flow rate. If this is insufficient, the solution parameters would need to be re-visited and further optimisation would be required.

The third and final force is the Bending or Whipping instability, and it occurs as the jet travels continuously away from the nozzle, looping towards the collector and thereby increasing the gap distance and jet elongation [75]. Unlike Rayleigh instability, bending instability is believed to be crucial to electrospinning and in fact beneficial to the formation of fibres in the nano-range [76]. An image depicting the three different instabilities is shown in Figure 1.8.

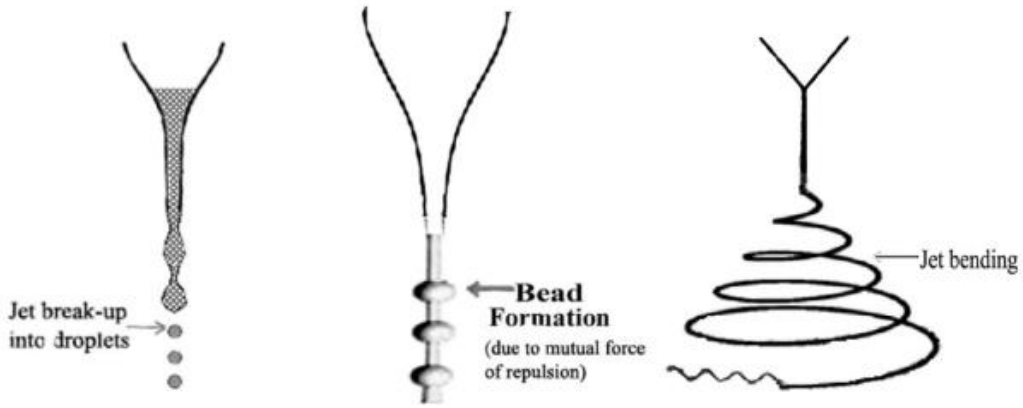

Figure 1.8. Different modes of jet instabilities. Image taken from Bagchi *et al.* (2015) [74].

Therefore, altering the process and solution parameters can affect the instabilities mentioned and therefore the quality of the fibres produced. Table 1.2 and Table 1.3 show the effect of increasing various factors on fibre beading and fibre diameter, respectively.

Table 1.2. Process, solution, and environmental variable effects on fibre beading.

Parameter	**Effect of increase** [77]
Applied Voltage	Bead formation **decreases,** up to a critical point, then increases [71]
Flow rate	Bead formation **increases** above a critical value [71]
Gap Distance	Beading **increases**
Polymer concentration	**Reduced likelihood** of beaded fibres, up to a critical point. If **viscosity** increases above a certain point needle clogging occurs which can result in beaded fibres [75]
Solvent	Mixing alcohol in dramatically **reduces formation of beads**, because it increases conductivity
Addition of salt	**Reduce beading** by increasing **conductivity**
Humidity	**Increases** beading
Temperature	Increases solvent evaporation and decreases viscosity, which in turn may **increase** beading

Table 1.3. Process, solution, and environmental variable effects on fibre diameter.

Factor	Parameter	Notes	**Effect of increase** [69]
Process	*Applied Voltage*	There is an optimum range for a given polymer-solvent system to form fibres	Fibre diameter **decreases** initially and then increases after a definite point
	Flow Rate	Affects the diameter, porosity, and geometry of fibres formed	Fibre diameter **increases**
	Gap Distance	The longer the distance travelled the more the jet has a chance to thin, thereby affecting the size and morphology of the fibres formed	Fibre diameter **decreases**
Solution	*Polymer concentration*	Increases **viscosity** improving chain entanglement. Affects **surface tension**, which in turn determines the electrospinnability of the solution	Fibre diameter **increases**
	Solvent	A lower boiling point indicates a rapid evaporation rate. However, if volatility is too high the solution may evaporate at the capillary tip and cause clogging, obstructing the flow of the polymer solution	A more conductive solvent will give rise to a fibre with a **smaller diameter**
	Salt Addition	The solution **conductivity** and the surface charge density of the solution jet increase	Fibre diameter **decreases**
Environmental	*Humidity*	Humidity cause changes in the nanofibres' diameter by controlling the solidification process of the charged jet [78]	Fibre diameter **decreases**
	Temperature	Temperature increases the rate of evaporation of solvent and it decreases the viscosity of the solution [78]	Fibre diameter **decreases**

1.4.2.2 Electrospinning as a Taste Masking Platform

Electrospinning has previously been used to manufacture age-appropriate and taste-masked dosage forms, with the aim of improving compliance in the paediatric population. Poller *at al*. (2017) [79] loaded prednisolone into PVP nanofibres using electrospinning. The fibres were compressed into 2 mm minitablets intended for use in young children. As mini-tablets can be taste-masked via coating and are easy to swallow, they are considered age-appropriate dosage forms [80]. No taste-assessment was conducted in this study. Paracetamol and caffeine fibres were loaded into PVP and electrospun into nanofibres that were formulated into a fast-dissolving dosage form. Similar to mini-tablets, fast-dissolving films are good candidates for a paediatric formulation as they are easy to swallow, however, their taste-masking is not as straightforward. The authors report the addition of raspberry flavouring agents; however, no taste-assessment is reported [81].

Meloxicam was loaded into PVP with cyclodextrin and electrospun into nanofibre mats intended for use as orally dissolving films. Cyclodextrins act as taste-masking systems as they enclose the bitter API in their core. In addition, menthol and aspartame were added to the blends as flavouring and sweetening agents, respectively. The films were taste-assessed by six human volunteers in an ethically approved trial, which showed successful reduction in the bitter taste [82]. The same authors published a report in 2017, with very similar dataset and findings [83]. Mouthfeel evaluation results were added in this paper, mentioning that the six volunteers found the electrospun fibre mats smooth. This is the only research found to report a human taste panel for electrospun fibre mats, nonetheless, with only six volunteers, the power of the study was low.

Co-axial electrospinning has also been utilised to develop a fast-dissolving film, incorporating Helicid, a plant extract used to treat headaches and insomnia. As the plant extract has a bitter taste, and a rapid onset is needed, the oral film needed to be taste-masked effectively. The authors report the use of PVP and sucralose, a sweetener, in the shell layer, and PVP with helicid in the core. It is claimed that the sucralose should effectively mask the bitter taste of the API, however, no taste-assessment was performed [84].

Although other researchers have explored electrospinning's usage as a taste-masking manufacturing technology, there is still a gap in this area. It is to be noted that none of the research articles found in the literature used the E-tongue to taste-assess electrospun fibre mats, and therefore this is one area of novelty of the work presented here.

1.4.3 Multi-axial Electrospinning

Multi-axial electrospinning results in fibres that are composed of more than one layer. This allows the incorporation of APIs in each of the layers, or the addition of different polymers or performance enhancing excipients in each of the layers. In addition, it has been reported that having a multi-layered fibre can alter the release profile of the delivery system, whereby an outer layer can burst release an API followed by sustained release from an inner layer. Multi-layered fibres can also offer improved stability of loaded substances [85].

1.4.3.1 Co-axial Electrospinning

Co-axial electrospinning comprises of two needles, one embedded inside the other. Figure 1.9 shows a schematic of the co-axial electrospinning setup. This gives rise to

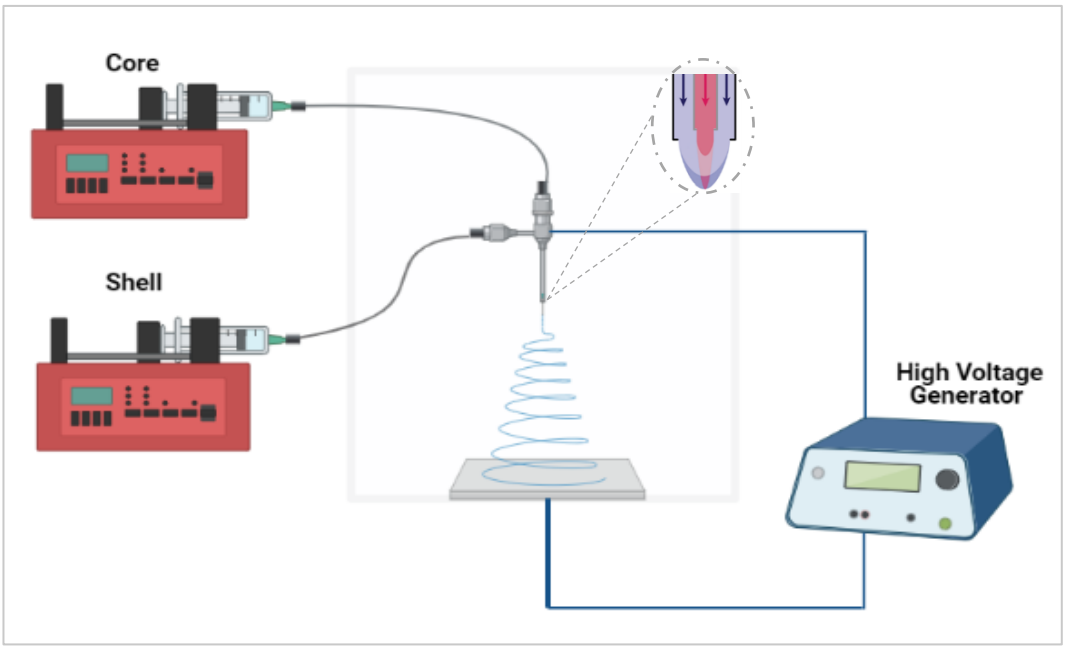

Figure 1.9. Co-axial electrospinning setup schematic. Created with BioRender.com.

a core-shell structure that can have various functions depending on the polymers used. Some of the applications of co-axially electrospun fibres includes controlled release, multi-drug formulations, protection of encapsulating a biological drug in the core [86], and also taste-masking [87]. Two syringe pumps are connected to a spinneret to form a coaxial structure showing a core and a shell, as shown in the inset.

1.4.3.2 Tri-axial Electrospinning

As the name suggests, tri-axial electrospinning comprises of three needles that are embedded within each other, giving rise to a multi-layered structure upon solvent evaporation. The first reported tri-axial electrospinning research was in 2007 by Lallave *et al.*[88] followed by Kalra *et al*. in 2009 [89]. There were no reports found of using multi-axial electrospinning for taste-masking.

1.4.3.3 Tetra-axial Electrospinning

Only one report could be found in the literature on researchers electrospinning four-layer fibres. The study by Labbaf *et al.* (2014) [90] provides a proof-of-concept study that combining layers via multi-axial electrospinning coincides with current trends in polypharmacy and therefore may be a way to improve patient compliance. The study however did not investigate optimising APIs in this way and the solutions were all drug-free.

1.5 Taste-assessment

Human and non-human taste-assessment tools have been utilised to ensure medicines are sufficiently taste-masked, and therefore acceptable, and palatable, for patient use. The paediatric population is the most sensitive to palatability of medicines. Unacceptable sensations are bitter tastes and gritty mouthfeel, therefore most taste-assessment techniques methods evaluate the aversiveness of both those aspects [60]. The following section presents an overview of some *in-vivo* and *in-vitro* methods used for taste-assessment.

1.5.1 *In-vitro* Techniques

In-vitro taste-assessment techniques mainly comprise of the use of an E-tongue or the use of dissolution methods to quantify drug amount [4]. These methods are easier to use than *in-vivo* methods mainly due to ethical and safety considerations.

1.5.1.1 Electronic Taste Sensing Systems

Electronic taste sensing systems, or E-tongues, are based on potentiometric measurement principles to assess a sample's taste. The two most commonly used E-tongues in the pharmaceutical industry are α-Astree and Insent, shown in Figure 1.10 [4].

The taste sensors are connected to reference sensors, and both of them are equipped with a silver electrode inside them. The reference electrode has a known potential; the difference between the electrodes appears as a mV reading using a voltmeter [91].

A basic E-tongue consists of a working lipid taste sensor and a reference taste sensor, with a known electric potential difference [92]. The difference between the two readings of both sensors represents a numerical output of a taste quality of a substance, for example bitterness [93].

The sensors compose of lipids, plasticiser and PVC. Positively charged lipid membranes comprise of quaternary ammonium salts, and negatively charged lipid membranes comprise of ester phosphates [91]. AN0, AC0 and BT0 are the negatively charged taste sensors used in this thesis. They all comprise of the same negatively charged artificial lipid (phosphoric acid di-n-decyl ester), but in differing amounts. They differ in their plasticiser component, which affects the hydrophobicity of the taste sensors, and therefore its selectivity and sensitivity. AN0 and AC0 contain dioctyl phenylphosphonate as a plasticiser, whereas the newer sensor contains another plasticiser, Bis(1-butylpentyl) adipate Tributyl O-acetylcitrate (BT0) [91].

As opposed to dissolution measurements, which merely quantify drug concentration, electronic taste sensors are able to detect taste substance interactions such as

suppression effects of bitterness caused by adding sucrose to a constant concentration of a bitter substance [94].

Basic bitter drug molecules are detected using negatively charged taste sensors. When the membrane is immersed in an aqueous solution, an electrical double layer is formed by the dissociation of the acid group in the lipid molecule. This is based on the Gouy-Chapman theory. This causes a change in membrane potential and the surface becomes negatively charged [95], causing the bitter positively charged hydrophobic molecules to adsorb onto the membrane surface. Because bitter drug molecules adsorb strongly onto the negative membrane surface, if washed with a reference solution only, the molecules remain detectable by the E-tongue. This gives rise to CPA, or change of membrane potential caused by adsorption, a reliable aftertaste bitter taste measurement. This value is significant for evaluating bitter and astringent substances, because they are also strongly adsorbed on the human tongue [95]. In terms of CPA, BT0 shows improved selectivity and sensitivity to hydrochloric salts, but nonetheless is suitable for other bitter salts.

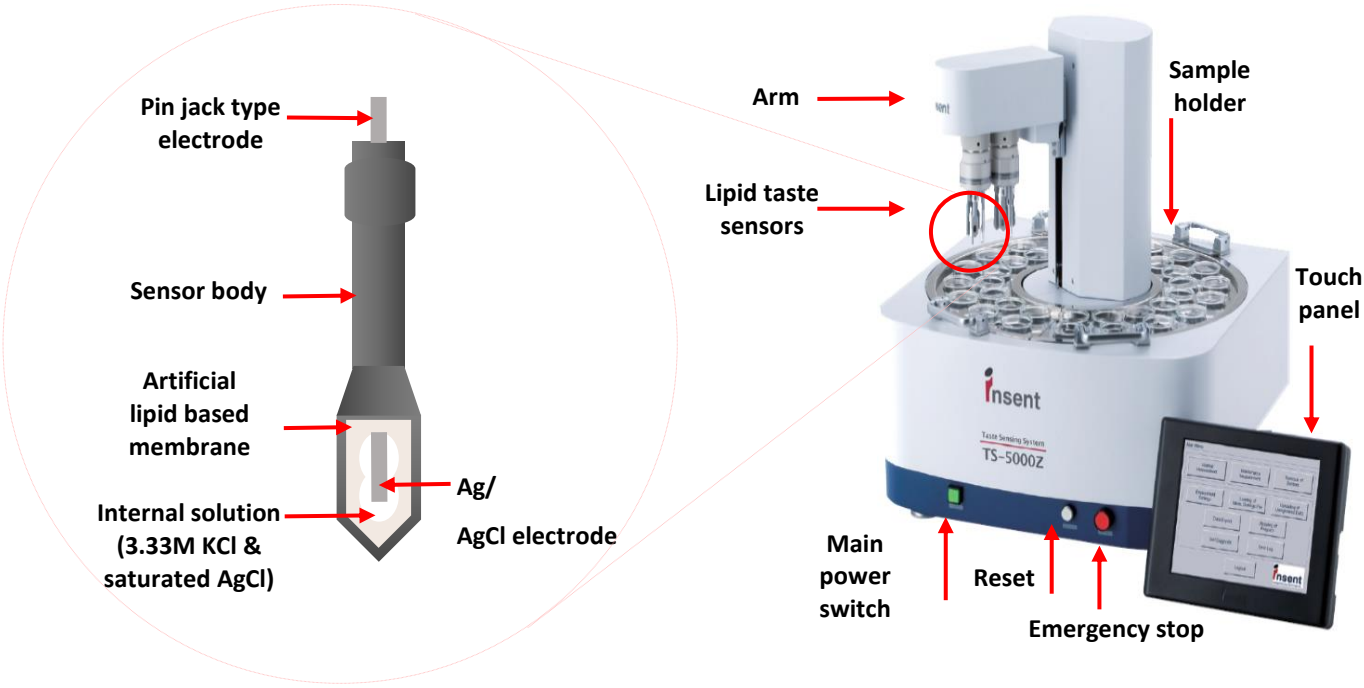

Figure 1.10. Insent TS-5000Z E-tongue set up. Adapted from www.insent.co.jp, with an inset of a schematic of a typical taste sensor.

A comparison between the two E-tongues' sensors and taste measurements is summarised in Table 1.4. Both systems can be used to assess taste by comparing the final taste-masked formulation to pure API, other excipients, and a placebo formulation. For a successfully taste-masked formulation, there should be little to no difference between the taste of the final taste-masked formulation and the placebo, and equally, the larger the taste difference between the final formulation and the pure API the more successful the taste-masking has been [4].

Table 1.4. A table comparing the two commercial E-tongues, α-Astree and Insent [4].

SA401, SA402/ TS-5000z **Insent (AtsugiChi, Japan)**	**α-Astree** **(Alpha M.O.S. Toulouse, France)**
Lipid membrane sensors	Chemical modified field effect technology (ChemFET) with polymeric sensors
Specific taste sensors, with partial cross selectivity: AAE for Umami CT0 for Saltiness CA0 for Sourness AE1 for Astringency AC0, AN0, & BT0 for Basic Bitterness C00 for Acidic Bitterness	*Cross selectivity across the different taste sensors; three sets of seven sensors that differ in composition:* 1) For Pharmaceutical application: ZZ, AB, GA, BB, CA, DA & JE 2) For food application: ZZ, BA, BB, CA, GA, HA &JB 3) Bitterness intensity measurement of a New Chemical Entity: BD, EB, JA, JG, KA, OA & OB
Initial taste (Relative Value) Aftertaste **(**CPA)	Initial taste only

1.5.1.2 Dissolution testing

Dissolution testing is an indirect method to assess the taste of medicines. It is based on quantifying drug release in a simulated oral cavity, and hence the amount of drug exposed to taste receptors. A drug concentration above a known bitter threshold would therefore be classified as being aversive. The quantifying is done through an analytical method such as UV-Vis spectrophotometry. It is essential to accurately mimic the oral cavity, controlling the volume, temperature, pH and osmolarity of saliva. A common limitation to pharmacopeial dissolution assays is the use a very high unnatural volumes of saliva media [96].

1.5.2 *In-vivo* Techniques

1.5.2.1 Human Taste Panels

Human taste panels are the most common and reliable methods for taste-assessment. They typically involve participants assessing a drug or medicine on a numerical intensity scale, or a hedonic scale, indicating how aversive a formulation or drug is. This enables the quantitative evaluation of taste. As previously mentioned, smell, mouthfeel and the overall appearance of a formulation can impact the palatability of a medicine. Therefore, human taste panels can be subjectively dependent on the participant, and a certain number of participants would be needed to give the study the appropriate power and therefore statistical significance. Ideally, panellists should be young healthy non-smokers [97]. This method is limited by the fact that it is usually performed in adults for paediatric applications. Also, taste perception changes between healthy and sick individuals. Human taste panels' use is also restricted by a Research Ethics Committee (REC) approval and safety concerns if testing medicines with limited toxicity data [4]. Therefore, human taste panels are usually conducted alongside other taste-assessment methods.

1.5.2.2 Animal Models

The other *in-vivo* testing methods currently in use are animal models. Dogs, cats, rats, mice, or even fish or drosophila can be used [52]. These are very useful in screening

taste in early stage drug development, as trials in humans are only possible once toxicology data is available later on in the development stage.

The rodent Brief-Access Taste Aversion (BATA) model is a useful tool that is currently used to assess the bitter taste of pharmaceuticals. Samples are presented in a random fashion to rodents in sipper tubes alongside a control, usually water. The number of licks recorded by the apparatus, known as a lickometer, is inversely proportional to the aversiveness of the samples presented [52].

1.6 Thesis Aim

The overall aim of this project was to investigate the utility of using electrospinning as a taste-masking technique using a BCS class I model drug for paediatric drug delivery. The work in this thesis aimed to design an optimised taste-masked age-appropriate formulation using various characterisation and taste-assessment methods, most notably the E-tongue. Further details of the research completed are outlined below in Thesis Overview, section 1.7.

1.6.1 Objectives

1. Design a medicine by choosing a bitter model drug and appropriate polymer to electrospin.
2. Preliminary experiments to define the design space using Quality by Design principles.
3. Production of taste-masked fibres with low diameters and no beading defects by utilising a design of experiment (DoE) approach in the optimisation of electrospinning parameters.
4. Using co-axial electrospinning to further enhance taste-masking.
5. Taste-assessment of raw materials and electrospun fibres using the E-tongue.
6. Human panel to assess acceptability of an electrospun fibre mat.
7. Film forming of the final optimal formulation into an orally disintegrating film, using multi-axial electrospinning.

1.7 Thesis Overview

An overview of the remaining sections of this thesis is provided below.

Chapter 2 – Materials and Methods

Reviews the materials and methods used throughout this project, provides instrument information, material sourcing and some experimental details. Specific experimental parameters are located in each experimental chapter.

Chapter 3 – Electrospinning optimisation of Eudragit E PO with and Without Chlorpheniramine Maleate Using a Quality by Design Approach

The first experimental chapter of the thesis which focuses on the optimisation of electrospun Eudragit E PO. In this chapter a Design of Experiment is used to achieve bead-free fibres in the nano-range. Advanced characterisation techniques are used to ascertain various properties of the materials and fibres. The E-tongue is used to assess the taste-masking efficiency of the fibre mats [98].

Chapter 4 – The Use of Co-axially Electrospun Eudragit E PO and Kollicoat Smartseal to Taste-mask Chlorpheniramine Maleate

Co-axial electrospinning of Eudragit E PO and Kollicoat Smartseal 30 D to achieve superior taste-masking of Chlorpheniramine Maleate. Solid state characterisation and thermal analysis techniques used to ascertain various properties of the fibre mats. A newer more sensitive E-tongue sensor is used for taste-assessment and the bitterness threshold of the drug is calculated.

Chapter 5 – Formulation and Assessment of Electrospun Films for use in the Paediatric Population

The formulation comprising of the two taste-masking polymers was further formulated into an elegant pharmaceutical dosage form using other polymers such as PVP and

PVA as an outer layer. This was achieved using tri-axial and tetra-axial electrospinning. Film characterisation techniques, solid state assessment, and thermal analysis techniques were all used to ascertain properties of the films. E-tongue and release studies were employed to ascertain functionality of the films.

To assess the acceptability of a PVA coated electrospun film in humans, a human taste panel assessed the mouthfeel of both solvent cast and electrospun films of drug-free PVA [99].

Chapter 6 – Conclusions and Future Work

Provides a summary of the main conclusions that can be drawn from the research performed during this project and suggests avenues for future work.

Chapter 2

Materials and Methods

2.1 Clinical Application

As previously mentioned, this PhD will focus on developing an innovative formulation for paediatric oral drug delivery. The formulation of choice needs to mask the bitter taste of an aversive API and overcome swallowing issues in the paediatric population. The rationale for drug and polymer choice is discussed below.

2.1.1 Choice of Drug

A model drug as chosen as per the following criteria: it should be commonly prescribed to children and therefore present a current challenge; it should be inexpensive to obtain and safe to handle; and the drug of choice needs to be bitter so that taste-masking can be demonstrated. To identify a list of bitter drugs, the following process was completed:

- Searched on bitterDB database [100];
- All compounds were browsed; 687 entries identified to be bitter in November 2016;
- Results were arranged by number of associated receptors;
- 208 compounds were associated with one or more human bitter receptors. The hypothesis is the more receptors the compound will affect the stronger the bitter response;
- Visual scanning of compounds to see if there are any drugs suitable for use as paediatric medicines. Three drugs were chosen: **chlorpheniramine maleate:** a promiscuous bitter drug that acts on eight bitter receptors; **paracetamol** and **erythromycin,** both of which are selective to one bitter receptor each [101].

It was noted that BitterDB is not a conclusive database and does not include other widely recognised bitter drugs. Other review papers listed drugs such as ranitidine, sildenafil and ibuprofen, to be bitter [47]. A review of the literature to identify research conducted on electrospinning of the aforementioned bitter drugs was completed via ScienceDirect, PubMed, and Web of Science on 22 November 2016. The following search terms were used:

- Paracetamol AND nanofib* - 1 relevant paper found by illangakoon *et al.*[81]
- Chlorpheniramine and Nanofib* - 1 result - ion exchange paper found [102]
- Erythromycin and Nanofib* - no relevant results

Therefore, it was identified that chlorpheniramine maleate and erythromycin were not previously electrospun. Certain formulations such as orodispersible films can only accommodate up to 40 mg of drug [103]. Paracetamol has been studied numerous times and a range of oral formulations are currently available. In addition, the dose range of 500 mg to 1 g is beyond that of an orodispersible film. Erythromycin has a large therapeutic dose, 125 mg to 1000 mg [104], which will limit the use of a film in the future. Chlorpheniramine maleate can be loaded into oral films owing to the low doses, between 1 mg and 4 mg [105], and therefore makes a suitable candidate. In addition, there is a market need due to the low amount of licensed age-appropriate formulations.

Chlorpheniramine has the extra challenge of being a BCS class I drug, being highly soluble at the pH of saliva and therefore exerting a bitter taste. Chlorpheniramine maleate has been chosen to be used in in this taste-masking project.

2.1.2 Choice of Polymer

The polymer of choice for the taste-masked formulation needs to be capable to be electrospun and has a taste-masking functionality. The polymer needs to be accepted in paediatric formulations with the amount used being within the accepted daily limits. In addition, the polymer chosen must complement the lipophilicity of the API chosen, so that the co-solvent system used can sufficiently dissolve both materials. Eudragit E PO and Kollicoat Smartseal both fulfilled these criteria and were used to taste-mask chlorpheniramine maleate.

2.2 Electrospinning Materials

2.2.1 Eudragit E PO

Eudragit E PO, Figure 2.1, is a synthetic cationic copolymer, based on dimethylaminoethyl methacrylate (x), butyl methacrylate (y), and methyl methacrylate

(z) with a ratio of 2:1:1. It has an average molar mass (M_w) of approximately 47,000 g/mol. It has a literature reported glass transition temperature (T_g) of approximately 57 °C [106]. E-EPO was donated by Evonik (Darmstadt, Germany).

E-EPO is insoluble in saliva which has a reported pH of between 5.3 and 7.8 [96] and therefore achieves safe taste-masking. E-EPO consists of a dimethylaminoethyl group that ionises and allows the polymer to dissolve in acidic pH [107] and thus It is freely soluble in gastric juice up to pH 5.0 [108]. The polymer, therefore, is ideal for taste-masking and has been used for that purpose using different fabrication techniques such as hot melt extrusion [61,63] and microencapsulation [109]. It has been electrospun before with and without drug [110,111]. It serves as a taste-masking polymer, and is suitable for use in paediatric formulations [112]. It is a lipophilic polymer that is freely soluble in ethanol and is practically insoluble in water. The allowed dosage of basic methacrylate copolymer, or Eudragit, as a food additive is 16 mg/ kg per day for children aged between 4 and 18 years [113].

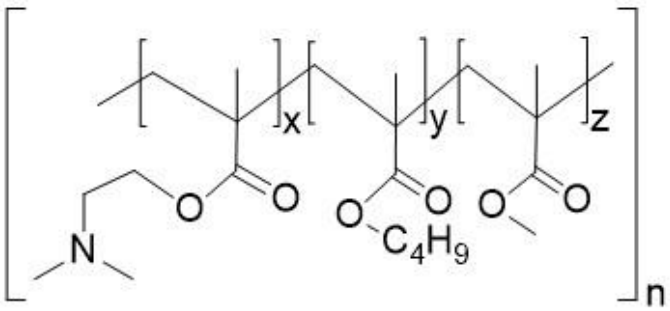

Figure 2.1. Eudragit E PO, drawn using ChemDraw.

2.2.2 Kollicoat Smartseal

Kollicoat Smartseal (KCT) is a methyl methacrylate and diethylaminoethyl methacrylate (7:3) copolymer and was kindly donated by BASF (Ludwigshafen, Germany) [114]. The structure is shown in Figure 2.2.

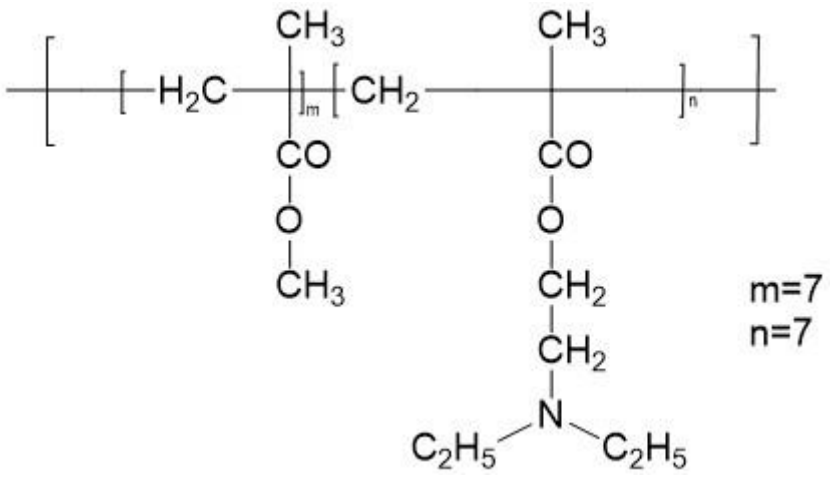

Figure 2.2. Kollicoat Smartseal, drawn using ChemDraw.

KCT is a pH sensitive polymer and insoluble in neutral pH, thereby making it a good candidate as a taste-masking polymer. It is readily soluble at pH <5.

KCT 30D is an aqueous polymer dispersion that is used for film forming and taste-masking purposes, and contains 30 % (w/v) of the polymer [114].

To our knowledge the polymer has not been electrospun before and was chosen because of its taste-masking function; it has been used for that purpose using various fabrication methods such as spray coating and spray drying [115,116]. The polymer's T_g is approximately 63 ^oC.

2.2.3 Chlorpheniramine Maleate

Chlorpheniramine, (3*RS*)-3-(4-Chlorophenyl)-*N*,*N*-dimethyl-3-(pyridin-2-yl)propan-1-amine hydrogen (*Z*)-butenedioate, Figure 2.3, is a bitter tasting first generation antihistaminic drug. It is indicated for symptomatic relief of all allergic conditions responsive to antihistamines, including hay fever, vasomotor rhinitis, urticarial, angioneurotic oedema, food allergy, drug and serum reactions and insect bites. It is also licensed in the UK for the symptomatic relief of itch associated with chickenpox [117]. It is a commonly used medicine in the paediatric population.

The drug is a lipophilic weak base that when added to maleic acid forms the salt chlorpheniramine maleate (CPM), improving its aqueous solubility. CPM is a BCS

class I drug [118] (high solubility, high permeability), that is freely soluble in water and 96 % soluble in ethanol [119]. It has a pKa of 9.13 and theoretical LogP of 3.38 [120]. Its toxicity profile is as follows: Oral LD_{50} (rat): 306 mg/kg; Oral LD_{50} (mice): 130 mg/kg.

Chlorpheniramine maleate is a chiral molecule, with all UK approved commercial formulations being in the racemic mixture. The S-(+)- enantiomer was shown to be approximately 100 times more potent than the R-(-)-enantiomer [121]. It has not been investigated whether both enantiomers exhibit the bitter taste or not.

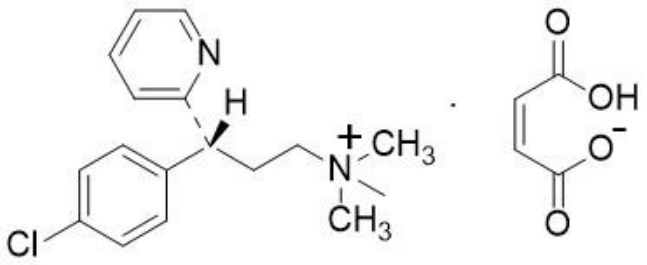

Figure 2.3. Chlorpheniramine maleate, drawn using ChemDraw.

CPM was purchased from Cambridge Bioscience (Cambridge, UK), molecular weight 390.864 g/mol.

2.2.4 Polyvinyl Alcohol

Polyvinyl alcohol (PVA) is a synthetic polymer commonly used a film forming polymer for oral films [99,122,123]. The polymer's structure is shown in Figure 2.4. PVA with a molecular weight of 31-50 kDa (87 – 89 % hydrolysed) was purchased from Sigma-Aldrich (Dorset, UK). This percentage was chosen as it was reported that at this %, electrospun PVA forms the most uniform fibres compared to a higher or lower value [124]. It is reported that the degree of hydrolysis also affects the solubility of PVA, with an improved solubility when it's under 90 % [124]. The polymer is generally highly soluble in water.

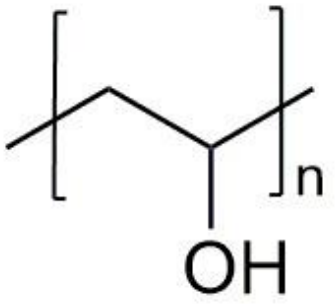

Figure 2.4. Polyvinyl alcohol's chemical structure, drawn using ChemDraw.

PVA has been electrospun a number of times [122,123] and is generally regarded as safe for human oral consumption [125]. It is intended to provide an outer layer to the electrospun taste-masked fibre mat giving it pharmaceutical elegance.

PVA is commonly used for both food and pharmaceutical preparations, due to its non-toxicity, biocompatibility and thermal stability. It has been used for the taste-masking of electrospun sumatriptan and naproxen [126]. The polymer is strongly hydrophilic and is soluble in water.

2.2.5 Polyvinylpyrrolidone

Polyvinylpyrrolidone (PVP) is a water-soluble synthetic polymer that is commonly used in various medical and pharmaceutical applications. PVP is biocompatible, non-toxic, and water soluble, making it a suitable candidate in designing an oral film for the paediatric population [127]. PVP is commonly used in electrospinning especially as a carrier for harder to spin materials [128], therefore it is intended to be used as a candidate for the outer-most layer of the multi-axial system. The chemical structure is shown in Figure 2.5.

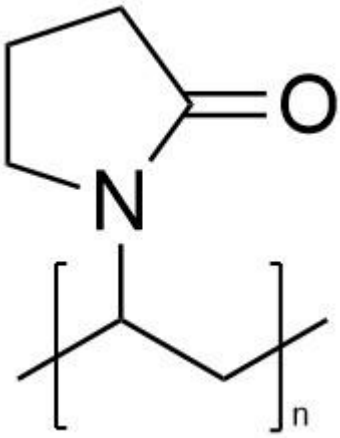

Figure 2.5 Polyvinylpyrrolidone's chemical structure, drawn using ChemDraw.

PVP with an average Mw of 1,300,000 was used and purchased from Sigma-Aldrich (Dorset, UK).

PVP is a good polymer of choice for film formation. It has been electrospun before with cyclodextrins for taste-masking potential, and is suitable for oral use [82]. It dissolves in water and ethanol. It is hydrophilic, with a LogP of 0.4.

2.2.6 Rhodamine B

Rhodamine B, [9-(2-carboxyphenyl)-6-(diethylamino)xanthen-3-ylidene]-diethylazanium;chloride, is a staining fluorescent dye and was used to detect the core of the electrospun co-axial fibre mats. This method has been used before in other co-axial electrospinning research [129]. It has a bright pink colour hence its synonym Brilliant Pink B [130]. The chemical structure is shown in Figure 2.6.

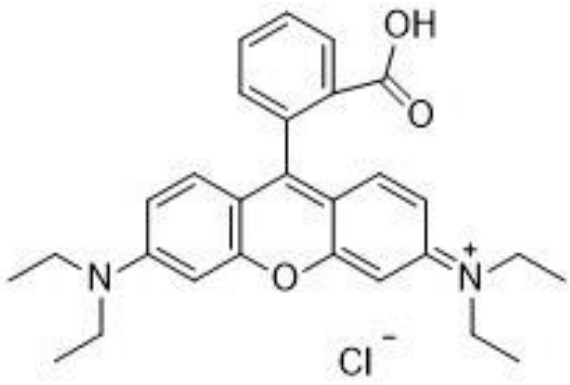

Figure 2.6. Rhodamine B's chemical structure, drawn using ChemDraw.

2.2.7 Solvents

Acetone, ethanol, dimethylsulfoxide (DMSO) and *N,N*-dimethylacetamide (DMAc) were all used. They were all purchased from Sigma-Aldrich (Dorset, UK), and were used as received.

2.3 E-tongue Materials

2.3.1 Quinine HCl dihydrate

Quinine HCl is an anti-malarial alkaloid agent derived from the cinchona bark. It is widely recognised as being bitter and is considered to be the gold standard with regards to bitter drugs, and is accordingly used as a standard for pharmaceutical taste-assessment. In this study, it is used to derive the aversiveness threshold for the bitter drugs used. The drug was purchased from Sigma-Aldrich (Dorset, UK), and its chemical structure is shown in Figure 2.7.

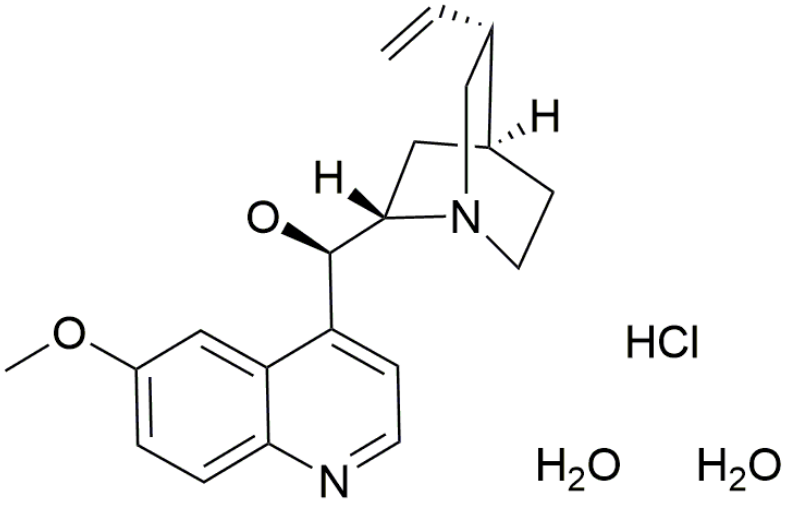

Figure 2.7. Quinine hydrochloride dihydrate's chemical structure, drawn using ChemDraw.

2.3.2 Other Reagents

Tartaric acid, potassium chloride, potassium hydroxide, monosodium glutamate, tannic acid and quinine hydrochloride were obtained from Sigma-Aldrich (Dorset, UK). Iso-alpha acid was obtained from Insent (Atsugi-shi, Japan). Hydrochloric acid was obtained from Fisher Chemicals (Loughborough, UK). All substances were used as received.

2.4 Methods

2.4.1 Electrospinning

A Spraybase® electrospinning instrument (Spraybase, Dublin, Ireland) was used to manufacture the fibres. A detailed explanation of the electrospinning process is included in Section 3.1. In the electrospinning process, the prepared solution was drawn in a 5 mL Terumo syringe (Surrey, UK), attached to a syringe pump. The syringe was connected to a stainless-steel needle, with varying diameters, via a PTFE connector tube. The viscous solution was fed through the needle at varying flow rates, using an automatic syringe pump also provided by Spraybase. Applied voltages up to 30 kV were applied to the polymer solutions, evaporating the solvent, allowing the solid fibres to deposit on a grounded metal plate collector 14.5 cm x 23 cm. The collector was covered in aluminium foil for ease of fibre removal. The gap distance between the

needle and the collector plate was set between 10 cm and 25 cm. Room temperature (ºC) and relative humidity (%) readings were recorded.

Monoaxial and multilayer electrospinning were both performed in this study. Further details are included in Chapters 3, 4 and 5.

2.5 Characterisation Techniques

2.5.1 Viscosity

Rheology is the study of the flow of matter, primarily in the liquid state. As stress is applied to some liquids, including polymer solutions, their viscosity changes; these are known as non-Newtonian fluids. The viscosity of samples was measured using a Bohlin Gemini HR nano dynamic rheometer (Malvern Instruments Ltd., Malvern, UK) at a shear stress of 1 to 30 Pa. Approximately 2 mL of polymer solution was placed on the measurement plate, and a cone geometry size of 4 mm was attached to the rheometer for measurement. Instantaneous viscosity values quoted are those recorded at a shear stress of approximately 5 Pa, for consistency.

2.5.2 pH and Conductivity

The conductivity and pH of samples were measured using SciQuip 902 (SciQuip, Wem, UK) conductivity metre. pH of a solution is measured by measuring hydrogen or hydroxyl ions. For conductivity, two electrodes with a fixed distance are inserted in the solution and the resistance is measured. A low resistivity indicates a material readily allows the flow of electric current, and therefore gives a high conductivity reading. Resistance is the reciprocal of conductivity. Ohm's law describes resistance measurement; Equation 2.1 [131].

Equation 2.1

$$\boldsymbol{V = IR}$$

where ***V*** = known voltage, ***I*** = current, and ***R*** = resistance.

The probes were calibrated using reference solutions as per the manufacturer's instructions.

2.5.3 Light Microscopy

A simple light microscope consists of a light source and a number of lenses that possess differing functions. The light source can be an incandescent bulb, a light-emitting diode (LED) or a laser. The collector lens collects the light from the source, and the condenser lens, as the name suggests, condenses that light and emits it onto the sample. After the light passes through the sample, an objective lens passes the collected rays to a tube lens, which focuses the light into the oculars, re-projecting the light to the retina of the observer or onto a detector such as a camera, allowing the sample to be viewed under high magnification [132]. The position of the objective lens can be varied by the user which in turn determines the magnification level viewed.

Light microscopy was used to examine the morphology of the electrospun fibres. Fibres were collected directly on microscope slides and viewed under various magnifications using the Leica (Lecia Microsystems, Wetzlar, Germany) DM2700 M microscope (25 x magnification). Images were saved directly using a connected camera and saved onto a connected computer. Images were taken using Studio86 Design capture software.

2.5.4 Scanning Electron Microscopy

Electron microscopes have much shorter wavelengths than light microscopes, therefore enabling better resolutions and are particularly useful for viewing materials in the nano-range, as little as 3 nm. Scanning Electron Microscopy (SEM) produces images by scanning electrons on top of samples with a high energy beam of electrons.

The electrons are emitted by an electron gun which consist of a tungsten filament firing the electrons, and an anode that directs the electrons towards the sample. The beam of electrons travels through a condenser lens followed by an objective lens, before it reaches the sample. Samples that are non-metallic need to be coated with a metallic layer to deem them conductive to the electrons. As the electrons interact with the sample, secondary electrons and x-rays are generated and are picked up by a detector

forming a computer viewable image. SEM can only be used to image the surface of the materials, and other techniques need to be used to get a cross-sectional view of materials [133].

SEM analysis was performed by Dr Andrew Weston at the Electron Microscopy Unit at UCL School of Pharmacy. A sample of the fibre collected was adhered onto aluminium SEM stubs (TAAB Laboratories, Aldermaston, UK) using carbon-coated double-sided tape. To make them conductive they were then given a thin coating of gold (~10 nm) in a Quorum Q150T Sputter Coater (Quorum Technologies Ld. East Sussex, UK) in an argon atmosphere. The imaging is performed under a strong vacuum so that gaseous molecules do not interfere with the path of the electron beam and the image produced.

The coated stub was then transferred and imaged with a FEI Quanta 200 FEG (FEI Company, Oregon, USA) SEM at an acceleration voltage of 5 kV.

2.5.5 Transmission Electron Microscopy

Transmission electron microscopy (TEM) is an imaging technique where an electron beam is transmitted under an accelerated voltage through a sample, unlike SEM, where the electrons only scan the surface. A TEM instrument is composed of an electron gun source at the top that fires electrons at the sample, which is followed by an objective lens and finally a viewing screen at the bottom of the TEM. Similar to a light microscope, a TEM consists of a condenser system, but instead of condensing the photons, it controls and condenses the beam of electrons onto the sample [134].

TEM allows the operator to image the finer details of an internal structure of the sample, as well as improved resolution, reaching as low as 0.2 nm. Because of the intricate nature of this technique, samples need to be very thin and porous, so that electrons are allowed to pass through, rather than just scan the surface of the samples. As the electrons pass through the sample, the objective lens forms an image from the scattered beam [135].

In this project, fibres were collected on a copper grid (to allow passage of electrons) during electrospinning. They were then stained with 2 % aqueous uranyl acetate solution prior to imaging with a FEI CM120 BioTwin TEM (FEI Company, Oregon, USA) at an accelerating voltage of 120 kV. The grids are stained in order to either absorb the electrons or scatter part of the electron beam, thereby improving the image contrast. TEM analysis was performed by Dr Andrew Weston at the Electron Microscopy Unit at UCL School of Pharmacy.

2.5.6 Fluorescently Labelled Optical Microscopy

Fluorescence is the emission of light that occurs after excitation of a susceptible sample by a light source. Fluorescence microscopy (FM) has similar working principles to light microscopy, however, the light applied to the sample is of a shorter wavelength in order to excite the fluorochromes. In addition, specific filters and lenses are fitted into the instrument to ensure the light emitted from the fluorochrome is separated and therefore visible to the observer. The light emitted from the sample has a longer wavelength than that of the absorbed excitation light. This difference is known as the Stokes shift. The larger this difference, the easier it is for the light to be separated. Optical filter cubes are fitted in the microscope to separate the excitation light from the emitted light, thereby correctly viewing the fluorochrome [136]. In this study Rhodamine B was used as a fluorochrome to stain the core structure in co-axial fibres. Rhodamine B's excitation wavelength is reported to be 555 nm, therefore a filter with a complementary range was used [137]. The Texas Red filter cube was chosen as it has an excitation wavelength range between 542 nm to 582 nm [138].

Core solutions were dyed with the fluorochrome Rhodamine B, electrospun, and samples collected on a glass microscope slide. Slides were then viewed on an EVOS FL imaging system (Thermo Fisher Scientific, Loughborough, UK) under Texas Red light. Images were saved and visually inspected for the core-shell structure.

2.5.7 Fibre Diameter Analysis

ImageJ 1.46R software (National institute of health, Maryland, USA) was used to measure the diameters of the electrospun fibres. On all occasions either 100 fibres

were measured, and their mean and standard deviation calculated. The range of the fibre distribution was noted. Histograms of the data showing the fibre diameter distribution were then plotted using OriginPro 9.4 (OriginLab, Massachusetts, USA). The histograms aided in identifying any data skewness and also if there were any outliers in the dataset. Fibre diameter distribution is an important parameter in electrospinning, as it can influence the end-function of the fibres if the data were heavily skewed. Drug release, absorption and therefore bioavailability can be affected as well as batch-to-batch variations, which potentially can influence clinical outcomes. Therefore, a uniformly distributed fibre-set is desirable and a positive indicator of a controlled experiment set-up.

2.5.8 Ultraviolet Spectrophotometry

Spectrophotometry is a method based on the absorption of light by a substance. An appropriate solvent with the drug is added to a cuvette and placed in the spectrophotometer. A light is passed through the cuvette, and the amount of light absorbed by the sample is proportionate to the drug concentration. The amount absorbed is measured by subtracting the light transmitted through the cuvette, which is picked up by an end-detector. The length of the cuvette is known as the path length, and usually this is 1 cm. UV spectrophotometry is based on Beer-Lambert's law as described in Equation 2.2.

Equation 2.2

$$\boldsymbol{A = \varepsilon c l}$$

where $\boldsymbol{A}$ is the absorbance, $\boldsymbol{\varepsilon}$ is the molar absorption coefficient, $\boldsymbol{c}$ is the molar concentration, and l is the optical path length, which is usually 1 cm [139].

Materials are measured at their λ_{max}, which the wavelength at which a substance has its strongest photon absorption. The UV-vis range is between 200 nm to 800 nm.

A calibration curve of CPM was constructed at a wavelength of 262 nm using Jenway 6305 UV-vis spectrophotometer (Bibby Scientific, Staffordshire, UK). A quartz cuvette with a wavelength of 1 cm was used. This was then used for determination of drug

loading of the electrospun fibres and also for assessment of drug release in dissolution studies.

2.5.9 Differential Scanning Calorimetry

Differential Scanning Calorimetry (DSC) is a thermal analysis technique that has been used in this project mainly for solid state characterisation and the assessment of amorphous solid dispersion formation upon electrospinning.

The basic principles of DSC comprise of applying heat to a sample and measuring the heat flow, allowing thermal events such as melting, crystallisation and glass transitions to be detected and quantified.

There are two types of DSC, heat-flux and powder compensation. In this study heat-flux DSC was used. A standard heat-flux DSC consists of two thermocouples, one for the sample being measured and another for an empty reference pan. These two pans are exposed to the same heat signals at all times as they are placed adjacently in a furnace, so that the recorded heat flow is a direct difference between the sample and reference. This is represented by the following equation, where the heat flow is proportional to the temperature difference, as described in Equation 2.3.

Equation 2.3

$$\frac{\boldsymbol{dQ}}{\boldsymbol{dt}} = \frac{\boldsymbol{\Delta T}}{\boldsymbol{R}}$$

where ***Q*** is heat, ***t*** is time, ***ΔT*** is the temperature difference between the furnace and pan, and ***R*** is the thermal resistance of the heat path between the furnace and pan [140].

DSC experiments must be carried out in an inert atmosphere which may be achieved by purging the cell with an inert gas, in this case it was nitrogen. A constant flow of purge gas enhances heat flow between the cell and the sample pan while also allowing removal of volatile compounds. Samples were heated under nitrogen gas flow rate of 50 mL/min. To ensure the accurate performance of the instrument, routine calibration processes using high purity indium were carried out.

Modulated temperature DSC (MTDSC) is an extension of conventional DSC in which typically a sinusoidal wave is used when the heating rate is applied. MTDSC improves upon traditional DSC since it measures the total heat flow plus its heat capacity component (reversing) and obtains the kinetic component (non-reversing) from their difference. The separation procedure is represented by Equation 2.4.

Equation 2.4

$$\frac{dQ}{dt} = Cp\frac{dT}{dt} + f(t,T)$$

where Cp represents heat capacity, T is absolute temperature, t is time and $f(t,T)$ is a function of time and temperature which governs the response associated with the physical or chemical transformation [141].

The heating rate used for MTDSC is much slower than that used for conventional DSC ranging from (1 to 5) °C/min, compared to (10 to 20) °C/min for the latter. This low underlying heating rate is combined with large modulation amplitudes, typically in the range of ± (0.1 to 1) °C. The modulation period is generally 30 s to 80 s long. In order to enable complete separation it is necessary to have at least six modulation cycles throughout the duration of each thermal event [142].

MTDSC thermograms of pure drug and polymer were recorded using TA instruments Q2000 calorimeter (TA Instruments, New Castle, Delaware, USA). Heating rate was set at 2 °C/min, amplitude was set at ± 0.212 °C for a period of 40 s. Samples' weights ranged from 4 mg to 8 mg and were sealed in a 40 µL aluminium Perkin Elmer standard pan. A pinhole was manually formed in the lids to allow for solvent evaporation. Samples were analysed in triplicate unless stated otherwise. Data analysis was carried out with TA Universal Analysis software, Version 4.5A.

2.5.10 Powder X-ray Diffraction

Powder X-ray diffraction is a non-destructive characterisation technique that is used to determine the solid state of materials, providing information on crystalline and amorphous structures. The process occurs in an X-ray diffractometer, where the X-

rays are generated by heating a filament, acting as a cathode. The electrons are then attracted to an anode, which is composed of a transition material such copper or silver. As the X-rays move between both electrodes, they pass through the sample and interact with the electron clouds of the molecules in the material, which causes the X-rays to scatter. The resultant interference caused by the X-ray scattering is recorded by a detector. This process is governed by Braggs law, as described in Equation 2.5 [143].

Equation 2.5

$$n\lambda = 2d\ sin\theta$$

where n is the order of the diffracted beam, λ is the wavelength of the incident X-ray beam, d is the distance between adjacent planes of atoms and θ is the angle of incidence of the X-ray beam. By altering θ during scanning, the distance between adjacent planes of atoms, or d-spacing, can be varied. By plotting beam intensity against angle of emergence a diffractogram with peaks corresponding to lattice spacing is obtained which gives an insight into the molecular arrangement and orientation of atoms within a sample.

Materials which are crystalline produce diffractograms with sharp peaks, which correspond to ordered lattice arrangements of the molecules assessed. On the other hand, materials which do not have long-range order appear as broad signals with no defined peaks, known as amorphous halos.

For PXRD analysis, the sample should consist of a fine powder. Providing the particle size is sufficiently small and no preferred orientation effects are occurring, the particles in the sample should cover the whole range of possible orientations. This results in an average diffraction effect being measured for the bulk powder, meaning diffraction rings are produced from crystalline samples rather than the individual spots generated by single crystals [144].

In this study, solid-state characterisation of raw materials and samples was completed using a Rigaku MiniFlex 600 X-Ray Diffractometer (Rigaku, Tokyo, Japan); CuKα radiation, operating power: 40 mV, 15 mA. RAW files produced were converted to

XRD data files using PowDLL Version 2.51 file converter software. The data were then viewed on X'Pert Data Viewer version 1.2F.

2.5.11 Thermogravimetric Analysis

Thermogravimetric analysis (TGA) is a thermal analysis technique in which a sample is heated in a closed furnace and weight change is monitored as a function of changing temperature. Typically, this technique is used to measure solvent loss, indicating residual solvent, or lack of. It is also used to measure degradation temperature which informs maximum heating temperatures in DSC and other thermal techniques.

In a TGA experiment, the sample is placed in a pan which is placed on a sample holder, which is suspended and attached to an internal balance by a metal wire. This internal balance holds a reference pan on the other side, also connected using a fine metal wire. The heating furnace covers the test sample holder, allowing temperature to be controlled whilst weight is simultaneously measured. Both the sample chamber and the balance are purged with nitrogen gas to establish a stable environment and remove any volatiles from the furnace [141].

In this project TGA was used to determine if there was any residual solvent left after electrospinning, an important consideration to check considering the fibre mats are intended for us a paediatric formulation. TGA was also used to determine the maximum heating temperature to be used in DSC, to avoid running samples beyond the degradation point.

Thermal analysis of pure drug and polymer were carried out using a TA Instruments Hi-Res 2950 thermogravimetric analyser (TA Instruments, New Castle, Delaware, USA), operating with a nitrogen gas flow rate of 60 mL/min through the furnace and 40 mL/min through the TGA head. Samples were tared and analysed in an open aluminium Perkin Elmer pans. Data analysis was carried out with TA Universal Analysis software, Version 4.5A.

2.5.12 Attenuated Total Reflection - Fourier Transform Infrared Spectroscopy

Fourier transform infrared spectroscopy (FTIR) is a spectroscopic technique that works by passing polychromatic infrared radiation (in the mid-IR region of 4000 to 400 cm^{-1}) through a sample and detecting the amount of radiation that is transmitted or absorbed at each wavenumber. Photons of light are absorbed by bonds in the sample when the frequency of the radiation is equal to the energy required for a particular bond to vibrate. This gives rise to useful information regarding the chemical bonds and hence functional groups present, which allows identification of the structure or indeed if any impurities are present. FTIR also allows investigation of interactions within multi-component systems due to wavenumber shifts of bonds involved in intermolecular interactions. This feature was used in this project to confirm the drug was molecularly dispersed in the amorphous polymer following electrospinning.

Some FTIR models are attached to an attenuated total reflection (ATR) crystal, which is made of a high refractive index material such as thallium bromide, thallium iodide or zinc selenide. The main advantage of the use of ATR is to avoid the need for sample preparation. The samples are placed on the opposite side of these transparent crystalline materials. The radiation is set to an angle at which the internal reflections occur between the sample and the crystal interface before it travels to the detector [145].

FTIR studies were performed using a Spectrum 100 FTIR spectrometer (Perkin-Elmer, Massachusetts, USA) and spectra were collected in the range of 4000 cm^{-1} to 650 cm^{-1} with a total of 16 scans and a resolution of 2 cm^{-1}, unless otherwise stated. Background scans were performed in all experiments and each sample was analysed in duplicate to check the reproducibility of the spectra.

2.5.13 Atomic Force Microscopy

Atomic force microscopy (AFM) provides topographical images of surfaces and can also be used to provide nanomechanical information. An AFM consists of a cantilever which scans across a solid sample mounted onto a stage. The cantilever tip's location

is noted by a laser detector. As it scans across the sample, the height and width of the atomic structure is detected by the probe. These movements are recorded and a three-dimensional map of the sample's surface is recorded and translated into an image [146]. A technique known as amplitude modulation-frequency modulation (AM-FM) was employed to provide maps of Young's modulus of electrospun fibres. AM-FM is an extension of conventional tapping made, where the cantilever is operated at two simultaneous resonances. The first resonance, AM, is used for the traditional tapping-mode imaging. The second higher frequency resonance in FM is responsible for providing information on the elasticity of the sample. The output resonance frequency from both signals describes tip-sample interaction; a higher frequency recording indicates a stiffer material [147].

The Cypher ES (Oxford Instruments, Abingdon, UK) low noise high resolution system was used. The cantilever oscillated at two frequencies: one used for tapping-mode imaging, the other used for mechanical measurements. Tracking changes in frequency and amplitude of the 2nd frequency can provide information on viscoelastic properties. The outputs recorded were images of topography, Young's modulus and dissipation. Measurements were performed at Oxford Instruments by Dr Jonathan Moffat.

2.5.14 Film thickness and Folding Endurance

3 cm x 2 cm films were cut. Their thickness were measured using a stainless steel digital calliper D03196 (DuraTool, Taichung, Taiwan) [103]. The calliper had a resolution of 0.01 mm and repeatability of 0.1 mm. Three measurements were taken and an average was calculated.

Folding endurance is defined as the number of times a film can be folded without breaking or visibly cracking. Folding endurance was determined by repeatedly folding the films in the same place. After 30 folds the experiment was stopped and films were determined to be flexible. For each formulation, three samples were examined. This method has been used repeatedly by other researchers [122,148,149].

2.5.15 *In-vitro* Dissolution Studies

Dissolution studies are used to assess the release behaviours of drugs in various media. Drug molecules must be in solution to be absorbed in the gastrointestinal tract and therefore exert a pharmaceutical effect. Dissolution testing is therefore an important tool for characterising the performance of pharmaceutical systems.

Dissolution consists of two major steps, the first being the breaking down of the solute molecules and for new solute-solvent bonds to be form. The second step is for these solute molecules to diffuse away from the saturated solid boundary. These processes are affected by a number of factors, described in the Noyes-Whitney equation [150]; Equation 2.6.

Equation 2.6

$$\frac{\boldsymbol{dm}}{\boldsymbol{dt}} = \boldsymbol{A} \,.\left(\frac{\boldsymbol{D}}{\boldsymbol{h}}\right) .(\boldsymbol{Cs} - \boldsymbol{C})$$

where $\frac{dm}{dt}$ is the solute dissolution rate, ***m*** is the mass of solute dissolved, *t* is time, *A* is the surface area of the solute, ***D*** is the diffusion co-efficient (related to solvent viscosity), ***h*** is the thickness of the diffusion layer at the surface of the dissolving material, $\boldsymbol{C_s}$ is the saturated solubility of the solute in the solvent and *C* is the solute concentration in the bulk media.

In this project, pH sensitive polymers were used to taste-mask a bitter drug. To ensure gastrointestinal release is not affected, and therefore bioavailability, release in gastric media was assessed. The calibration curve for the drug was obtained in pH 1.2 gastric media prepared by the addition of 0.1 M HCl to phosphate buffer saline (PBS) solution. The PBS solution was prepared by adding 1 tablet of PBS per 100 mL of distilled water. PBS tablets were purchased from VWR Chemicals (Avantor, Pennsylvania, USA). A standard curve was plotted using absorbance data from a Jenway 6305 UV−vis spectrophotometer (Bibby Scientific, Staffordshire, UK). Absorbance was recorded at 262 nm (λ_{max}). Drug released was calculated by using the slope = 0.0171 and intercept = 0.04801 of the standard curve (R^2 = 0.9999).

The amount of drug released from the films was determined by placing a known amount of the fibres (approximately 10 mg) into a glass container. A metal mesh cover was then added onto the film and 15 mL of the release media was added. The volume of the dissolution medium was at least 3 to 10 times the saturation volume of the predicted drug amount, thereby creating sink conditions. At pre-specified time intervals 1 mL of the solution was removed and 1 mL of fresh media was added. This experiment took place in an Incu-Shake Mini shaking incubator (SciQuip, Shropshire, UK) at 37 ^{o}C and shaking speed of 50 RPM. This modified method, adapted from Tawfik *et al.* (2020) [151] was used as no pharmacopeial dissolution test exists for electrospun fibre mats.

2.6 *In-vitro* Taste-assessment

2.6.1 E-tongue

The TS-5000Z (Insent Inc., Atsugi-shi, Japan) was equipped with lipid membrane sensors and corresponding reference electrodes (New Food Innovation Ltd, UK). Positively charged membrane sensors included C00, responding to acidic bitterness, and AE1, responding to astringency. Negatively charged membrane sensors included AC0 and AN0, both responding to basic bitterness at different sensitivity and selectivity levels. The newer BT0 sensor, also negative, was used for basic bitterness measurement.

2.6.1.1 Sensors

Sensor and reference electrodes were purchased from New Food Innovation Ltd (Nottingham, UK). The sensors compose of lipids, plasticiser and polyvinyl chloride (PVC). Positively charged lipid membranes are composed of quaternary ammonium salts, while negatively charged lipid membranes are composed of ester phosphates. The sensors are summarised in Table 2.1.

Table 2.1 Lipid membrane sensor names and corresponding tastes measured.

Type	Sensor name	Corresponding taste
Positively charged membrane	C00	Acidic Bitterness
	AE1	Astringency
Negatively charged membrane	AC0	Basic Bitterness
	AN0	Basic Bitterness
	BT0	Basic bitterness

2.6.1.2 Standard Solutions

All standard solutions were stored in the refrigerator upon preparation. The expiration date was one month.

2.6.1.3 Alcohol Solutions

2.6.1.3.1 Negatively Charged Washing Solution

150 mL ethanol was added to 250 mL deionised water and mixed thoroughly. 50 mL 1 M hydrochloric acid solution was added and the solution was made up to 500 mL using deionised water. 1 M HCl solution was prepared by measuring 4.74 mL of 32 % (v/v) concentrated HCl and making it up to 50 mL of deionised water.

2.6.1.3.2 Positively Charged Washing Solution

3.73 g potassium chloride was added to 250 mL deionised water and stirred thoroughly. 150 mL ethanol and 5 mL 1 M potassium hydroxide solution were added and thoroughly mixed before making up to 500 mL with deionised water. 1 M KOH solution was prepared by dissolving 561 mg of KOH in 10 mL of deionised water.

2.6.1.4 Preconditioning solutions

2.6.1.4.1 Internal Solution

248.2 g potassium chloride was added in about 900 mL deionised water and mixed thoroughly before being made up to 1 L with deionised water. The solution was then transferred again to a different container; 10 mg silver chloride were dissolved and the solution was stirred for at least 8 hours.

2.6.1.4.2 3.33M Potassium Chloride Solution

248.2 g potassium chloride was dissolved in about 900 mL deionised water and mixed thoroughly before being made up to 1 L with deionised water.

2.6.1.4.3 Standard Reference Solution

0.045 g tartaric acid and 2.25 g potassium chloride were dissolved in about 900 mL of deionised water. The solution was stirred thoroughly before being made up to 1 L with deionised water.

2.6.1.5 Maintenance Solutions

2.6.1.5.1 Salty Reference Solution

0.045 g tartaric acid and 22.37 g potassium chloride were dissolved in about 900 mL deionised water a mixed thoroughly before being made up to 1 L with deionised water.

2.6.1.5.2 Umami Reference Solution

0.045 g tartaric acid and 2.25 g potassium chloride were dissolved in about 900 mL deionised water. 1.87 g of monosodium glutamate was then added a mixed thoroughly before making up to 1 L with deionised water.

2.6.1.5.3 Astringent Reference Solution

0.045 g tartaric acid and 2.25 g potassium chloride were dissolved in about 900mL deionised water. 0.50 g tannic acid was added and mixed thoroughly before making up to 1 L with deionised water.

2.6.1.5.4 Bitter (-) Reference Solution

0.045 g tartaric acid and 2.25 g potassium chloride were dissolved in about 900 mL deionised water. 100 µL iso-alpha acid was added and mixed thoroughly before being made up to 1 L with deionised water.

2.6.1.5.5 Bitter (+) Reference Solution

0.045 g tartaric acid and 2.25 g potassium chloride were dissolved in about 900 mL deionised water. 0.04 g quinine hydrochloride was added and mixed thoroughly before being made up to 1 L with deionised water.

2.6.1.5.6 Sour Reference Solution

0.45 g tartaric acid and 2.25 g potassium chloride were dissolved in about 900 mL deionised water and mixed thoroughly before being made up to 1 L with deionised water.

2.6.1.6 Procedure

Each lipid sensor was filled with 0.2 mL inner solution and was soaked in standard solution for 24 hours before measurement to precondition. The reference sensors were completely filled with inner solution and were soaked in 3.33 M potassium chloride solution for 24 hours before measurement to precondition. BT0 sensors need to be preconditioned for at least 48 hours. During preconditioning all sensors were placed in a beaker separately that was covered with Parafilm. The TS-500Z (Insent Inc., Atsugi-shi Japan) E-tongue was used for all the experiments. Calibration of instrument as per manual was consequently performed. The sour, salty, umami, astringent, bitter (+) and (-) standard solutions were used for the maintenance measurements. Calibration was also periodically completed every month.

A sensor check was conducted routinely before each measurement. Each measurement cycle consisted of the following elements:

1- Measurement of reference potential (V_r) in reference solution for 30 s
2- Measurement of electric potential (V_s) in sample (initial taste) for 30 s (Equation 2.7)
3- Lightly washing of sensors in reference solution for 2 s x 3 s

4- Measurement of electric potential (V_r^1) in reference solution again (aftertaste) for 30 s. This aftertaste is also called CPA value – Change of membrane Potential caused by Adsorption (Equation 2.8).
5- Refreshing of sensors in alcohol solution to give them a complete wash before the measurement of the next sample, for 330 s.

Equation 2.7

$$V_s - V_r = initial\ taste$$

Equation 2.8

$$V_r^1 - V_r = aftertaste$$

All measurements were repeated four times. The data from the first run were discarded (as recommended by Insent) to allow for the conditioning of sensors. In this study, a solution of 10 mM KCL was used as a control sample and the corresponding sensor responses were subtracted from the sensor responses of the samples. Hence, all data produced are a mean of three measurements and represent relative sensor responses. If more than ± 5 mV is recorded by the sensors, this implies that the drug displays this taste quality to some degree.

2.6.1.7 Maintenance Measurement

A maintenance measurement was carried out once a month or after measuring 100 samples as recommended by the manufacturer. Sensors are exposed to standard solutions which represent salty, sour, bitter and astringent taste attributes. Each sensor is expected to respond only to the taste attribute for which it is designed. If any sensor response to a standard solution for which it is not designed, then it is considered defective and must be replaced. Therefore, this measurement tests for sensor accuracy. BT0 does not need to have a maintenance measurement as it is for one use only.

2.6.1.8 Sensor Check

Prior to commencement of each experiment a sensor check was carried out. This involves washing the sensors in alcohol washing solutions for 2 s x 120 s before

washing for 90 s in reference solution. Following the washing of sensors, they are immersed in reference solutions and the voltage readings of each sensor is recorded. The voltage readings must be within a certain range (Table 2.2) and the procedure is repeated up to twenty times until the sensor gives the required reading on three consecutive occasions with a reading of ± 0.5 mV. This therefore measures for sensor precision. If the required voltage reading is not achieved after twenty attempts then the sensor is marked as defective.

Table 2.2. Sensor response maintenance ranges for the various sensors.

Sensor	C00	AE1	AC0	AN0	BT0
Response to reference solution (mV)	+80 to +160		-80 to -30		-110 to -90

2.6.1.9 Measurement

For all the measurements, the samples were stirred in 10 mM KCL, as a supporting electrolyte. All solutions were made up to 100 mL in a volumetric flask. Fibres were mixed at 37 °C for 1 minute in 100 mL 10 mM KCl. The taste extracted liquid was then removed through a 0.22 µm filter (Merck- Millipore, Cork, Ireland).

2.6.1.10 Data Analysis

Multivariate Principal Component Analysis (PCA) was completed on the data collected. This aided in the visualisation of the high number of data points on a two dimensional map. The dataset is projected onto a space relative to their distance from the two main principal components, which represent the axes of the map and correspond to the variance in the data. Differences between samples were assessed by determining the Euclidean distances which were calculated from the Cluster Centre. All data analysis was carried out using OriginPro 9.4 (Origin Lab, Massachusetts, USA).

2.6.2 Biorelevant Dissolution Model

A biorelevant dissolution method (Figure 2.8) that mimics the oral cavity volume was used to assess the amount of drug released and hence the bitter taste associated with it. An acrylic model was connected to a peristaltic pump Perista-Pump A2110 (Atto Corporation, Tokyo, Japan) at a rate of 1 mL / min at which stimulated saliva fluid (SSF) was pumped through. The SSF composition was taken from Guhmann *et al.* (2012) [152]. Three samples of 100 mg to 120 mg of fibres were finely ground with a mortar and pestle. The column was manually loaded with the fibres. The fibres were retained in the column by wire mesh discs placed either side. Samples were taken at 60, 80, 100, 120, 180, 240 and 300 s and 100 µL aliquots were added to 900 µL SSF and assayed using UV at a wavelength of 262 nm and using a 1 cm quartz cuvette. UV calibration curve of equation was, ***y = 12.787x + 0.019*** and R^2 = 0. 993.The values measured in 100 µL aliquots were used to calculate the amount of drug in mg/mL; these data were analysed and plotted using OriginPro 9.4 (Origin Lab, Massachusetts, USA).

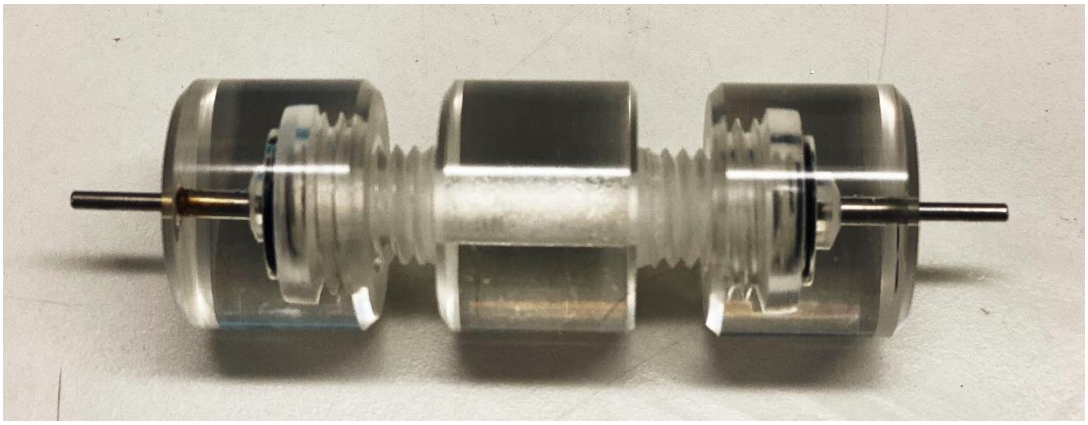

Figure 2.8. A picture of the biorelevant dissolution model mimicking the oral cavity, loaded with ground fibre.

2.7 *In-vivo* Assessment

2.7.1 Human Panel

Human panels are the gold standard for taste and mouthfeel assessment in humans. The human panel conducted in this thesis aimed to assess the mouthfeel of

electrospun oral films compared to more traditional manufacturing method, namely solvent casting.

Solvent-casting is a well-established technology that was driven by the needs of the photographic industry. In the drug-delivery arena, it has become the most traditional method for manufacturing oral films. The method entails dissolving polymers, APIs and other excipients in an appropriate solvent and then drying off the mixture. The mixture is usually dried by passing it through a drying apparatus such as an oven. The resultants dried film is then cut into strips of pre-determined sizes and individually sealed in specialised packaging. It is imperative for the solution to set without entrapped air bubbles to ensure a homogenous film is formed [153].

The participants were asked to swallow two GMP manufactured polyvinyl alcohol films, one prepared by either manufacturing method. These were manufactured by Bioincia (Valencia, Spain). A break of five minutes between the samples was observed to allow their palates to clear. A full description of this study is given in Chapter 5.

Chapter 3

Electrospinning Optimisation of Eudragit E PO with and Without Chlorpheniramine Maleate Using a Quality by Design Approach

3.1 Introduction

Electrospinning is based on the ultra-fast removal of solvents from a fluid mixture to form solid micro- and nanofibres [154]. The method utilises a high voltage electric field to form a continuous jet of liquid that subsequently dries and deposits on a collector plate as fibrous material. The applications of this technology include filtration, production of protective clothing, tissue engineering and more recently drug delivery [155]. In the therapeutics arena, electrospun fibres are promising candidates for drug delivery owing to their high surface area to volume ratio for release, their structural flexibility and their ability to encapsulate high drug loadings in polymeric matrices, the polymers allowing a range of performance functions in the body [81]. One such recent application of electrospinning is as an approach to taste-masking for bitter drugs [79,81,82,87,126]. Poor palatability of medicines is one of the main compliance barriers within the paediatric population, making most liquids unsuitable, and yet large coated solid dosage forms cannot be swallowed by children. By using taste-masking polymers, bitter drugs can be encapsulated in a form that can be both palatable and easy to swallow. Electrospun fibres can then be formulated into age-appropriate dosage forms such as oral films or mini-tablets [79,81,156]. While systems such as microspheres have been extensively studied, the use of nanofibres is a relatively new approach and little is known with regard to production optimisation, particularly concerning the effects of drug addition on fibre characteristics and the associated taste-masking performance.

To develop electrospinning within the pharmaceutical field, it is necessary to thoroughly explore the spinning properties of polymers relevant to therapeutic use while also being mindful of the need for therapeutic, as well as production, performance. Relatively recently, the understanding of scalability of electrospinning has increased very considerably, thus opening up the potential for viable oral delivery which require high volume manufacture [157].

In this study, the production of E-EPO is explored, both alone and incorporating chlorpheniramine maleate (CPM), an antihistamine used by children for conditions such as urticaria, hay fever and relief of itching associated with chicken pox but which is also known to have a bitter taste [158]. E-EPO is a pH sensitive polymer that masks

the bitter taste of CPM by physically encapsulating the drug and only releasing it at pH < 5 [159]. This means CPM would not be released in mouth saliva, which has a pH of approximately 7.4 [160]. In particular, the production of loaded and unloaded fibres is studied in detail, so as to provide a guide for others intending to use this polymer in nanofibre formulations and also to provide insights into the potential effects of drug addition on spinning parameter optimisation. In addition, the taste of the fibres using a biosensor approach is investigated so as to allow early screening and product optimisation to facilitate the design of the final dosage form.

Electrospinning production is influenced by a number of parameters that can be generally classified as solution, process and environmental factors which have been widely studied for small scale production [161]. Desired characteristics of a fibre can range from morphological to pharmaceutical activity considerations, while the range of manufacturing parameters, and the possibility of their interaction on influence, render a single parameter approach inappropriate and necessitate multifactorial methodologies in order to identify key production characteristics.

For pharmaceuticals, a systematic understanding of parameter influence is extremely helpful. Although there are several studies that have involved factorial or Design of Experiment (DoE) approaches [77,162–170] for electrospinning there is a particular need for pharmaceuticals for information pertinent to Quality by Design (QbD) approaches; these allow for the quality of an end-product to be built in by design, rather than reaching these attributes empirically. This is in line with the recommendations given by the ICH Q8 pharmaceutical development guidelines [171].

The DoE in this study was used to screen for the most influential factors in producing smooth E-EPO nanofibres. Smooth fibres were defined as fibres with no bead-on-strings and those that have the most uniform fibre diameter distribution. The factors chosen to be controlled represent the critical material attributes (CMAs) and were polymer concentration and solvent mixture. The critical process parameters (CPP) explored were flow rate, applied voltage and gap distance. The output criteria of smooth fibres represent the critical quality attributes (CQA) of the fibres formed. Figure 3.1 shows a summary of the DoE design space. Once E-EPO fibres were electrospun

with and without drug, taste-masking assessment of CPM-loaded fibres was performed.

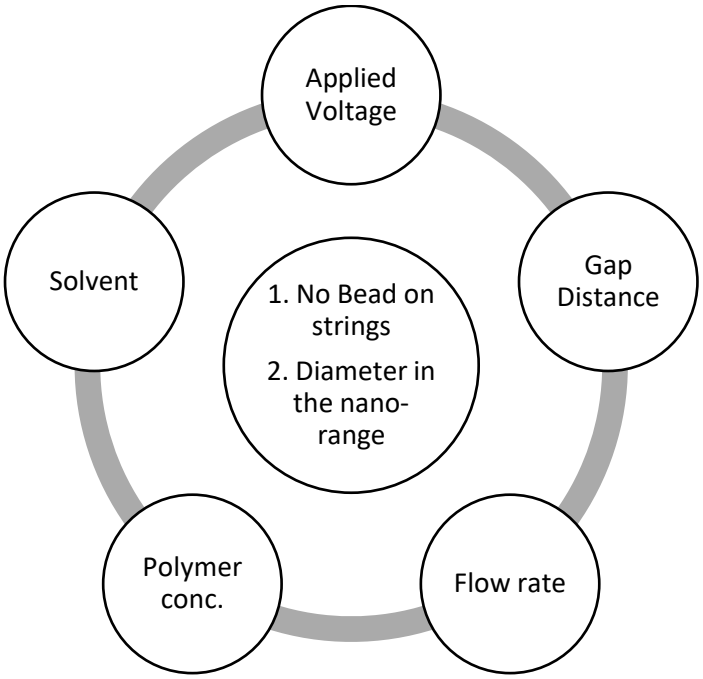

Figure 3.1 Design of Experiment design space, with Critical Quality Attributes (CQA) in the inner circle and Critical Process Parameters (CPP) /Critical Material Attributes (CMA) in the peripheral circles.

Using the E-tongue, taste-masking efficiency of electrospun CPM fibres were assessed compared to placebo fibres and physical mixtures. To our knowledge, this is the first study to use an E-tongue for taste-assessment of electrospun nanofibres. In this manner it is intended that the study may provide a blueprint for the design and characterisation of taste-masked electrospun fibres, the approach being designed with a view to both pharmaceutical production requirements and therapeutic acceptability [98].

3.1.1 Quality by Design

A trial and error approach is an inefficient way to manufacture high quality pharmaceutical products; quality should instead be built in by design. Electrospinning is affected by a number of material and process parameters and therefore it would be beneficial to use a QbD approach to manufacturing. QbD principles can be broadly classified into the following objectives [172]:

1. The product to have performance-based quality specifications and to deliver its intended outcomes.
2. To achieve optimum manufacturing conditions, by improving process capability and reducing product variability.
3. Having a systematic approach and therefore enhancing the ability to identify the root cause of any failure. This in turn increases product development and manufacturing efficiencies.

3.1.2 Elements of QbD

The FDA encourages the adoption of QbD principles in drug product development and manufacturing. Pharmaceutical QbD consists of the following elements [172]:

- Quality target product profile (QTPP) – Defining the efficacy and quality characteristics of the drug product by considering the route of administration, dosage form, dissolution and stability.
- Critical Quality Attributes (CQAs) – These are the output characteristics of the finished product that will impact its overall quality and should be within appropriate limits.
- Critical Material Attributes (CMAs) – Characteristics of input parameters that are essential for desired quality and therefore should be within an appropriate range.
- Critical Process Parameters (CPPs) – A process parameter whose variability has an impact on a CQA and therefore should be controlled to ensure the desired quality.
- Risk Assessment – Defines and ranks parameters that can potentially impact the product, which can be studied through a design of experiment (DoE) approach.
- Design of Experiment (DoE) – DoE allows for the most significant parameters to be identified, that can then be further studied, through another DoE or other mathematical models, leading to a higher level of process understanding.
- Design Space – Once DoE data is collected, statistical analysis can be used to determine whether certain parameters are critical or not. All this information is then to be used to create a design space which will include acceptable

ranges of both CMAs and CPPs. This is represented in Figure 3.2.The figure depicts that the CQAs of the output materials are a result of the fine-tuning of the combined effect of pre-optimized CPPs and CMAs.

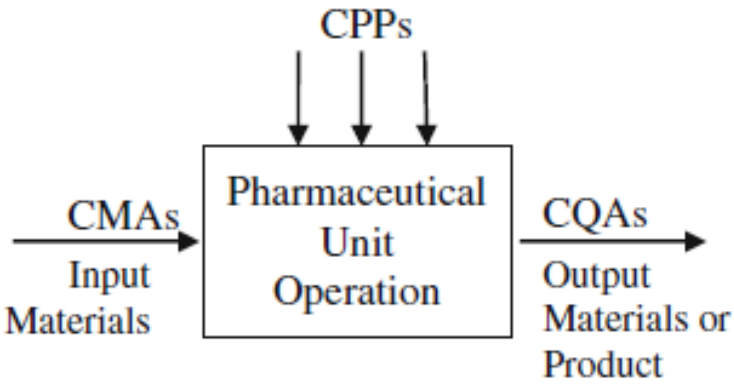

Figure 3.2 Shows the relationship between input CMAs and CPPs and output CQAs. Adapted from [172].

3.1.3 QbD Plan

A QbD approach was used as a guide to plan for an age-appropriate formulation. Table 3.1 shows the different elements considered when planning the dosage form design in this research project. The overall aim of this chapter was to manufacture a taste-masked fibre mat that has acceptable physical considerations.

Table 3.1. Using a QbD approach to plan for the formulation manufacturing.

QTTP	CQA	CMA	CPP
Palatable oral dosage form	Taste-assessment data of finished product to be different from pure API as tested by the E-tongue	Polymer Concentration Drug Concentration	Choice of E-tongue sensor Accuracy and precision of sensors
Dissolution profile	Fibre diameters to be minimised. Dissolution studies to be consistent with current formulation	Type of polymer used	Temperature Humidity Applied Voltage
Reproducible manufacturing	Morphology of fibres to be smooth and reproducible	Co-solvent mixture	Gap Distance Flow rate Collector type
Easy to swallow	Film thickness, stickiness and overall handling to be acceptable	Solvent type Addition of other excipients	Spinneret diameter Needle clogging Ease of removal of fibre mat

3.1.4 Aims and Objectives

The overarching aim of this chapter was to optimise the electrospinning of E-EPO with and without drug using QbD principles, in particular DoE. Objectives included identifying optimised parameters via structure and performance characterisation, which included thermal analysis, imaging, and taste-assessment using the E-tongue.

3.2 **Methods**

3.2.1 Electrospinning

Solutions of E-EPO were prepared in either absolute ethanol or ethanol in addition to 10 – 20 % (v/v) distilled water. E-EPO solutions were prepared by dissolving 15 to 50 % (w/v) E-EPO in absolute ethanol, or ethanol in combination with water. The mixture was then magnetically stirred at a temperature of 40 ºC for 2 to 3 hours. Drug-loaded E-EPO solutions were prepared by adding CPM directly to the polymer solution in ratios of 1:2 to 1:10 drug to polymer. The mixture was magnetically stirred at a temperature of 40 °C for 2 to 3 hours. Spraybase® electrospinning instrument (Spraybase, Dublin, Ireland) was used to manufacture the fibres.

The chain entanglement concentration of E-EPO was determined [173] by plotting the concentration of E-EPO against the corresponding viscosity.

Initially, a trial and error approach was taken to electrospin E-EPO, whilst varying the process and solution parameters one factor at a time (OFAT). The initial conditions used were adapted from Balogh et al [110]. This approach proved very time consuming and also did not highlight multi-factorial interactions.

These were the solution and process parameters used initially:

- E-EPO concentration: 25 % (w/v)
- Solvent used: Ethanol
- Applied Voltage: 25 kV
- Flow Rate: 5 mL/h
- Gap Distance: 20 cm

The spinneret used had an internal diameter of 0.9 mm. Connector tube F (1 mm diameter) was purchased from Spraybase® and used to connect the syringe to the spinneret. The fibres were collected on a metal grounded plate (14.5 cm x 23 cm) covered with aluminium foil.

The following were investigated:

- Effect of using different flow rates
- Effect of using different gap distance
- Effect of using water as a co-solvent
- Effect of voltage
- Effect of spinneret diameter
- Effect of adding CPM

3.2.2 Viscosity

Viscosity measurements of E-EPO at increasing concentrations were taken to determine the chain entanglement concentration as described in Chapter 2, Section 2.5.1.

3.2.3 Conductivity and pH

The technique was used as described in Chapter 2, Section 2.5.2.

3.2.4 Design of Experiment

A DoE approach was utilised to optimise the electrospinning of E-EPO on its own, using a definitive screening design. JMP Pro 12.0.1 (SAS institute) was used for design and data analysis. A DoE approach uses a reduced number of runs to identify the most influential parameters in producing a particular outcome. A DoE also takes account of parameter interaction using analysis of variance (ANOVA) [168]. Definitive screening designs help to detect the main effects of input parameters on a particular outcome in the most efficient way possible. Classical or factorial designs generally study the parameters at two levels, a high and a low, detecting only linear relationships. A definitive screening design can detect non-linear relationships as three levels are tested, an additional medium level. In addition, this allows for detection of effects caused by parameter interactions [174]. Smooth unbeaded fibres, with uniform diameters in the nano-range, were desired. A stable Taylor cone, with reduced needle clogging and a peelabe fibre mat were used as secondary success criteria. Five factors were investigated at three levels of each, as shown in Table 3.2. The experiments were performed over two different days, or blocks. The sequence in which

these runs were carried out was randomised. The temperature ranged between 23.5 °C to 24 °C and the relative humidity (RH) ranged between 27 % to 28 %. The data were fitted to a standard least squares model, yielding linear regression and ANOVA results.

Table 3.2. A table displaying the factors screened by the DoE and the three corresponding levels for each. Solvent used is ethanol.

Factor	Low	Medium	High
Applied voltage (kV)	10	17.5	25
Flow rate (mL/h)	0.5	1.25	2
Gap distance (cm)	15	20	25
E-EPO concentration (% w/v)	25	35	45
Water in solvent (% v/v)	0	10	20

3.2.5 Addition of Drug

The drug was added and electrospinning of E-EPO before and after addition of CPM was compared. CPM was added to the physical mixture in a range of amounts as a ratio to E-EPO as follows: 1:2, 1:3, 1:4, 1:5, 1:6, 1:7, 1:8, 1:9 and 1:10 CPM: E-EPO.

3.2.6 Light Microscopy

Fibres were collected directly on microscope slides during electrospinning and then viewed under the light microscope Leica DM2700 M (Leica Microsystems, Wetzlar, Germany). Background information on the light microscope can be found in Chapter 2, Section 2.5.3.

3.2.7 Scanning Electron Microscopy

The samples were analysed by SEM as described in Chapter 2, Section 2.5.4. Fibre size analysis was performed by measuring the diameter of 100 fibres using ImageJ 1.46R software (National institute of health, Maryland, USA).

3.2.8 Thermogravimetric Analysis

The technique was used as described in Chapter 2, Section 2.5.11; samples were tared and analysed in an open aluminium Perkin Elmer pans with a heating rate of 10 °C/min from 30 °C to 500 °C.

3.2.9 Differential Scanning Calorimetry

Method as described in Chapter 2, Section 2.5.9. Samples were heated under nitrogen gas (flow rate 50 mL/min) at a rate of 2 °C/min ramped up to 150 °C, amplitude ± 0.212 °C and a period of 40 s. Samples' weights ranged from 4 mg to 8 mg and were sealed in a 40 µL aluminium Perkin Elmer standard pan.

3.2.10 Powder X-Ray Diffraction

Characterisation of the solid-state of CPM and E-EPO before and after electrospinning was completed using a Rigaku MiniFlex 600 X-Ray Diffractometer (Rigaku, Tokyo, Japan) as described in Chapter 2, Section 2.5.10. Patterns were recorded over the 2θ range 3º to 40º at a scan rate of 3 º/min, with an interval of 0.02 º.

3.2.11 Fourier Transform Infra-Red Spectroscopy

The background to the method is described in Chapter 2, Section 2.5.12. FTIR studies were performed using a Spectrum 100 FTIR spectrometer (Perkin-Elmer, USA) and spectra were collected in the range of 4000 cm^{-1} to 650 cm^{-1} with a total of 16 scans and a resolution of 2 cm^{-1}, unless otherwise stated. Background scans were performed in all experiments and each sample was analysed in duplicate to check the reproducibility of the spectra.

3.2.12 Determination of Drug Loading

λ_{max} of CPM was determined by scanning CPM at a concentration range of (5 to 50) µg/mL between (200 to 300) nm, with steps of 5 nm, using a UV-vis spectrophotometer (SpectraMax, Molecular Devices, San Jose, CA, USA). Data were collected using SoftMax Pro software. Standard solutions of CPM with the concentration range of (5

to 50) µg/mL were prepared in ethanol. A standard curve (R^2 = 0.9988) of CPM was plotted using absorbance data recorded using a Jenway 6305 UV-vis spectrophotometer (Bibby Scientific, Staffordshire, UK). Absorbance was recorded at 205 nm (λ_{max}). Drug loading was calculated by using the slope = 0.07525 and intercept = 0.03447 of the standard curve. All measurements were taken in triplicate.

Film samples weighing approximately 10 mg were dissolved in 10 mL of ethanol. This was repeated three times. Each sample was tested three times using UV spectroscopy. Therefore, nine samples were tested for each formulation to ensure the reading is both accurate and precise. For each sample, the exact theoretical drug-load was calculated. Using the calibration curve, actual drug amount was calculated.

3.2.13 Atomic Force Microscopy

The technique was used as described in Chapter 2, Section 2.5.13. The samples were prepared by pressing onto double sided tape. It was decided that smaller areas of interrogation were desirable to try and minimise the effect of surface topography.

To ensure consistency, a diamond coated probe was used as any changes to the tip will adversely affect the Young's modulus values. To check consistency, a reference sample of polystyrene was imaged before and after measurements to ensure that the tip had not changed during measurements. For each sample, a 20 µm x 20 µm scan was acquired and then at least three flat locations were selected on fibres for 1 x 1 µm scans.

3.2.14 E-tongue Taste-assessment

The TS-5000Z (Insent Inc., Atsugi-shi, Japan) was equipped with four lipid membrane sensors and two corresponding reference electrodes (New Food Innovation Ltd, UK). Positively charged membrane sensors included C00, responding to acidic bitterness, and AE1, responding to astringency. Negatively charged membrane sensors included AC0 and AN0, both responding to basic bitterness at different sensitivity and selectivity levels. The full measurement description is described in Chapter 2, Section 2.6.1.6.

3.2.14.1 Sample Preparation of the Fibres

Taste extracted liquids were used for biosensor assessment of the electrospun fibre mats and materials that are solid in the media's pH, such as KCT and E-EPO. Measurement of fibres were calculated as the corresponding mass of fibre that will contain 20 paediatric doses of CPM (20 mg) in a 100 mL, which equates to 0.5 mM. For example. For a 1:6 (14.30 % w/w) drug to polymer ratio fibre, the amount measured was 140 mg. The fibres were added to 100 mL of 10 mM potassium chloride solution, as a supporting electrolyte, at 37 ºC and gently stirred for 1 min. The mixture was then filtered through 0.22 µm filters (Merck-Millipore, Cork, Ireland), removing any suspended particles.

3.2.14.2 Data Analysis

All measurements were repeated four times. The data from the first run were discarded to allow for the conditioning of sensors. In this study, a solution of 10 mM potassium chloride was used as a control sample and the corresponding sensor responses were subtracted from the sensor responses of the samples. Hence, all data produced are a mean of three measurements and represent relative sensor responses. Multivariate PCA was performed on the data collected. PCA was used to compress the data from the four sensors into a two-dimensional space whilst preserving taste information. PCA allows the data responsible for the highest variance to be displayed as Principal Component 1 and Principal component 2 [175]. This aided visualisation of the high number of data points on a two-dimensional map. Differences between samples were assessed by determining the Euclidean distances which were calculated from the cluster centre [63]. Euclidean distances were calculated according to the following, Equation 3.1:

Equation 3.1

$$d(p,q) = \sqrt{\sum_{i=1}^{n}(p_i - q_i)^2}$$

Where d is the distance, p and q are two samples and n is all the variables included in the multivariate analysis [176].

Data compilation and analysis were carried out using OriginPro 9.4 (Origin Lab, Massachusetts, USA). Statistical significance tests were completed using a one sample t-test using GraphPad Prism 7.04 (GraphPad inc., San Diego, CA, USA).

3.2.15 Biorelevant Dissolution Taste-assessment

A column of 1 mL volume capacity was used to assess the taste of a drug-loaded fibre, as described by Keeley et. al.[115]. The column was connected to a peristaltic pump which set to a flow rate of 1 mL/ min, mimicking natural saliva flow in the human mouth. The column was filled with a sample of fibre which corresponds to 35 % (w/v) E-EPO + 3.5 % (w/v) CPM (theoretical drug loading is 9.1 % (w/w) relative to polymer).

Stimulated saliva fluid (SSF) was used as the dissolution media, prepared as described by by Guhmann *et al.* (2012) [160]; Table 3.3.

Table 3.3. A table displaying the components of the SSF prepared.

Compound	Concentration
Potassium dihydrogen phosphate	12 mM
Sodium chloride	40 mM
Calcium chloride	1.5 mM
Sodium hydroxide	To pH 7.4
Deionised water	To 1 L

Sample size tested was 115.93 mg ± 11.08 mg, therefore theoretical drug load was 10.45 mg ± 1 mg.

At specified time intervals 100 µL aliquots were collected. 900 µL of SSF was added to the samples collected to make them into 1 mL samples. Samples were analysed using UV spectroscopy at wavelength of 262 nm. Equation of calibration curve: $y = 12.787x + 0.019$, $R^2 = 0.993$.

3.2.16 *In-vitro* Dissolution Study

A Sciquip mini shaker (SciQuip, Wem, UK) was used to investigate the release of CPM in stomach conditions of pH 1.2. 0.1 N HCl was used as the dissolution media. 1 mL aliquots were removed and replaced with fresh media at the following time intervals: (1, 5, 10, 15, 20, 30, 45, 60, 90 and 120) minutes. Removal and replacement of fluid was taken from the same position on all occasions. Sink conditions were achieved by ensuring the volume of solvent used was 10 times or more the solubility of the drug. CPM has a solubility of 10 mg/mL to 50 mg/mL [120] therefore a media volume of 15 mL was used. Samples were placed in glass vials and the mesh cover dropped over them at the beginning of the time. Drug amount released was measured using UV spectrophotometry at wavelength of 262 nm. Fibre samples measured 10.56 mg ± 0.2 mg and had a theoretical drug load of 9.1 % (w/w). Equation of calibration curve in release media: $y = 0.0197x + 0.021$, $R^2 = 0.993$. A 1 mL quartz cuvette was used and all experiments were performed in triplicate. Data were collated and analysed using OriginPro 9.4 (Origin Lab, Massachusetts, USA).

3.3 Results and Discussion

3.3.1 One Factor At a Time Electrospinning

3.3.1.1 Effect of Polymer Concentration

Concentrations of E-EPO ranging from 20 % (w/v) to 50 % (w/v) were electrospun and their viscosity measured, to determine a chain entanglement concentration as described by Kong *et al.* (2014) [173]. This is defined as the intercept between the two fitted lines representing untangled and entangled regions, as shown Figure 3.3. The entanglement concentration is the boundary between the semi-dilute unentangled region and the semi-dilute entangled region. The former defines the conditions where the polymer chains overlap one another but not enough to cause entanglement, whereas the latter describes the polymer chains' significant overlap and constraint into a formed structure [177]. Electrospun fibres therefore only form beyond the chain entanglement concentration, and a continuous polymer fibre formation is also

dependent on crossing this threshold. The chain entanglement concentration of E-EPO was determined to be approximately 32.5 % (w/v) in ethanol.

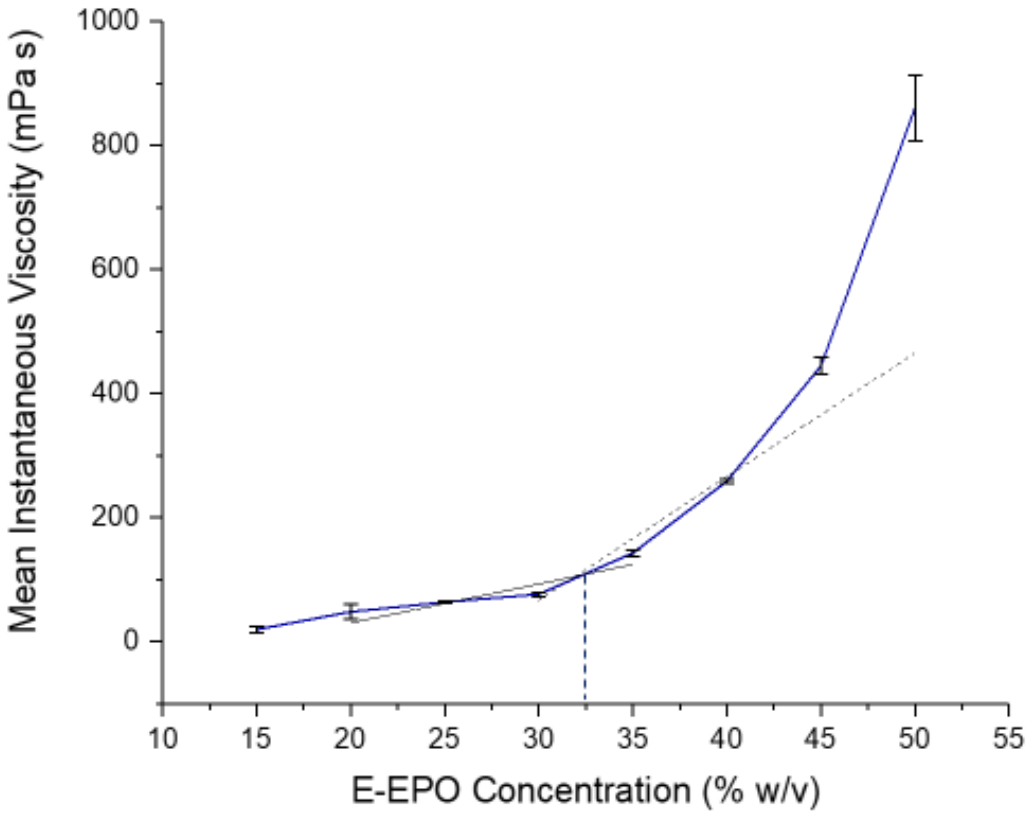

Figure 3.3. Instantaneous viscosity, at a shear stress of 5 Pa, versus concentration of E-EPO.

To support the viscosity measurements, SEM visual representations of the electrospun fibres are shown in Figure 3.4 and Figure 3.5. They show that as the polymer concentration increases, a transition between spraying and electrospinning occurs.

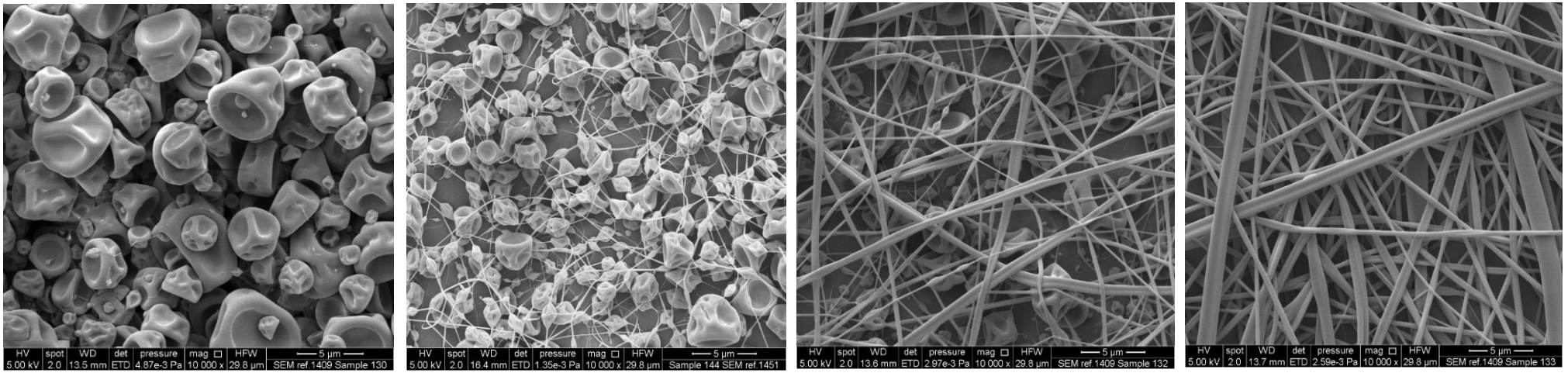

Figure 3.4. SEM images of electrospun E-EPO fibres- 15 %, 20 %, 25 %, 30 % (w/v). All fibres were processed at applied voltages of 10-20 kV, flow rate of 1 mL/h, and gap distance of 20 cm. Temperature: 26 ºC, and RH: 32 %.

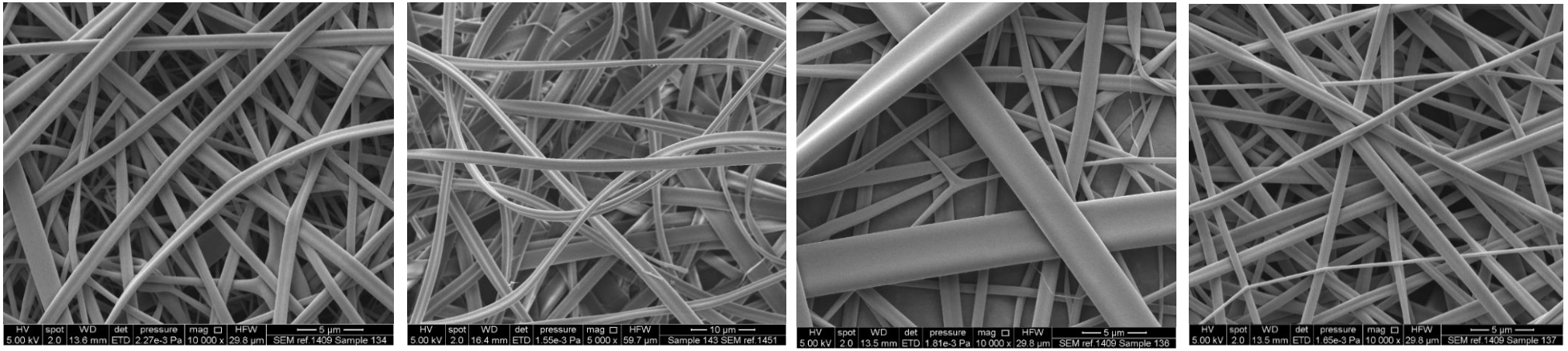

Figure 3.5. SEM images of electrospun E-EPO fibres- 35 %, 40 %, 45 % and 50 % (w/v). All fibres were processed at applied voltages of 10-20 kV, flow rate of 1 mL/h, and gap distance of 20 cm. Temperature: 26 ºC, and RH: 32 %.

In Figure 3.4, the first image shows 15 % (w/v) E-EPO solution forming beads or particle-like structure, akin to electrospraying. This is because the solution viscosity is insufficient to enable the formation of fibres. The next image at 20 % (w/v), thin fibres start to form between the beads forming a spindle-like structure. As the polymer concentration is increased so is the viscosity and therefore the polymer chain's entanglement with one-another. At 25 % (w/v), electrospinning starts to take place and fibres are formed albeit with some beading. This forms the beginning of the chain entanglement, however, does not represent the optimum polymer concentration to form bead-free fibres. It was noted in the literature that to spin bead-free fibres, the polymer concentration should be 1.2 to 2.7 times the chain entanglement concentration [177,178]. This is to allow sufficient entanglement beyond the semi-dilute entangled region. The SEM images support the chain entanglement concentration findings, and it can be seen that at concentrations of 30 % (w/v) E-EPO and above, smooth fibres were formed. Figure 3.5 shows the fibres electrospun at a polymer concentration of 35 %, 40%, 45% and 50 % (w/v). At 35 and 40 % (w/v), smooth bead-free fibres are formed. Even though the fibres are sufficiently entangled at 45 % and 50 % (w/v) forming smooth fibres, the high viscosity becomes problematic causing needle clogging and affecting the running of the experimental procedure.

Fibre diameter was also measured. It can be seen from Figure 3.6 that as polymer concentration increases, average fibre diameter also increases, which can be attributed to the fact that more polymer is dispensed through the needle as well as higher entanglement causing larger fibres. In addition, with an increased polymer concentration, fibre diameter increases due to an increase in viscosity [179]. This correlation has been recorded by Song *et al* (2008) [180], showing that electrospun gelatin fibres increase in diameter as the polymer concentration is increased. Using a linear fit analysis, the regression between the two parameters was calculated to be R^2 = 0.99. It is to be noted no data is plotted for 15 % (w/v) E-EPO as no fibre formation occurred and therefore diameter could not be measured. The error bars represent the diameter range of the fibres. It can be seen that at lower concentrations where electrospraying is occurring the diameter distribution is narrow due to minimal jet fluctuations. As the concentration reaches entanglement, and the viscosity rises, the fibre diameter distribution range widens greatly. This is likely due to fluctuations in the Taylor cone caused by charge density changes due to voltage optimisation during the process [181].

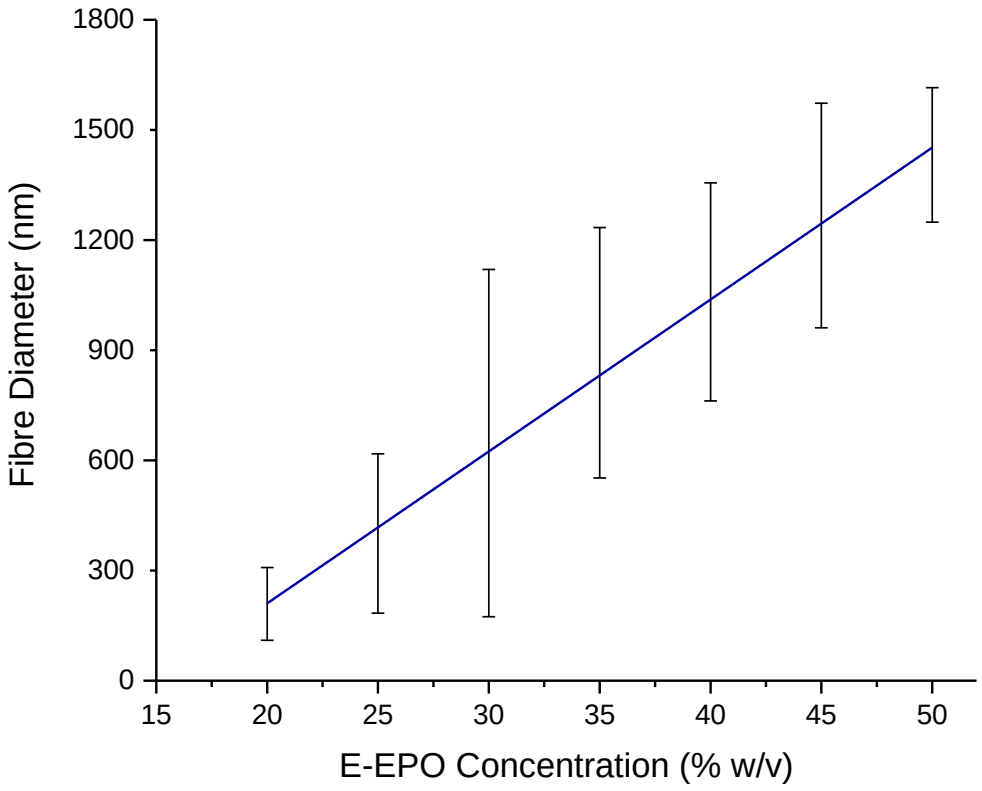

Figure 3.6. Linear fit showing mean fibre diameter versus concentration of E-EPO.

3.3.1.2 Effect of Voltage

The effect of increasing voltage on fibre morphology was investigated. 35 % (w/v) E-EPO was processed at a gap distance of 15 cm and a flow rate of 2 mL/h. As the applied voltage increased, fibres went from wavy structures with bead-on-strings, to smooth straight uniform fibres at a point of optimal voltage. This is consistent with findings by Deitzel *et al.* (2001) [182], where they report that optimising the applied voltage is highly correlated with bead-free fibres. An optimum applied voltage is one of the most important electrospinning parameters. When applied voltage was increased beyond the optimal value, waviness was observed again, with fibres forming loops, followed by spindle formation. The applied voltage is required to overcome the surface tension of the dripping solution and the axisymmetric instability [71]. This electric charge promotes the elongation of the fibre jet towards to grounded collector, rendering the electrospinning process possible. Optical images of the fibres are shown in Figure 3.7.

It can be seen that spindle formation occurs between 14 kV and 16 kV which is likely due to insufficient electric charge to fully overcome the surface tension, giving rise to axisymmetric instability, where some beading still occurs in between the formation of stable fibres [71,74]. Once that instability is overcome, stable smooth fibres are observed between 18 kV and 24 kV. Beyond that optimum point, as the applied voltage is increased further, the polymer jet starts to spin at a higher speed resulting in the electrospun fibres arriving at the collector not fully dry and defective [182], as seen in the fibres spun at 26 kV, viewed under optical microscopy.

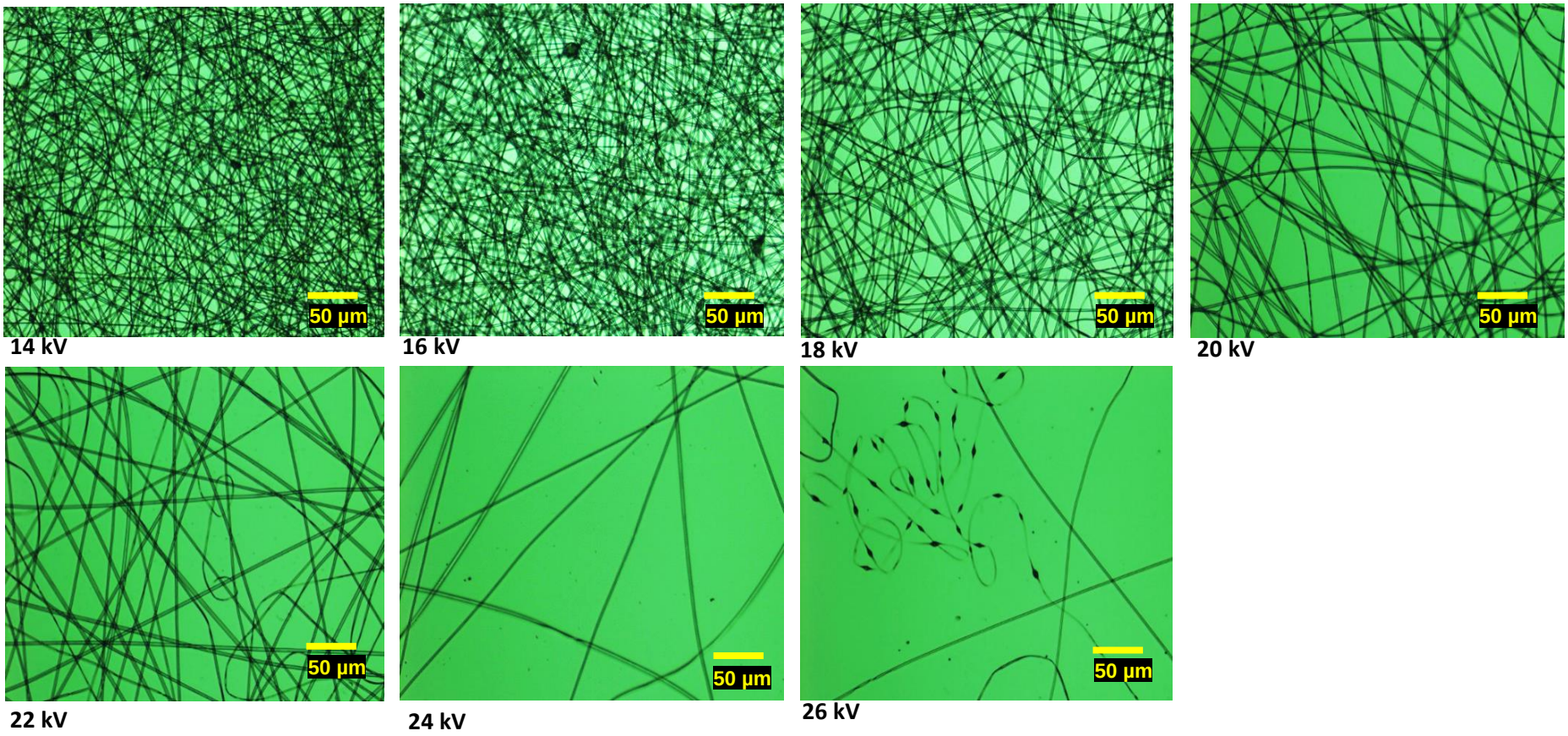

Figure 3.7. Optical microscopy images of 35 % (w/v) E-EPO processed at 15 cm and 2 mL/h. Images show different morphologies of fibres as the applied voltage increases from 14 kV to 26 kV.

3.3.1.3 Effect of Water Addition

Formulation 1 conditions were derived from literature [110]. Fibres were formed but with beads; it was thought here to increase the viscosity by adding water in the solvent mixture, as E-EPO is insoluble in water, therefore acting as an non-solvent [183]. This was performed in order to attempt to reach a viscosity similar to that of the chain entanglement concentration. The flow rate was also reduced. The results are shown in Table 3.4 The addition of water increased the conductivity of the solutions and reduced beading up to a point. Beyond that optimum point, beading reinitiated because water was not evaporating by the time the fibres deposited on the collector. It appears, however, that the water addition did not cause a noticeable difference in the morphology of the fibres, as shown in Figure 3.8. In addition, the fibre diameters were all in the nano-range and water addition did not cause a reduction in the mean fibre diameter, therefore offered no apparent advantage. Temperatures ranged between 23 °C and 25 °C whilst relative humidity ranged between 30 % and 33 %. All the formulations were electrospun at a gap distance of 15 cm and applied voltage of 20 kV to 25 kV.

Table 3.4. Electrospinning conditions for the first six formulations adapted from conditions found in the literature. All contained 25% (w/v) E-EPO.

F	Water (% v/v)	Flow Rate (mL/h)	Conductivity (µS/cm)	Mean Diameter ± SD (nm)
1	0	5	3.24 ± 0.39	794 ± 357
2	10	1	6.38 ± 0.33	397 ± 152
3	15	1	8.41 ± 2.42	349 ± 103
4	20	1	9.57 ± 0.45	872 ± 284
5	22.5	1	14.31 ± 4.59	559 ± 194
6	25	1	14.35 ± 1.76	817 ± 216

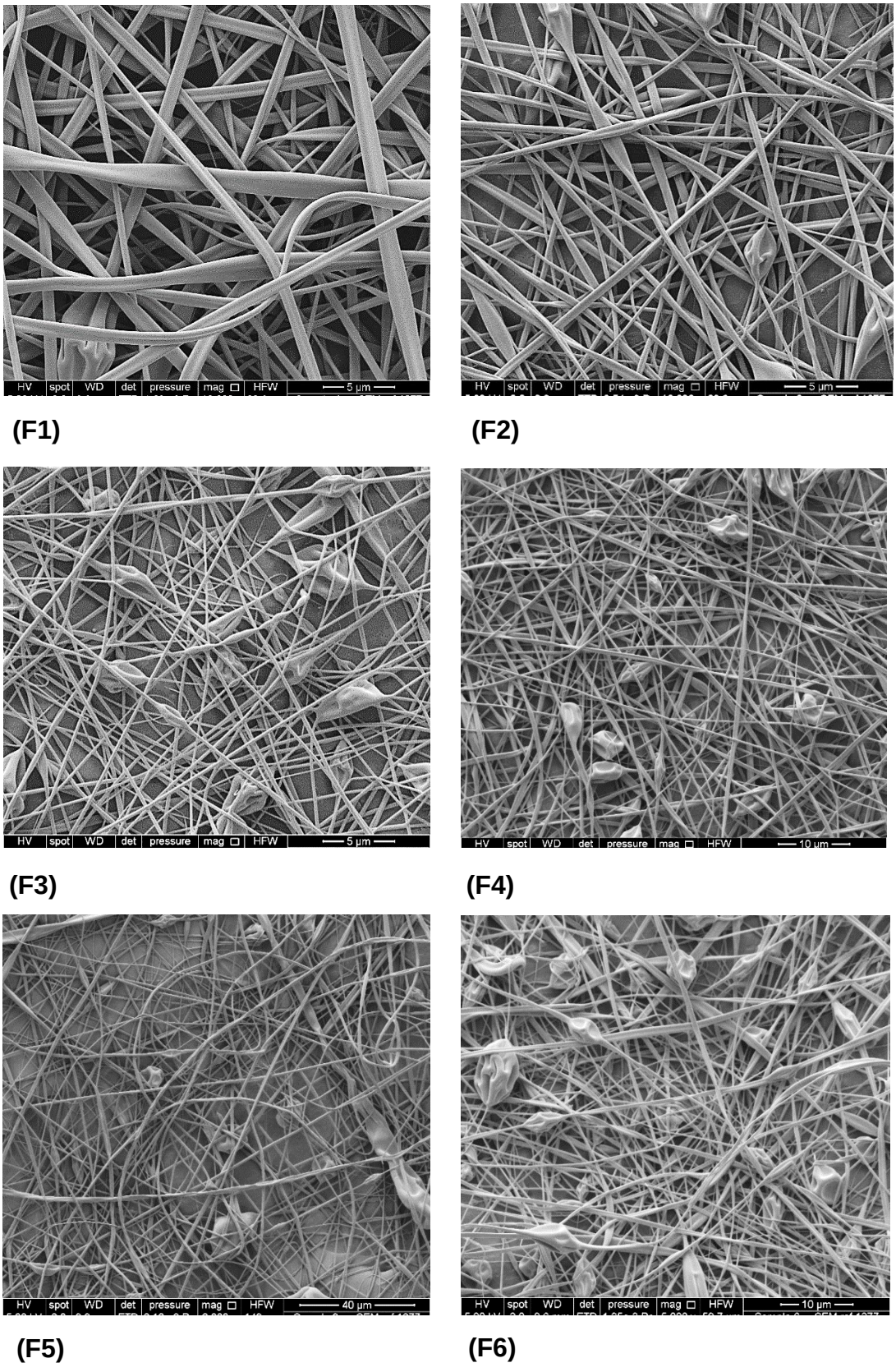

Figure 3.8. SEM images of formulations 1 to 6 showing general fibre morphology as a function of changing water content in the solvent mixture.

3.3.1.4 Effect of Spinneret Diameter

To investigate whether the spinneret diameter had an effect on E-EPO fibre diameter, Formulation 1 which had the smoothest morphology, was electrospun using different spinneret sizes as shown in Table 3.5. The solution was electrospun at 1 mL/h. There was no linear relationship found between the increase of spinneret diameter and mean fibre diameter. SEM images of the different fibres are shown in Figure 3.9. It can be seen that all the fibres had smooth-bead free morphology. A narrow needle can be used to produce fibres with lower diameters, depending on the polymer, it can also be helpful in reducing beading, however it is more prone to becoming clogged [68]. In this case, fibres with a larger diameter were observed when using a smaller needle; this can be explained by a higher pressure being required to form a Taylor cone which in turn resulted in thicker fibres [184]. Generally, spinneret diameter would need to be increased as the viscosity increases, as otherwise the flow of the solution through the orifice will become more challenging. Since E-EPO fibre diameter was not significantly influenced by spinneret size, a spinneret with an internal diameter of 0.9 mm was used thereafter, as needle clogging was reduced with this size. In addition, the relative standard deviation (RSD) was calculated to be 26 % which represented the 2nd lowest variation in fibre diameter after the 0.55 mm spinneret, which was deemed unsuitable due to clogging.

Table 3.5. Mean diameter, SD and RSD of E-EPO fibres when electrospun at different spinneret diameters.

Spinneret diameter (mm)/ gauge	Mean Fibre diameter ± SD (nm)	RSD (%)
0.45 (26 G)	892 ± 375	42
0.55 (24 G)	775 ± 141	18
0.7 (22 G)	903 ± 308	34
0.9 (20 G)	817 ± 216	26
1.2 (18 G)	750 ± 471	63
1.6 (16 G)	628 ± 379	60

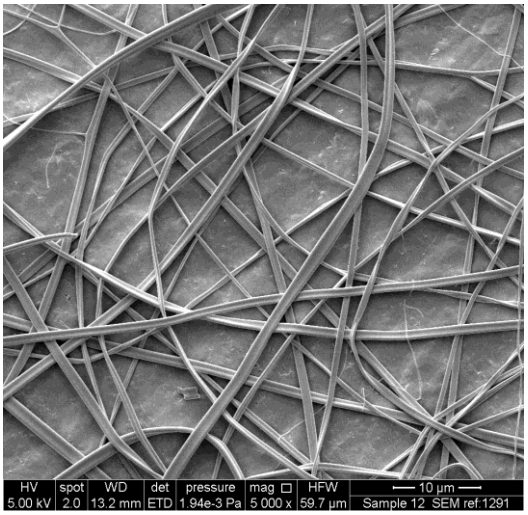

(26 G)

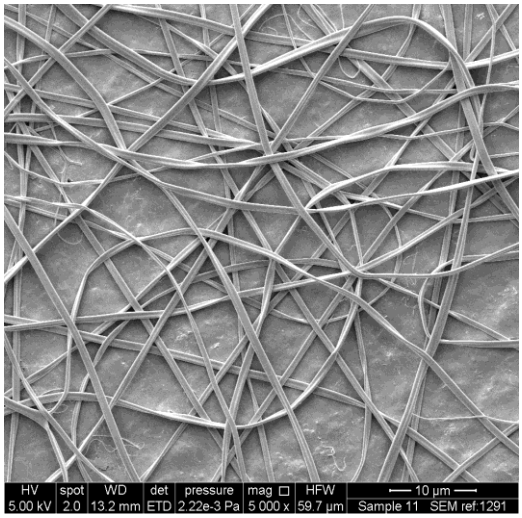

(24 G)

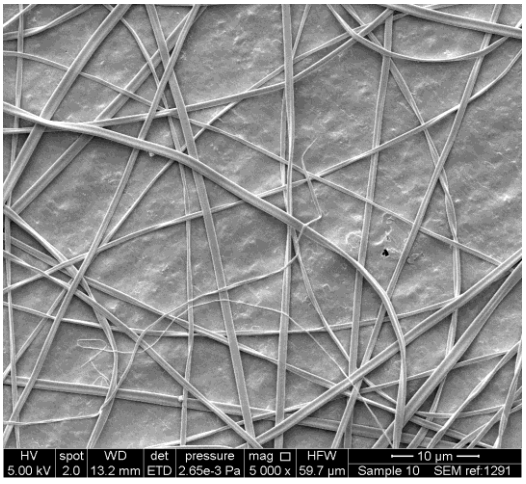

(22 G)

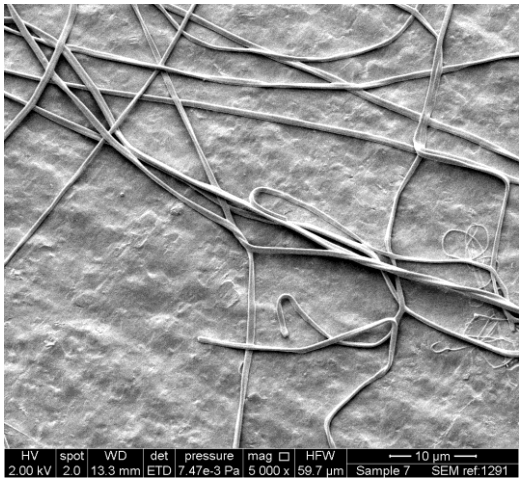

(20 G)

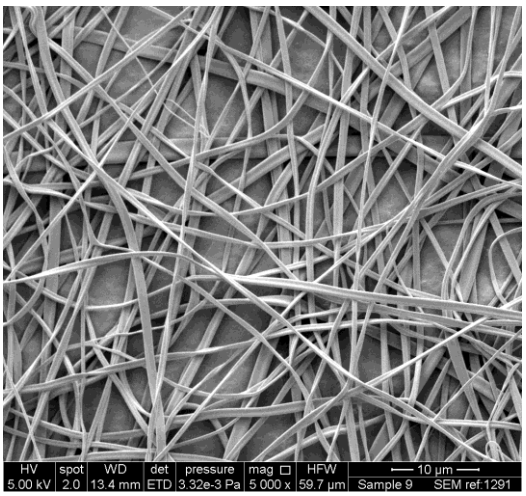

(18 G)

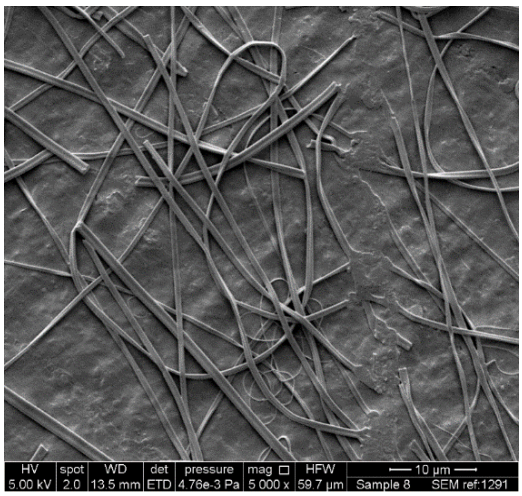

(16 G)

Figure 3.9. SEM images of E-EPO fibres, electrospun using different spinneret diameters.

3.3.1.5 Effect of Flow Rate

As flow rate was increased from 1 mL/h to 5 mL/h for formulation 1, it was observed that a larger applied voltage is needed to counteract dripping to overcome surface tension and the axisymmetric instability [71]. Formulations 2, 3, 4 and 5 were also electrospun at flow rates of 0.5 mL/h, 1 mL/h, 2 mL/h and 3 mL/h and an increased voltage was required to counteract the surface tension. An increased gap distance is also required when the flow rate is high, and this is to allow a longer flight time of the jet and therefore to allow complete evaporation of the solvent [185]. Depending on the formulation, when the flow rate was increased beyond an optimum point, dripping contributed towards beading formation, which can be undesirable. This can be explained by the fact that the jet returned to displaying a Rayleigh instability, where a column of liquid ejected is inclined to break up into droplets with smaller individual surface areas, as explained in Section 1.4.2.1. Generally, for a given fluid, there will be a range of flow rates and associated applied voltages at which the electrospinning process will be possible. These will be determined by the solution parameters such as the polymer concentration and solvent content, which influence the viscosity and density of the solution; these affect the flow resistance thereby affecting the rate applied [186].

3.3.1.6 Effect of the Addition of API

CPM salt was added to 25 % (w/v) E-EPO and 20 % (v/v) water. All solutions were processed at a gap distance of 15 cm, 1 mL/h flow rate and Taylor-cone forming applied voltage between 20 kV and 25 kV. SEM images shown in Figure 3.10. 1:6 drug to polymer ratio was the only combination that yielded fibres, even though they were defective. As the amount of drug increases in the solution mixture, spinning of fibres does not occur and only mild spraying is observed. As the drug-to-polymer ratio is decreased, conductivity is increased. Due to drug-loaded solutions being highly conductive, electrical discharge in the surrounding air can occur [68], causing multiple jets to form at the nozzle and this may explain the broken fibre strands seen in the SEM images of 1:4 and 1:5 fibres. There were no fibres produced at 1:3 drug to polymer ratio, indicating that the API amount above this point halts the electrospinnability of the solution. As CPM is a salt, it is hypothesized that as the salt concentration is further increased, specific viscosity is decreased, and therefore so is

the chain entanglement. This is in line by findings by Li *et al.* (2017) [187], where salt addition beyond an optimum point interrupted the electrospinning of pullulan fibres. In addition, Du and Zhang (2007), discussed the effect of a salt on the solvation power of the solvent on the carrier polymer. As the added salt or API interacts with the solvent, the polymer chains experience less coil expansion, which manifests as a reduction in viscosity [188].

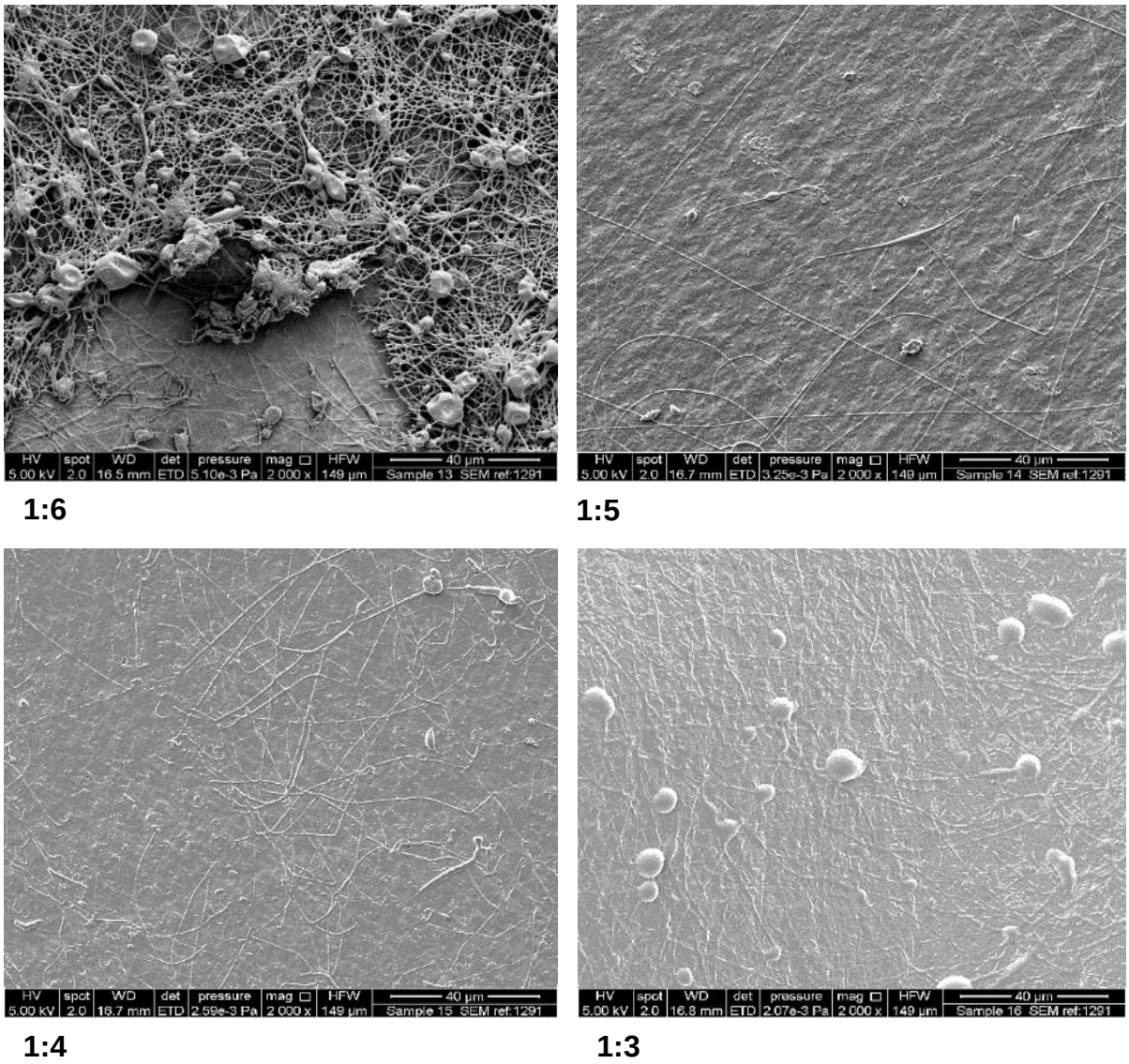

Figure 3.10. SEM images of electrospun drug loaded E-EPO at ratios of 1:6, 1:5, 1:4 and 1:3.

3.3.1.7 Summary of OFAT Findings

Table 3.6 summarises the observational findings of the various parameters investigated, as each of the parameters listed are increased. These tie in with the effect of process and solution parameters discussed in the introduction of this thesis, section 1.4.2.1.. Nonetheless, an OFAT approach does not detect multi-parameter interactions and makes it difficult to predict optimum conditions accurately and hence the use of a DoE to accurately optimise the electrospinning of E-EPO.

Table 3.6. Effect of parameter increase on solution and fibre properties.

Parameter	Taylor Cone	Morphology	Diameter
Polymer Concentration	Clogging increases at tip	A transition is seen from spraying to beaded and spindled curly fibres to ribbons then tubular fibres.	⬆
Water addition	Clogging increases at tip due to lower evaporation	Beading decreases as a result of increases viscosity but then increases with a large water %	⬇
Applied Voltage	Stable up to a point; Sheets or yarns mid-air if voltage is set beyond optimum point.	Decreases beading to a point then increases again	⬇
Flow rate	Dripping – as flow rate increases, voltage needs to be increased	Beading increases slightly	⬆
Gap distance	If too large then electric range is disrupted and Taylor cone formation weakened.	Beading increases slightly	⬇

3.3.2 DoE Electrospinning

The DoE definitive screening design aimed to find the most influential factors affecting diameter and beading. Table 3.7 shows the parameters investigated, the levels tested of each and the associated results. This type of DoE requires only a small number of runs to identify most important factors quickly and efficiently. If a systematic approach was used to run experiments for all combinations of the five chosen factors at three levels for each, this would have resulted in 3^5, or 243 separate experiments. The definitive screening design allowed for screening with only 14.

Figure 3.11 shows the statistical significance level of each of the parameters investigated on both outputs when modelled together. *P*-value is expressed on the log scale; the vertical dashed line represents the statistically significant level of log (*p*-value) = 0.05. Polymer concentration was found to be the only statistically significant factor. If increased, it reduced beading defects, while if decreased it reduced fibre diameter.

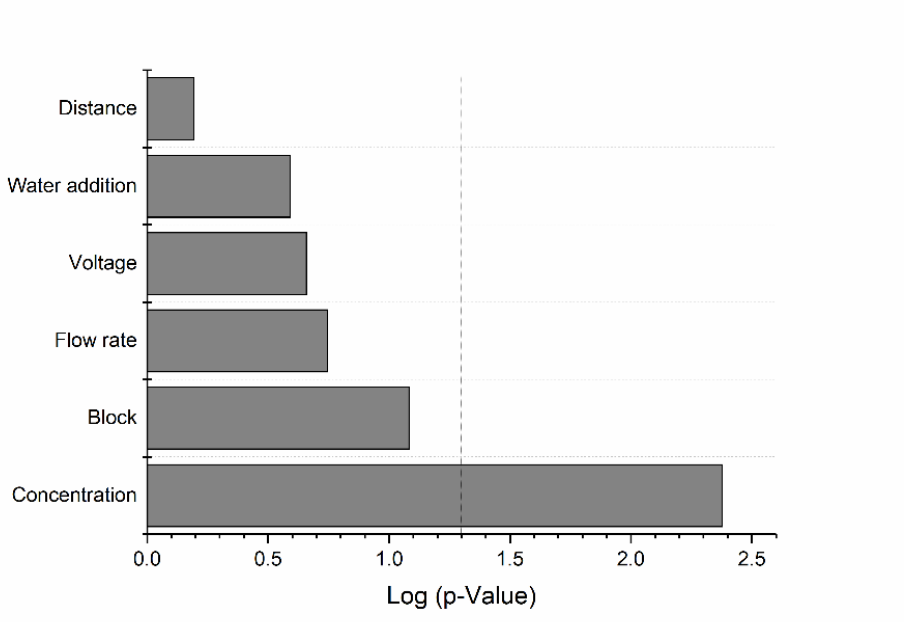

Figure 3.11. Pareto chart showing the statistical significance of the various parameters in producing bead-free fibres with a small diameter. The vertical dashed line represents significance level of Log *p*-value = 0.05.

Table 3.7. DoE definitive screening design; parameters investigated and findings.

Formulation	Block	Applied Voltage (kV)	Flow rate (mL/h)	Gap Distance (cm)	Water (% v/v)	E-EPO Concentration (% w/v)	Beading *	pH	Conductivity (µS/cm)	Viscosity ± SD (mPa s)	Mean Diameter ± SD (nm)
1	1	25	2	15	10	45	0	8.4	6.20 ± 0.44	1650 ± 43	2358 ± 782
2	1	17.5	2	25	20	45	0	8.9	5.65 ± 0.61	2068 ± 47	3078 ± 741
3	1	25	1.25	15	20	25	105	8.7	9.57 ± 0.45	76 ± 6	259 ± 58
4	1	10	1.25	25	0	45	0	8.3	2.03 ± 0.15	444 ± 14	4207 ± 78
5	1	10	0.5	25	10	25	NF	8.6	6.38 ± 0.33	51 ± 6	N/A
6	1	17.5	0.5	15	0	25	60	8.7	3.24 ± 0.39	63 ± 2	483 ± 181
7	CP-1	17.5	1.25	20	10	35	0	8.9	5.01 ± 0.15	176 ± 17	1574 ± 535
8	2	25	2	25	0	25	145	8.9	3.24 ± 0.39	63 ± 2	416 ± 359
9	2	25	0.5	20	0	45	0	8.9	2.03 ± 0.15	444 ± 14	2557 ± 395
10	2	10	2	20	20	25	NF	9.2	9.57 ± 0.45	76 ± 6	N/A
11	2	10	0.5	15	20	45	0	9.2	5.65 ± 0.61	2068 ± 47	2789 ± 677
12	CP-2	17.5	1.25	20	10	35	65	8.7	5.01 ± 0.15	176 ± 17	436 ± 162
13	2	25	0.5	25	20	35	65	8.9	6.90 ± 0.20	133 ± 25	260 ± 68
14	2	10	2	15	0	35	NF	8.5	2.17 ± 0.09	143 ± 5	N/A

*Approximate number, counted in SEM x 5000 mag image. No fibres (NF) recorded when spraying occurred and no fibres were formed; those data were excluded from prediction model.

3.3.2.1 Fibre Diameter

The effect of adding water to ethanol in the solvent mixture was not found to be a statistically significant factor for E-EPO fibre diameter reduction *(p*-value = 0.2572). Water increases the dielectric constant of the solvent and can lead to a reduced diameter of the fibre due to increased stretching of the fibres, as in the case of F11(see Table 3.7), where the addition of 20 % (v/v) water to the solvent yielded a mean fibre diameter of 2789 nm ± 677 nm. On the other hand, F4 had no water in the solvent mixture and it had a mean fibre diameter of 4207 nm ± 78 nm. Water addition can also increase the viscosity of a solution, and therefore can lead to an increased diameter, as is the case with F2 (20 % (v/v) water) yielded a diameter of 3078 nm ± 741 nm, as compared to F1 (10 % (v/v) water), which yielded a diameter of 2358 nm ± 782 nm [189].

Similar to the addition of water, applied voltage was not found to be statistically significant in reducing the diameter of E-EPO fibres (*p*-value = 0.2197). Nonetheless, as applied voltage increases the electric field is enhanced accelerating the jet and hence its stretching giving rise to smaller fibres. However, although minor, an increase in applied voltage can also cause an increase in polymer drawn, thereby increasing fibre diameter. Therefore, depending on conditions, it can lead to either an increase or decrease, or have no effect at all on fibre diameter. While an increase in flow rate was observed to show an increase in fibre diameter this was not found to be statistically significant (*p*-value = 0.8203). An increase in gap distance increases the flight jet time and elongates the polymer jet stretching out, and therefore can reduce fibre diameter, but it was also not found to be statistically significant (*p*-value = 0.6413).

The screening design showed that out of those parameters studied in the stated ranges, polymer concentration was the only statistically significant factor in reducing fibre diameter (*p*-value = 0.0076).

The ANOVA data shows that the input parameters studied explain the reduction in mean fibre diameter observed. The error's sum of squares is less

than the model's sum of squares, and therefore the variance in the fibre diameter is explained by the statistically significant effect of the input parameters (*p*-value = 0.0362) and not by pure chance or error. The sum of errors is shown as the corrected total, or C.Total. The degrees of freedom (DF) represent how many values in the calculation have the freedom to vary. The model's DF represents the parameters investigated which is 6, whereas the error's DF is equal to the number of observations minus the number of parameters studied in the model +1. The error's DF is calculated as follows: 14 - (6+1) = 7 and as 3 datapoints were excluded because no fibres were formed, that results in 4. The 6 parameters were applied voltage, flow rate, gap distance, solvent, polymer concentration and block. The ANOVA data is shown in Table 3.8.

Table 3.8. ANOVA data for reduced diameter.

Source	DF	Sum of Squares	Mean Square	F Ratio
Model	6	17828619	2971437	7.4530
Error	4	1594765	398691	Prob > F
C. Total	10	19423384		**0.0362**

3.3.2.2 Fibre Beading

The effect of water addition was not found to be statistically significant on beading (*p*-value = 0.764). The addition of water increased the conductivity of the solutions which reduced beading on some occasions, however, in other instances, beading increased because water was not evaporating by the time the fibres deposited on the collector. An increase in applied voltage can reduce beading by improving Taylor cone stability through overcoming the surface tension and eventually stopping dripping [71]. This effect was not statistically significant on the reduction of beading in E-EPO fibres (*p*-value = 0.7778). Flow rate can increase beading as it can lead to Taylor cone instability, and therefore interruption of the jet stream. This however was not found to be statically significant on reducing beading (*p*-value = 0.180). An increase in

gap distance can lead to increased beading due to a weakened electric field and therefore reduced solvent evaporation [68]. However, this effect was not found to be statically significant on the reduction of beading (*p*-value = 0.6966). Similar to its effect on fibre diameter, polymer concentration was the only statically significant parameter in reducing beading (*p*-value = 0.0042).

The ANOVA data shows that the input parameters studied explain the reduction in beading observed. The error's sum of squares is less than the model's sum of squares, and therefore the variance in the beading recorded is explained by the statistically significant effect of the input parameters (*p*-value = 0.0287) and not by pure chance or error. The ANOVA data is shown in Table 3.9.

Table 3.9. ANOVA data for reduced beading.

Source	DF	Sum of Squares	Mean Square	F Ratio
Model	6	24573	4095	8.5
Error	4	1926	481	Prob > F
C. Total	10	26500		**0.0287**

As polymer concentration was found to be the only statistically significant factor in affecting beading and fibre diameter, the morphology of the fibres as a function of E-EPO concentration is further discussed.

3.3.2.3 25 % (w/v) E-EPO

It can be seen from Figure 3.12 that at 25 % (w/v) E-EPO beading and spindle formation occurs, likely due to the solution being insufficiently viscous. In fact, samples in this category had the highest beading and the lowest viscosity measurements as compared to other samples. F10 shows sprayed particles; no spinning occurred as the applied voltage was very low at 10 kV. There is

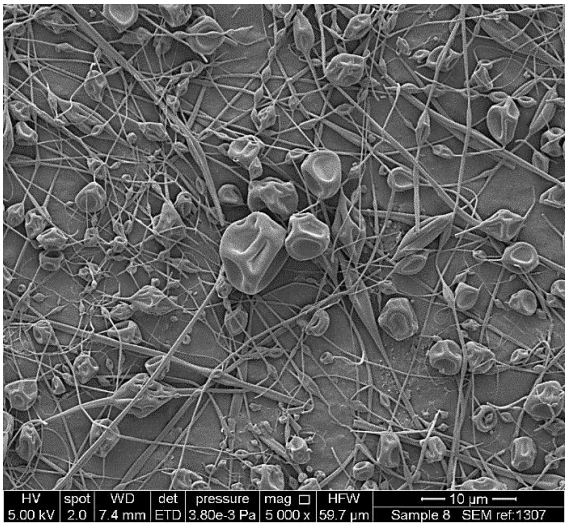

DoE F8

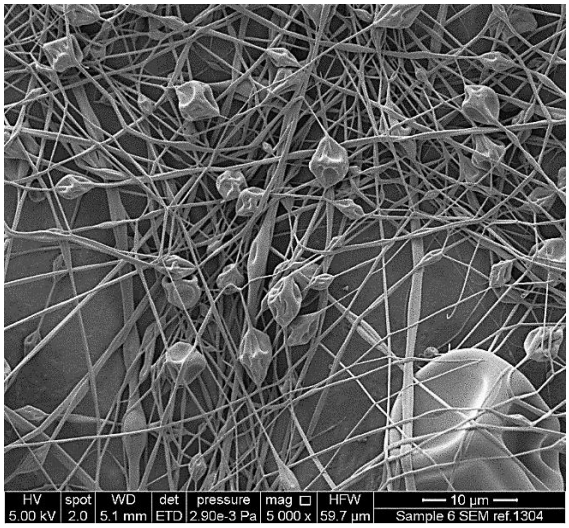

DoE F6

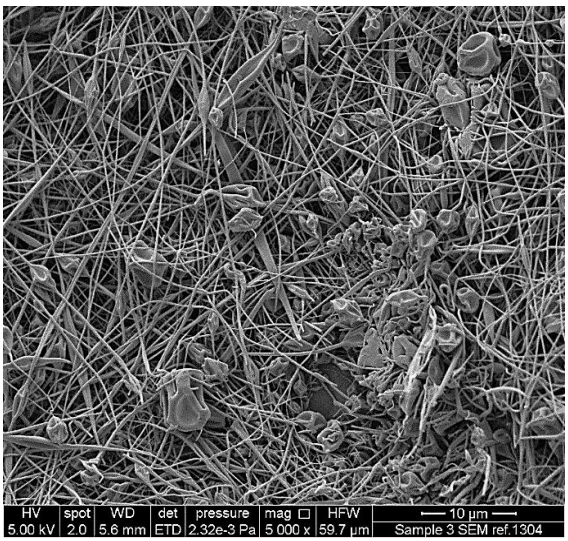

DoE F3

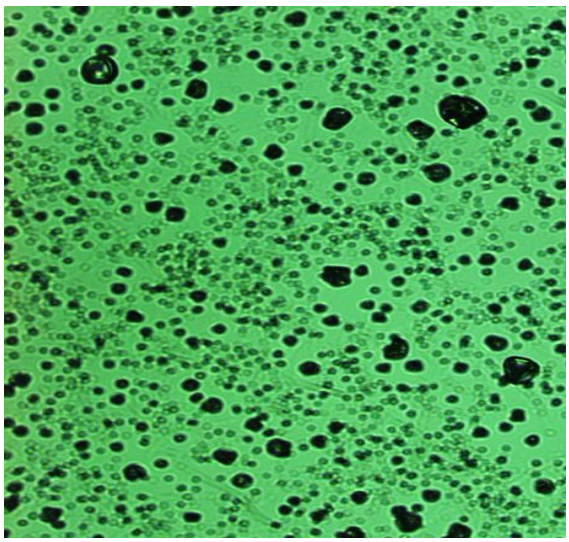

DoE F10

Figure 3.12. SEM and optical microscopy images of 25 % (w/v) E-EPO electrospun fibres, processed at: F8: no water, 25 kV, 2 mL/h, and 25 cm, F6: no water, 17.5 kV, 0.5 mL/h, and 15 cm, F3: 20 % (v/v) water in solvent, 25 kV, 1.25 mL/h, and 15 cm, F10: 20 % (v/v) water in solvent, 10 kV, 2 mL/h, and 20 cm.

no image for F5 as it also did not electrospin any fibres due to the low concentration combined with the very low applied voltage setting. F6 and F8 had the same solution parameters, but were electrospun at a flow rate of 0.5 mL/h and 2 mL/h, respectively. This explains why F6 had less beading than F8. F3 had a flow rate of 1.25 mL/h and with a slightly more viscous solution (70 mPa s) than the other sample, it had slightly less beading than F8 and F5. Due to high beading caused by a low concentration and therefore splitting streams of polymer jet, the diameters in this category were the smallest as compared to other concentrations.

3.3.2.4 35 % (w/v) E-EPO

It can be seen in Figure 3.13 that F7 and F12 were both run at the same conditions, known as centre points (CP) of the design. It was noted that F12 yielded beaded fibres, while F7 was electrospun into smooth fibres. It is well documented that environmental conditions affect electrospun fibres, and it is a factor that needs to be taken into consideration with electrospinning [185]. This might have been due to the difference in humidity. F14 did not electrospin at 10 kV due to the low applied voltage; an image of the solution processed at 14 kV is instead provided to illustrate the importance of an optimum applied voltage. F13 yielded beaded fibres even though it was electrospun at a low flow rate and high gap distance; this might be explained by the high-water percentage in the solvent. The water particles might not have evaporated by the time it reached the collector plate and therefore caused beading. Water-containing solvent mixtures can be more difficult to electrospin owing to low evaporation point of water, as well as the high surface tension that needs to be overcome to form stable fibres [180].

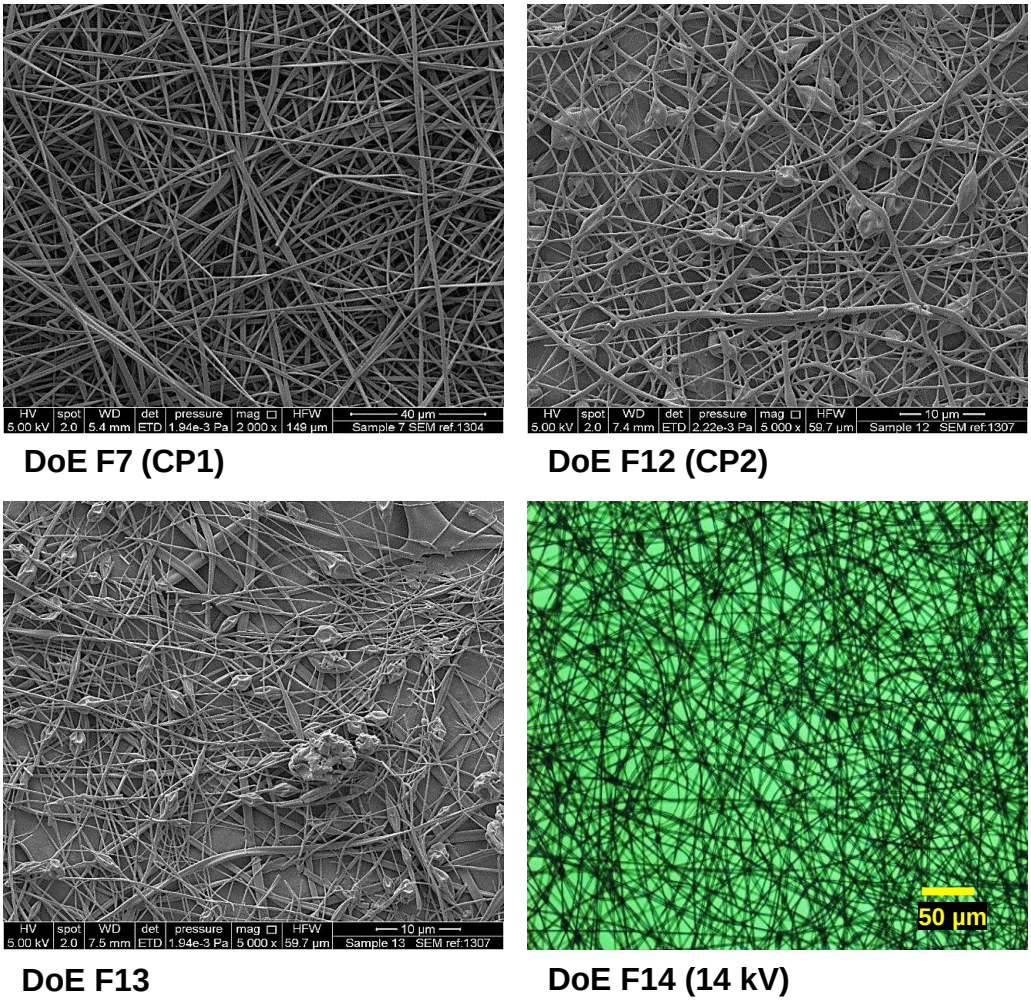

Figure 3.13. SEM and optical microscopy images of 35 % (w/v) E-EPO electrospun fibres, processed at: F7: 10 % (v/v) water in solvent, 17.5 kV, 1.25 mL/h and 20 cm, F12: 10 % (v/v) water in solvent, 17.5 kV, 1.25 mL/h and 20 cm, F13: 20 % (v/v) water in solvent, 25 kV, 0.5 mL/h and 25 cm. F14: No water, 10 kV, 2 mL/h and 15 cm.

3.3.2.5 45 % (w/v) E-EPO

In Figure 3.14 F4 appears as a mesh of fibres that has not completely dried off; this may be due to the low applied voltage (10 kV). F9 which has the same solution parameters as F4, also has a mesh structure, but with a drier appearance. This could be explained by the high applied voltage used and also the lower flow rate, which gives extra time for the fibres to dry and deposit on the collector. F1, F2 and F11 yielded smooth non-beaded fibres, due to the high polymer concentration. However, a rate limiting factor at this stage was needle clogging due to high viscosity. Cleaning of the needle tip manually was

repeated which would have resulted in discontinuation of a single continuous fibre and hence explains the breakage seen in F2.

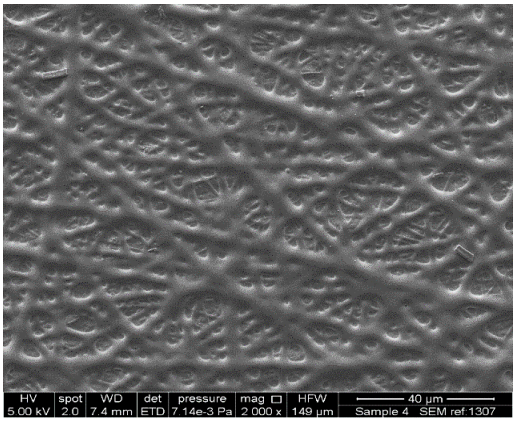

DoE F4

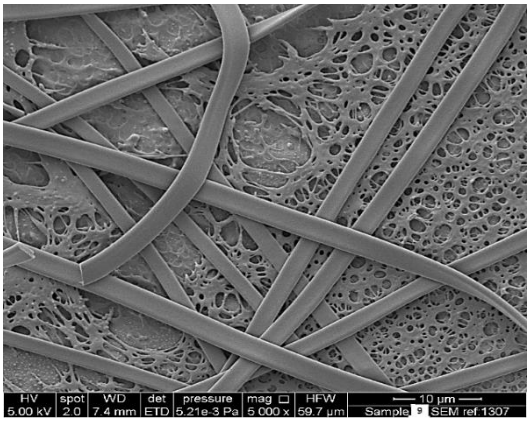

DoE F9

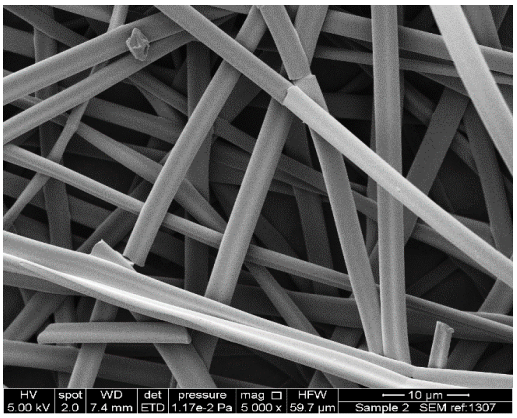

DoE F2

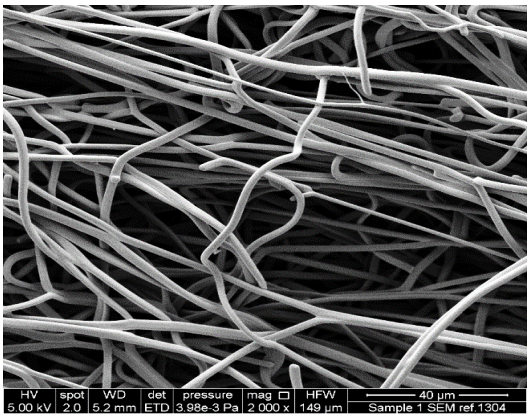

DoE F1

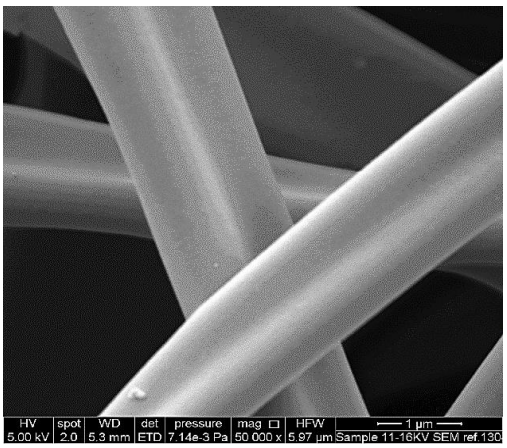

DoE F11

Figure 3.14. SEM images of 45 % (w/v) E-EPO electrospun fibres, processed at; F4: no water, 10 kV, 1.25 mL/h and 25 cm, F9: no water, 25 kV, 0.5 mL/h and 20 cm. F2: 20 % (v/v) water in solvent, 17.5 kV, 2 mL/h and 25 cm, F1: 10 % (v/v) water in solvent, 25 kV, 2 mL/h and 15 cm, F11: 20 % water (v/v) added in solvent, 10 kV, 0.5 mL/h and 15 cm.

3.3.3 DoE Validation

Using standard least squares regression analysis model, a predictive tool was used to predict fibre diameter and beading number. To determine the reliability of the predictive model, a summary of the fit is shown in Figure 3.15. The regression model for the reduction of fibre diameter data had an R^2 of 0.92, which means that 92 % of the predicted diameters are within the confidence intervals of the actual diameters recorded. Similarly, the predicted beading regression analysis, R^2 = 0.93, also had a very positive correlation with the actual beading numbers recorded, showing 93 % of the model predictions are within the confidence intervals of the actual beading data recorded. Both confidence curves cross the horizontal lines which indicates that the predictions are statistically significant to the actual measurements.

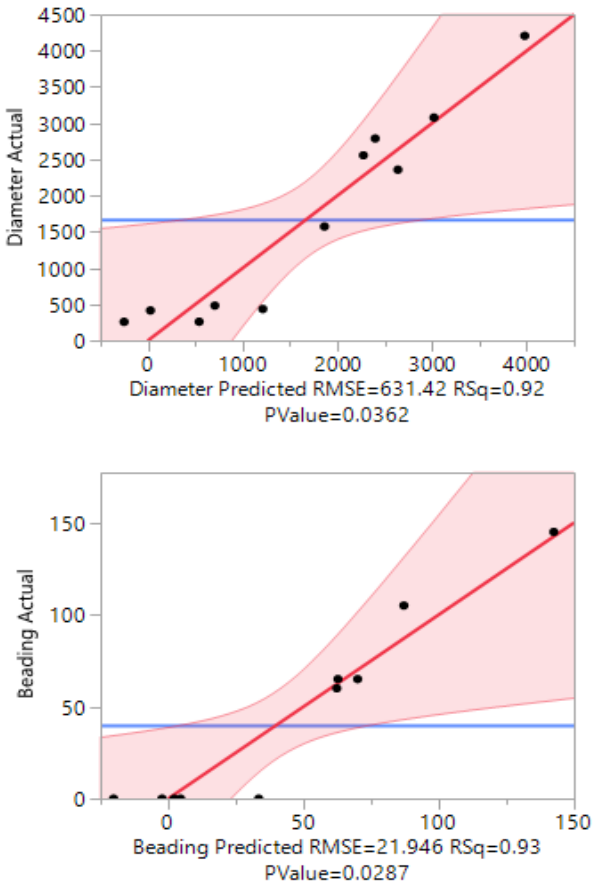

Figure 3.15. Summary of fit predicting diameter and number of beads in electrospun E-EPO fibres. Block line represents the linear fit, dashed outer lines represent the confidence curve, whilst the horizontal dashed line represents the hypothesised predicted outcomes at optimum conditions.

3.3.3.1 Minimising Beading

As well as screening key parameters, the definitive screening design approach can also be used to predict optimum conditions; shown in Figure 3.16. In the profiler graph, the x-axis represents input parameters and the y-axis represents the outcomes predicted and the desirability. From the prediction profilers, the operating conditions for producing nanofibres with the desired outcomes can be predicted [162]. The prediction profiler models a particular outcome depending on the interaction between the various variables, and therefore results may differ from linear observations made for each parameter [190].

The desirability value refers of likelihood of outcome being produced using the stated input variables. For bead-free fibres, these were predicted to be 45 % (w/v) E-EPO, 20 % (v/v) water, flow rate of 0.9 mL/h, applied voltage of ~21 kV and gap distance of 15 cm, with an R^2 of 0.93. This was validated experimentally, thereby lending weight to the predictive approach (Temp 19 ^oC, RH 32 %). The fibres had a mean diameter of 4317 nm ± 1942 nm and were bead-free as per the predictor.

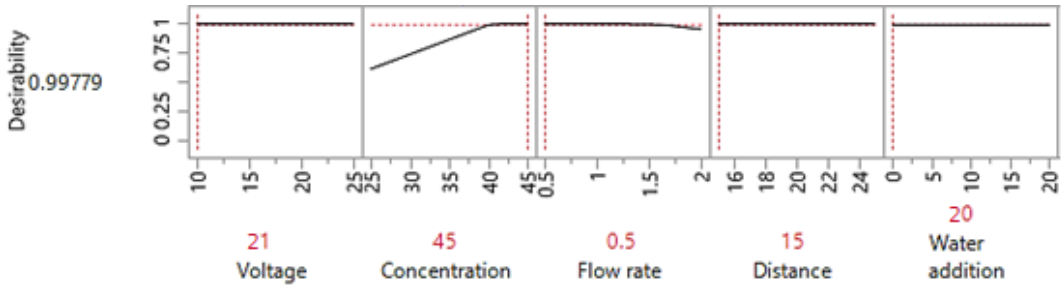

Figure 3.16. Prediction profiler tool for predicting the optimum conditions for electrospinning bead free fibres.

3.3.3.2 Minimising Diameter

Minimising fibre diameter was most affected by a decrease in polymer concentration (*p*-value = 0.008), the only statistically significant factor in the limits tested. The optimum parameters were predicted (Figure 3.17) to be 28 % (w/v) E-EPO, 20 % (v/v) water, flow rate of 0.5 mL/h, applied voltage of 25 kV and a gap distance of 15 cm to generate fibres with a mean diameter of 155 nm, R^2 = 0.92.

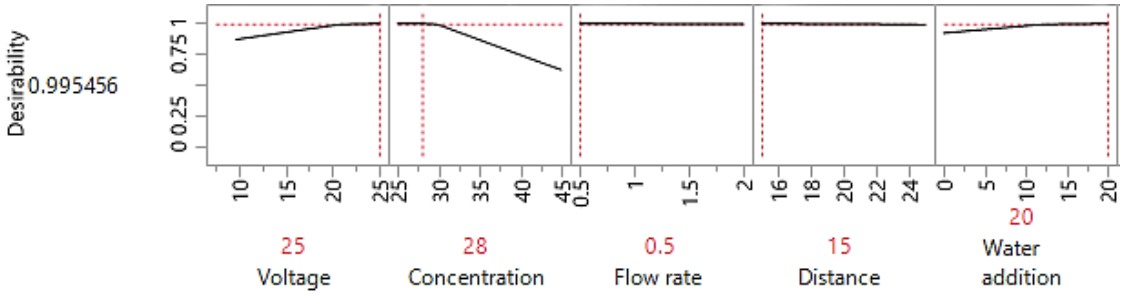

Figure 3.17. Prediction profiler tool for predicting the optimum conditions for electrospinning fibres with reduced diameter.

Experimental validation produced non-beaded fibres with a mean diameter of 930 nm ± 348 nm, Temp: 28 ºC, RH 36 %. An SEM image of the electrospun fibres is shown in Figure 3.18.

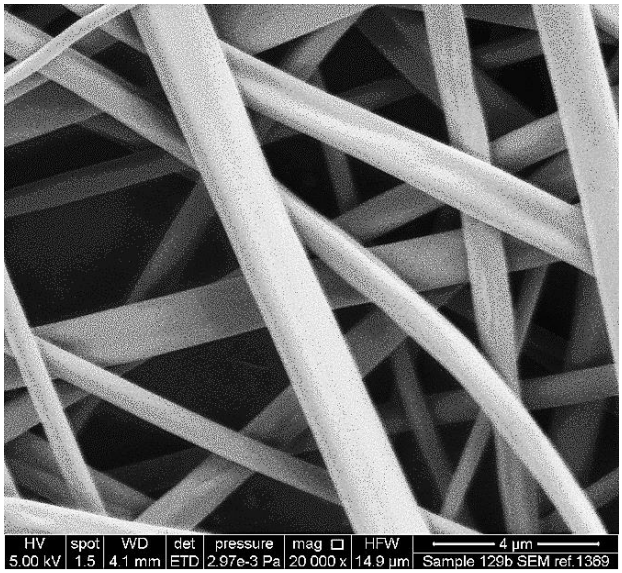

Figure 3.18. SEM image of electrospun 28 % (w/v) E-EPO; DoE predicted parameters for fibres in the nano-range.

3.3.3.3 Minimising Beading & Diameter Together

When both outcomes were modelled together, the prediction profiler tool, shown in Figure 3.19, predicted that at an applied voltage of 25 kV, polymer concentration of 35 % (w/v) E-EPO, 0.5 mL/h flow rate, gap distance of 15 cm and addition of 20 % (v/v) water, fibres with a mean diameter of 621 nm will be formed. They will also contain 37 beads per 3 square millimetre (i.e. very low beading). The desirability column shows negative sloped lines indicating the desire to minimize beading and fibre diameter. The dashed lines show the intersection between the values of the input and output parameters. The block lines show the relationship between input parameters and the outputs over the range.

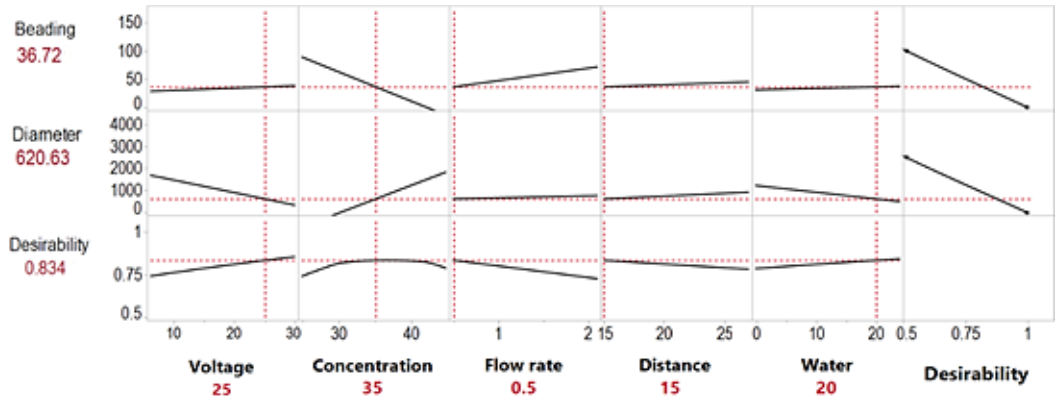

Figure 3.19. Prediction tool showing the relationship between the parameters and outcomes.

When validated experimentally non-beaded fibres with an average diameter of 1508 nm ± 250 nm were formed, SEM of fibre shown in Figure 3.20; Temp: 28 ^{o}C, RH 36 %. A potential reason why the projections are slightly different to the actual results is because of the hard-to-change factors such as humidity and temperature, which are not actually part of the predictive model.

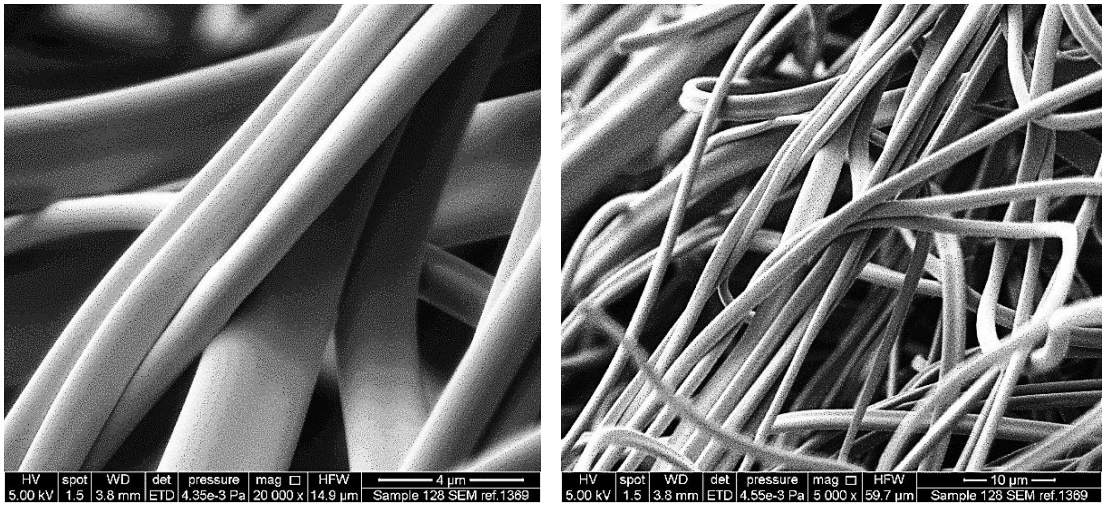

Figure 3.20. SEM image of electrospun 35 % (w/v) E-EPO; DoE predicted parameters for bead-free fibres in the nano-range.

3.3.4 Adding CPM

Using the definitive screening design, concentration was identified as the most influential factor in electrospinning smooth E-EPO fibres. Using the OFAT approach, CPM was previously electrospun with 25 % (w/v) E-EPO at ratios ranging from 1:2 to 1:6, and it was shown that fibre formation started to occur at ratios above 1:6. CPM was added using the defined optimised condition ranges, at drug ratios of 1:5 to 1:10. Input parameters and output parameters, namely conductivity, fibre diameter and drug loading measurements are recorded in Table 3.10. The fibres had a mean pH of 7.49 ± 0.202, which is neutral and therefore should not be irritating for the oral mucosa. All solutions were electrospun at a flow rate 1 mL/ h and a gap distance of 17.5 cm. Temperatures ranged between 20 °C and 24 °C whilst relative humidity ranged between 22 % and 49 %.

Table 3.10. Solution and process parameters used to electrospin CPM with 35 % (w/v) E-EPO; mean diameter, drug loading and conductivity results ± SD are recorded.

F	API	Applied Voltage (kV)	Conductivity (µS)	Mean Diameter (nm)	Theoretical drug loading (w/w %)	Actual drug loading (w/w %)	Drug loading efficiency (%)
1	**1:5**	15	244 ± 5	2471 ± 449	16.70	15.7 ± 0.4	95.0 ± 3.9
2	**1:6**	15	304 ± 42	2225 ± 389	14.30	14.0 ± 0.6	98.1 ± 3.9
3	**1:7**	15	232 ± 12	1566 ± 273	12.50	12.2 ± 0.5	97.5 ± 4.2
4	**1:8**	25	209 ± 4	1047 ± 437	11.10	9.8 ± 0.3	88.2 ± 2.9
5	**1:9**	25	203 ± 3	1102 ± 315	10.00	8.7 ± 0.5	86.6 ± 5.3
6	**1:10**	25	207 ± 15	708 ± 175	9.10	9.3 ± 0.6	102 ± 6.1

As the drug-to-polymer ratio is decreased, conductivity is increased. CPM is a salt, and therefore ionises in solution adding to its conductivity. Conductivity measurements were significantly higher than those without drug due to the salt nature of CPM. As the conductivity increases, the more easily charge can build up sufficiently to overcome the surface tension and therefore a lower applied voltage is needed to initiate electrospinning [68]. This knowledge was used to set the applied voltage at 15 kV for formulations 1 to 3, whereas for solutions with lower drug amounts, formulations 4 to 6, an increased applied voltage was applied (up to 25 kV). Due to drug-loaded solutions being highly conductive, electrical discharge in the surrounding air can occur [68], causing multiple jets to form at the nozzle and this may explain the large range of fibre diameter distribution shown by the standard deviation. SEM and fibre diameter distribution histograms of formulations 1 to 3 are shown in Figure 3.21.

It can be seen from the SEM images that for formulations 1 to 3, that the fibres did not have a smooth appearance. Formulation 1 had a drug to polymer ratio of 1:5, formulation 2's ratio was 1:6 and formulation 3's ratio was 1:7, All three formulations displayed similar defective morphology. This can be explained by the fact that when the polymer jet reached the collector, residual solvent was present causing this webbed appearance, which may have been caused as

the applied voltage not being set at the optimum value. As the partially solidified jets come into contact, they fuse together in a process known as conglutination [191]. The consequence of these connections are that they cause the mechanical properties to be altered, particularly the brittleness of the fibre mat to be increased, which is not ideal for an oral film formulation [69]. This is an indication that either the process or the solution parameters are not ideal and further optimisation is therefore needed. It is hypothesised that due to the increased drug amount in the solution causing an increased conductivity, as discussed, the multiple jets formed give rise to formation of multiple fibres strands that fuse together either on their flight or upon contact on the collector. The drug amount was therefore reduced. SEM and fibre diameter distribution histograms of formulations 4 to 6 are shown in Figure 3.22. Drug loading values were comparable to theoretical values indicating the drug is not chemically altered by the process.

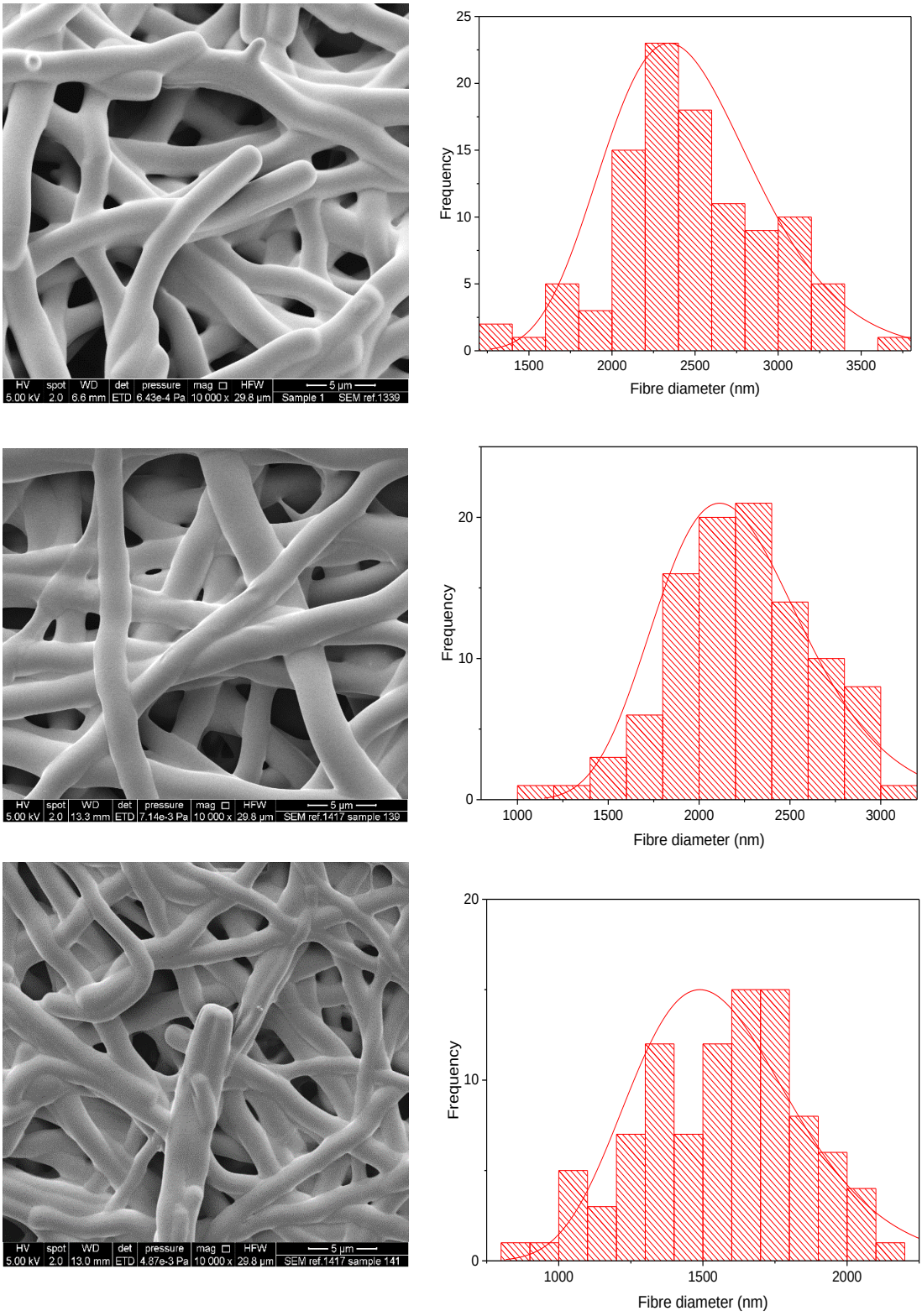

Figure 3.21. SEM and fibre diameter distribution histograms for formulations 1 to 3 (top to bottom).

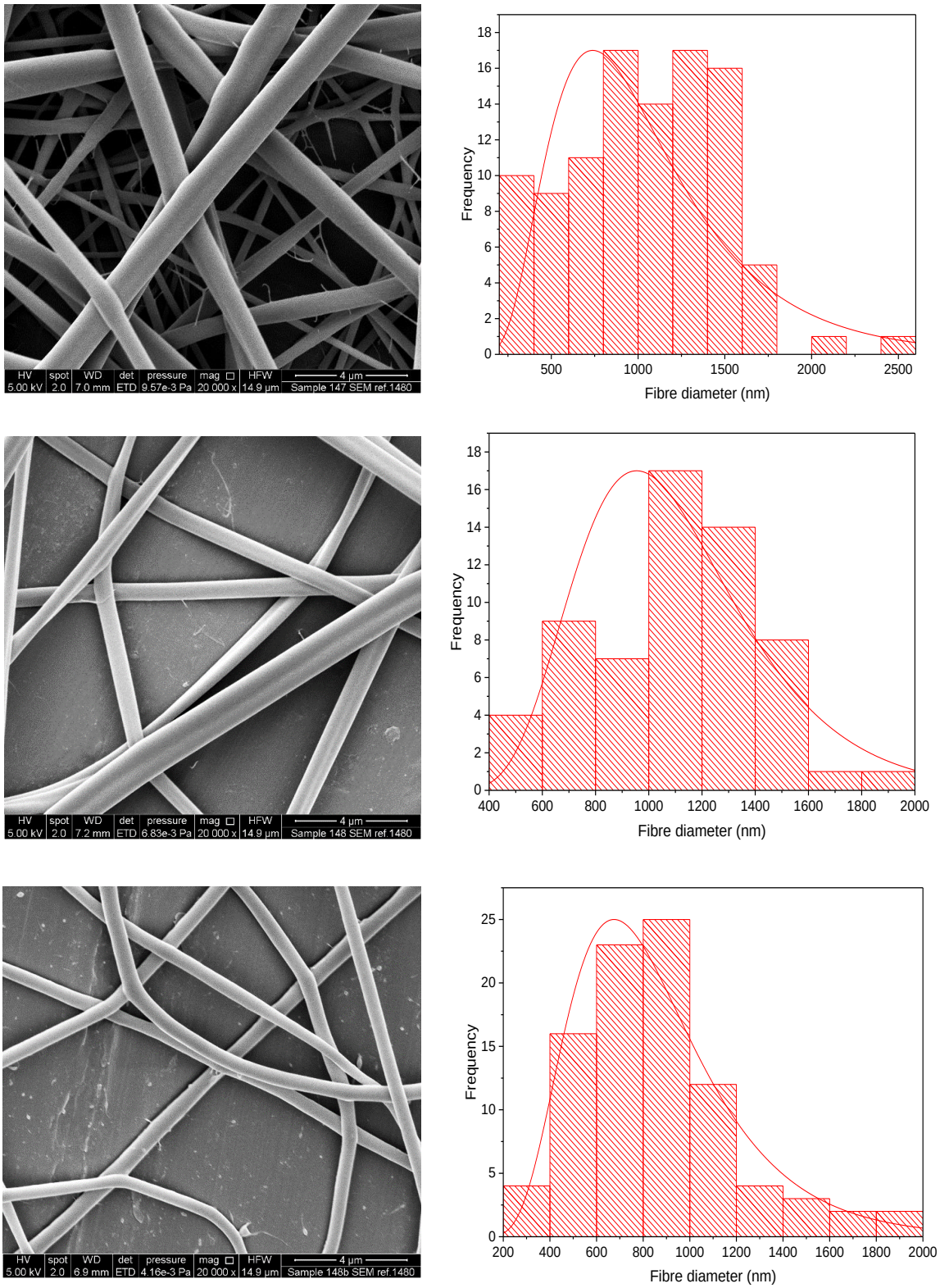

Figure 3.22. SEM and fibre diameter distribution histograms for formulations 4 to 6 (top to bottom).

It can be seen that as the drug amount is reduced, the fibres become smoother in appearance and more comparable to the placebo fibre morphology. All three formulations have a similar defect-free morphology as shown by their SEM images. Formulations 4 and 5 had a comparable mean fibre diameter and distribution. They were all electrospun at higher voltage compared to formulations 1 to 3, which appears to have contributed to more stable fibre formation and reduced fibre diameter size and distribution. Formulation 6 had a mean fibre diameter of 708 nm ± 175 nm, representing the lowest fibre diameters of all the drug-loaded formulations, likely due to the lower amount of drug and stability of the solution. In addition, this is the lowest diameter distribution, as shown by the SD and histogram representation, again indicating improved stability of the polymer jet and resultant fibre mat. The three formulations also showed drug loading in good agreement with the theoretical drug load, likely due to a more stable solution.

3.3.4.1 Multi-factorial Interactions

The main effects of polymer concentration, water addition, applied voltage, flow rate, gap distance and the addition of a drug, have so far been discussed in the electrospinning of E-EPO. The DoE completed for manufacturing optimisation of E-EPO aimed at screening for the most influential factors. Multi-factorial interactions are useful to gain a deeper understanding of the electrospinning process. 42 experiments of drug-loaded E-EPO were completed (see Appendix A). The effect of each parameter and multi factorial interactions were investigated on reducing fibre diameter. Beading was not explored at this stage, as it was completely eliminated by electrospinning the drug-loaded solutions above the critical entanglement concentration of E-EPO.

Figure 3.23 showed that both polymer concentration and flow rate were statistically significant effects on reducing fibre diameter of drug-loaded E-EPO fibres. It is to be noted that the flow rate's significant effect was likely not due to the drug addition in itself versus E-EPO on its own, but due to the higher number of experiments run and therefore increased power.

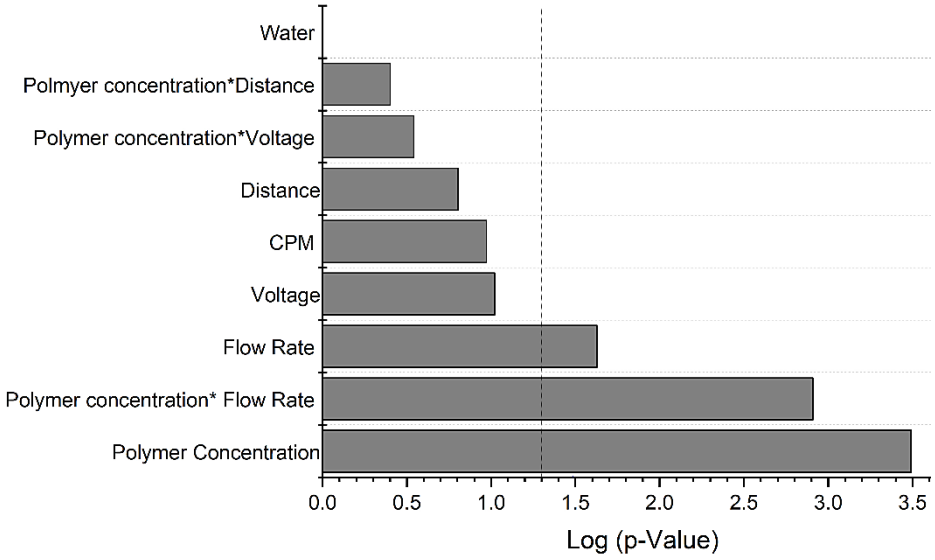

Figure 3.23. Pareto chart showing the statistical significance of the various parameters in producing drug-loaded E-EPO fibres with a small diameter. The vertical dashed line represents significance level of Log *p*-value = 0.05.

In summary, the optimised polymer concentration for both drug-loaded and placebo fibres was found to be 35 % (w/v). Polymer solution of 35 % (w/v) E-EPO was electrospun in 100 % ethanol at an applied voltage of 15 kV, flow rate of 1 mL/h and a gap distance of 17.5 cm. TEM image shows a smooth, non-beaded placebo nanofibre with a diameter of 260.54 nm, shown in Figure 3.24.

It was shown that at a drug to polymer ratio of 1:8 onwards at a polymer concentration of 35 % (w/v) E-EPO is the optimum concentration of drug that allows for the transfer of process conditions, at an applied voltage of up to 25 kV, flow rate of 1 mL/h and a gap distance of 17.5 cm. The TEM image shows a representative smooth, non-beaded placebo nanofibre with a diameter of 491.92 nm, shown in Figure 3.24. Electrospinning at ratios of 1:10 offered the

advantage of smaller nanofibres and a more accurate drug loading, likely due to better solution stability.

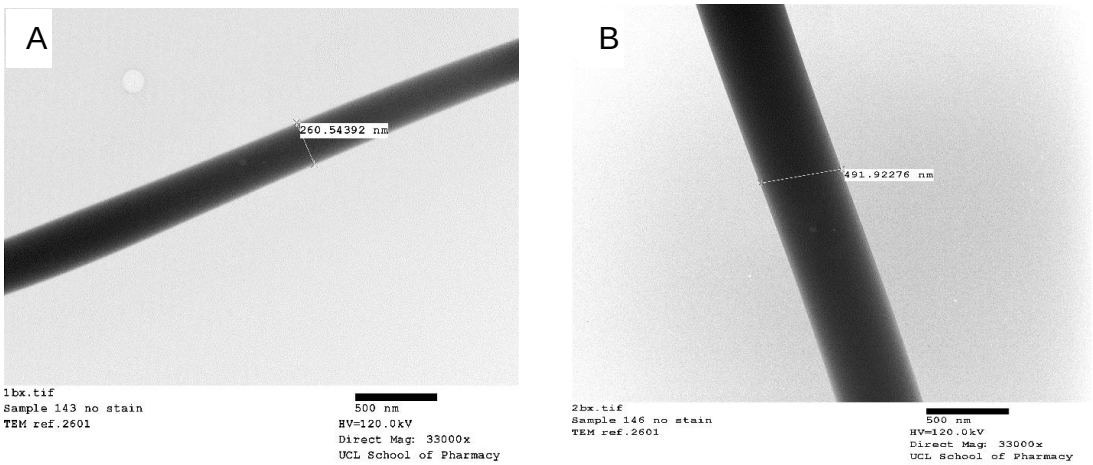

Figure 3.24. A: TEM image of 35 % (w/v) E-EPO placebo fibre, B: TEM image of drug-loaded 35 % (w/v) E-EPO fibre, 1:6 CPM, electrospun at 15 kV, 1 mL/h and a gap distance of 17.5 cm.

3.3.5 Solid State Characterisation

3.3.5.1 Powder X-Ray Diffraction

The XRD diffraction pattern shown in Figure 3.25 shows distinct peaks of CPM indicating a crystalline state, whereas E-EPO shows a halo which indicates an amorphous state. CPM distinctive peaks have been recorded on the figure; main peaks were seen at 13.19 º, 19.48 º, 20.43 º and 22.06 º. Similarly, E-EPO's main peak is seen around 17.51 º, and this peak is also seen in the PM and the electrospun fibres (Figure 3.26), confirming the sample composition. This reading is in close agreement with the literature reported value of 18 º [192].

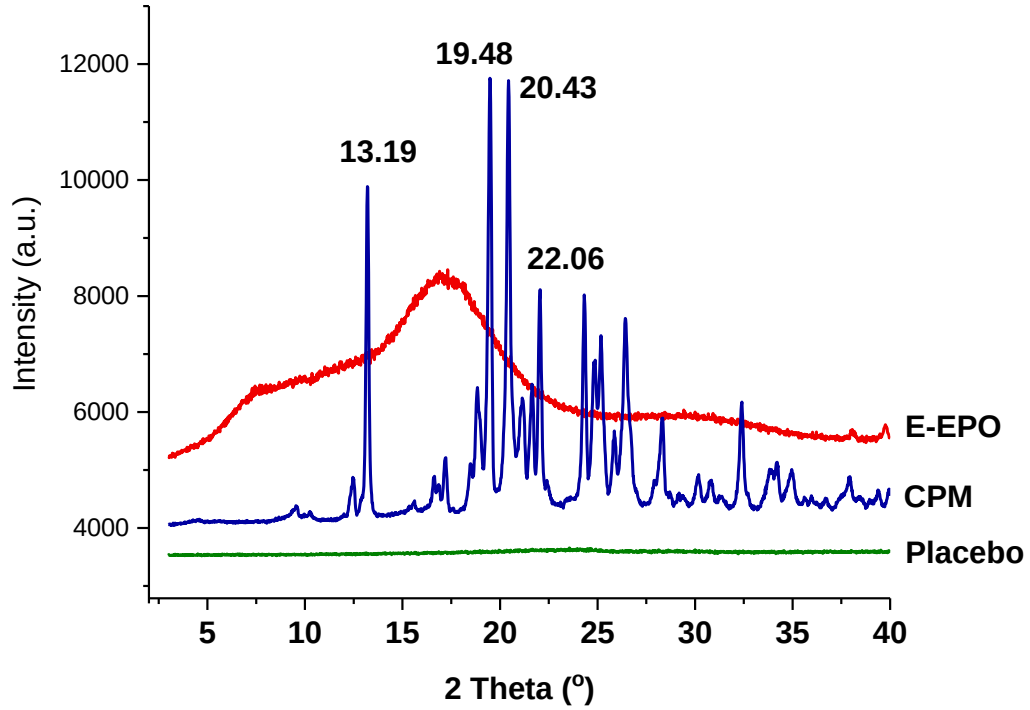

Figure 3.25. An XRD diffraction pattern of raw E-EPO, raw CPM and placebo 35 % (w/v) E-EPO fibre.

Even though no distinct peaks can be seen for the placebo electrospun fibres, the halo is very flat. In addition, it has been reported that peak patterns are less intense for processed materials of Eudragit E PO [192]. Nonetheless, the flat appearance may be due to the low sensitivity slow scanning rate used, at 3 ^{0}/min. To confirm this, drug-loaded fibres and PM were recorded over the ranges of 3 ^{o} to 40 ^{o}, at a scan rate of 10 ^{o}/min, improving the sensitivity of the diffraction pattern recorded [193]. The diffraction pattern is shown in Figure 3.26. Both drug loaded fibres show halos indicative of an amorphous state. This shows that CPM changes to the amorphous state following electrospinning.

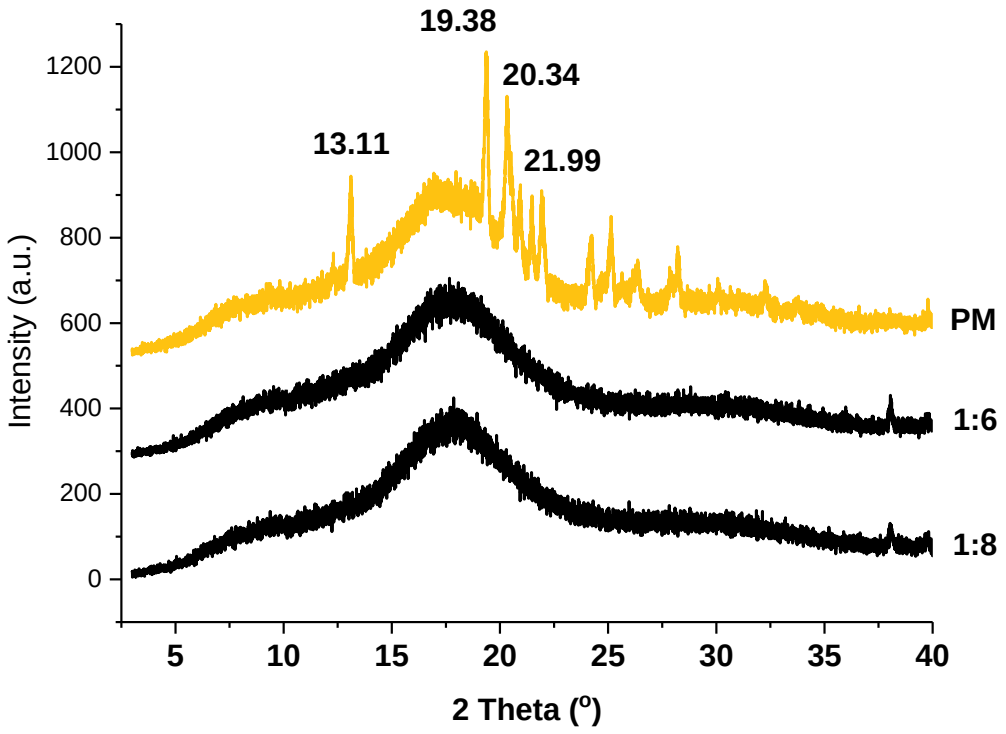

Figure 3.26. An XRD diffraction pattern of E-EPO and CPM physical mixture, 35 % (w/v) E-EPO + 1:6 CPM: E-EPO and 35 % (w/v) E-EPO + 1:8 CPM: E-EPO electrospun fibres.

3.3.5.2 Fourier Transform Infra-Red

In Figure 3.27, the most intense peak observed in E-EPO at 1150 cm^{-1} is characteristic of the C-O bond. The peaks observed at 1265 and 1237 cm^{-1} are also characteristic of this ester group. This is in agreement with the literature ranges of 1150 cm^{-1} to1190 cm^{-1} and 1240 cm^{-1} to1270 cm^{-1} [192]. The second most intense peak observed at 1724 cm^{-1} is characteristic of the C=O bond stretching [123], and is in similar agreement with the literature value of 1730 cm^{-1} [192]. The peaks observed around 2808 cm^{-1} to 2823 cm^{-1} correspond to the dimethyl-aminoethyl group present in E-EPO, and responsible for its ionisation in an acidic environment and eventual unloading of the API. These peaks are in agreement with literature values quotes to be 2770 cm^{-1} to 2830 cm^{-1} [192]. Other significant peaks noted at 1452 cm^{-1} and 2946 cm^{-1} are characteristic of the hydrocarbon chain vibrations and are in close agreement of literature values of 1450 cm^{-1} and 2950 cm^{-1} [192]. All the aforementioned peaks were also present in the physical mixture and the

electrospun fibres, confirming the presence of E-EPO in all of them. Both the placebo fibre and the drug-loaded fibre's spectra are almost identical, indicating no bonds were formed between the polymer E-EPO and the drug CPM, further validating the XRD data that an amorphous solid dispersion was formed.

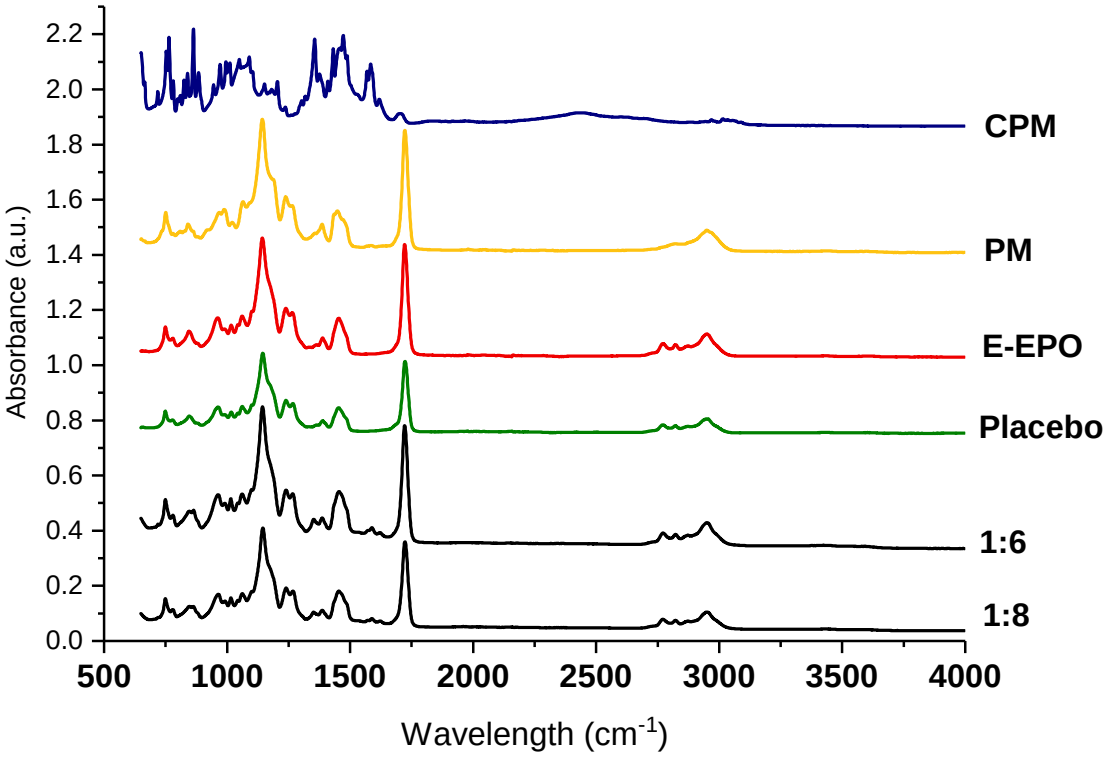

Figure 3.27. FTIR spectra of unformulated raw CPM, E-EPO, their physical mixture, 35 % (w/v) E-EPO placebo fibre and 1:6 and 1:8 CPM: E-EPO drug-loaded fibres.

3.3.6 Thermal Characterisation

3.3.6.1 Thermogravimetric Analysis

The degradation profiles for pure E-EPO and CPM were analysed using TGA. Representative thermograms are shown in Figure 3.28 and Figure 3.29, respectively. No water loss was observed in the temperature range for water evaporation for both drug and polymer.

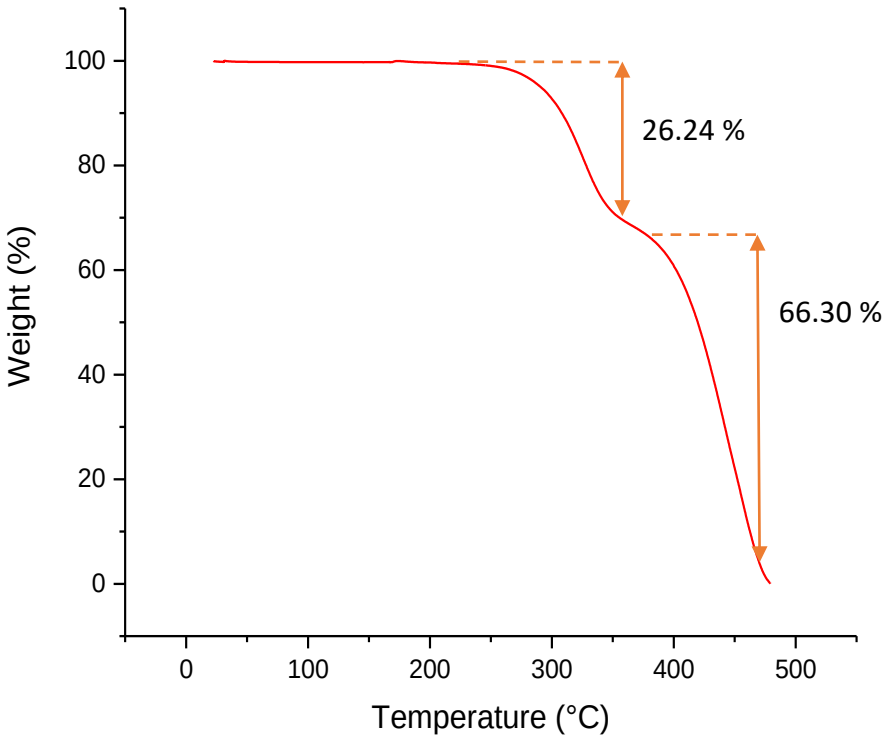

Figure 3.28. TGA thermogram of E-EPO raw material showing the % weight loss as temperature increases.

It can be seen from Figure 3.28 that E-EPO's TGA thermogram displays a biphasic profile. The first weight loss is seen around 276 °C, with approximately 26 % of the sample mass degrading. This is then followed by a larger weight loss of almost the rest of the sample, approximately 66 % which has an onset point of around 361 °C. E-EPO is a co-polymer formed from methacrylate dimethyl-aminoethyl, butyl-methacrylate and methyl-methacrylate groups [192]. This pattern indicates that the polymer breaks down into its components in a stepped process. Nonetheless, for purposes of DSC experimental conditions, the first decomposition temperature is noted as the onset point.

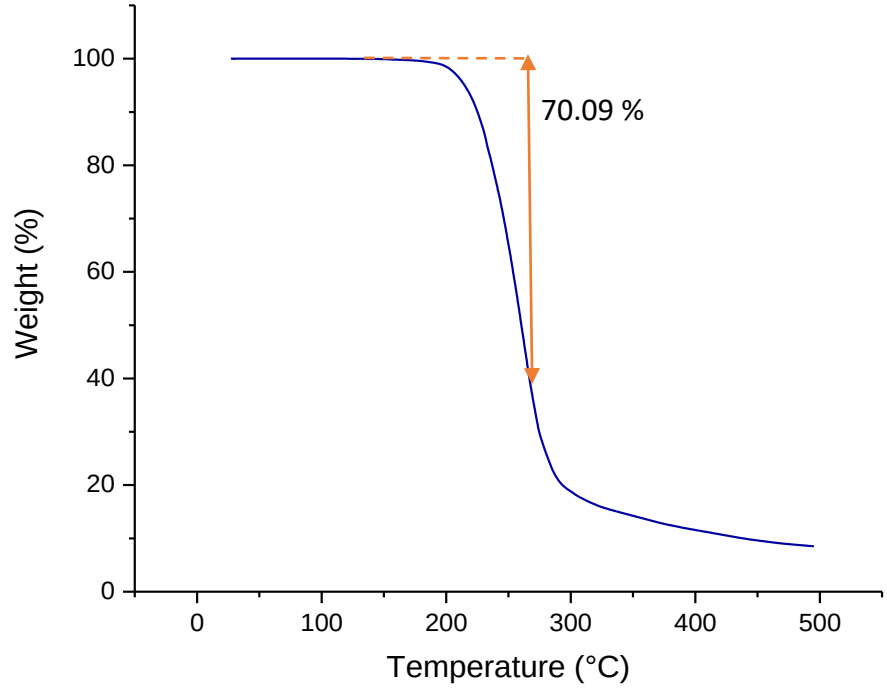

Figure 3.29. TGA thermogram of CPM raw material showing the % weight loss as temperature increases.

Degradation onset point for E-EPO, CPM and active fibres are shown in Table 3.11. It can be seen that weight loss due to degradation of CPM starts at around 215 °C where almost 70 % of its weight degrades over the next 50 °C. This information was used to determine the maximum heating temperatures used in DSC.

Table 3.11. TGA degradation temperatures for pure E-EPO, CPM and drug loaded fibres.

Sample	Mean onset point ± SD (°C)
E-EPO	276.1 ± 8.0
CPM	215.7 ± 5.9
Physical mixture	216.2 ± 2.8
Placebo fibre	278.4 ± 2.8
35 % (w/v) E-EPO; 1:8	215.7 ± 0.6

A representative thermogram of an electrospun drug-loaded fibre is shown in Figure 3.30. It can be deduced that there is little to no residual solvent in the electrospun fibres, as no significant mass loss is seen around ethanol's, 78.4 °C, or water's boiling point, 100 °C [194]. The thermogram displays a similar shape to that of E-EPO, showing that the drug is incorporated in it as a dispersion. The onset point however shifts to a lower temperature, 216 °C, closely matching that of the drug.

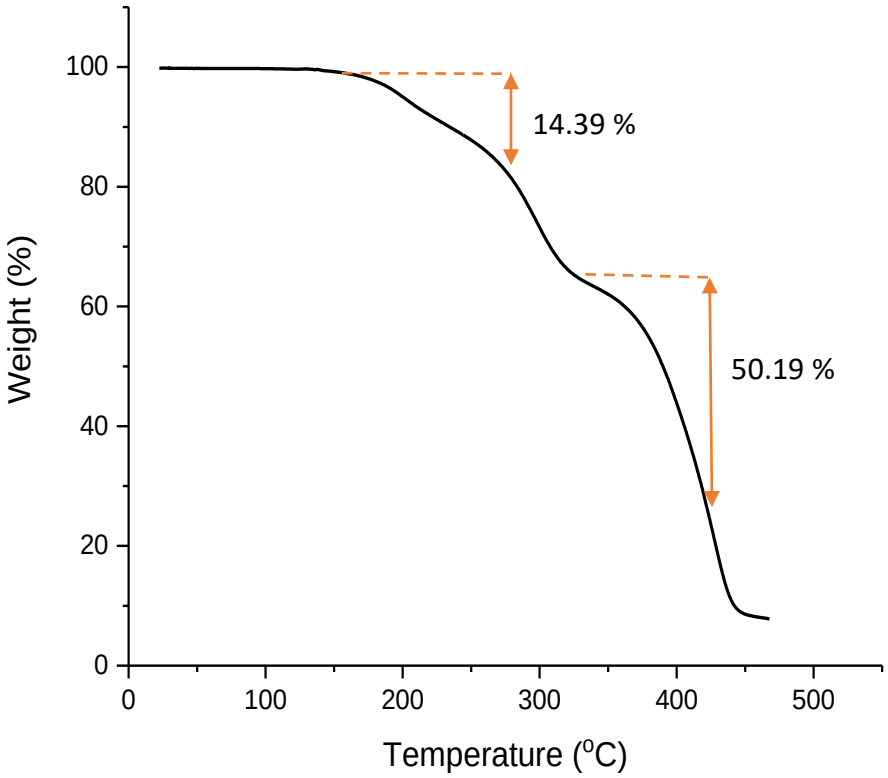

Figure 3.30. TGA thermogram of 35 % (w/v) E-EPO fibre with a CPM drug load of 1:8 showing the % weight loss as temperature increases.

3.3.6.2 Modulated Temperature Differential Scanning Calorimetry

Modulated temperature differential scanning calorimetry (MTDSC) measurements were carried out to determine the melting point (T_m) of CPM and the glass transition (T_g) of E-EPO. Midpoint values were recorded. E-EPO's T_g was recorded as 50.9 °C ± 1.1 °C, consistent with literature findings [106]. CPM's T_m was recorded as 133.24 °C ± 0.1 °C, in close agreement with the reported literature value of 130 °C to 135 °C [120]. When the physical

mixture of CPM and E-EPO was tested, both an endothermic melting trough at 133.5 °C ± 0.4 °C and a T_g shift at 49.7 °C ± 0.9 °C were observed, indicating both compounds were detected. The intensity of the melting peak was less in the physical mixture than in pure CPM which could be explained by the dilution effect of polymer [195].

Electrospun fibres were then tested. An E-EPO placebo fibre was tested and an endothermic shift was observed at 50.7 °C ± 0.7 °C indicating a T_g shift. Drug loaded fibres did not display a melting peak which indicates the conversion of crystalline CPM to the amorphous state. DSC thermograms shown in Figure 3.31.

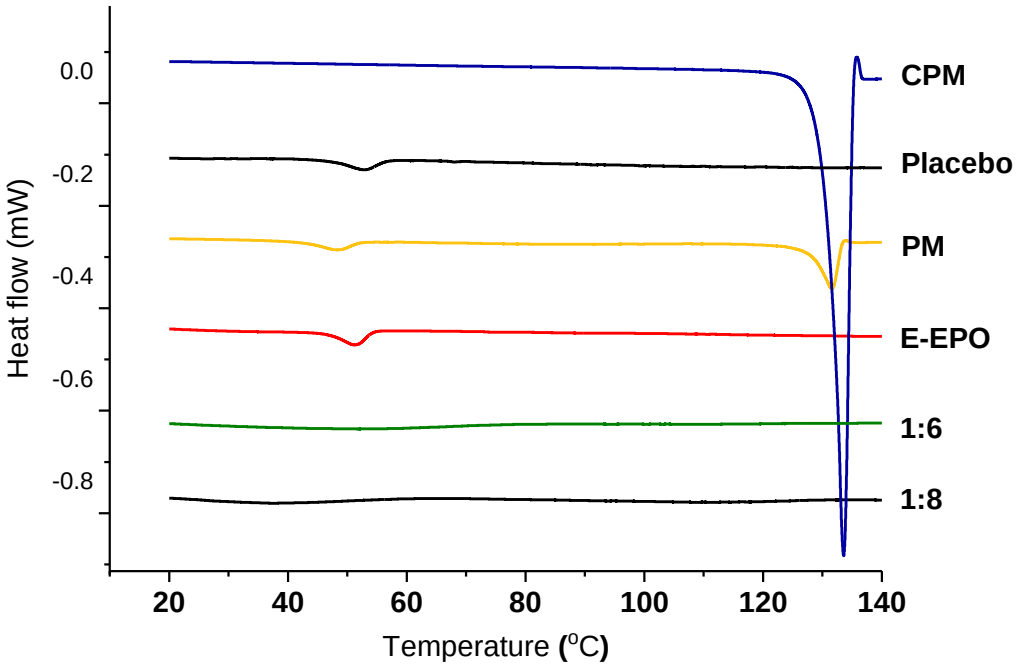

Figure 3.31. A MTDSC reversing heat flow thermogram of: pure CPM, placebo 30 % (w/v) E-EPO fibre, physical mixture (PM), pure E-EPO, 35 % (w/v) E-EPO + 1:6 CPM and 35 % (w/v) E-EPO + 1:8 CPM fibres. Exo up.

Heat-cool-heat cycles are commonly used to erase the thermal history of the material (i.e. the physical aging), allowing the T_g to be measured [141]. A heat-cool-heat cycle of CPM by itself was completed to understand the thermal behaviour of the drug further. The drug was heated to 150 ^oC, then cooled to -100 ^oC, then heated again to 150 °C. A representative DSC thermogram is shown in Figure 3.32. The drug formed an amorphous structure upon cooling and reheating and therefore a T_g was observed at 4.60 °C.

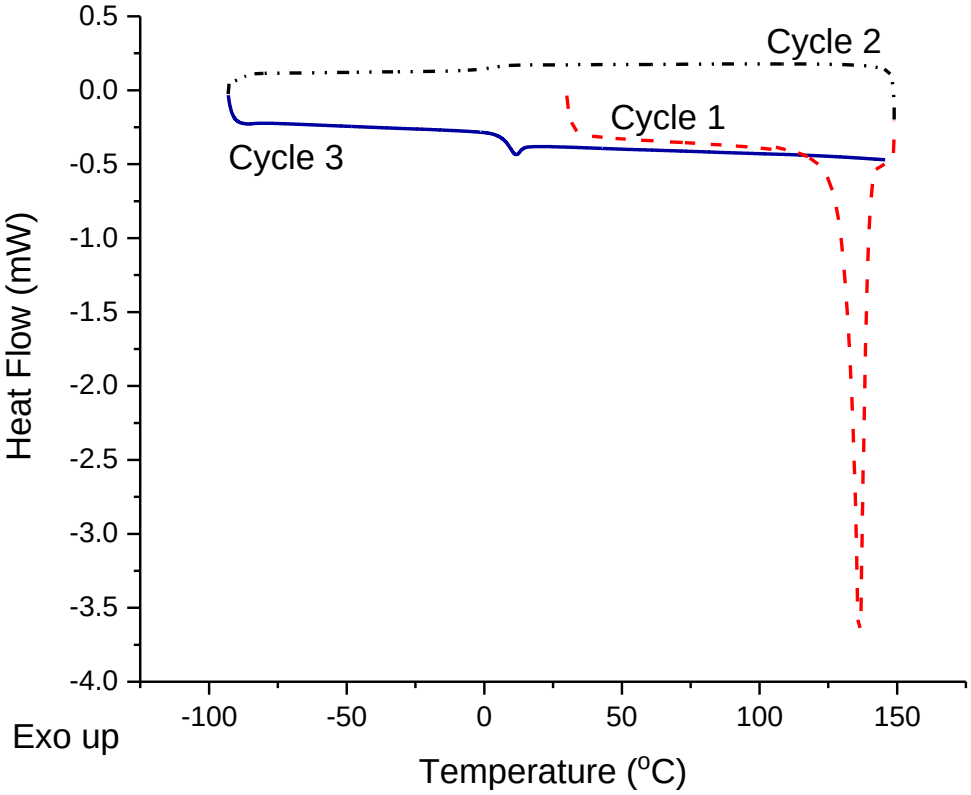

Figure 3.32. DSC thermogram of raw CPM showing the thermal events due to a heat-cool-heat cycle.

3.3.7 Atomic Force Microscopy

A technique termed amplitude modulation-frequency modulation (AM-FM) was employed to characterise the stiffness of the samples. It operates by using two cantilevers that are excited at two different resonances simultaneously. The resulting deflected resonance from the AM cantilever indicates the topography of the sample, whereas the FM resonance indicates the stiffness and elasticity

of the sample [147]. This resonance can be quantified as the change from the ingoing resonance to the outgoing resonance, which was used to calculate Young's modulus of the fibres, an indicator of stiffness.

AFM was used to obtain topographical images of placebo E-EPO fibres. As shown in Figure 3.33, the topography is smooth, as supported by the SEM data. The placebo E-EPO fibre showed a mean Young's modulus of approximately 5 GPa.

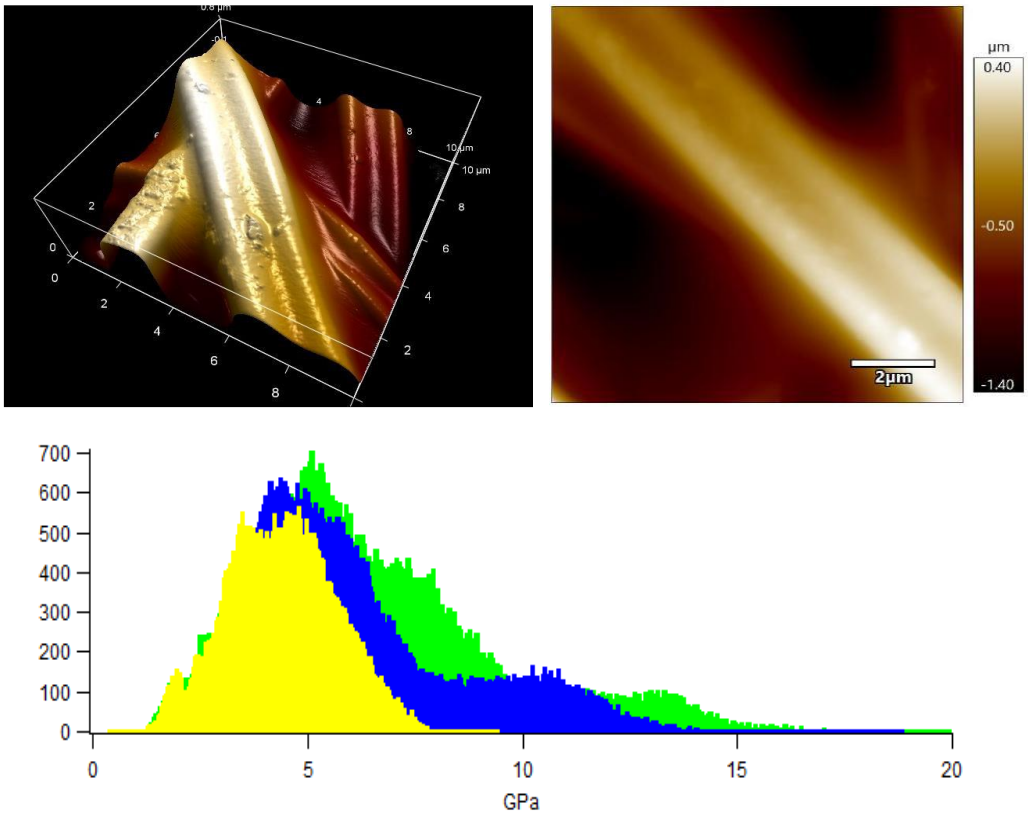

Figure 3.33. Placebo 35 % (w/v) E-EPO fibre 3D/ topography image, showing the structure of the fibre. Histogram showing distribution of young's modulus for three different fibre samples. Y-axis represents the frequency.

It can be seen in Figure 3.34 that as the drug amount increase from 1:10 ratio to 1:6 ratio, the average GPa or Young's modulus decreases. This reduction in elasticity indicates that the drug has a softening effect on the fibres, which is supported by the T_g shift (see Section 4.3.4.2) of the system as the drug is added showing a plasticising effect [196]. This elasticity effect offers an advantage when these mats are further to be used as oral films, whereas in solvent casting, plasticizer addition is necessary. It is hypothesised that

electrospinning of film-forming polymers such as E-EPO enhances its plasticity. This is believed to be due to the non-woven matrix formation of the nanofibres, allowing voids between the fibres and therefore reducing the cohesive forces, giving rise to a more elastic structure [197].

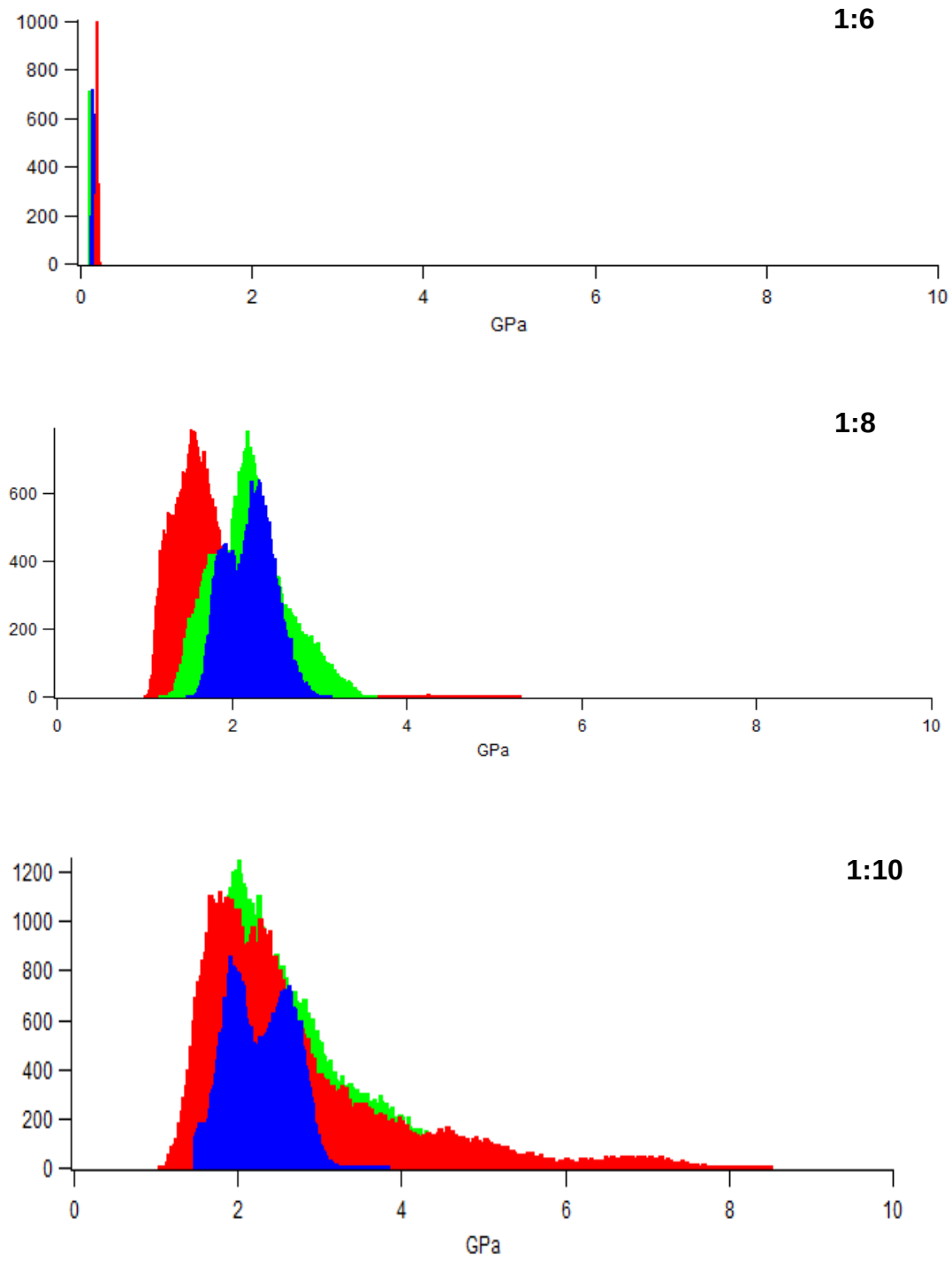

Figure 3.34. Drug-loaded 35 % (w/v) E-EPO fibre Young's Modulus histogram graphs, for 1:6, 1:8 and 1:10 drug-loaded E-EPO fibres. The three histogram curves per graph represent n = 3. Y-axes represents the frequency.

3.3.8 Dissolution Study

The *in-vitro* release profiles of the raw crystalline drug as well as the drug-loaded formulation are shown in Figure 3.35. The dissolution experiment was performed in a buffer solution of pH 1.2, mimicking fasted gastric conditions. Children over 2 have a similar gastric pH to adults, which is generally between 1.0 and 2.5 [198]. E-EPO is a pH dependent polymer that is insoluble over pH 5.0 therefore release in pH 6.8 buffer was not performed. It can be seen that the electrospun film releases at a very comparable manner to crystalline CPM, owing to the nanofibre's high surface area to volume ratio, and therefore a high release rate is expected. It can be seen that the film released approximately 100 % of the drug amount at 45 minutes, which is in line with an immediate release formulations' guideline of releasing 70 % of the drug in that timeframe (Ph. Eur. 5.17.1) [199]. The formulation is expected to release fully in the stomach, where no adverse effect due to the taste-masking on absorption is anticipated.

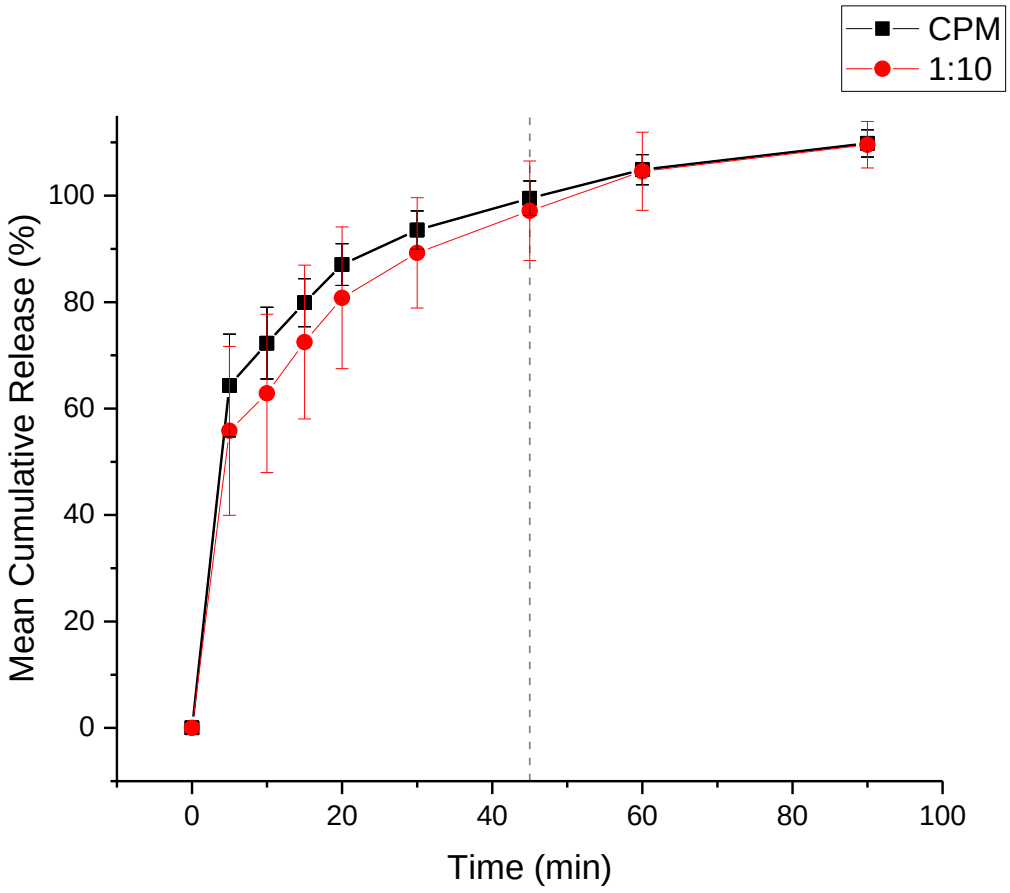

Figure 3.35. Dissolution profile in pH 1.2 of raw crystalline CPM and an E-EPO drug-loaded fibre with a 1:10 drug-to-polymer ratio of CPM. The dashed line represents 45 minutes.

3.3.9 *In-vitro* Taste-assessment

3.3.9.1 E-tongue

One of the main limitations of the E-tongue is that it can only detect drugs ionisable in the medium used for measurement [200]. The first step was to, therefore, determine if the drug in question, CPM, was detectable by the E-tongue's taste sensors. As chlorpheniramine is a basic drug, calculation of its ionisation percentage was completed using the Henderson-Hasselbalch equation, Equation 3.2 [201]:

Equation 3.2

$$pH = pKa + log\frac{[A^-]}{[HA]}$$

As the pH of the measurement media, 10 mM KCl, was measured to be 5.7, and the pKa of chlorpheniramine is quoted to be 9.13, the percentage ionisation was calculated to be 99.96 %.

Taste sensor output was obtained by measuring a difference in electric potential between the taste sensor and the reference electrode. It was confirmed that CPM is detectable by the E-tongue as a bitter drug. All sensors showed a concentration dependent response to CPM as shown in Figure 3.36. The drug demonstrates basic bitterness as well as astringency.

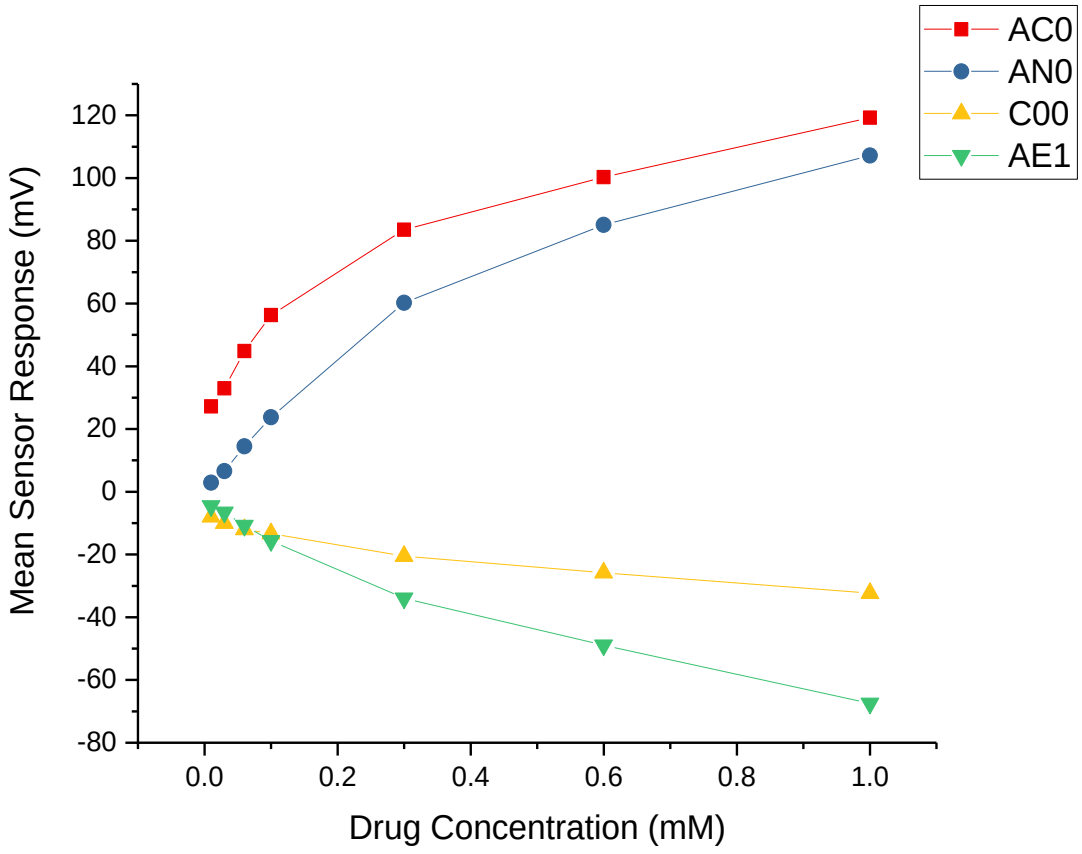

Figure 3.36. Analysis of sensor responses to various concentrations of CPM: AC0 – basic bitterness; AN0 – basic bitterness; C00 - acidic bitterness; AE1 – astringency.

Table 3.12 shows the data for Euclidean distances between pure CPM and pure E-EPO, physical mixture, placebo fibre and 1:8 and 1:6 drug-loaded fibres. Euclidean distance is defined as the distance between the cluster centre between one sample to another sample. The lower the distance between two samples, the closer and more similar they are [202]. As anticipated, pure E-EPO and placebo fibres tested had the largest Euclidean distance, an arbitrary distance from the pure bitter drug; the higher the distance, the lower the bitterness of the sample [202]. This was followed by drug-loaded fibres and finally by the physical mixture. Drug-loaded fibres had a larger distance than the physical mixture, indicating better taste-masking. It is to be noted that the 1:8 and 1:6 drug-loaded fibres tested both were tested in amounts that have an equivalent of 20 mg/ 100 mL CPM, or 0.5 mM. The difference between the two would be that the 1:6 formulation would have less E-EPO protecting the drug than the 1:8, and therefore it is expected that bitterness would be slightly higher. According to the Euclidean distance, 1:8 was indeed further away from CPM, indicating better protection of the drug.

Table 3.12. Euclidean distances of pure E-EPO, physical mixture, placebo and drug loaded fibres from pure 20 mg /100 mL CPM, or 0.5 mM, corresponding to data from the four sensors: AC0, AN0, AE1 and C00.

Sample	Euclidean distance
Physical Mixture	4.12
1: 6 Active fibre (14.3 % (w/w) drug load)	7.89
1: 8 Active fibre (11.1 % (w/w) drug load)	8.99
Placebo fibre	21.82
Pure E-EPO	22.84

Figure 3.37 shows a PCA bi-plot illustrating the distances from pure CPM. PCA showed that the basic bitterness sensor AC0 was responsible for Principal Component 1 (94.98 % of variance). AN0, the second basic bitterness sensor was responsible for the second principal component. The dataset is projected onto a space relative to their distance from the two main principal components,

which represent the axes of the map and correspond to the variance in the data.

This has a cumulative variance of 99.7 % which indicated that the change in data observed can be explained by the true change in taste as detected by the bitterness sensors. The upper right quadrant in the bi-plot shows pure CPM located in the direction of the AN0 and AC0 vectors, indicating its basic bitter taste. Pure E-EPO seems to elicit an acidic bitter response relative to the other samples; when formulated by electrospinning, the placebo fibre's C00, or acidic bitterness response, was decreased compared to pure E-EPO. The physical mixture and drug-loaded fibres, are neither located in the basic bitterness or acidic bitterness quadrants. This indicates that both the addition of the taste-masking polymer E-EPO and the process of electrospinning reduces the bitterness sensor response, relative to the other samples tested, concluding that the technique is capable of effectively coating bitter drugs.

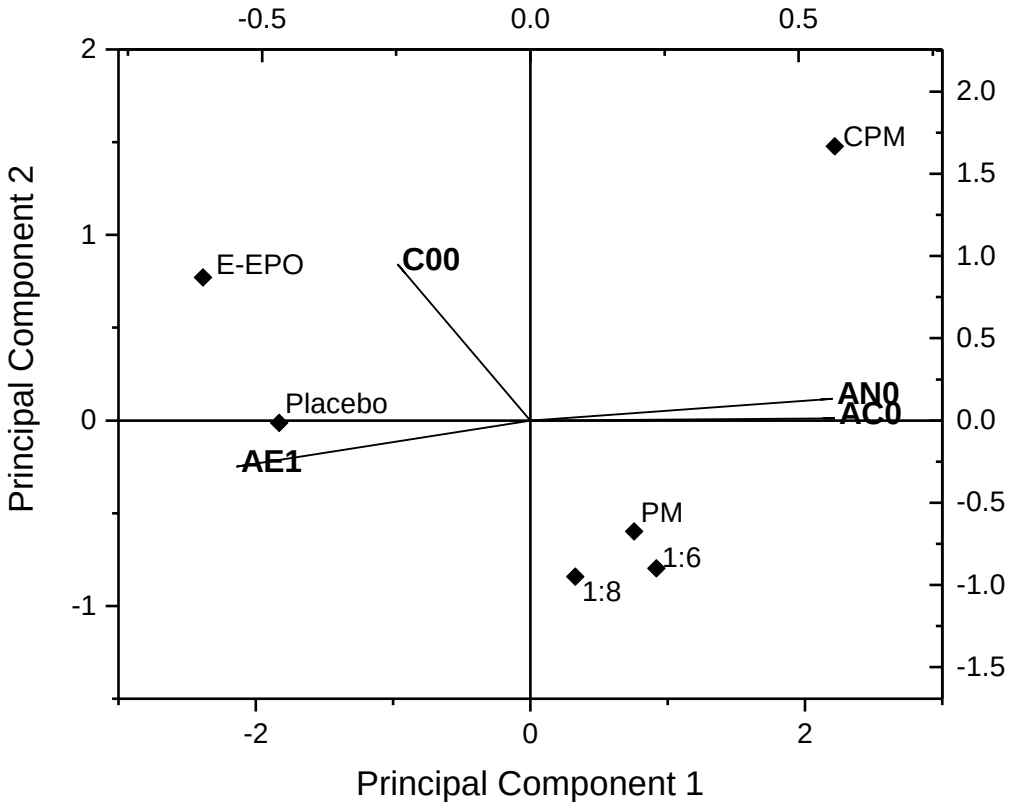

Figure 3.37. PCA biplot of drug loaded fibres compared to their physical mixtures, placebo fibre, pure E-EPO and pure CPM.

In addition, astringency seems to be evident as seen in Figure 3.36, but when the formulations are taste-masked, this seems to be reduced. Figure 3.38 shows the taste-masking effect of electrospinning CPM with E-EPO on the astringency profile. The difference between CPM and the physical mixture was not statistically significant (*p*-value = 0.0736), whereas the difference between CPM and the and drug-loaded and placebo fibres were statistically significant and all had a *p*-value of less than 0.0001. No astringent aftertaste was detected in the samples using this sensor.

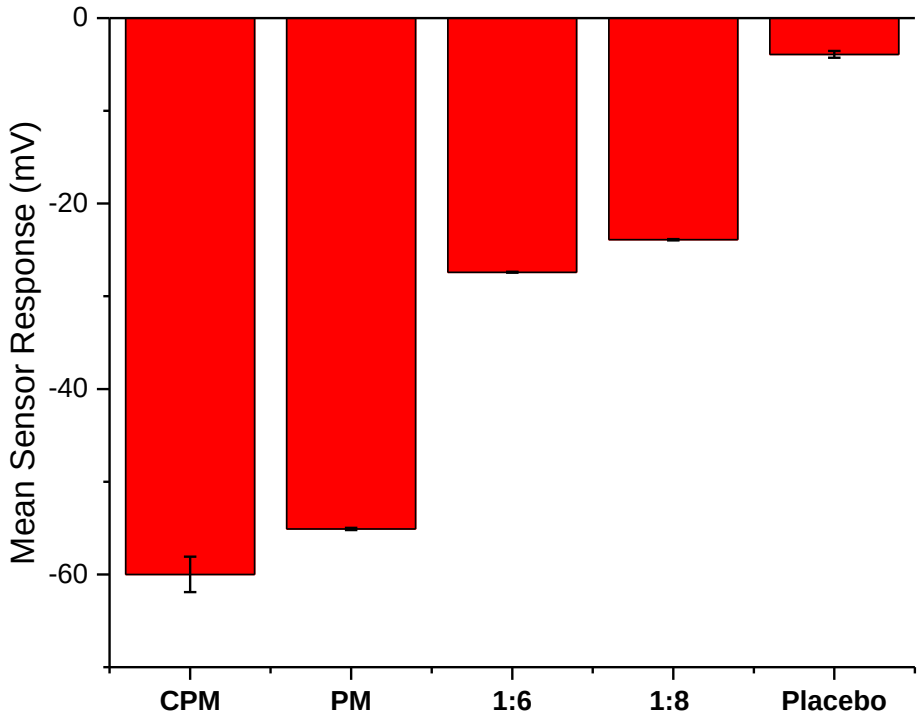

Figure 3.38. Bar chart showing astringency output for raw materials and electrospun fibres. CPM amount tested = 20 mg / 100 mL or 0.5 mM.

3.3.9.2 Biorelevant Dissolution

A bio-equivalent flow-through oral dissolution apparatus was used to further confirm the taste-masking of the drug-loaded E-EPO nanofibres [115]. Figure 3.39 shows the release of CPM from an electrospun film in SSF as well as the bitterness threshold of the drug in humans, 0.506 mg/mL, a value derived from the literature [115].

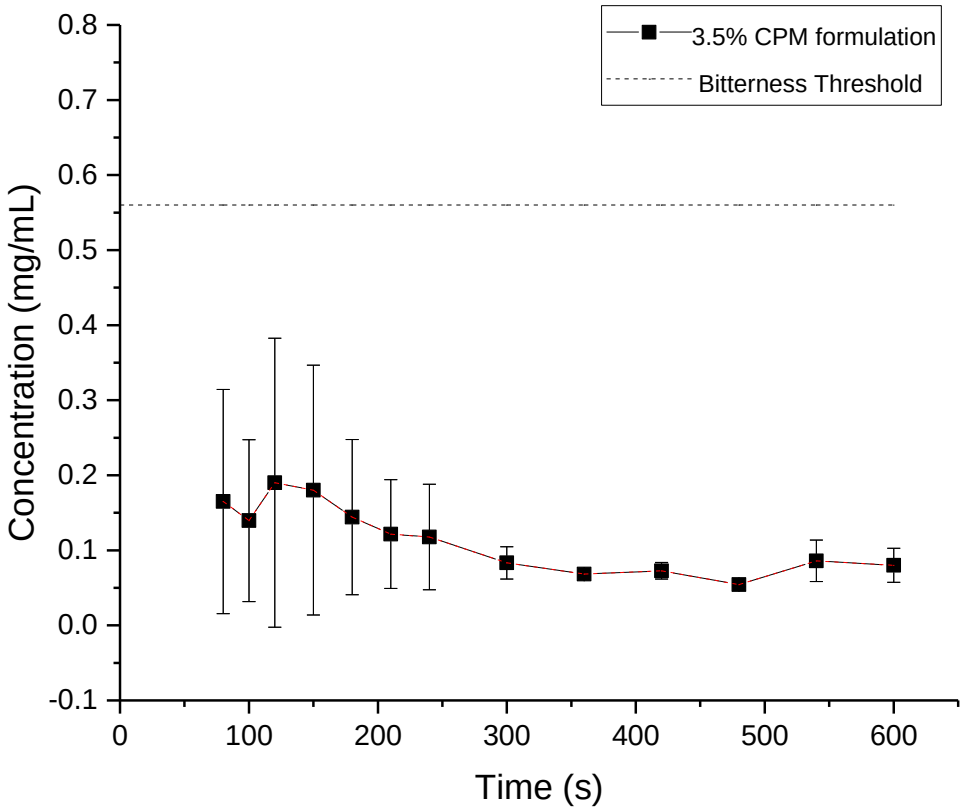

Figure 3.39. Release of CPM in SSF in a bio-equivalent dissolution apparatus. The dashed line represents CPM's bitterness threshold in human.

The fibres tested contained a theoretical amount of 10.54 mg ± 1 mg of CPM. The bitterness threshold of CPM, represented by the dashed line, is 0.506 mg/mL. The concentration of drug released at different time points up to 600 s (10 minutes) are represented on the scatter plot. It can be seen that at the dose tested, the electrospun fibres did not allow CPM release over the ten minutes sufficient to exceed the bitterness threshold and therefore indicating adequate taste-masking. It is to be noted that, similar to the E-tongue results, some drug release is observed and therefore if a higher dose is to be administered further taste-masking will be required.

3.4 **Conclusions**

In summary, electrospinning is a promising technique in the formulation of a taste-masked paediatric dosage form, however, it is affected by a number of parameters. Although using an OFAT approach initially did help gain some

understanding of the effects of certain parameters such an optimum flow rate, applied voltage and gap distance, it is not very methodical and can be time-consuming.

Utilising a DoE definitive screening design aided in gaining a deeper understanding of the effect of process and solution parameters on the electrospun fibres. The DoE definitive screening design has allowed both the screening of the most influential manufacturing conditions for nano-diameter fibres and absence of beading as well as the prediction of optimal conditions for both outcomes when combined. Polymer concentration was found to be the most influential factor in producing optimised E-EPO placebo fibres, with a chain entanglement concentration of 32.5 % (w/v) in ethanol. The study has therefore not only suggested parameters for producing E-EPO fibres but has also developed an approach for the rational choice of electrospinning conditions, which guided the next stage of the project; electrospinning drug loaded E-EPO.

Adding CPM to E-EPO changed both the conductivity and viscosity of the solutions, and therefore yielded fibres with a different morphology. At ratios higher than 1:4, fibre formation decreases, and particles are observed. At polymer concentrations higher than 35 % (w/v), spinneret clogging becomes very problematic and disrupts the continuation of manufacturing. In summary, the optimised polymer concentration for both drug-loaded and placebo fibres was found to be 35 % (w/v). It was shown that at a drug to polymer ratio of 1:6, 35 % (w/v) E-EPO is the optimum percentage of drug that allows for the transfer of process conditions. 35 % (w/v) E-EPO fibres that have drug loads of 1:6 to 1:10 yielded reproducible smooth, non-beaded fibres. The drug-loading assessment showed that the fibre samples tested actually showed a higher drug amount than anticipated, which may be a result of needle clogging and therefore an increased drug amount per polymer present in the final formulation. This will need to be addressed in future work through further optimisation of the Taylor cone stability.

TGA identified decomposition temperature of raw materials and showed that there was no residual solvent left in the fibres, an important parameter for an oral dosage form intended to be used in children. XRD and MTDSC confirmed the presence of the drug in the electrospun fibre matrix as an amorphous solid dispersion. In addition, FTIR studies showed that no new bonds were formed, confirming these findings. AFM analysis showed that the drug's addition to the fibres made them less brittle which may be a desirable feature for an oral film in terms of handling and acceptability.

The final formulation choice was dependent on a functional assessment output; taste-assessment. A biorelevant *in-vitro* dissolution model showed that the 1:10 formulation did not release a drug amount higher than that of the human bitterness threshold, therefore showing adequate taste-masking. Nonetheless, if a higher dose is required, more taste-masking will be needed. Using the E-tongue, drug loaded fibres were found to have a larger Euclidean distance than the physical mixture, indicating taste-masking. 1:8 fibres had a larger distance than 1:6, indicating a drug-loading relationship. However, drug loaded fibres' Euclidean distances were closer to the physical mixtures than the placebo fibre, which may indicate some drug release, or drug presence on the fibre surface. Fibres with an even lower drug load might yield a better taste-masked formulation, which can be part of the future work planning.

Finally, the fibre's release study showed that they released all the drug content at a very similar time to the raw drug, and within the pharmacopeial (Ph. Eur. 5.17.1) requirements of 70 % release within 45 minutes for a formulation to be considered immediate release. Therefore, the taste-masking strategy used does not seem to affect the drug release and hypothetically the pharmacological action of the drug.

Chapter 4

The Use of Co-axially Electrospun Eudragit E PO and Kollicoat Smartseal to Taste-mask Chlorpheniramine Maleate

4.1 Introduction

In the previous chapter [98], Quality by Design (QbD) principles were applied to optimise the electrospinning of Eudragit E PO (EPO), a pH sensitive taste-masking polymer. This involved the incorporation of a model bitter drug, chlorpheniramine maleate (CPM), a bitter anti-histamine commonly used in children. A Design of Experiment approach was utilised to identify the optimum electrospinning process and solution parameters to produce bead-free nanofibres. It was found that E-EPO's chain entanglement concentration is between 30 % (w/v) and 35 % (w/v) and the optimum solvent to use to optimise the parameters mentioned is ethanol.

The initial phase of optimising E-EPO focused on the mechanical properties of the fibres, resulting in unbeaded fibres in the nano-range. To maximise the taste-masking potential of the electrospun fibre mat, co-axial electrospinning was used. In this study, the plan was to incorporate another taste-masking polymer: Kollicoat Smartseal (KCT). Co-axial electrospinning incorporates two needles embedded within each other, creating a core solution and a shell solution [203], [204]. Different materials can be used to produce a fibre mat with varying functions, such as controlled release [151] or taste-masking. It has been reported that both solutions need not to be electrospinnable, especially the core solution, as the shell solution can ensure the viability of the electrospinning process [68]. On the other hand, If the shell solution is unspinnable and the core solution is what drives the process forward, this is termed modified electrospinning and allows the generation of fibres from a wider range of materials [205]. In co-axial electrospinning, the API can be incorporated in either the core or the shell depending on the final function. Using a bi-layered approach, it becomes possible to incorporate more than one drug with differing release patterns by altering the carrier polymers [206]. It is worth noting that as with monoaxial electrospinning, careful optimisation of both solutions is required to ensure the presence of a stable Taylor cone and consequently defect-free fibres.

In this work, co-axial electrospinning was utilised for its taste-masking potential. Only one report was found to explicitly state using co-axial electrospinning for this purpose; a fast-dissolving film incorporating helicid and PVP in the core, and sucralose, a sweetener, in the shell layer [84]. A PVP/acyclovir core was prepared with a PVP/sucralose/sodium dodecyl sulfate shell. The sucralose was added to hide the metallic taste of the drug, although no taste-assessment was performed [207]. Co-axial electrospinning was also used to prepare fast-disintegrating films of quercetin with PVP in the core and PVP in the shell; taste-assessment was not performed [208].

As a continuation of our previous research, the model bitter drug used was CPM. In addition to using E-EPO, KCT was also used to taste mask the bitter drug. KCT is a moisture and pH sensitive polymer that conceals bitter tastes and creates a moisture barrier around the formulation [114], therefore, was an ideal candidate for the oral film formulation design.

Oral films have a considerable potential to be used in children due to their numerous advantages including thin feel, improved swallowability compared to other solid dosage forms, and lack of water necessity [209]. There are no reports in the literature of KCT being electrospun before. Here, therefore, it is initially explored whether KCT can be electrospun at all. If the aforementioned proves successful, co-axial electrospinning using the two taste-masking polymers will be tested to assess whether the use of both of them is more effective than using either of the polymers alone with regards to taste-masking.

Taste-assessment of a pharmaceutical dosage form is very important to ensure a medicine will be deemed palatable by the target population [210]. In this study an E-tongue was used to taste-assess the formulations produced. Our overarching aim for this study was to find the best polymer combination to produce a fully taste-masked formulation as verified by the E-tongue.

4.2 Methods

4.2.1 Preparation of Precursor Solutions

E-EPO solutions were prepared by dissolving (30 to 35) % (w/v) E-EPO in absolute ethanol. The mixture was then magnetically stirred for approximately two hours. Drug-loaded E-EPO solutions were prepared by adding CPM directly to the polymer solution at a concentration of 3.5 % (w/v).

KCT 30D, an aqueous solution, is miscible with ethanol at a ratio of 1:3. As the polymer is supplied as a 30 % (w/v) solution, after dilution with ethanol a 7.5 % (w/v) polymer solution is formed. Drug-loaded KCT solutions were prepared by adding CPM directly to the polymer solution at a concentration of 3.5 % (w/v). Rhodamine B (0.01 % w/v) was added to the core solutions for viewing with fluorescence microscopy.

4.2.2 Electrospinning

In case of monoaxial electrospinning of KCT, the syringe was connected to a stainless-steel needle, with a diameter of 0.9 mm, via a connector tube. The viscous solution was fed through the needle at flow rates between 0.5 mL/h and 2 mL/h. Applied voltages of up to 25 kV were applied to the polymer solutions, evaporating the solvent, allowing the solid fibres to deposit on a grounded metal plate collector 14.5 cm × 23 cm. The gap distance between the needle and the collector plate was set between 10 cm and 20 cm. Room temperature (°C) and relative humidity (RH) (%) readings were recorded. The temperature ranged between 21 °C and 28 °C and the RH ranged between 26 % and 46 %.

4.2.3 Co-axial Electrospinning

The co-axial emitter used had a diameter of 0.9 mm for the outside needle and 0.45 mm for the inside needle. A representative image is shown in Figure 4.1. Inside and outside needles were the same length at 10 mm from the hub. In order to find the optimum formulation for taste-masking CPM, 7.5 % (w/v) KCT

and 35 % (w/v) E-EPO were alternated between the core and shell solutions. The flow rates used were 0.45 mL/h for both the core and shell solution. The gap distance was set between 15 cm and 17.5 cm and the applied voltage was between 15 kV and 20 kV.

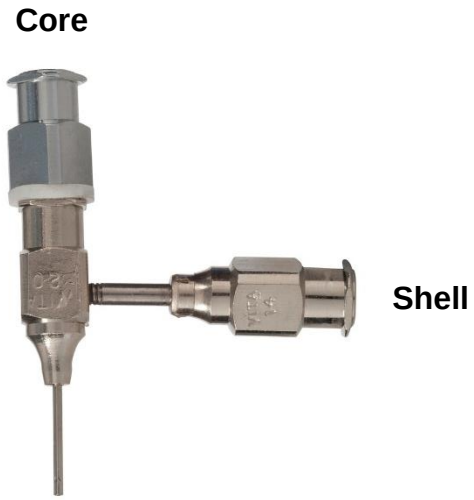

Figure 4.1. A picture of a co-axial emitter. Taken from www.spraybase.com.

4.2.4 Light Microscopy

Fibres were collected directly on microscope slides during electrospinning and then viewed under the light microscope Leica DM2700 M (Leica Microsystems, Wetzlar, Germany). Background information on the light microscope can be found in Chapter 2, Section 2.5.3.

4.2.5 Fluorescence Microscopy

Core solutions were dyed with the flurochrome Rhodamine B, electrospun, and samples collected on a glass microscope slide. Slides were then viewed on an EVOS FL imaging system (Thermo Fisher Scientific, Loughborough, UK) under Texas Red light. Images were saved and visually inspected for the core-shell structure. Background details of the technique are described in Chapter 2, Section 2.5.6.

4.2.6 Scanning Electron Microscopy

The samples were analysed by SEM as described in Chapter 2, Section 2.5.4. Fibre size analysis was performed by measuring the diameter of 100 fibres using ImageJ 1.46R software (National institute of health, Maryland, USA).

4.2.7 Transmission Electron Microscopy

Fibres were collected on a copper grid (to allow passage of electrons) during electrospinning. They were then stained with 2 % aqueous uranyl acetate solution prior to imaging with a TEM FEI CM120 BioTwin (FEI Company, Oregon, USA) at an accelerating voltage of 120 kV. This technique is described in further detail in Chapter 2, Section 2.5.5.

4.2.8 Thermogravimetric Analysis

The technique was used as described in Chapter 2, Section 2.5.11; samples were tared and analysed in an open aluminium Perkin Elmer pans with a heating rate of 10 °C/min from 30 °C to 500 °C.

4.2.9 Differential Scanning Calorimetry

The method was as described in Chapter 2, Section 2.5.9. Samples were heated under nitrogen gas (flow rate 50 mL/min) at a rate of 2 °C/min ramped up to 150 °C, amplitude ± 0.212 °C and a period of 40 s. Samples' weights ranged from 4 mg to 8 mg and were sealed in a 40 µL aluminium Perkin Elmer standard pan.

4.2.10 UV Spectroscopy and Drug Loading

The background to the method is described in Chapter 2, Section 2.5.8. A standard curve (R^2 = 0.9998) of CPM was plotted using absorbance data recorded using a Jenway 6305 UV-vis spectrophotometer (Bibby Scientific, Staffordshire, UK). Absorbance was recorded at 262 nm (λ_{max}). Drug loading

was calculated by using the slope = 0.01248 and intercept = 0.04057 of the standard curve. All measurements were taken in triplicate.

Film samples weighing approximately 10 mg were measured out and dissolved in 10 mL of ethanol. This was repeated three times. Each sample was tested three times using UV spectroscopy. Therefore, 9 samples were tested for each formulation to ensure the reading is both accurate and precise. For each sample, the theoretical drug-load was calculated as follows:

Equation 4.1

$$Concentration\ of\ each\ Polymer\ (\%\ w/v)\ \times flow\ rate\ \left(\frac{mL}{h}\right) = sum\ of\ all\ polymer\ content\ (\%\frac{w}{v})$$

$$API\ concentration\ (\ 3.5\ \%\ w/v)\ \times flow\ rate\ \left(\frac{mL}{h}\right) = drug\ content\ (\%\frac{w}{v})$$

$$Theoretical\ Drug\ loading\ \left(\%\frac{w}{w}\right) = \frac{drug\ content\ (\%\frac{w}{v})}{sum\ of\ all\ polymer\ and\ drug\ content(\%\frac{w}{v})}$$

For example, for a 35 % (w/v) E-EPO core and 7.5 % (w/v) KCT shell formulation, the polymer content sum is (0.45 x 35 = 15.75) + (0.45 x 7.5 = 3.375) = 19.125; the drug content is (0.45 x 3.5 = 1.575); and the theoretical drug load therefore is; 1.575/ (19.125 + 1.575) *100 = 7.6 % (w/w). Using this theoretical percentage, the amount of the drug in the samples tested was calculated. The absorbance readings for the samples tested were inserted in the calibration curve to give a concentration measurement. After accounting for dilution factors, a mean number was calculated, which is represents the actual drug-loading in the results section. This value was then divided by the theoretical drug amount and multiplied by a 100; this gave rise to a % drug loading efficiency of the actual drug amount divided by the theoretical drug amount.

As the core and shell solution's flow rate were set at a 1:1 ratio, the theoretical drug-load of the co-axial system was calculated as follows; for co-axial system 3 which contained 35 % (w/v) in both the core and shell, the drug loading was 4.76 % w/w. For co-axial system 4 that contained 7.5 % (w/v) of KCT in both the core and shell solutions, the drug loading was 18.9 % w/w. For co-axial systems 2 and 5 which contained both 35 % (w/v) E-EPO plus 7.5 % (w/v) KCT in either the shell or the core, the drug loading was 7.6 % (w/w). In all systems the amount of drug actually added was the same at a concentration of 3.5 % (w/v).

4.2.11 Powder X-Ray Diffraction

Characterisation of the solid-state of KCT in addition to the co-axial formulations were completed using a Rigaku MiniFlex 600 X-Ray Diffractometer (Rigaku, Tokyo, Japan) as described in Chapter 2, Section 2.5.10. Patterns were recorded over the 2θ range 3º to 40º at a scan rate of 3 º/min, with an interval of 0.02 º.

4.2.12 Fourier-Transform Infrared Spectroscopy

The background to the method is described in Chapter 2, Section 2.5.12. FTIR studies were performed using a Spectrum 100 FTIR spectrometer (Perkin-Elmer, USA) and spectra were collected in the range of 4000 cm^{-1} to 650 cm^{-1} with a total of 16 scans and a resolution of 2 cm^{-1}, unless otherwise stated. Background scans were performed for all experiments and each sample was analysed in duplicate to check the reproducibility of the spectra.

4.2.13 Statistical Analysis

All experiments were conducted in triplicate unless otherwise stated. All data were presented as mean value ± standard deviation.

4.2.14 E-tongue Taste-assessment

The method is as described in Chapter 2, Section 2.6.1. BT0 taste sensor was used to ascertain the bitterness of the films. To ensure the data produced by this sensor was reliable, a non-linear Boltzmann fitting function was performed on the initial and aftertaste responses. This was completed using OriginPro 9.4 (Origin Lab, Massachusetts, USA).

4.2.14.1 Bitterness Threshold

The bitterness threshold of CPM was calculated as a comparison to Quinine HCl, a commonly used bitter standard drug with known bitterness and aversiveness levels in humans. In human taste panels, bitterness thresholds are determined by selecting the concentration of the drug that produces half of the maximal rating (100), known as the EC_{50} [211]. For the E-tongue, bitterness thresholds are deduced by using the human EC_{50} for quinine hydrochloride dihydrate, and finding the corresponding mean sensor response at that value [91].

Sensor output is proportional to the logarithmic concentration of a test substance, which is based on the Nernst equation:

Equation 4.2

$$U = U^0 + \frac{RT}{zF} \ln a_i$$

where U = electrode potential; U^0 = standard electrode potential; R = universal gas constant; T = temperature (K); z = ionic valence of the substance; F = Faraday constant; a_i = activity of the substance.

Equation 4.3

$$a_i = f_i c_i$$

where c_i = concentration of the substance; f_i= activity coefficient of the substance [212].

Therefore, sample concentrations equivalent to intervals on the logarithmic scale were prepared (0.01 mM up to 10 mM). To benchmark CPM, other standard bitter drugs were tested for their bitterness, and a rank order was prepared and compared to literature data of human sensory analysis. This work was conducted with the help of Ms Wan Ting Quek. The drugs were purchased as follows; caffeine citrate (MP biomedicals, Leicester, United Kingdom), ethambutol dihydrochloride (Sigma Aldrich, London, United Kingdom), sildenafil citrate (Fagron, Newcastle upon Tyne, United Kingdom) and ibuprofen sodium (Santa Cruz, Heidelberg, Germany). Dose response curves were plotted using GraphPad Prism 7.04 (GraphPad Inc., San Diego, CA, USA).

4.2.14.2 Sample Preparation of the Fibres

Taste extracted liquids were used for biosensor assessment of the electrospun fibre mats, and materials that are insoluble in the media's pH, such as KCT and E-EPO. Measurement of fibres were calculated as the corresponding mass of fibre that will contain 20 paediatric doses of CPM (20 mg) in a 100 mL, which equates to 0.5 mM. For example, for co-axial systems 2 and 5 that had a theoretical drug-load of 7.6 % (w/w), 263 mg of fibres needed to be measured for assessment of a 100 mL. The fibres were added to 100 mL of 10 mM potassium chloride solution, as a supporting electrolyte, at 37 °C and gently stirred for 1 min. The mixture was then filtered through 0.22 µm filters (Merck-Millipore, Cork, Ireland), removing any suspended particles.

4.2.14.3 Data Analysis

All measurements were repeated four times. The data from the first run were discarded to allow for the conditioning of sensors. In this study, a solution of 10 mM potassium chloride was used as a control sample, and the corresponding sensor responses were subtracted from the sensor responses of the samples. Hence, all data produced are a mean of three measurements and represent relative sensor responses. Multivariate PCA was performed on the data collected; this aided visualisation of the high number of data points on a two-dimensional map. Differences between samples were assessed by

determining the Euclidean distances which were calculated from the cluster centre [63]. All data analysis was carried out using OriginPro 9.4 (Origin Lab, Massachusetts, USA).

4.2.15 Dissolution

The full method is described in Chapter 2, Section 2.5.15. A Sciquip mini shaker (SciQuip, Wem, UK) was used to investigate the release of CPM in stomach conditions of pH 1.2. 0.1 N HCl was used as the dissolution media. 1 mL aliquots were removed and replaced with fresh media at the following time intervals: (1, 5, 10, 15, 20, 30, 45, 60, 90 and 120) minutes. Removal and replacement of fluid was taken from the same position on all occasions. a media volume of 15 mL was used. Samples were placed in glass vials and the mesh cover dropped over them at the beginning of the time. Drug amount released was measured using UV spectrophotometry at wavelength of 262 nm. Fibre samples measured 12.30 mg ± 0.7 mg and had a theoretical drug load of 4.76 %, 7.6 % or 18.9 % (w/w). Equation of calibration curve in release media: $y = 0.0197x + 0.021$, $R^2 = 0.993$. A 1 mL quartz cuvette was used, and all experiments were performed in triplicate. Data were collated and analysed using OriginPro 9.4 (Origin Lab, Massachusetts, USA).

4.2.16 Film Thickness and Folding endurance

Method as described in Chapter 2, Section 2.5.14.

4.3 Results and Discussion

4.3.1 Electrospinning

4.3.1.1 Kollicoat Smartseal 30 D

The KCT polymer solution was successfully electrospun alone at an applied voltage of 20 kV, flow rate of 1 mL/h and gap distance of 17.5 cm. Figure 4.2 shows KCT fibres using SEM imaging, with a histogram showing the fibre diameter distribution. The mean fibre diameter was measured as 565 nm ±

206 nm, which is in the desired nano-range. It can be seen from the image that the fibres were not perfectly bead-free, with some spindle formation. As this is planned to be used as part of a co-axial electrospinning process, there is leeway for the solution to be less electrospinnable than the 2nd solution to be used in the process [68]. The drug-loaded fibre had a mean fibre diameter of 1222 nm ± 250 nm and was electrospun at an applied voltage of 8 kV, flow rate of 0.5 mL/h and gap distance of 17.5 cm. An image of the fibres and the histogram fibre diameter distribution is shown in Figure 4.3. It can be seen that the fibres had overall a narrow fibre diameter distribution and generally had a smooth appearance with no apparent beading. There are no reports in the literature of Kollicoat Smartseal being electrospun before.

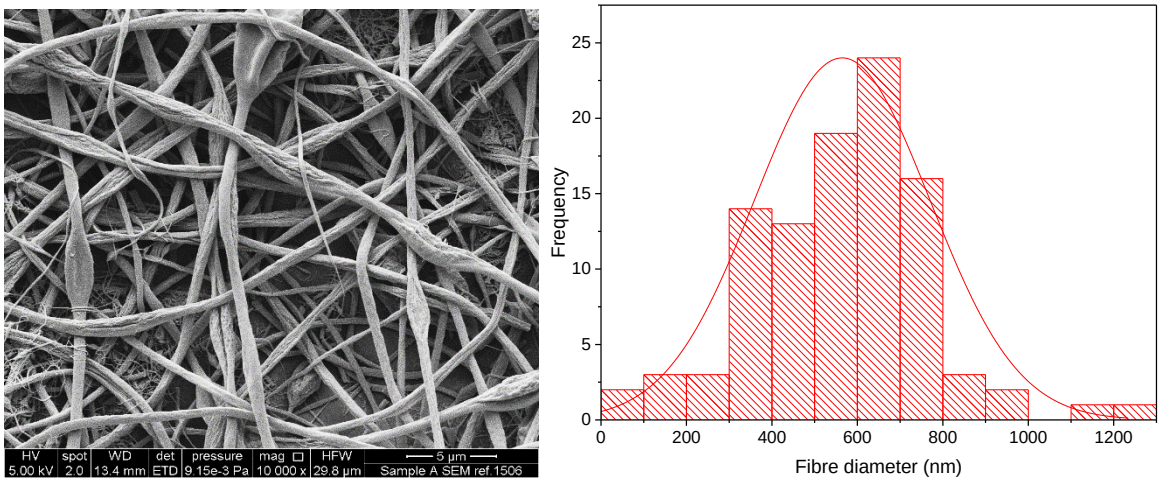

Figure 4.2. SEM of Electrospun KCT fibres in addition to a fibre diameter distribution histogram.

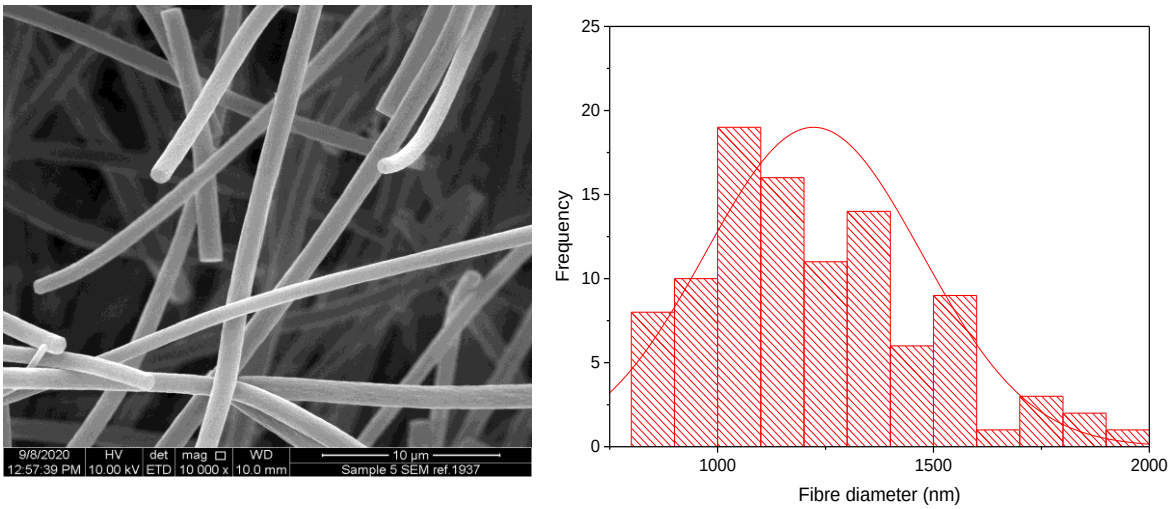

Figure 4.3 SEM of drug-loaded Electrospun KCT fibres in addition to a fibre diameter distribution histogram.

4.3.2 Co-axial Electrospinning

Optimum electrospinning parameters for E-EPO were taken from Abdelhakim et al [98]. In combination with KCT, the two polymers were alternated between core and shell positions and co-axially electrospun together. The reason they were alternated was to find the most optimum bead-free fibres as well as a fully taste-masked formulation for the bitter drug CPM.

Table 4.1 shows the composition of the different co-axial solutions spun and also contains the drug-loading efficiency and the mean nanofibre diameter.

Table 4.1. The formulations tested had KCT and E-EPO alternating between the core and shell solutions. CPM was always added at 3.5 % (w/v) in the core apart from sample 1, a placebo. The table shows the drug loading efficiency and mean diameter of the nanofibres.

Co-axial Sample	Core	Shell	Theoretical drug loading (% w/w)	Actual drug loading ± SD (% w/w)	Drug loading efficiency ± SD (%)	Mean ± SD Diameter (nm)	Diameter RSD (%)
1	**KCT**	E-EPO	N/A	N/A	Placebo	1220 ± 501	41
2	**KCT**	E-EPO	7.6	7.4 ± 0.4	97.5 ± 5.3	795 ± 505	64
3	E-EPO	E-EPO	4.8	5.3 ± 0.2	111.3 ± 4.2	616 ± 228	37
4	**KCT**	**KCT**	18.9	17.8 ± 3.6	94.2 ± 19.0	967 ± 262	27
5	E-EPO	**KCT**	7.6	7.0 ± 1.6	92.1 ± 21.1	633 ± 271	43

It can be seen from that the two polymers were alternated (samples 2 and 5) as well as repeated (samples 3 and 4) in the core and shell structure. This was to compare taste-masking outcomes and to determine whether there was a real difference. Sample 1 is a placebo structure that contained E-EPO in the shell and KCT in the core. This arrangement was chosen because E-EPO solution is more electrospinnable than KCT solution hence was placed in the shell, believed to be the dominant driving solution for the co-axial process [213].The placebo fibres had the largest average fibre diameter, likely due to

the lack of drug presence and therefore low charge density [71]. The drug loading efficiency of the co-axial 4 and 5 fibres had a large distribution as indicated by the SD %, and this is likely due to intermittent needle clogging and hence uneven distribution of drug particles in some areas of the fibre mat [214]. The sample with the narrowest drug loading distribution was 3, which consisted of only E-EPO. This can be explained by the fact that E-EPO is well optimised to be electrospun therefore the jet stream is consistent with minimal clogging or interruption, leading to uniform fibre formation.

Figure 4.4 shows the morphology and fibre diameter distribution of the five different formulations spun. It can be seen that samples 1 to 3 generally have a smooth structure, whereas samples 4 and 5 are more spindled. This is likely due to the fact that KCT is in the shell portion of the co-axial structure in those formulations, and due to its low spinnability compared to E-EPO, the fibres are less smooth. Fibres 1 and 2 contain both KCT and E-EPO, with E-EPO being in the shell. As previously mentioned the needle tip did get clogged and due to cleaning it, breakages happen in the fibre, as seen on the SEM images. System 1 is placebo, whereas system 2 is drug loaded. This is reflected in the fibre diameter, as the drug-loaded system is expected to have a higher charge density and therefore leads to thinner fibre formation [215].

Systems 2 and 3 are fairly similar because E-EPO is in the shell of both of them, nonetheless, system 3 has smaller average fibre diameters due to the improved electrospinnability and therefore jet elongation and stretching [191]. System 4 had wavy fibres that were not as smooth as E-EPO alone, and this is because KCT is not as well electrospun on its own due to its high-water content and therefore this webbed appearance may occur due to lack of enough time to allow for solvent evaporation. With this in mind, system 5 had KCT in the shell and therefore also is less smooth compared to the systems with E-EPO in the shell, however, is still smoother than 4 because it has E-EPO in the core. System 5 had a significantly smaller diameter than the rest of the systems, due to the elongation of the fibres between the formed spindles. The spindles likely formed as this modified co-axial system was not fully optimised, where the core solution is spinnable but the shell is not [216].

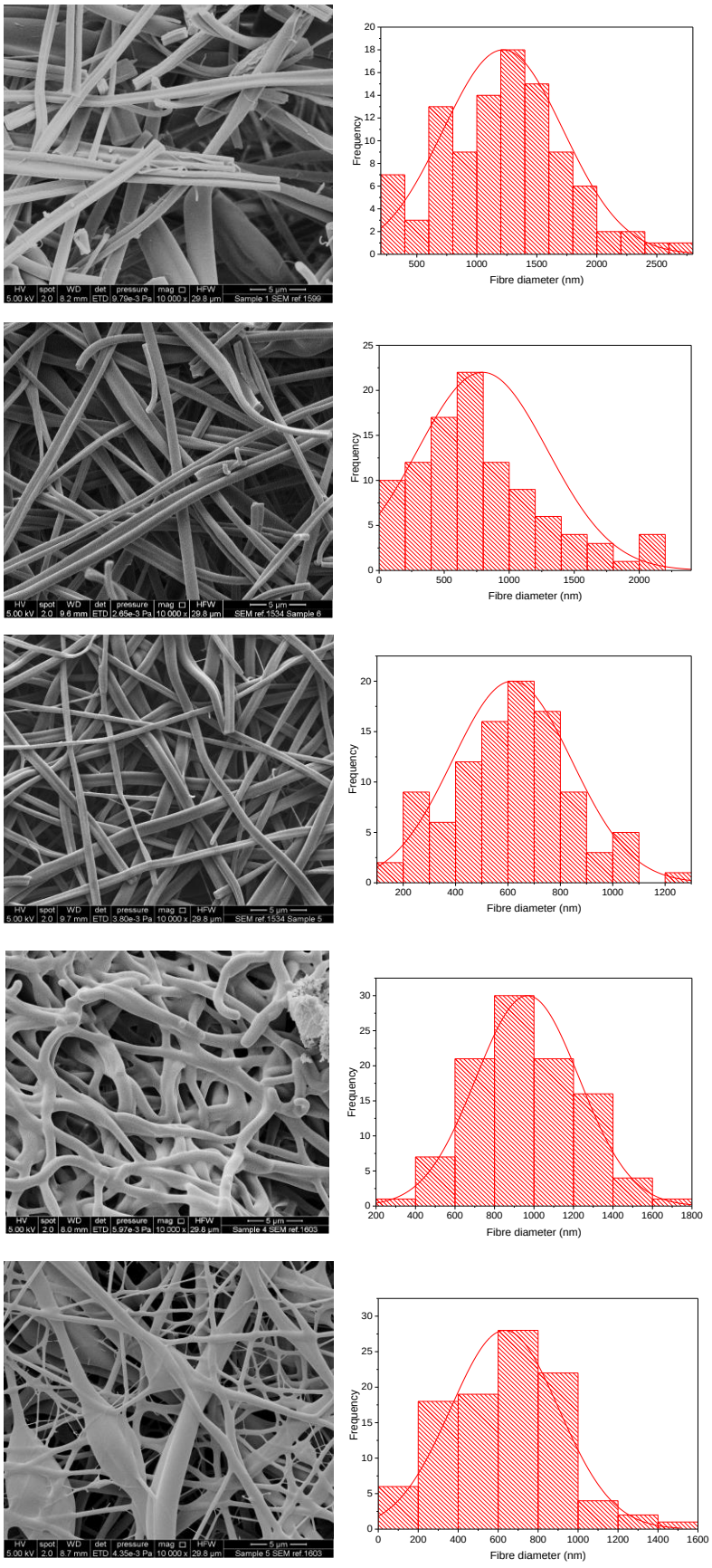

Figure 4.4. SEM Images of the five co-axial formulations tested. The histograms represent distribution of fibre diameters. The images from top to bottom represent samples 1 to 5.

Figure 4.5 shows the FL microscopy images of the samples in both black and white and with the Texas Red light filter on, which illuminates Rhodamine B that was loaded in the core of all the formulations tested. Both the optical microscopy images and the fluorescent images have an identical appearance, indicating that all the nanofibres represented were successfully loaded with the drug-loaded core solution that contained rhodamine. As the fluorescent image shows homogenous distribution of the dye, it can be assumed that the drug has been loaded homogenously in the nanofibres [217].TEM images are also shown in Figure 4.5. It can be seen that the five co-axial formulations imaged, a separate core-shell structure was not seen. This is likely due to the fact that the solutions were miscible and therefore a definite barrier was not formed. Nonetheless, co-axial electrospinning here was used to improve the taste-masking barrier, which is discussed in further detail in Section 4.3.7.

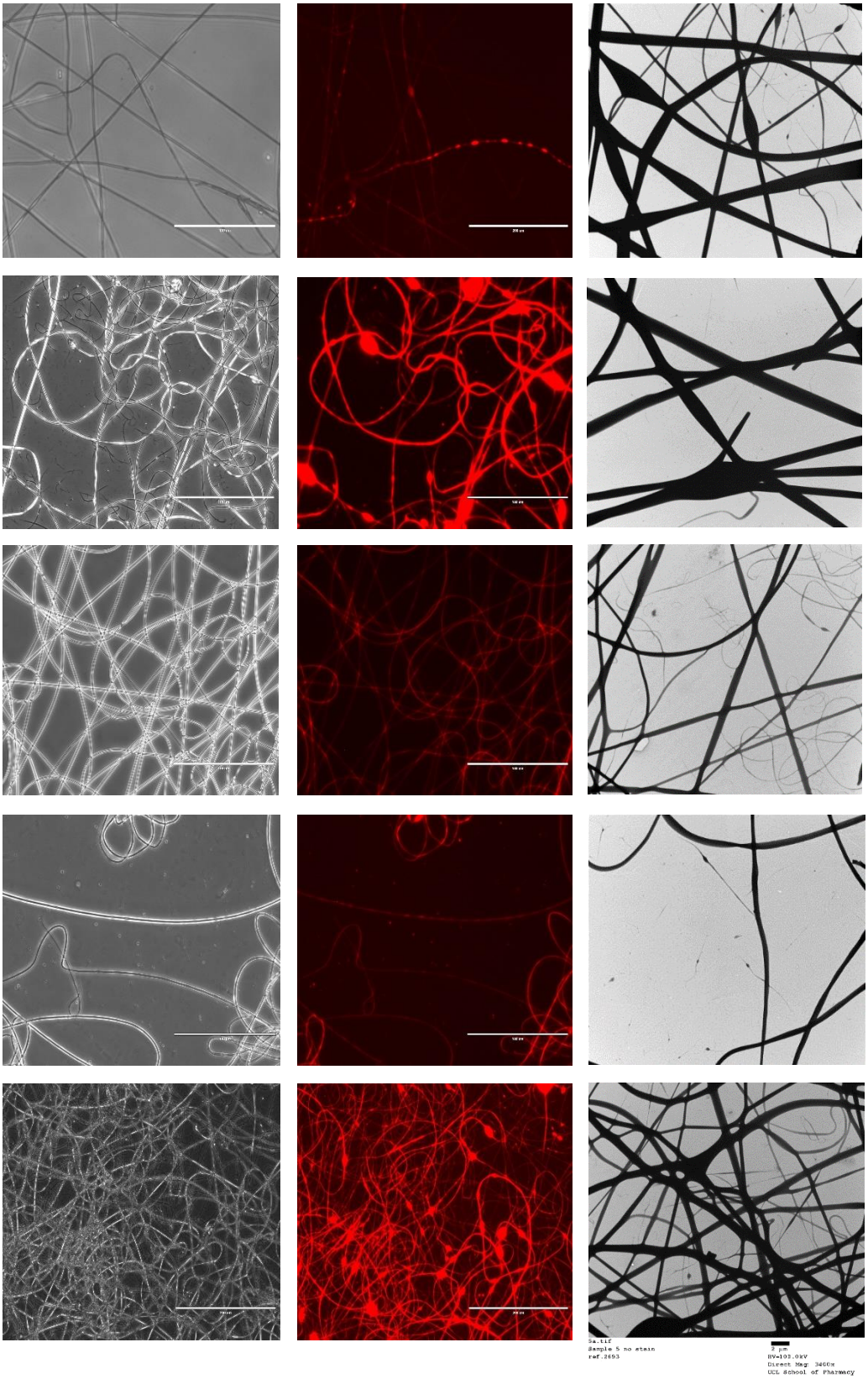

Figure 4.5. The five co-axial formulations are shown as 1 to 5 from top to bottom. Left column images represent light microscopy. Middle column represents FL microscopy and TEM images are represented in the final column.

4.3.3 Solid State Characterisation

4.3.3.1 Powder X-Ray Diffraction

Figure 4.6 shows the XRD diffraction pattern of all the co-axial systems and the raw drug and polymers. CPM shows a crystalline structure as identified by the clear diffraction peaks. KCT and E-EPO show amorphous structures as shown by the halos. The electrospun fibres clearly lack the distinctive diffractions peaks observed in the crystalline CPM pattern, indicating an amorphous molecular dispersion formation. The placebo fibre shows a similar diffraction pattern to the drug-loaded diffractograms, confirming this finding.

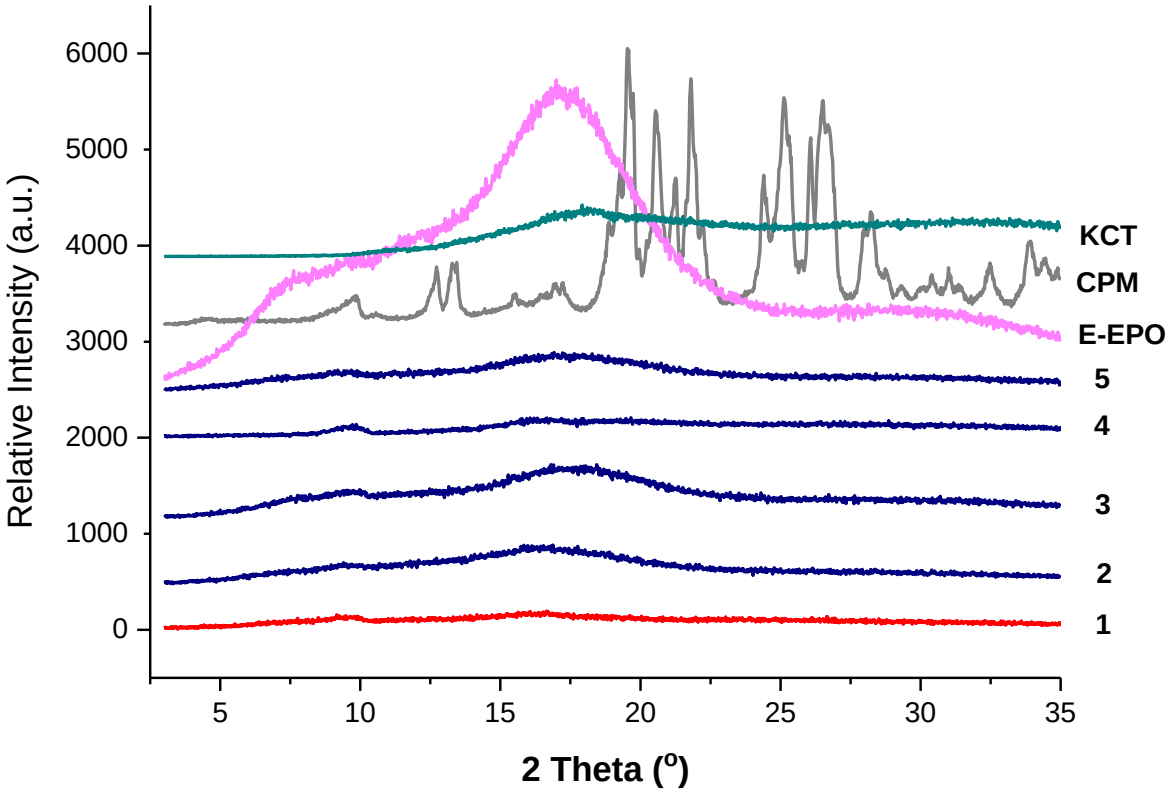

Figure 4.6. XRD diffraction patterns of pure CPM, E-EPO, KCT and the five co-axial systems electrospun.

4.3.3.2 Fourier Transform Infra-Red

Figure 4.7 shows the FTIR spectra of the raw ingredients and the electrospun co-axial systems. Methacrylate polymers have characteristic peaks at around 1730 cm^{-1}, due to the presence of C=O groups in their molecules.

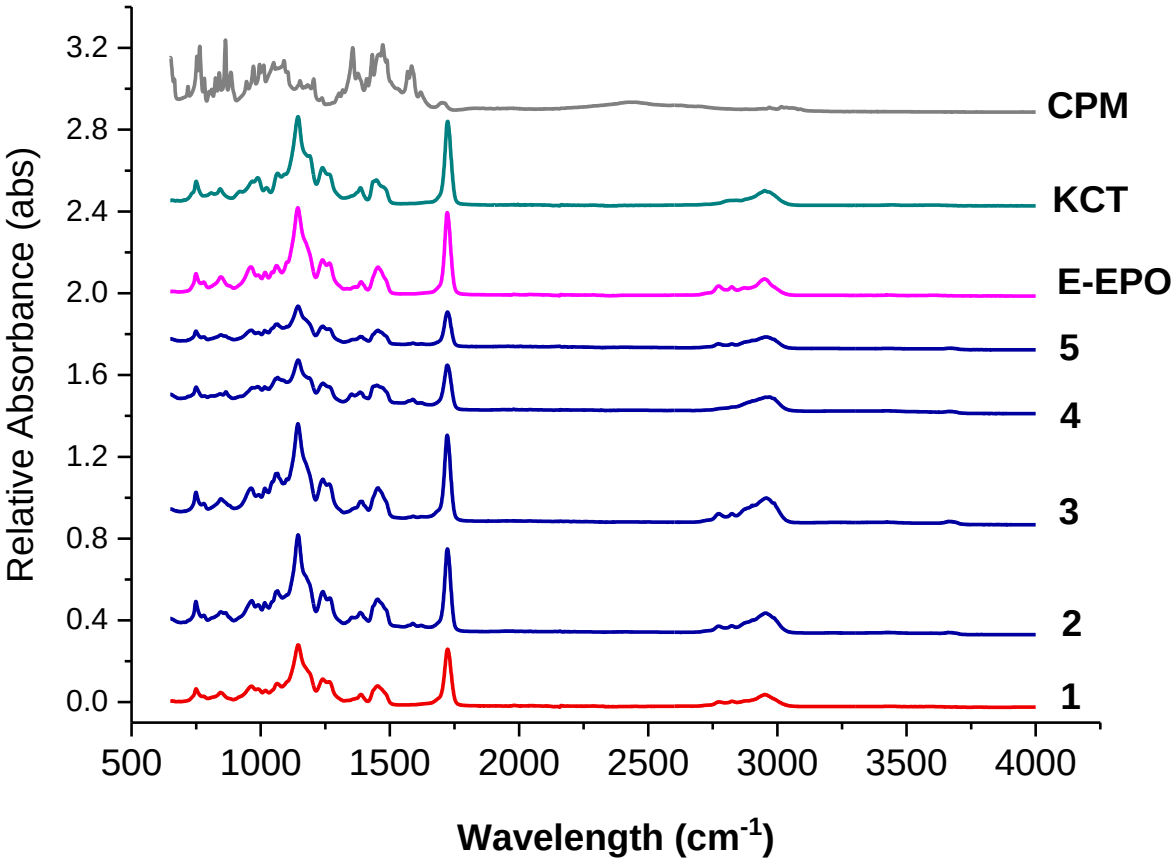

Figure 4.7. FTIR spectra of pure CPM, raw E-EPO, KCT and the five co-axial systems electrospun.

These peaks are observed in both KCT and E-EPO spectra. The peak observed in both polymers around 1210 cm^{-1} is characteristic of the C−O bond, also very abundant in both these polymer types. Both those prominent peaks are present in all the co-axially spun fibres (systems 2 to 5), as well as the placebo system, number 1. The spectra of the polymers and fibres are very similar which indicates that no strong bonds were formed between the polymers and the drug CPM, further validating the XRD data that an amorphous solid dispersion was formed. The drug CPM shows characteristic peaks at: 850 cm^{-1} responsible for the C-Cl stretching; 1700 cm^{-1} indicative of

C=O stretching; and 1355 cm^{-1} which is indicative of an aromatic amine [218]. These peaks do not seem to present anymore in the fibres which indicates that the functional groups within the drug could have formed hydrogen bonds with the methacrylate polymers. These interactions give an indication of compatibility and therefore stability of the drug in the co-polymer matrix [213]. These results indicate that CPM was amorphously dispersed in the polymeric carriers, which was also validated in the XRD data.

4.3.4 Thermal Characterisation

4.3.4.1 Thermogravimetric Analysis

A representative thermogram of co-axial system 2 is shown in Figure 4.8. An analysis between 40 ˚C and 120 °C showed that a weight loss of 0.01269 mg was observed, accounting for 0.31 % of the total sample weight. This indicates that minimal residual solvent was present in the representative electrospun fibres. The thermogram displays a similar shape to that of E-EPO, showing that the drug is incorporated in it as a dispersion. The onset point however shifts to a lower temperature, 215 °C, closely matching that of the drug.

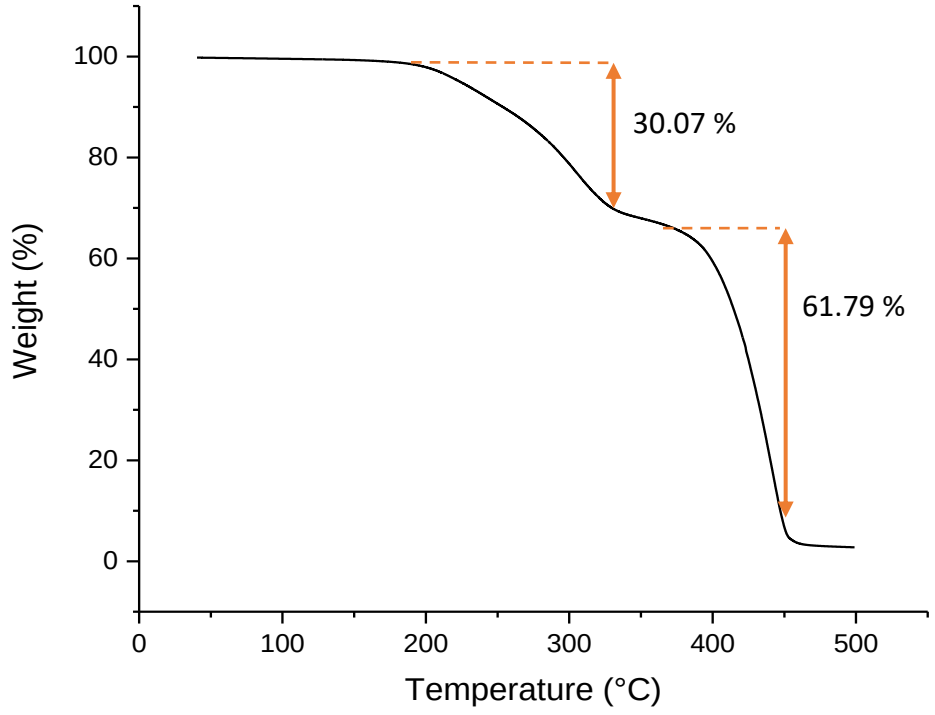

Figure 4.8. TGA thermogram of co-axial system 2 showing the % weight loss as temperature increases.

4.3.4.2 Modulated Temperature Differential Scanning Calorimetry

The thermal characteristics of KCT were determined using MTDSC. The polymer's T_g was measured to be 68.0 °C ± 0.5 °C; the mid-point temperature was used. This is in close proximity of literature findings of 63 °C [114]. This variation is likely due to a difference in heating rate used. In addition, polymers can show great variability between batches. A representative thermogram is shown in Figure 4.9, showing the glass transition as shown by the separated reversing heat flow thermogram [142]. A melting peak was not observed for this polymer suggesting it is in an amorphous state.

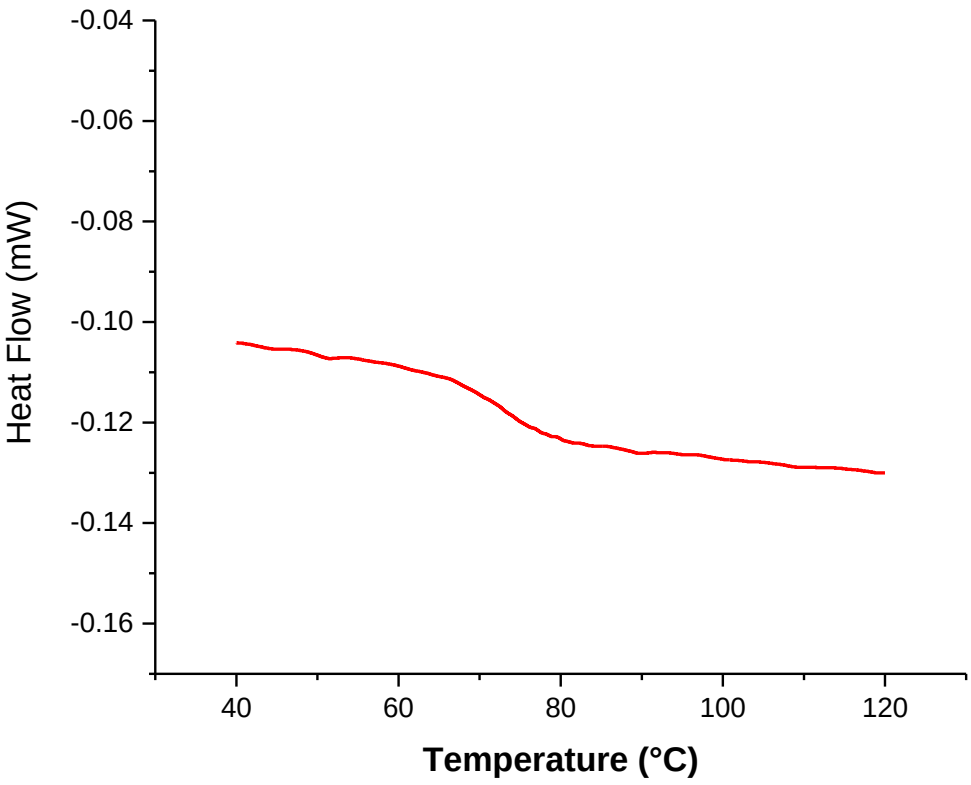

Figure 4.9. MTDSC reversing heat flow thermogram of raw Kollicoat smartseal. Exo up.

Figure 4.10 shows the MTDSC thermograms of co-axial system 2. This system was shown here as it contains both polymers alternating between core and shell, and contains the drug CPM in the core. From Chapter 3, the data for CPM's melting point was 133.24 °C; E-EPO's glass transition temperature was

50.9 °C, whilst KCT's glass transition temperature was measured around 68 °C. The total heat flow as well as the reversing and non-reversing components are displayed. MTDSC allowed the separation of the glass transition which appears in the reversing heat flow signal, where the non-reversing signal shows the relaxation endotherm [142]. The addition of the drug lowered the T_g of the system, to approximately 44 °C, a plasticising effect [219].

The drug-loaded co-axial system did not display a melting peak which indicates the conversion of crystalline CPM to the amorphous state in the co-polymer matrix. This can be considered a stable drug-delivery system, as it has been suggested that the formulation's T_g should be between 10 °C to 20 °C higher than the storage temperature [66].

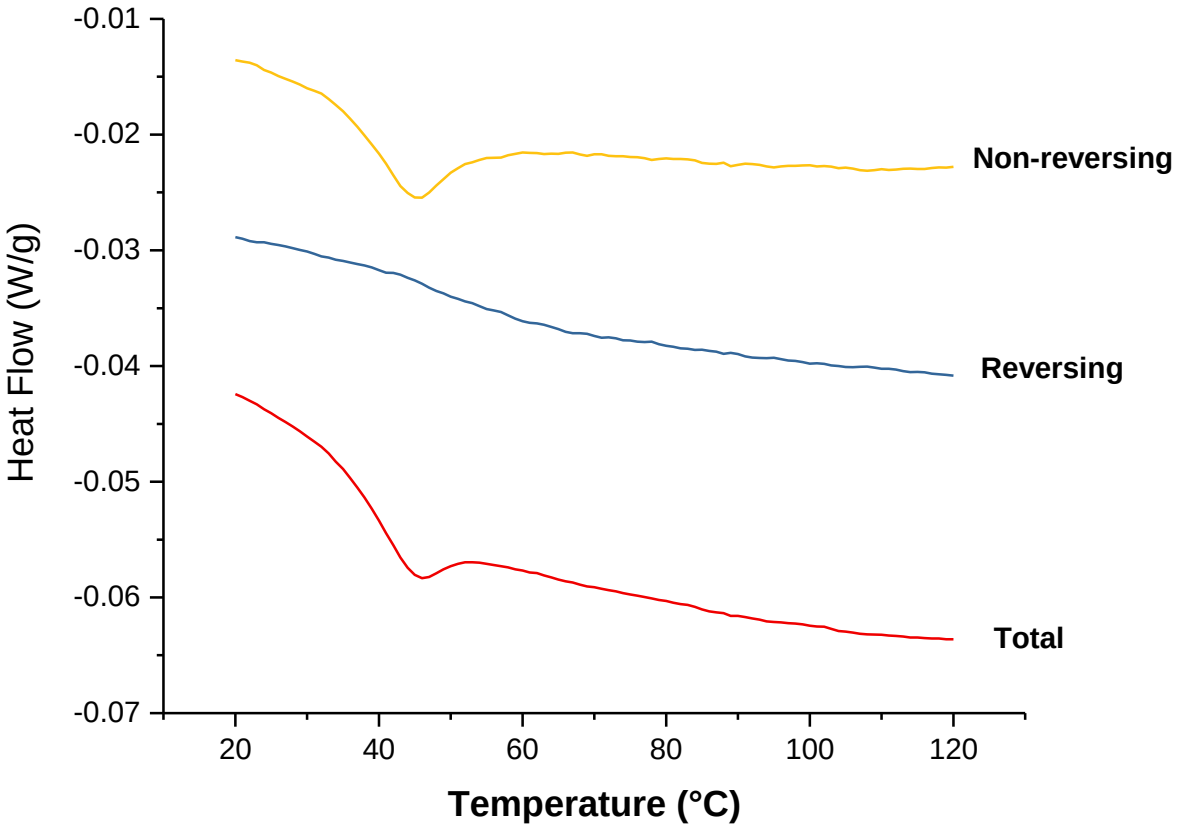

Figure 4.10. MTDSC thermogram of co-axial system 2. Exo up.

4.3.5 Dissolution Study

The *in-vitro* release profiles of co-axial formulation 2 is shown in Figure 4.11. The dissolution experiment was performed in a buffer solution of pH 1.2, mimicking fasted gastric conditions. Children over 2 have a similar gastric pH to adults, which is generally between 1.0 and 2.5 [133]. Both KCT and E-EPO are pH dependent polymers that are insoluble over pH 5.0 therefore release in pH 6.8 buffer was not performed. It can be seen that the co-axial electrospun film releases rapidly owing to its high surface area to volume ratio, and therefore a high release rate is expected. It can be seen that the film released approximately 75 % of the drug amount at 45 minutes, which is in line with an immediate release formulations' guideline of releasing 70 % of the drug in that timeframe (Ph. Eur. 5.17.1) [134]. The formulation is expected to release fully in the stomach, where no adverse effect due to the taste-masking on absorption is anticipated.

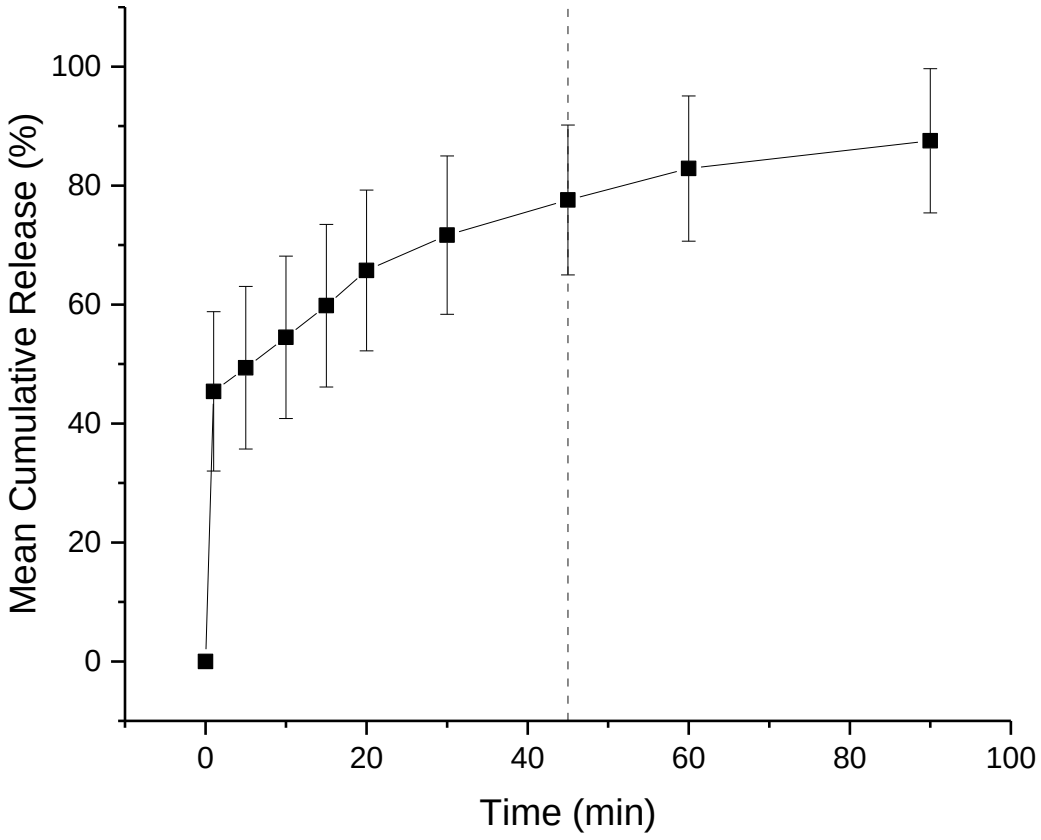

Figure 4.11. Dissolution profile in pH 1.2 co-axial formulation of KCT and CPM in the core, and E-EPO in the shell. The dashed line represents 45 minutes.

4.3.6 Film thickness, pH and Folding endurance

The thickness of the films is of one of the main acceptability parameters for patients. The thickness of a 3 cm x 2 cm co-axial 2 film was taken and the average measurement was found to be 100 µm ± 20 µm. These thickness levels are in line with literature recommendations [53,220,221], nonetheless, they can easily be altered by increasing the time of electrospinning and therefore the amount fabricated.

In addition to thickness of films, folding endurance is a very important parameter for the formulation to effectively be taken by the patient. The films were folded in the same position, and it was found that after bending them for 30 times they did not break, which is considered high endurance and the experiment was stopped [122,148,149]. The fact that the films have high folding endurance indicates that they will be well handled and easily ingestible.

The pH of the films when dissolved in distilled water was 6.63 ± 0.28, which is approximately neutral pH and within consistent values of saliva's natural pH levels. This indicated that the formulation is not expected to cause any irritation due to its pH levels [103,222].

4.3.7 E-tongue Taste-assessment

4.3.7.1 Dose Response Curve

It is known that CPM is detectable by the E-tongue's basic bitterness (AN0 and AC0), acidic bitterness (C00) and astringency (AE1) sensors as verified by our previous study [98]. The E-tongue utilises sensors of various qualities to detect a taste of a substance relative to a reference point. In this case basic bitterness sensors were used and compared the taste of the various formulations to the raw unformulated drug. Bitterness is associated with adsorption of molecules on the surface of the sensors. Consequently, aftertaste or 'Change of membrane Potential caused by Adsorption' (CPA) can be a reliable measure of those tastes. If more than ± 5 mV is recorded by the sensors, this implies that the drug displays this taste quality to some degree.

BT0 is the newest basic bitterness sensor with improved selectivity and sensitivity [223] and therefore data from it was used for comparisons. Figure 4.12 shows BT0's response as initial taste and aftertaste output (CPA) to raw CPM at concentrations ranging between 0.01 mM to 10 mM, to ensure detectability. It can be seen that CPM is detected by this sensor and has a perceived basic bitter taste profile. The aftertaste results indicate that this bitterness persists through after light washing, and therefore taste-masking is required. CPM was previously assessed using AC0 and AN0 sensors (section 3.3.9.1), both also responsible for detecting basic bitterness taste qualities. AC0, AN0 and BT0 all possess different plasticisers that allow them to have different affinities and therefore sensitivities to differing bitter molecules. Even though the measurements are very similar to that of AN0's, BT0 has been shown the be more selective [224] and therefore will be used to calculate the bitterness threshold of CPM.

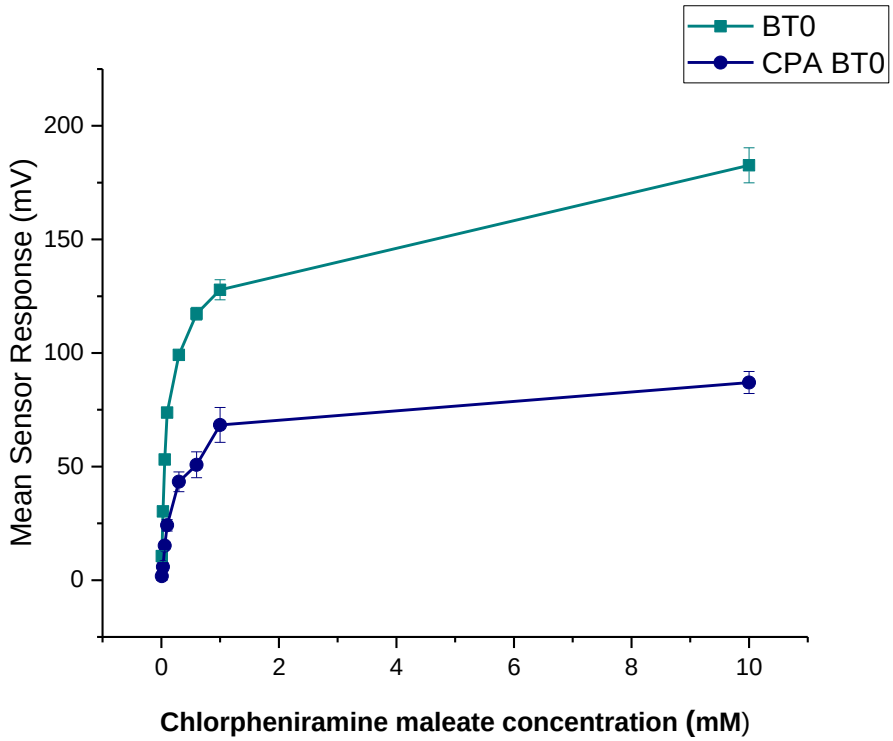

Figure 4.12. Dose response curve representing initial taste and aftertaste (CPA) for CPM as detected by BT0 sensor.

To ensure BT0 was an appropriate sensor for further analysis and comparison with standard bitter drugs, a non-linear Boltzmann fitting was completed on the data-set for both initial taste and aftertaste. A Boltzmann fitting produces a

sigmoidal curve which is indicative of an effect plateauing off when reaching a measured maximum [225]. The effect of taste response is not linear but instead logarithmic as explained by the Weber-Fechner law that states that the relationship between a stimulus and the corresponding perceived intensity is logarithmic [91] [212]. As shown in Figure 4.13, the initial taste represents a sigmoidal curve and thus successful Boltzmann fitting, indicating the use of BT0's initial taste curve for further analysis is appropriate. The fitting produced an $R^2 = 0.99$ for initial taste and $R^2 = 0.98$ for aftertaste. It was decided to use the initial taste data to calculate the bitterness threshold.

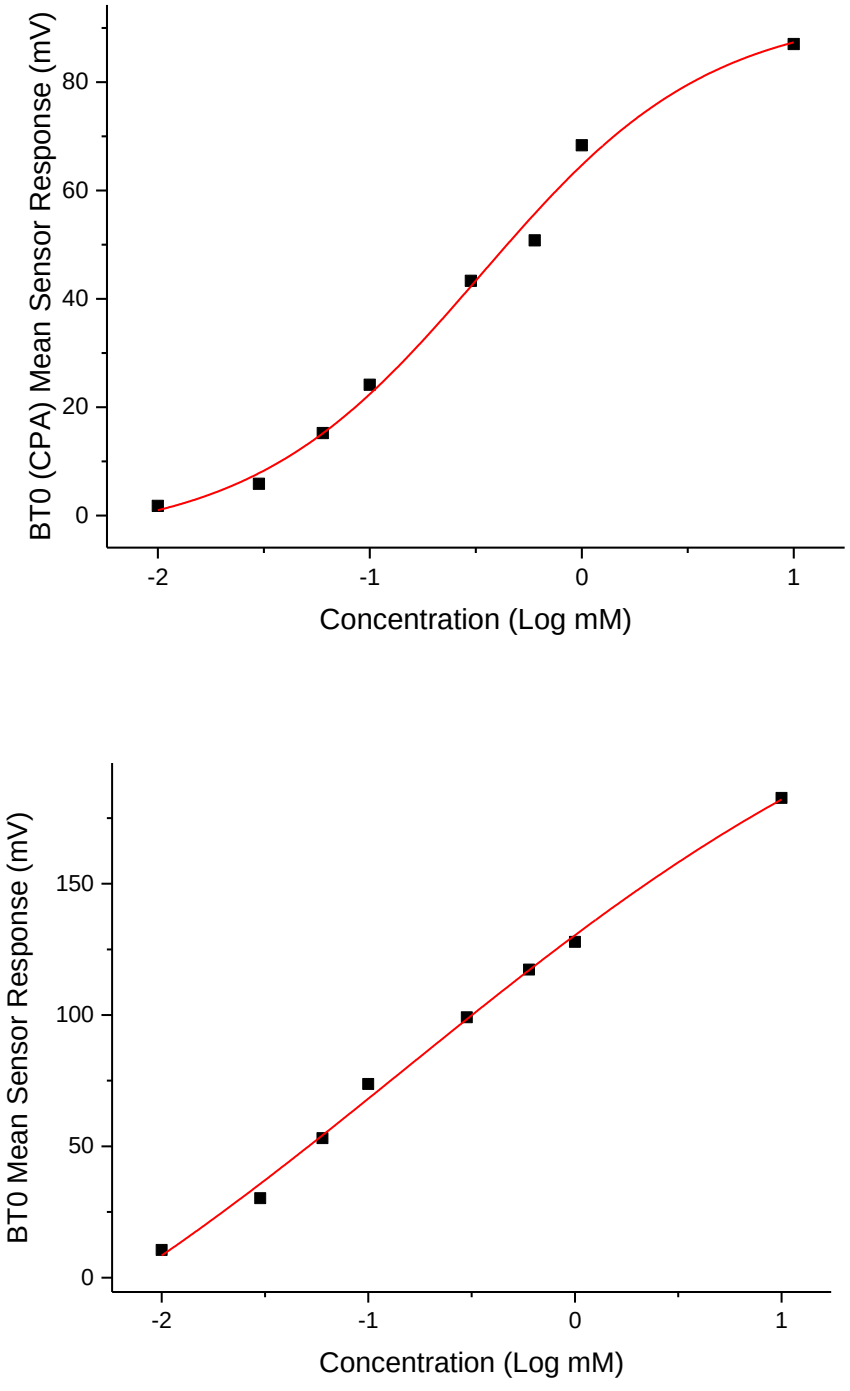

Figure 4.13. Non-linear Boltzmann fitting of (bottom) the initial taste (BT0 sensor) and (top) aftertaste (BT0 CPA sensor) of chlorpheniramine maleate.

4.3.7.2 Bitterness Threshold

Quinine HCl, an anti-malarial drug, is a commonly used bitter drug standard in taste-assessment studies [226]. To ensure it is detectable by the E-tongue's BT0 sensor, it was tested. The dose response curve is shown in Figure 4.14. The drug is well detected by the E-tongue for both initial taste and aftertaste measurements, therefore data derived from it's logarithmic fit will be used to determine the bitterness threshold for CPM.

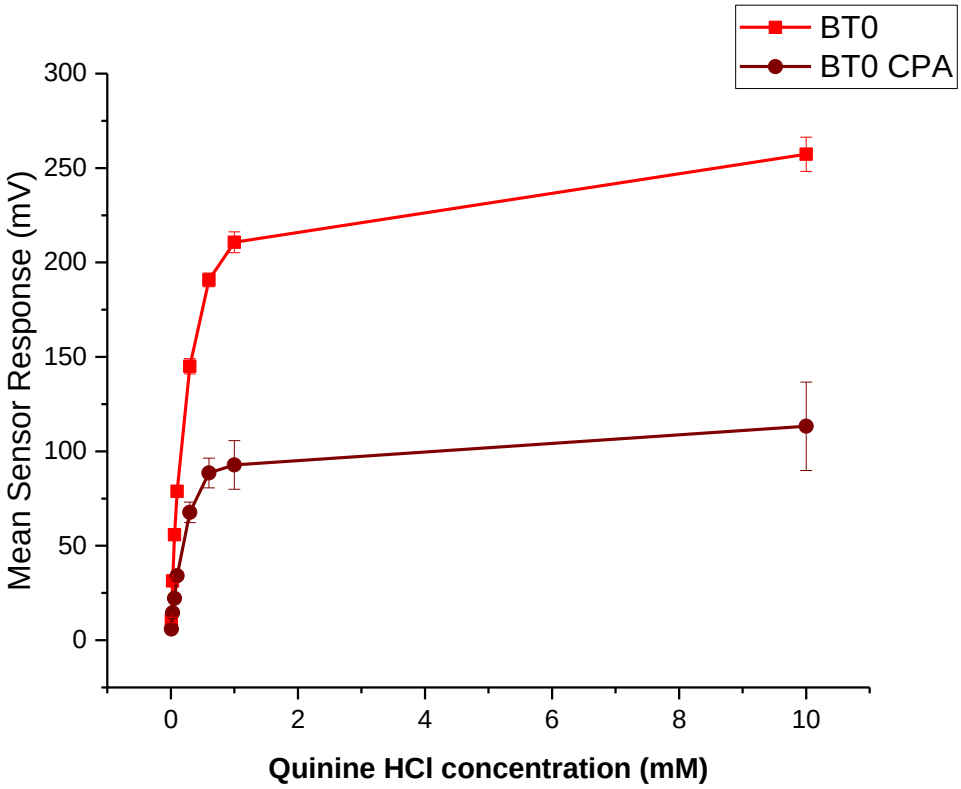

Figure 4.14. Dose response curve representing initial taste and aftertaste (CPA) for Quinine HCl as detected by BT0 sensor.

Taste response was found to follow a logarithmic concentration sensor response. The bitterness threshold for quinine HCl from a human sensory test was determined to be 0.26 mM [211] which equates to an E-tongue BT0 sensor output of 132 mV when fitted on a logarithmic trend-line using the equation in Figure 4.15.

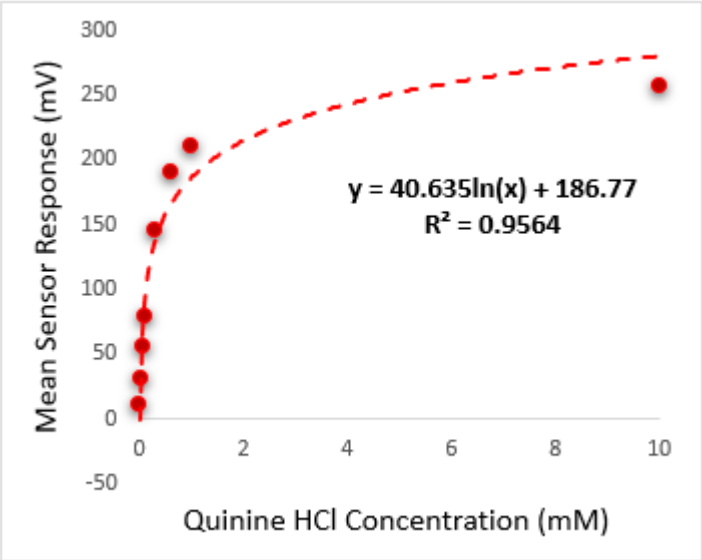

Figure 4.15. Quinine HCl dihydrate response shown as a logarithmic trend-line as determined by BT0 sensor.

To estimate the bitterness threshold of CPM, this value was used and substituted into the corresponding logarithmic equation to generate a mean drug concentration that matches quinine's known bitter mean sensor response (132 mV). The logarithmic fitting of the data is shown in Figure 4.16. Using data from the BT0 sensor, the bitterness threshold of CPM was calculated to be 1.2 mM or 0.47 mg/mL, meaning any concentration above this point is expected to exert a bitterness response by the person tasting it, and therefore requires taste-masking. Since the clinical CPM dose is between 1 mg and 4 mg [105], and the average human secretes 1 mL of saliva per minute [227], this threshold is below the clinical dose and therefore taste-masking of this drug is essential. In the literature the human bitterness threshold of CPM was reported to be 0.506 mg/mL or approximately 1.3 mM [115]. This means that the E-tongue is reporting a slightly lower value, which may indicate higher sensitivity compared to *in-vivo* findings. This can be expected as humans vary in sensitivity levels, with a proportion of people classified as non-tasters, thereby potentially skewing aversiveness results [44]. This subjectivity limitation is therefore eliminated when using a biosensor. Nonetheless, the values are in close agreement, indicating good E-tongue to human correlation.

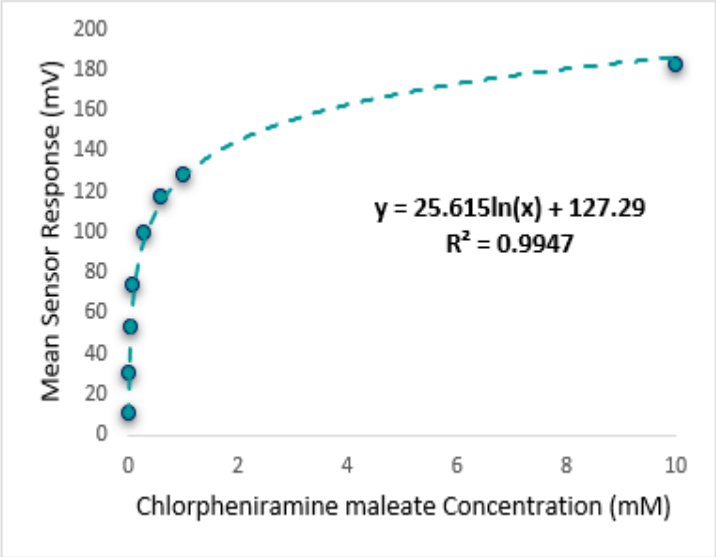

Figure 4.16. Chlorpheniramine maleate response shown as a logarithmic trend-line as determined by BT0 sensor.

4.3.7.3 Human Sensory Analysis Correlation and Benchmarking

A good correlation (R^2 = 0.822) between E-tongue generated bitterness scores by BT0 and those from a human taste panel was established for ten of the most commonly used bitter drugs [91]. Similarly, the astringency sensor had a high correlation with the human sensor score (R^2 = 0.95), where tannic acid solutions were used as standards and compared to known astringent compounds such as caffeic acid and gallic acid [91].

In addition, the E-tongue robustness has been demonstrated by a number of studies. Inter-laboratory testing of Insent E-tongues by five centres found that in conclusion, participating E-tongues can be declared to perform comparably [228], showing high sensitivity and data robustness. In a systematic testing series, which was based on the ICH guideline Q2 for validation of analytical methods, it was demonstrated that data of Insent taste-sensing system are reliable [91] according to the parameters of the guidelines, which are: accuracy; precision; specificity; detection limit; linearity; and range [91,212,229].

Data gathered has found that the ranking order of commonly bitter drugs matches the equivalent human taste panel data [211], as shown in Figure 4.17. Human sensory analysis by Soto et al. (2018) [211], has ranked the bitterness of the same drugs studied here in the following order from most to least bitter: Quinine HCl > chlorpheniramine maleate > sildenafil citrate > caffeine citrate> ethambutol> ibuprofen sodium.

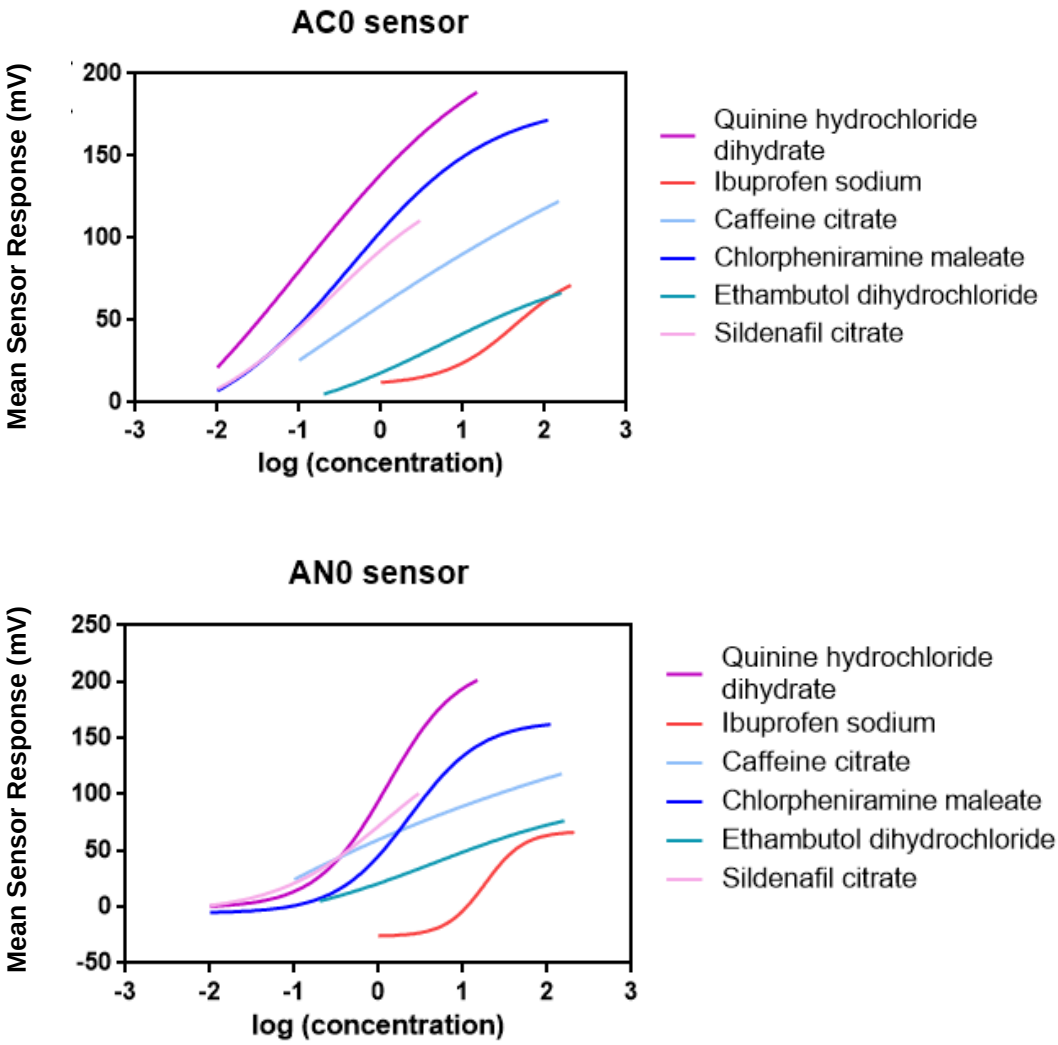

Figure 4.17. Rank order of common bitter drugs using data from the AC0 and AN0 sensors.

Figure 4.17 shows the AC0 and AN0 ranking as follows: Quinine HCl> chlorpheniramine maleate> sildenafil citrate > caffeine citrate> ethambutol > ibuprofen sodium. These results indicate high confidence of the data generated by the E-tongue to be used to measure bitterness and therefore predict aversiveness in humans.

CPM therefore was benchmarked to be a highly bitter drug with approximately half the bitterness of quinine HCl. It was found to be more bitter than all the other standard drugs tested.

4.3.7.4 Formulations Taste-assessment

AN0 and BT0 were both used to assess the formulations' taste difference from raw CPM. Results from the BT0 sensor, which had improved sensitivity, is shown in Figure 4.18.

It can be seen from the bar chart that the raw unformulated drug, CPM, gave the highest sensor response and is at the top of the chart indicating the highest bitterness. Co-axial system 4 (see Table 4.1) appeared to exhibit the weakest taste-masking. This is likely due to the fact that it did not contain any E-EPO, which was present in a much higher concentration thereby providing better protection of the enclosed API. Similarly, the next system was co-axial 3, which also contained one polymer in both the core and the shell, E-EPO. It did, however, exhibit much higher taste-masking that co-axial system 4. This is likely due to its more superior electrospinnability and therefore stability of the fibres formed. Also, E-EPO was electrospun at 35 % (w/v) whereas KCT was electrospun at 7.5 % (w/v). The higher concentration of E-EPO provided a thicker structure that gave rise to better formed fibres and superior taste-masking.

Co-axial system 5 contained E-EPO in the core and KCT in the shell. The combination of both polymers seems to be better than either polymer alone. However, looking at their SEM image Figure 4.4, the fibres formed were spindled due to low electrospinnability of KCT when placed in the shell of the structure.

Any mean sensor response between -5 mV and 5 mV is deemed undetectable by the E-tongue's sensors. Co-axial system 2 was deemed undetectable by the E-tongue, showing effective taste-masking. This is likely due to the fact that E-EPO was in the shell, and because it was used at a higher concentration than KCT, it is hypothesised that a thicker more protective shell was formed, causing the superior taste-masking. The placebo fibres were undetectable, as expected.

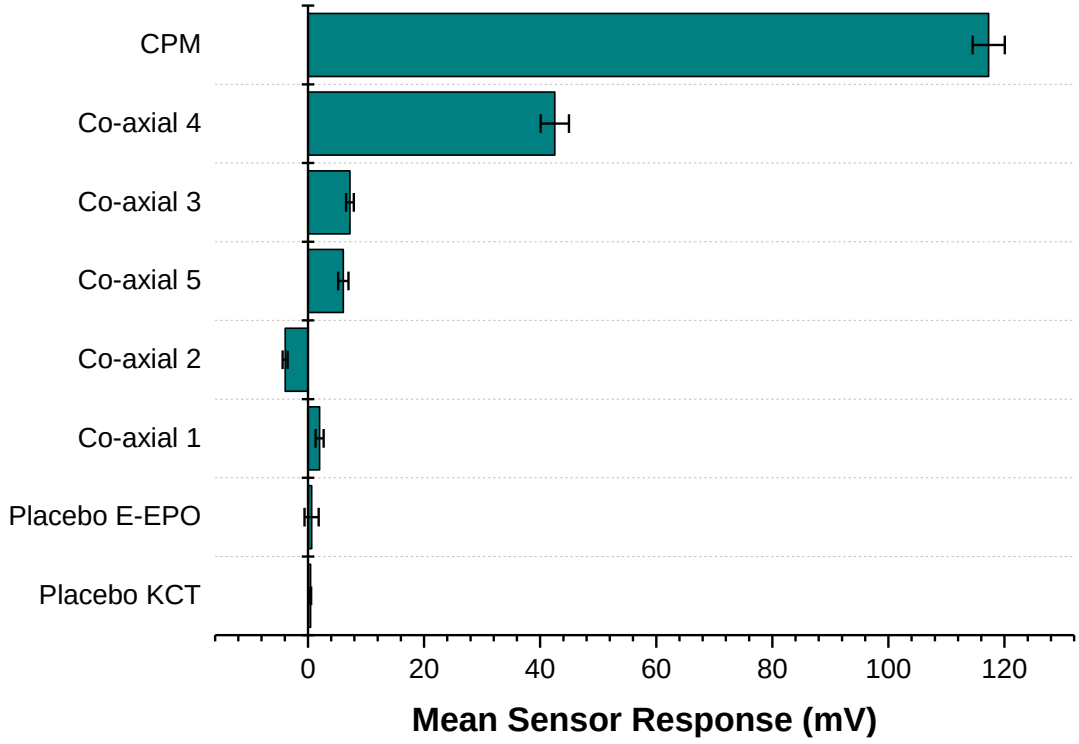

Figure 4.18. A bar chart representing the E-tongue's response to the various formulations tested as well as placebo fibres. The sensor used for this assessment was BT0, the newest generation basic bitterness sensor.

Principal component analysis was used to reduce data from the initial taste and aftertaste of BT0 and AN0 sensors into a two dimensional output [230]. Principal component 1 was responsible for 71.97 % of the variance in the data and it was determined by data outputs from the BT0 sensor, indicating it had most influence on the results. The 2nd principal component was determined by data from the AN0 sensor and was responsible for 27.83 % of the variance in the data. Both principal components therefore account for 99.82 % of the variance of the data demonstrating that these results are credible and not merely due to chance.

Table 4.2 shows the Euclidean distance calculated for the various formulations from the bitterest point, the raw drug. The further away the distance, the more taste-masked a formulation is. The most taste-masked formulation is co-axial formulation 2, which contained KCT in the core with the drug, and E-EPO in the shell. Perhaps this is a somewhat expected outcome as E-EPO electrospins well, and therefore when loaded in the shell of the formulation an intact and taste-masked fibre mat is formed.

Co-axial samples 3 and 5 were taste-masked similarly as shown by the comparable Euclidean distance values. Co-axial system 4 was the closest to the raw drug, indicating the least taste-masking and therefore the lowest Euclidean distance.

Table 4.2. Euclidean distance of the drug-loaded co-axial formulations from 20 mg / 100 mL or 0.5 mM CPM.

Sample	Euclidean distance
Co-axial 4	4.43
Co-axial 5	7.51
Co-axial 3	7.63
Co-axial 2	9.40

4.4 **Conclusions**

KCT Smartseal was successfully electrospun for the first time as far as I am aware. The conditions were optimised to produce smooth bead-free fibres. Using the optimised conditions, KCT and E-EPO were both used in conjunction to co-axially electrospin CPM for taste-masking. Co-axially electrospun fibres show improved taste-masking compared to raw drug. In addition, combining both polymers in one co-axial system improved taste-masking compared to either polymer alone. Using FL microscopy and TEM It was deduced that the drug was loaded homogenously throughout the fibre

mat. It was concluded that placing E-EPO in the shell solution drives the electrospinning process in a much more efficient manner versus KCT, as in co-axial system 2. Even though co-axial system 2 forms taste masked nanofibres that are confirmed to be an amorphous solid dispersion, needle clogging still is problematic. This will need to be optimised further in future experiments possibly through using different solvents or multi-axial spinning.

TGA analysis showed that there was negligible residual solvent left in the fibres, an important parameter for an oral dosage form intended to be used in children. XRD and MTDSC confirmed the presence of the drug in the electrospun fibre matrix as an amorphous solid dispersion. In addition, FTIR studies showed that no new bonds were formed, confirming these findings.

The fibre's release study showed that they released all the drug content at a very similar time to the raw drug, and within the pharmacopeial (Ph. Eur. 5.17.1) requirements of 70 % release within 45 minutes for a formulation to be considered immediate release. Therefore, co-axial electrospinning does not seem to affect the drug release and hypothetically the pharmacological action of the drug.

The films' thickness was comparable of literature values, were the folding endurance of the films was high, showing high potential acceptability of the films when handled by the patient. In addition, when the films were dissolved in distilled water, the pH measured was consistent with natural saliva pH, indicating low mucosal irritability as a result of the ingestion of this oral film.

The E-tongue's newer and more sensitive basic bitterness sensor BT0 was successfully used to measure the taste of CPM's bitterness as well as the associated formulations. The bitterness threshold of CPM was calculated which was used to ascertain whether the drug released from the formulation surpasses that value thereby eliciting aversiveness. In addition, six commonly known drug molecules were taste-assessed using the E-tongue and their ranking compared to literature values in humans. The bitterness ranking was

the same as the human data, leading to the conclusion that the E-tongue is a reliable tool in the taste-assessment of pharmaceuticals.

Overall, it was shown that co-axial electrospinning is a promising technique to manufacture taste-masked formulations that have the potential to be further formulated into age-appropriate dosage forms such as oral films, which are well suited for paediatric administration. As well as taste-masking and dosage form flexibility, this manufacturing method also offers the benefits of nanotechnology such as improved dissolution.

Chapter 5

Formulation and Assessment of Electrospun Films for use in the Paediatric Population

5.1 Introduction

This chapter is split into two parts, both aiming at reaching a clinic-ready age-appropriate oral film. Part A aims to assess the acceptability of orodispersible electrospun fibre mats using a human panel. Part B utilises multi-axial electrospinning to fabricate an orodispersible film (ODF) that is taste-masked.

5.1.1 Part A: *In-vivo* Assessment of Orodispersible Films

The overarching aim of this chapter was to further optimise the co-axial formulation to make it better suited for a clinic-ready ODF. In this study, polyvinyl alcohol (PVA) and polyvinylpyrridone (PVP) were trialled as a suitable outer layer of the film with a view to it being deemed a ready-to-administer dosage form.

A human panel was performed to assess the acceptability of fast-disintegrating PVA electrospun films compared to solvent cast orodispersible films (ODFs). ODFs fall under the category of oromucosal preparations in the European Pharmacopoeia (Ph.Eur. 10th). ODFs are suitable for the paediatric population because they do not pose a swallowing difficulty and can be taken without water. Solvent casting is the typical technique in manufacturing ODFs, however, batch-to-batch variations are seen due to entrapped air bubbles and therefore varied uniformity of drug content and distribution [231]. Solvent casting involves dissolving a film-forming polymer, excipients and an API in a suitable solvent then drying to form a film layer than can then be cut into various sizes. The number of polymers and solvents which can be used are limited. The process may sometimes require heat, and thus may be unsuitable for thermolabile excipients and active ingredients [232]. It also often requires the addition of excipients such as plasticisers to improve the formulation properties, for example to lower the glass transition temperature and thus improve the mechanical properties of the films. This can be especially undesirable for a dosage form intended to be used in the paediatric population [233]. Paediatric dosage forms should include the minimum amount of excipients possible, as detailed in the European Medicines Agency (EMA)

guidance document [234]. This is the case even for excipients which are generally recognised as safe (GRAS) in adults, because there is limited safety data on the effect of exposure to excipients on children's developing organ systems.

Hot-melt extrusion can also be used for manufacturing of oral films. In this process, no solvent is used and the API is blended with the film-forming polymer and excipients in the solid state. This blend is then heated and extruded into a film through a special die. This solvent-free process has advantages over solvent-casting as there is no risk of residual solvent or air bubble entrapment. On the other hand, thermolabile substances would not be suitable for processing using this method [149].

A recent review by Strickley [235] indicates that the most suitable paediatric formulation should ideally be: single use and therefore require no preservative; require no further manipulation (like reconstitution); require no intervention from care-giver (like volume measurement); be taste-masked; be easy to swallow; require no specialised dispensers or spoons; in addition to being a flexible dosage. Oral films were chosen as the most suitable dosage form for paediatric administration as they possess the parameters of a suitable paediatric formulation. Electrospun oral films offer advantages such as dose flexibility by simply perforating the films to be divided easily [236].

Orodispersible films are excellent candidates for age-appropriate formulations. They are thin, easy to swallow, can be formulated to be taste-masked and do not require water to be taken [237]. They also offer flexible dosing, possess no risk of choking and offer improved dose accuracy in comparison to syrups, which renders them suitable for paediatric drug delivery [103]. Oral films are suitable to be given to children, but key attributes such as stickiness, disintegration time and thickness need to be optimised to ensure maximum acceptability [238]. One limitation of ODFs is the potential for low drug loading, however, with a maximum of approximately 50 mg per film [239].

The first commercial success of oral thin films appeared in the United States (Listerine PocketPaks) by Pfizer, and they were used for mouth freshening. This was followed by Chloraseptic relief strips, and they were deemed to be the first therapeutic oral films on the market containing benzocaine intended to treat sore throats [103]. Although there is a number of oral films either fully launched on the market or are in clinical trials, only one paediatric film is on the market, ondansetron (Setofilm) [240]. Setofilm is licensed in children from the age of 6 months onwards for chemotherapy-induced nausea and vomiting. [241].

Due to safety and ethical concerns, there has been only two studies in the literature that assess the acceptability of oral films in children. The first study by Orlu *et al.* in 2017 investigated the acceptability of placebo ODFs in children aged between 6 months and 5 years. Their findings demonstrated that the ODFs showed high degree of acceptability amongst the children and their caregivers [242]. More recently in 2020, research by Klingmann *et al.* demonstrated that ODFs are in fact superior to syrup in terms of overall acceptability as well as palatability and swallowability as specific test parameters. Their study was performed on children from the age of 2 days to 12 months, thus demonstrating that ODF are a safe and promising alternative to liquid formulation even for children of a very young age [241]. Although two studies do not grant a definitive conclusion, it is widely considered that ODFs are acceptable for children of all ages.

As mentioned, oral films can be produced by manufacturing methods other than solvent casting, such as by hot melt extrusion, rolling and electrospinning [103]. The mechanical properties and plasticity of polymer films are influenced by the fabrication methods [197], and thus may also have an effect on mouthfeel acceptability. For instance, studies by Ghosal *et al*. (2018) showed that PVA films produced by solvent casting were brittle unless a high amount of glycerol was added, whereas electrospun films were more naturally flexible.

Electrospinning also requires little to no addition of excipients, unlike solvent casting. Further, it does not require heat (in contrast to hot melt extrusion)

therefore making it more suitable for application with a wider range of materials, particularly thermally labile drugs [154,189,243]. The process can be scaled up to industrial production levels, with multiple companies now offering high throughput and GMP manufacture of electrospun products [244]. However, while these advantages suggest that electrospinning may be a viable alternative in the preparation of ODFs, the question remains as to how patients will perceive films prepared in this manner. This is of fundamental importance for further development, as poor acceptability will undermine any performance advantages incurred by the nanofabrication approach.

In this study, the effect of the manufacturing method used to prepare ODFs on mouthfeel acceptability was explored. To do so, a human panel, the gold standard approach for assessing the palatability of a dosage form [97,211], was designed and undertaken. Its aim was to assess the ability and willingness of healthy volunteers to self-administer placebo PVA electrospun and solvent cast film formulations.

5.1.2 Part B: Multi-axial Electrospinning

Multi-axial electrospinning was utilised to enhance the acceptability of the previously optimised co-axial dosage form by adding a fast-dissolving polymer layer to the otherwise fairly hydrophobic taste-masked film. This will allow the final film formulation to disintegrate in the oral cavity aiding swallowability and mouthfeel. The resulting multi-layered structure is hypothesised to be easier to handle and administer in comparison to a fibrous mat, which is sensitive to physical impact and therefore can be a poor choice for a final dosage form [245]. The additional polymer layer provides strength and thus an improved final medicine ready for administration.

Dually taste-masked co-axial drug-loaded fibre mats have thus far proven acceptable when tested using the E-tongue. One of the main limitations seen in the co-axial formulation is the breakages in the fibres, likely due to needle clogging. In order to improve this parameter, solvent content will be altered

through the addition of DMAc and DMSO to optimise the Taylor cone and jet stability.

Electrospun fibre mats have been further optimised into secondary dosage forms frequently. A number of researchers have utilised electrospun mats for the formulation of orodispersible dosage forms. Casian *et al.* (2019) have formulated meloxicam into orodispersible tablets using both PVP and Eudragit E [236]. Electrospun indomethacin films were formulated with HPMC and ethyl-cellulose to produce a buccal dosage form [246]. Donepezil HCl, which is used in patients with Alzheimer's disease, was introduced into PVA and fabricated into orally dissolving films using electrospinning; this formulation offers a more acceptable and effective dosage form in older people and patients with dysphagia compared to traditional dosage forms [245]. Domokos *et al.* (2019) have produced orally dissolving webs of carvedilol by electrospinning on top of a pre-solvent cast pullulan layer on a wheel collector, deeming the system continuous and therefore advantageous [247]. Vrbata *et al.* (2013) have successfully incorporated sumatriptan succinate, naproxen and its salt as well as combinations of these into nanofibrous membranes electrospinning [126]. The researchers used PVA, PAA, PCL and chitosan as polymer carriers for the migraine treatment intended to be administered as an oral film sub-lingually.

In this study, tri-axial and tetra-axial electrospinning were both used to design a fully taste-masked easy to swallow ODF. There are a number of reports in the literature for using tri-axial electrospinning, with a 2021 review [248] reporting ten studies that utilised the modified process for various drug-delivery functions including: delivery of poorly soluble drugs; sustained release systems; and dual-drug delivery systems. Only one report of tetra-axial electrospinning [249] was found. None of the research papers found have used multi-axial electrospinning for taste-masking and therefore this is a novelty of the work presented here.

5.2 Methods

5.2.1 Part A: Human Panel

5.2.1.1 Research Ethics Committee

This study was a single centre, single blinded cross-over study and was conducted at the UCL School of Pharmacy. The study design was approved by the UCL Research Ethics Committee (REC; project ID: 15975/001). All data were handled in line with the General Data Protection Regulation 2018. Full application and materials used in advertising the panel is shown in Appendix B.

5.2.1.2 Formulation Preparation and Characterisation

Participants were given two samples of PVA oral films, one manufactured by electrospinning and one by solvent casting. The preparation details are outlined in this section.

PVA (Parteck® SRP 80 EMPROVE® ESSENTIAL Ph Eur, USP, JPE) oral films were purchased from Bioinicia (Valencia, Spain). These were manufactured in an ISO 7 clean room according to cGMP standards [250]. The Bioinicia plant has GMP certification issued by the Agencia Española de Medicamento, the Spanish agency that issues the permits required for the manufacturing of pharmaceutical products whose authorisations are worldwide harmonised and recognised. The plant also has ISO13485 accreditation to manufacture biomedical devices based on the electrospinning technology and ISO9001 to manufacture any items based on this technology.

A solution of 20 % (w/v) PVA in a mixture of deionised water and 2-propanol in a ratio 60:40 was used. The PVA was slowly added to the solvent mixture and then stirred at 450 RPM overnight at 50 °C. All the films were packaged in a clean environment. The films were packaged as follows: the primary packaging was an ultrapure silicon-free resin resealable bag and the

secondary packaging a pharmaceutical grade aluminised high oxygen barrier bag with zip closing mechanism, made of glossy aluminium. The packaging was labelled with batch number, expiry date, REC approval ID and a unique sample code.

5.2.1.3 Electrospinning

Electrospinning was performed using a Fluidnatek® LE-500 with a multi-needle spinneret (26 needles). The optimised parameters were 25 kV applied voltage, a flow rate of 15 mL/h (0.577 mL/h per needle) and a spinneret to collector gap distance of 15 cm. The temperature ranged between (20 to 21) °C and the relative humidity was 29 %. 25 gauge needles were used and fibres collected on a rotating drum (100 RPM) and the sweep speed was 30 mm/s. All the films were packaged in a clean environment. The packaging was labelled with batch number, expiry date, REC approval ID and a unique sample code.

5.2.1.4 Solvent Casting

The most common route to ODF preparation is solvent casting, in which a polymer and drug are dissolved in a solvent, charged into a die and then the solvent evaporated. There has been a limited amount of previous research comparing polymers and their molecular weights in terms of their effects on the acceptability attributes of solvent cast films. Scarpa *et al.* found that the chemical structure and molecular weight of a polymer influence stickiness perception and the molecular weight has a major influence on disintegration time [251]. They concluded that 39 kDa polyvinyl alcohol (PVA) shows acceptable mouthfeel properties, hence this grade was selected for use in this study.

The PVA solution was poured over a sterilised stainless-steel plate with dimensions 25 x 15 cm and allowed to dry in a controlled temperature and humidity chamber.

5.2.1.5 Characterisation of ODFs

Film thicknesses were measured using a digital micrometer (S00014, Mitutoyo, Corp., Kawasaki, Japan) with ± 0.001 mm accuracy. Measurements were performed in triplicate with no force applied. The morphology of the materials was determined with a field emission scanning electron microscope (FE-SEM, S-4800, Hitachi High Technologies Corp., Tokyo, Japan). Analysis of fibre diameter was carried out with ImageJ (National Institutes of Health, Bethesda, MD, USA). Prior to imaging, samples were sputtered for 2 minutes with gold/palladium. For the electrospun samples, at least 60 fibres from three different SEM images were randomly selected and measured to quantify fibre size.

5.2.1.6 Participant Recruitment

An email was sent out to UCL School of Pharmacy staff and students to recruit them to the study. Healthy volunteers between 18 and 60 years of age were recruited. Smokers and individuals who had received dental care up to 15 days before the panel or were taking any medical treatment known to affect saliva production, were excluded. Participants that had any allergies or known hypersensitivities to PVA were also excluded.

5.2.1.7 The Panel

Participants were individually seated in front of a computer monitor displaying a questionnaire designed using the Qualtrics software (SAP America Inc., Seattle, Washington, USA), which was used to record their answers. The two drug-free PVA films were presented to each participant in a random order with a 5 min break between them, to allow for palate cleansing. The participants were offered a plain cracker and water in this break, if they wished. Participants were not asked to cleanse their palates at the start of the experiment, nor were they discouraged from drinking water to aid in swallowing the films. A digital stopwatch was provided to allow participants to record disintegration time.

5.2.1.8 Data Collection

A five-point hedonic scale, as used in other taste panels [252], was used to capture the acceptability of different attributes of the oral films, as shown in Figure 5.1.

Figure 5.1. The five-point hedonic scale used to capture the perception of some the key acceptability attributes of the ODFs.

The six attributes investigated were the acceptability of the films' perceived size, stickiness, thickness, disintegration time, saliva thickening effect and handling. Questions evaluating the disintegration time, whether the full film was swallowed or not and the overall acceptability of the formulation were additionally included. For disintegration time, participants were instructed to start the stopwatch as soon as the film was placed on their tongue, then stop it and record the time in seconds when they felt it has disintegrated completely. The same questionnaire was completed by each participant for both samples. At the end of the survey the participants were asked to include any other open comments and to choose a preferred film from the two tested.

5.2.1.9 Data Analysis

Ordinal data were converted to discrete numerical values as detailed in Table 5.1. Data were then analysed using OriginPro 9.4 (Origin Lab, Massachusetts, USA).

Table 5.1. Conversion of ordinal quality attribute ratings into discrete numerical values.

Value	Quality attribute	Stickiness	Saliva thickening	Overall acceptability
1	Extremely uncomfortable	Extremely sticky	Extremely thickened	Extremely bad
2	Somewhat uncomfortable	Strongly sticky	Strongly thickened	Somewhat bad
3	Neither comfortable nor uncomfortable	Moderately sticky	Moderately thickened	Neither good nor bad
4	Somewhat comfortable	Slightly sticky	Slightly thickened	Somewhat good
5	Extremely comfortable	Not sticky	Not thickened	Extremely good

The numerical data from the acceptability attributes were then presented in a box plot, showing the median response and interquartile range (IQR). Significance tests were used to assess the magnitude of statistical associations. The data were non-parametric and therefore a Paired Sample Wilcoxon Signed-Rank Test was used. The significance level was set at *p*-value = 0.05. A Fisher's Exact Test was used to assess whether the overall preference difference between the two films was statistically significant.

Modal data were used to compare the attributes between both films. The mode here is the rating that occurs most frequently and is also regarded as the best way to measure the central tendency for data measured on a nominal scale [253].

5.2.2 Preparation of Precursor Solutions

Placebo E-EPO solutions were prepared by dissolving 40 % (w/v) E-EPO in 1 part DMAc, 2 parts DMSO and 6 parts absolute ethanol. The mixture was then magnetically stirred for approximately two hours. Drug-loaded E-EPO solutions were prepared by adding 3.5 % (w/v) CPM directly to a 35 % (w/v) E-EPO solution prepared in 1-part DMAc to 6 parts absolute ethanol.

KCT 30D, an aqueous solution, is miscible with ethanol at a ratio of 1:3. As it comes as a 30 % (w/v) solution, after dilution with ethanol a 7.5 % (w/v)

polymer solution is formed. When drug loaded, CPM was directly added to the polymer solution at a concentration of 3.5 % (w/v); 8 % (w/v) PVA solution was prepared by dissolving PVA in 90 % water and 10 % ethanol; and 10 % (w/v) PVP solutions were prepared in ethanol.

5.2.3 Electrospinning

In case of monoaxial electrospinning of PVP, PVA and the newly optimised E-EPO, the syringe was connected to a stainless-steel needle, with a diameter of 0.9 mm, via a connector tube. The viscous solution was fed through the needle at flow rates between 0.2 mL/h and 2 mL/h. Applied voltages of up to 25 kV were applied to the polymer solutions, evaporating the solvent, allowing the solid fibres to deposit on a grounded metal plate collector (14.5 × 23) cm. The gap distance between the needle and the collector plate was set between 10 cm and 20 cm. Room temperature (°C) and relative humidity (RH) (%) readings were recorded. The temperature ranged between 20 °C and 28 °C and the RH ranged between 25 % and 48 %.

5.2.4 Part B: Multi-axial Electrospinning

5.2.4.1 Co-axial Electrospinning

Following on from Chapter 4, the co-axial formulation that showed the most taste-masking, Formulation 2, was further optimised to stabilise the Taylor cone and therefore improve the drug-loading distribution throughout the fibre mat. The co-axial emitter used had a diameter of 0.9 mm for the outside needle and 0.45 mm for the inside needle. Inside and outside needles are the same length at 10 mm from the hub. The flow rates used were 0.45 mL/h for both the core and shell solution. The gap distance was set between 15 cm and 17.5 cm and the applied voltage was between 10 kV and 15 kV. The core solution consisted of KCT with 3.5 % (w/v) and a shell of 40 % (w/v) E-EPO in 1-part DMAc, 2 parts DMSO and 6 parts absolute ethanol.

5.2.4.2 Tri-axial Electrospinning

Tri-axial fibres have been prepared as follows; the core solution contained drug-loaded 7.5 % (w/v) KCT with 3.5 % (w/v) CPM; the middle solution contained of 40 % E-EPO in 1-part DMAc, 2 parts DMSO and 6 parts absolute ethanol; and the shell solution contained 10 % PVP. A tri-axial needle has been used with a diameter of 0.45 mm, an intermediate diameter of 0.9 mm and an outer shell diameter of 1.65 mm. The temperature ranged from 24 °C to 25 °C and relative humidity from 30 % to 40 %. The gap distance was set between 15 cm and 17.5 cm, whilst the applied voltage was set between 10 kV and 16 kV. The flow rates were set at 0.3 mL/h, 0.3 mL/h and 0.3 mL/h from core to shell. Using these flow rates the theoretical drug loading was calculated to be 7.51 % (w/w).

5.2.4.3 Tetra-axial Electrospinning

Tetra-axial fibres have been prepared as follows; the core solution contained drug-loaded 7.5 % (w/v) KCT with 3.5 % (w/v) CPM; the inner middle solution contained of 40 % E-EPO in 1-part DMAc, 2 parts DMSO and 6 parts absolute ethanol; the outer middle solution contained ethanol; and the shell solution contained 10% PVP. A tetra-axial needle has been used with a diameter of 0.45 mm, a middle diameter of 0.70 mm, an outer middle diameter of 1.2mm and an outer shell diameter of 1.6 mm. The temperature ranged from 24 to 25 °C and relative humidity from 30 % to 40 %. The gap distance was set between 15 cm and 17.5 cm, whilst the applied voltage was set between 10 kV and 16 kV. The flow rates were set at 0.3 mL/h, 0.3 mL/h, 0.3 mL/h and 0.3 mL/h from core to shell. Using these flow rates the theoretical drug loading was calculated to be 7.51 % (w/w).

5.2.5 Light Microscopy

Fibres were collected directly on microscope slides during electrospinning and then viewed under the light microscope Leica DM2700 M (Leica Microsystems, Wetzlar, Germany). Background information on the light microscope can be found in Chapter 2, Section 2.5.3

5.2.6 Scanning Electron Microscopy

The samples were analysed by SEM as described in Chapter 2, Section 2.5.4. Fibre size analysis was performed by measuring the diameter of 100 fibres using ImageJ 1.46R software (National institute of health, Maryland, USA).

5.2.7 Transmission Electron Microscopy

As described in Chapter 2, Section 2.5.5.

5.2.8 Thermogravimetric Analysis

The technique was used as described in Chapter 2, Section 2.5.11; samples were tared and analysed in an open aluminium Perkin Elmer pans with a heating rate of 10 °C/min from 30 °C to 500 °C.

5.2.9 Differential Scanning Calorimetry

The method was used as described in Chapter 2, Section 2.5.9. Samples were heated under nitrogen gas (flow rate 50 mL/min) at a rate of 2 °C/min ramped up to 150 °C, amplitude ± 0.212 °C and a period of 40 s. Samples' weights ranged from 4 mg to 8 mg and were sealed in a 40 µL aluminium Perkin Elmer standard pan.

5.2.10 UV Spectroscopy and Drug Loading

The background to the method is described in Chapter 2, Section 2.5.8. A standard curve (R^2 = 0.9998) of CPM was plotted using absorbance data recorded using a Jenway 6305 UV-vis spectrophotometer (Bibby Scientific, Staffordshire, UK). Absorbance was recorded at 262 nm (λ_{max}). Drug loading was calculated by using the slope = 0.01248 and intercept = 0.04057 of the standard curve. All measurements were taken in triplicate.

Film samples weighing approximately 10 mg were measured out and dissolved in 10 mL of ethanol. This was repeated three times. Each sample

was tested three times using UV spectroscopy. Therefore, 9 samples were tested for each formulation to ensure the reading is both accurate and precise. For each sample, the exact theoretical drug-load was calculated. Using the calibration curve, actual drug amount was calculated.

Theoretical drug-load of the multi-axial system was calculated as follows;

Equation 5.1

$$Concentration\ of\ each\ Polymer\ (\%\ w/v)\ \times flow\ rate\ \left(\frac{mL}{h}\right) = sum\ of\ all\ polymer\ content(\%\frac{w}{v})$$

$$API\ concentration\ (\ 3.5\ \%\ w/v)\ \times flow\ rate\ \left(\frac{mL}{h}\right) = drug\ content(\%\ \frac{w}{v})$$

$$Theoretical\ Drug\ loading\ \left(\%\frac{w}{w}\right) = \frac{drug\ content\ (\%\frac{w}{v})}{sum\ of\ all\ polymer\ amd\ drug\ content\ (\%\frac{w}{v})}$$

5.2.11 Powder X-Ray Diffraction

Characterisation of the solid-state of pullulan, PVA and PVP in addition to the multi-axial formulations were completed using a Rigaku MiniFlex 600 X-Ray Diffractometer (Rigaku, Tokyo, Japan) as described in Chapter 2, Section 2.5.10. Patterns were recorded over the 2θ range 3º to 40º at a scan rate of 3 º/min, with an interval of 0.02 º.

5.2.12 Fourier-Transform Infrared Spectroscopy

Background to method is described in Chapter 2, Section 2.5.12. FTIR studies were performed using a Spectrum 100 FTIR spectrometer (Perkin-Elmer, USA) and spectra were collected in the range of 4000 cm^{-1} to 650 cm^{-1} with a total of 16 scans and a resolution of 2 cm^{-1}, unless otherwise stated.

Background scans were performed in all experiments and each sample was analysed in duplicate to check the reproducibility of the spectra.

5.2.13 Statistical Analysis

All experiments were conducted in triplicate unless otherwise stated. All data were presented as mean value ± standard deviation.

5.2.14 E-tongue Taste-assessment

Full method details are described in Chapter 2, Section 2.6.1. Taste extracted liquids were used for biosensor assessment of the electrospun fibre mats and materials that are solid in the media's pH, such as KCT and E-EPO. Measurement of fibres were calculated as the corresponding mass of fibre that will contain 20 paediatric doses of CPM (20 mg) in a 100 mL, which equates to 0.5 mM. The fibres were added to 100 mL of 10 mM potassium chloride solution, as a supporting electrolyte, at 37 ºC and gently stirred for 1 min. The mixture was then filtered through 0.22 µm filters (Merck-Millipore, Cork, Ireland), removing any suspended particles.

5.2.15 Dissolution

Full method is described in Chapter 2, Section 2.5.15. A Sciquip mini shaker (SciQuip, Wem, UK) was used to investigate the release of CPM in stomach conditions of pH 1.2. 0.1 N HCl was used as the dissolution media. 1 mL aliquots were removed and replaced with fresh media at the following time intervals: (1, 5, 10, 15, 20, 30, 45, 60, 90 and 120) minutes. Removal and replacement of fluid was taken from the same position on all occasions. a media volume of 15 mL was used. Samples were placed in glass vials and the mesh cover dropped over them at the beginning of the time. Drug amount released was measured using UV spectrophotometry at wavelength of 262 nm. Tri-axial fibre samples measured 10.03 mg ± 0.12 mg and had a theoretical drug load of 7.51 % (w/w). Tetra-axial fibre samples measured 10.36 mg ± 0.21 mg and had a theoretical drug load of 7.51 % (w/w). Equation

of calibration curve in release media: $y = 0.0197x + 0.021$, $R^2 = 0.993$. A 1 mL quartz cuvette was used and all experiments were performed in triplicate. Data were collated and analysed using OriginPro 9.4 (Origin Lab, Massachusetts, USA).

5.2.16 Film Thickness and Folding Endurance

The method was used as described in Chapter 2, Section 2.5.14.

5.3 Results and Discussion

5.3.1 Part A: Human Mouthfeel Panel

5.3.1.1 Film Characterisation

The electrospun films had a mass in the range of (22 to 26) mg, with a mean mass of 24.94 mg ± 1.04 mg. They were cut to 3 cm x 2 cm, with a thickness of 253 (± 10) µm. The cast films were generated with an equivalent mass or 25.35 mg ± 1.40 mg, resulting in dimensions of 2 cm x 1.7 cm and a thickness of 83 µm ± 10 µm. A representative image of the electrospun and solvent cast films is shown in Figure 5.2 It is clear that the two formulations have different sizes and colours, which could impact acceptability attributes such as handling.

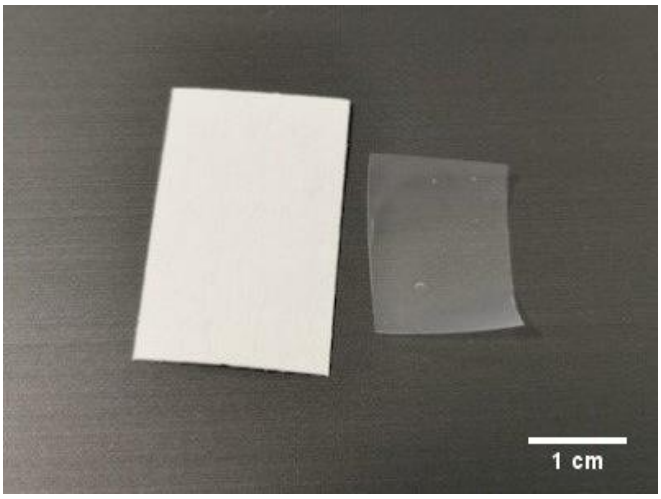

Figure 5.2. Images of the oral films. Left: the electrospun film; right: the solvent cast film.

The films were imaged using SEM as shown in Figure 5.3. The electrospun films show a fibrous structure whereas as expected the solvent-cast films do not. The electrospun fibres had a mean fibre diameter of 566 nm ± 94 nm.

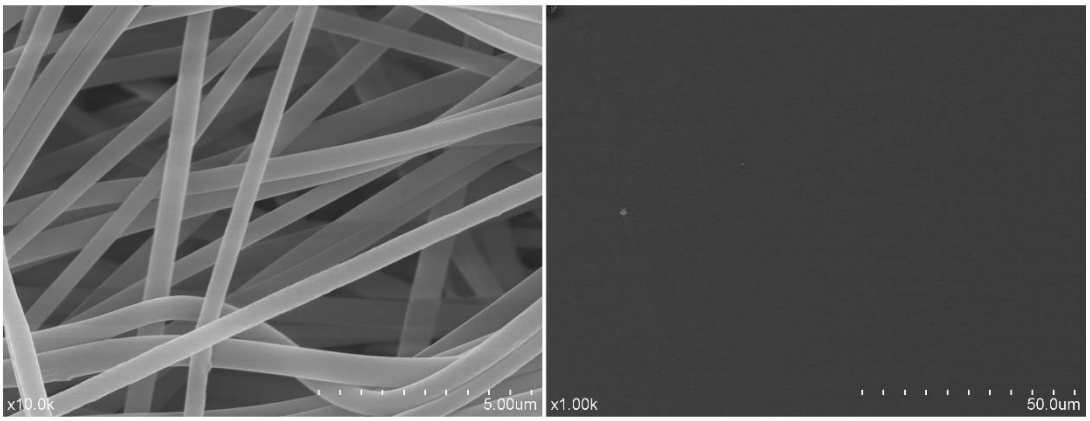

Figure 5.3. SEM images of the electrospun (left) and solvent cast (right) PVA films tested.

5.3.1.2 Sample Acceptability

50 participants (14 male and 36 female) were recruited for the study. The median age was 22 (min: 18; max: 49). Each participant received one sample of an electrospun film and one of a solvent cast film. The order the films were presented in was alternated between participants. No adverse effects associated with sample intake were reported by any participants during or after the study.

The hedonic-scale question in the survey assessed a number of characteristics that could affect the overall mouthfeel acceptability of the films. Box plots showing how the participants scored the films are given in Figure 5.4., with the top red box-plots showing the results for the electrospun films and the bottom blue box-plots showing the results for the solvent cast films. Stickiness was the only attribute that had a median score of 3 for the solvent-cast films. The median score for the remaining five of the six attributes was 4, denoting a somewhat comfortable formulation. This is consistent with the literature, reaffirming that solvent cast oral films are acceptable for use by end-users [238]. Outliers were observed in the data collected for the saliva

thickening effect and handling of the solvent cast films, yet these were only noted with 2 or 3 out of 50 measurements.

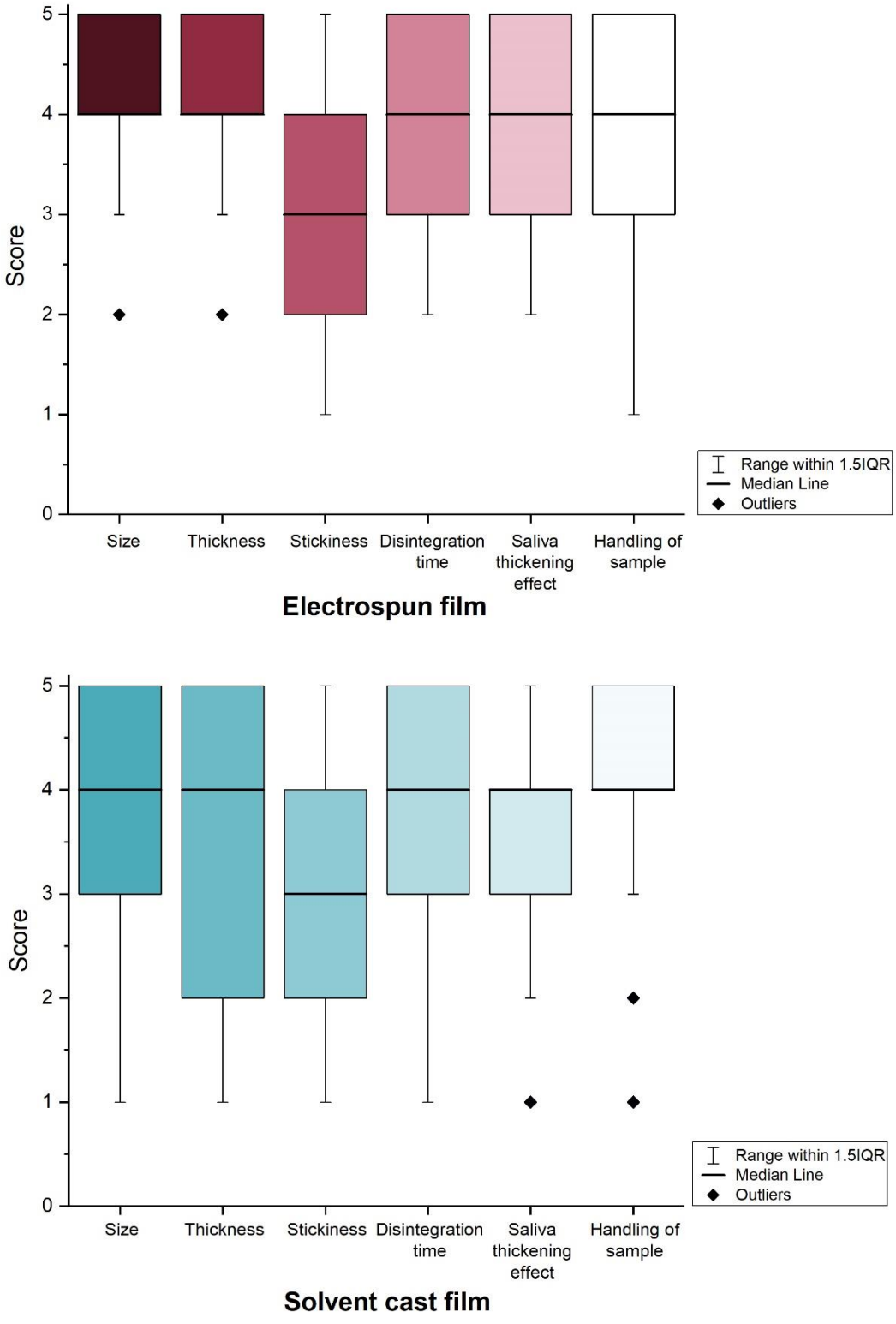

Figure 5.4. Box plots depicting key quality attributes of the electrospun and solvent cast films.

The decision was taken to match the ODFs by mass rather than size, because research by Scarpa *et al.* (2018) [251] showed that the polymer mass represents the most reliable way to compare formulations. It was not possible to match both size and mass in the same experiment, but controlling for size instead is an important avenue that will be explored in future work. For the electrospun formulation, perceptions of size and thickness in the mouth scored particularly highly, with 88 % of the participants choosing 5 (extremely comfortable) or 4 (somewhat comfortable). Similar to the solvent cast films, both those attributes had a median score of 4 overall. There was one outlier score of 2, or a somewhat uncomfortable formulation, for both size and thickness. It seems therefore that the participants preferred larger and thicker films, which may be explained by the fact that they are easier to administer into the mouth, not necessarily because they were electrospun or solvent cast.

Participant assessments of disintegration time and saliva thickening effect were similar, with a median score of 4 but a slightly larger range. Handling of the sample also had a median score of 4, but the range of responses extended to 1 (an extremely uncomfortable formulation). Stickiness scores were lower, with a median of 3 (neither comfortable nor uncomfortable), which is the same as the electrospun films, denoting that stickiness may be the largest barrier for films' acceptability from the attributes tested [238].

At first glance, the acceptability attributes scoring of both sets of films are very similar. The median values are the same for size, thickness, disintegration time, saliva thickening effect, stickiness and handling of the films.

Differences between the formulations can be seen when considering the modal values (Table 5.2). Because the rankings cover a small range of only 5 choices, a modal value can present a more reliable way of comparing acceptability since there are a lot of repeated values in this dataset. Table 5.2 also shows the quality attributes scoring the most 5s or extremely comfortable for both films.

Table 5.2. Modal ratings of quality attributes for the PVA ODFs manufactured by both methods. % demonstrates attributes scoring the most 5s or extremely comfortable.

Quality attribute	Electrospinning		Solvent casting	
	Modal value	Score = 5 (%)	Modal value	Score = 5 (%)
Thickness	5	48	4	26
Size	4	42	4	34
Disintegration time	5	38	4	30
Handling	4	34	5	46
Saliva thickening effect	4	26	4	18
Stickiness	2	16	2	10

The percentage of participants ranking any of the attributes as extremely comfortable (5) was higher for every quality attribute when comparing electrospun to solvent cast films, apart from handling of the films (34 % vs 46 %). There was a positive difference of 8 % for scores of extremely comfortable for the perceived film size in the mouth, saliva thickening effect and disintegration time of the electrospun film. The differences between fabrication methods in the acceptability of size and thickening effect on saliva were statistically significant, with *p*-values of 0.03096 and 0.0012, respectively. However, as previously mentioned, the sizes of the films were different, and therefore it is believed the participants may have preferred the larger films for the ease of administration, and not necessarily because they were electrospun. Disintegration time differences were not found to be statistically significant (*p*-value = 0.35).

The samples were controlled for mass, and because the electrospun films are less dense they had a larger size of 3 cm x 2 cm (thickness approximately 250 µm), whereas the solvent cast films were 2 cm x 1.7 cm in size (thickness approximately 85 µm). It was not possible to make the solvent cast films larger in size and keep their mass comparable to fibres, because this would have resulted in them being too thin to handle. The acceptability results for size and thickness of the films therefore do not necessarily represent superiority of either method, but relate to the general acceptability of size/ thickness of films.

The thickness and handling of the samples show the clearest differences between the electrospun and solvent cast films. The different densities of the films can impact the thickness perception, with 22 % more participants selecting extremely comfortable for the thickness of the electrospun film. This difference was, however, not statistically significant, with *p*-value = 0.66. The thickness of the electrospun films was the most highly rated attribute, whereas for solvent cast films this was the 4th attribute in rating order. It can be concluded that participants prefer thicker films therefore, irrespective of fabrication method. In contrast, handling was the highest rated acceptability attribute for the cast film. The ease of handling of the films was the only attribute where participants ranked the solvent cast system more highly, but this was not statistically significant (*p*-value = 0.09). With regards to stickiness, a positive difference of 6 % was observed for electrospun films, but this again was not a statistically significant finding (*p*-value = 0.53). This is to be expected, given that stickiness is a factor mostly dependent on the film composition (polymer), which is identical for both formulations.

5.3.1.3 Stickiness Intensity

It is recognised that stickiness of oral films can be undesirable [251]. It was hypothesised that as the stickiness intensity increases so will the undesirability of the formulation. it is shown that stickiness scored lowest amongst the acceptability attributes, with a median of 3 and mode of 2 for both manufacturing methods. Figure 5.5 is a bar chart depicting the stickiness intensity. This refers to the perception the user experiences when placing the film in their mouth, rather than comfort or discomfort associated with that feeling. For example, an individual may find a film sticky yet comfortable, or vice versa.

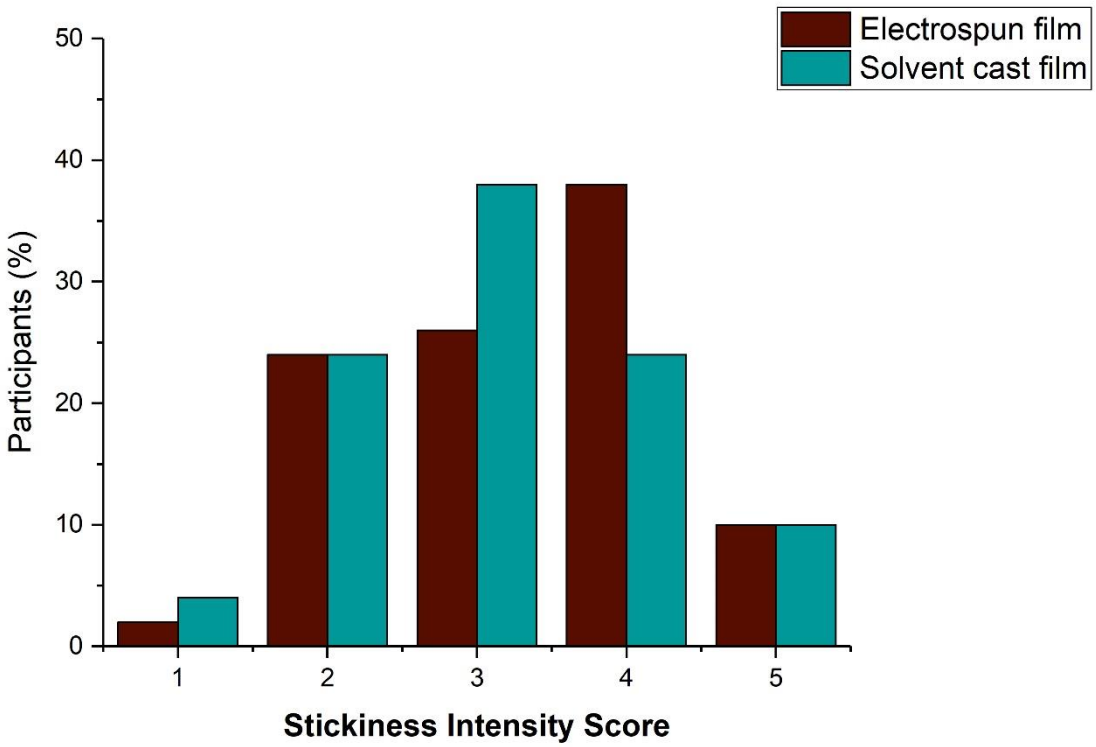

Figure 5.5. Bar chart representing stickiness intensity scoring for both ODF manufacturing methods.

It can be seen in Figure 5.5 that the modal score for the electrospun films is 4, or only slightly sticky, and for solvent cast films the mode is 3, or moderately sticky. Actual discomfort associated with stickiness scored lower (Table 5.2) with modal value of 2 for both manufacturing methods. This suggests that the threshold for discomfort associated with stickiness intensity is quite low, and some work is needed to overcome this hurdle. In addition, this finding disproves the earlier hypothesis that both reported outcomes are correlated.

For both films, an equal percentage of participants chose 5, which equates to the samples not being perceived as sticky. More participants ranked the electrospun films as 4 (only slightly sticky), indicating a slight increase in acceptability over the cast films where more participants gave a score of 3 (moderately sticky). However, the difference observed between the films in terms of stickiness intensity was not statistically significant (*p*-value = 0.07),

confirming the null hypothesis that both methods exhibit the same perceived stickiness.

5.3.1.4 Saliva Thickening Intensity

The thickening effect on saliva after placing the formulations on the tongue was the second least acceptable attribute for both manufacturing methods in terms of the number of participants selecting 5 or extremely comfortable. Similar to stickiness perception, a further question investigating the thickening effect intensity was asked. The saliva thickening perception was explored, rather than its subsequent comfort or discomfort (Figure 5.6). Again, it was hypothesised that the lower the thickening effect intensity was perceived to be, the more comfortable the mouthfeel. It can be seen from the bar chart that both methods had a modal value of 4 or only slightly thickened saliva. This agrees with the hypothesis that intensity of the saliva thickening perceived is correlated to the level of comfort or discomfort reported, as the modal value of this (Table 5.2) is also 4.

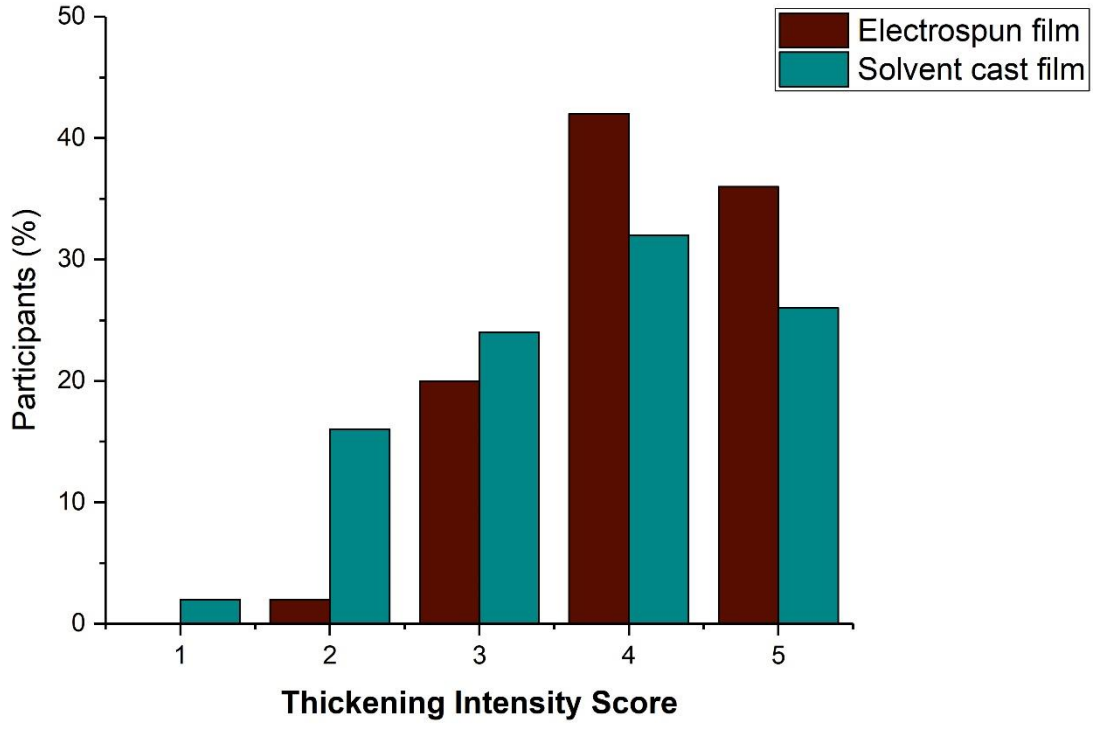

Figure 5.6. Bar chart representing saliva thickening intensity scores for both ODF manufacturing methods.

The data in Figure 5.6 indicate that participants preferred electrospun to solvent cast films in terms of saliva thickening intensity. The saliva thickening effect, and therefore intensity, is important because it might indicate further unfavourable outcomes such as mouth dryness and difficulty swallowing [254], which would be likely to reduce patient compliance. The difference observed between both methods was statistically significant (*p*-value = 7.21×10^{-4}). This concurs with the difference between comfort levels relating to saliva thickening effect, which was also found to be statistically significant.

5.3.1.5 Film Swallowing and Disintegration Time

Complete film swallowing data were captured in the final portion of the survey. Swallowing recorded represented a binary outcome of either swallowing the disintegrated film or spitting it out due to aversiveness. One participant spat out the whole electrospun film, stopping the timer at 12 s, and four others spat it out with partial loss only after having the film in their mouth between 27 and 60 s. This did not raise any safety concerns from the participants. The questionnaire did not allow for capturing the causes of film loss and so it is not clear why this happened. However, it can be assumed it is not taste related since both films had the same composition. This is one of the first studies investigating the acceptability of electrospun films in human participants, which means there are no baseline data. Nonetheless, it is known that 35 % of the general population have difficulty in swallowing oral solid dosage forms [255]. Although most participants preferred the larger size of the electrospun sample, this also could be a reason why the film was spat, with the larger size leading to difficulty in swallowing. However, the particular reasons for this will need to be explored further, and perhaps more researcher observed outcomes should be incorporated in future studies. None of the solvent cast films were spat out.

35 participants indicated that the electrospun films disintegrated in under 1 minute, whilst the remaining ten reported times between 1 and 3 minutes. 40 participants found that the solvent cast films disintegrated in under a minute, with the remaining ten recording a time between 1 and 3 minutes. The electrospun films had a median disintegration time of 30 s, with a minimum

value of 8 s and maximum of 120 s. The solvent cast films gave a median time of 34.5 s, with a minimum of 9 s and maximum of 136 s. Overall the solvent cast films took slightly longer to dissolve, but this difference was not statistically significant (*p*-value = 0.83).

Data shown here is supported by literature findings, where a pharmacokinetic study in rats demonstrated that drug release from PVA/PVP-blend electrospun ODFs is significantly faster than that of solvent cast films, which may be desirable for conditions requiring fast onset such as migraine relief [256].

5.3.1.6 Overall Acceptability

There is a comprehensive definition of a preparation's acceptability in the EMA's guidance on pharmaceutical development of medicines for paediatric use [234]. It is stated that acceptability is "defined as the overall ability of the patient to use a medicine as intended" and outlines the aspects involved as: palatability, swallowability (size and shape); appearance (colour, shape); the required dosing frequency; administration device, if needed; the primary and secondary container system; and the actual mode of administration to the child [234]. In this study, participants were asked to give their assessment of the acceptability of various attributes the authors deemed as key for an ODF's mouthfeel. At the end of the questionnaire, participants were asked to assess the overall acceptability of both films (Figure 5.7) by rating the formulations from extremely bad (1) to extremely good (5). The electrospun films scored slightly higher than solvent cast films for the extremely good rating, but this difference was not statistically significant (*p*-value = 0.54).

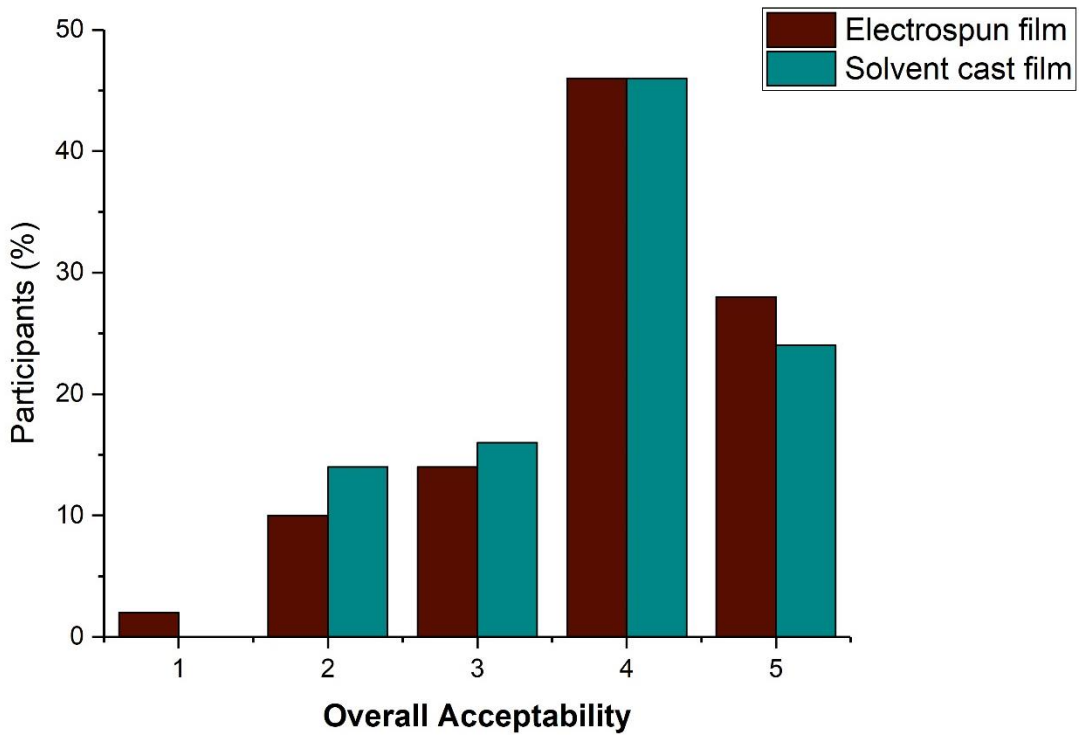

Figure 5.7. Overall acceptability scoring of the ODFs produced by both methods.

To further understand participants' overall preference, they were asked to choose a preferred formulation using a forced choice test of both formulations. Table 5.3 details the results. A difference of 28 % was observed for the male participants in their ranking of electrospun films as more preferable, while female participants had no overall preference with an equal split for both formulations. The reasons for these differences are not clear, and need further investigation [257]. It should also be noted that the male sample size was approximately 50 % of the number of female participants and therefore the data here have low power.

Table 5.3. Overall participant preference of the ODFs produced by both methods.

Participants (number)	Electrospun films (%)	Solvent cast films (%)
Total (50)	54 (27/50)	46 (23/50)
Male (14)	64 (9/14)	36 (5/14)
Female (36)	50 (18/36)	50 (18/36)

There was no statistically significant difference in preference between males and females, with a *p*-value of 0.37. Overall, 27 out of the 50 participants chose electrospun films as their preferred ODF over solvent cast films in a forced choice test, however, this difference is marginal and was not found to be statistically significant (*p*-value = 0.55).

Electrospun mats have been very widely explored as fast-dissolving film formulations, with a Web of Science search conducted on 17 January 2020 yielding 95 hits for “electrospinning” AND “fast dissolving”. It has been very well established that the amorphous physical form of the drug in electrospun fibres, coupled with their very high surface area to volume ratio, can lead to enhanced solubility and dissolution rate [258–265]. However, to date the patient acceptability of electrospun formulations has not been explored. This is a crucial facet of their onward development into medicines and is addressed for the first time in this work. It is shown here that electrospun formulations are at least as acceptable to adults as solvent cast films and appear to be more acceptable in some aspects. This is an important finding: it is widely recognised that solvent cast films are acceptable to end-users [62,221,251,266], and from the data presented in this work it is clear that electrospun formulations will also be acceptable. Electrospun films hence comprise viable alternatives to solvent cast films. Given that scale up to industrial throughput is now possible [244] and clinical trials of electrospun formulations underway, (Rivelin, 2019) these results pave the way for the clinical translation of electrospun fibre formulations.

5.3.2 Part B: Multi-axial Electrospinning

In order to successfully electrospin KCT with CPM and E-EPO using multi-axial electrospinning, the newly introduced third layer needed to be optimised separately before introduction to the multi-axial system. The aim of this design was to achieve a taste-masked fibre mat with a hydrophilic outer layer, which can be presented clinically as an orodispersible film with acceptable mouthfeel properties. The hydrophilic polymers PVA and PVP were selected as candidates for the outer layer due to their film-forming abilities and use in

ODFs [82,83,256,259,268]. In addition, E-EPO was re-optimised using a mixed solvent system to ensure the overall optimisation of the process when all three solutions were electrospun together.

5.3.2.1 Electrospinning of Polyvinyl alcohol

As the human panel showed positive results for electrospun PVA fibre mats, the electrospinning of PVA was optimised to be loaded into the outer layer of the multi-axial formulation. In addition, PVA has been electrospun previously for the formation of an ODF, incorporating riboflavin/caffeine [123] and donepezil [245]. Figure 5.8 shows an SEM and fibre diameter distribution histogram of electrospun 8 % (w/v) PVA. This concentration was optimised from conditions discussed by Zhang *et al.* (2005) [124]. The fibres had a mean diameter of 457 nm ± 146 nm. PVA's electrospinning conditions were optimised at the following; flow rate of 0.2 mL/h, applied voltage of 12 kV and gap distance of 15 cm. The fibres show smooth morphology with a narrow size distribution as indicated by the low SD. As PVA is practically insoluble in ethanol, when electrospun with a multi-axial needle with E-EPO or KCT ethanol-based solutions, needle clogging occurred due to solidification on point of contact and electrospinning was not possible.

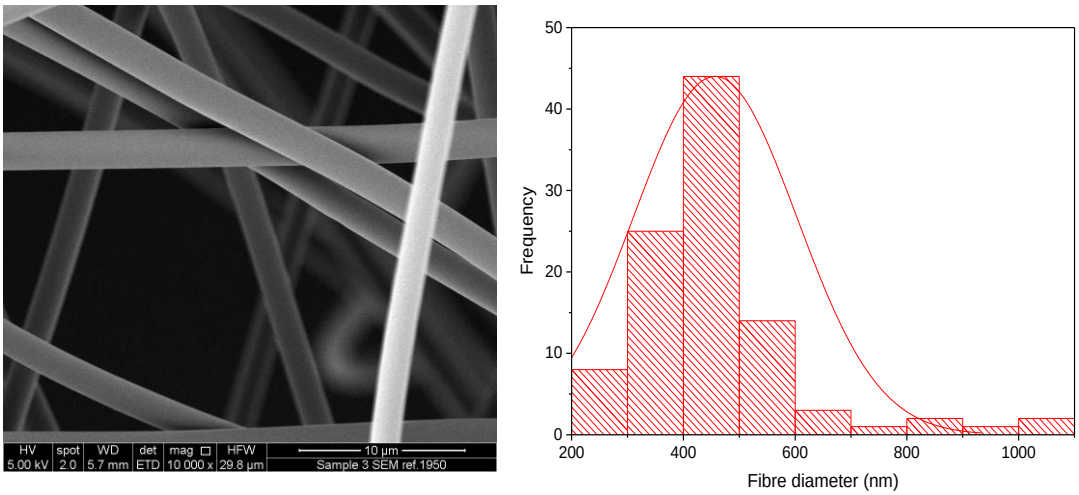

Figure 5.8. SEM and fibre diameter histogram of PVA fibres.

5.3.2.2 Electrospinning of Polyvinylpyrrolidone

In addition, PVP, which is soluble in ethanol, was optimised to be electrospun for use in the multi-axial systems. PVP can achieve rapid disintegration, drug release, and does not exert an aversive taste, all features essential in an ODF [82]. PVP has been used on numerous occasions in the electrospinning of oral films including: amlodipine/valsartan films [269]; paracetamol/caffeine [81]; meloxicam [82]; and helicid [87].

Figure 5.9 shows an SEM and fibre diameter distribution histogram of electrospun 10 % (w/v) PVP. This polymer concentration was derived from literature conditions which were found to be transferable [82]. The fibres had a mean diameter of 1520 nm ± 399 nm. PVP's electrospinning conditions were optimised at the following; flow rate of 0.7 mL/h, applied voltage of 12 kV and gap distance of 17.5 cm. The fibres show smooth morphology with a low average fibre diameter. These optimised conditions will be transferred for use in the multi-axial electrospinning of the taste-masked formulation of CPM.

Having an outer hydrophilic layer such as PVP will provide the formulation with the acceptable disintegration mouthfeel of a fast-disintegrating film [251].

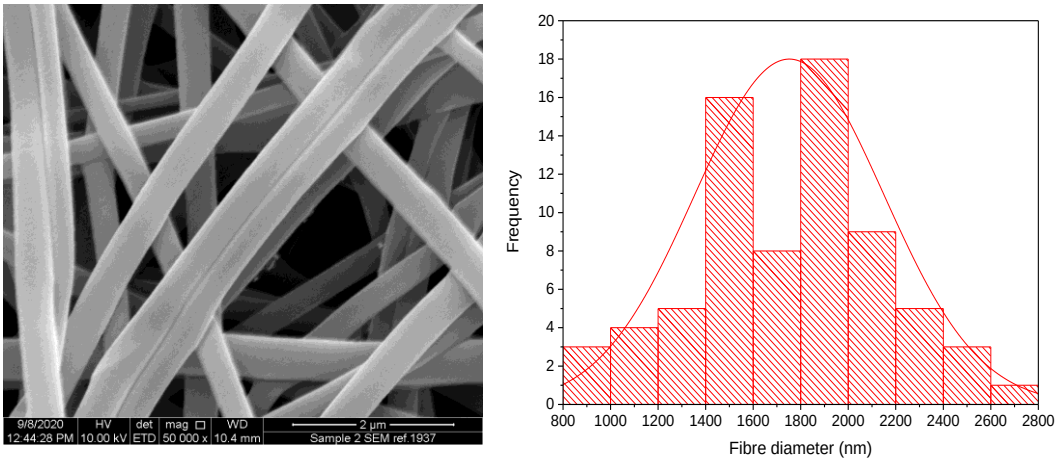

Figure 5.9. SEM and fibre diameter histogram of PVP fibres.

5.3.2.3 Re-optimising E-EPO electrospinning with mixed solvents

One of the main challenges with the monoaxial E-EPO fibres was the needle clogging. In addition, this problem was also evident with the co-axially electrospun fibres. In co-axial electrospinning only one solution needs to drive the electrospinning process forward. As it was concluded from the co-axial electrospinning experiments that the optimum conditions included E-EPO in the shell and KCT in the core, placebo E-EPO was re-optimised via using mixed-solvents to overcome the needle clogging.

The use of a co-solvent system can improve Taylor cone stability thereby reducing needle clogging [270]. This is in line with findings found in the literature where DMAc is used as co-solvent with acetone and ethanol [271,272]. DMAc and DMSO have high boiling points compared to ethanol and therefore they are less likely to evaporate at the needle causing clogging. DMAc's boiling point is 168 °C whilst DMSO is 189 °C [87].

Various ratios of co-solvents were used as shown in Table 5.4. For the placebo E-EPO formulation, all samples contained the polymer at the previously

optimised concentration of 35 % (w/v) E-EPO, were electrospun at a gap distance of 17.5 cm and were pumped at a flow rate of 1 mL/h. The combinations in Table 5.4 were electrospun to investigate Taylor cone stability and the associated needle clogging.

Table 5.4. Different co-solvent combinations to improve the Taylor cone stability of E-EPO.

F	Solvent ratio			Needle clogging	Stable TC
	DMAc	DMSO	EtOH		
F1	0	1	5	Clogged	
F2	1	1	7	Clogging delayed	
F3	1	1	4	Minor clogging	
F4	1	2	4	Minor clogging	Y
F5	2	1	9	Clogged	
F6	1	1	5	Clogging; Unstable jet	
F7	1	2	9	Minor clogging	Y
F8	1	3	2	Clogged	
F9	1	1	6	Medium clogging	
40 % (w/v) E-EPO; 15 kV; 1 mL/h and 15 cm.					
F10	1	2	6	No Clogging	Y

The best formulations at a concentration of 35 % (w/v) E-EPO were found to be F4 and F7. F4 fibres' SEM and mean diameter distribution are shown in Figure 5.10. The fibres had a mean diameter of 623 nm ±188 nm. Upon inspection of the morphology, the fibres did not have a smooth appearance and spindle formation was observed, indicating that these conditions were in the sub-optimal entanglement region.

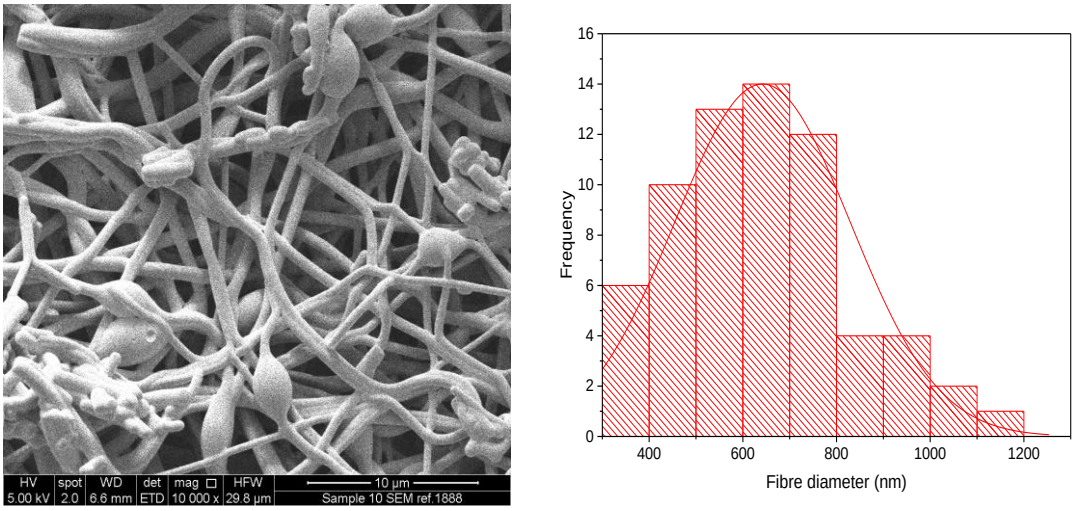

Figure 5.10 SEM and fibre diameter distribution of 35 % (w/v) placebo E-EPO fibres in a mixed solvent of 1-part DMAc, 2-parts DMSO and 4-parts ethanol.

F10 contained 40 % E-EPO, was electrospun at a voltage of 15 kV, flow rate of 1 mL/h and gap distance of 15 cm. DMSO has been used to lower the viscosity of systems whilst lowering the surface tension [270], which may explain the fact that the fibres stabilised at a polymer concentration of 40 % (w/v). It can be deduced that the chain entanglement concentration shifts with a different co-solvent system, which explains the higher E-EPO concentration needed for smooth fibres. The fibres produced were not brittle, and were easily peeled away from the metal collector. As the Taylor cone was stable, needle clogging did not occur leading to the formation of smooth fibres.

It was determined that placebo 40 % (w/v) E-EPO in 1-part DMAC, 2-parts DMSO and 6 parts absolute ethanol yielded smooth non-beaded nanofibres. An SEM image of the placebo fibres and histogram of fibre diameter distribution is shown in Figure 5.11. The solution was electrospun at an applied voltage of 15 kV, gap distance of 15 cm and flow rate of 1 mL/h. A stable Taylor cone was achieved at these conditions and no needle clogging was observed. The fibres show smooth morphology and mean fibre diameter was determined to be 565 nm ± 156 nm.

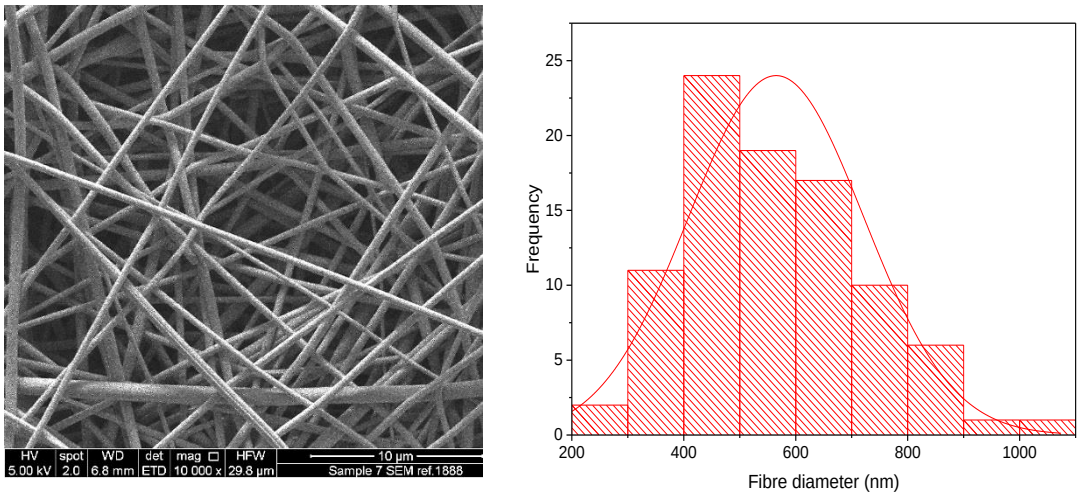

Figure 5.11. SEM and fibre diameter distribution of 40 % (w/v) placebo E-EPO fibres in a mixed solvent of 1-part DMAC, 2-parts DMSO and 6-parts ethanol.

Using the re-optimised placebo E-EPO conditions, co-axial formulation system 2 with drug-loaded KCT in the core and E-EPO in the shell was electrospun. No needle clogging was observed and smooth fibres were formed.

5.3.2.4 Tri-axial Electrospinning

Tri-axial electrospinning of 7.5 % (w/v) KCT with 3.5 % (w/v) CPM in the core, 40 % (w/v) E-EPO in the middle layer, and 10 % (w/v) PVP in the shell was undertaken. The fibres' SEM and diameter distribution are shown in Figure 5.12. The fibres show a smooth structure and diameter sizes with a mean fibre diameter 1061 nm ± 267 nm. The applied voltage was set at 15 kV and the gap distance at 17.5 cm. The flow rates of all three solutions were set at 0.3 mL/h. This gave rise to a stable Taylor cone and no needle clogging. In addition, at these flow rates, the theoretical drug-loading was determined to be 7.51 % (w/w) CPM, which is comparable to co-axial formulation 2 which had a drug-loading of 7.60 % (w/w). The film size needed at this theoretical drug-load is 26.67 mg for a 2 mg dose of CPM, which is similar to the film sizes assessed in the human panel. The actual drug-loading of the tri-axial films was determined to be 90.1 % ± 8.4 %, which is a positive indicator of the stability of the electrospinning process and therefore the drug distribution in the fibre mat.

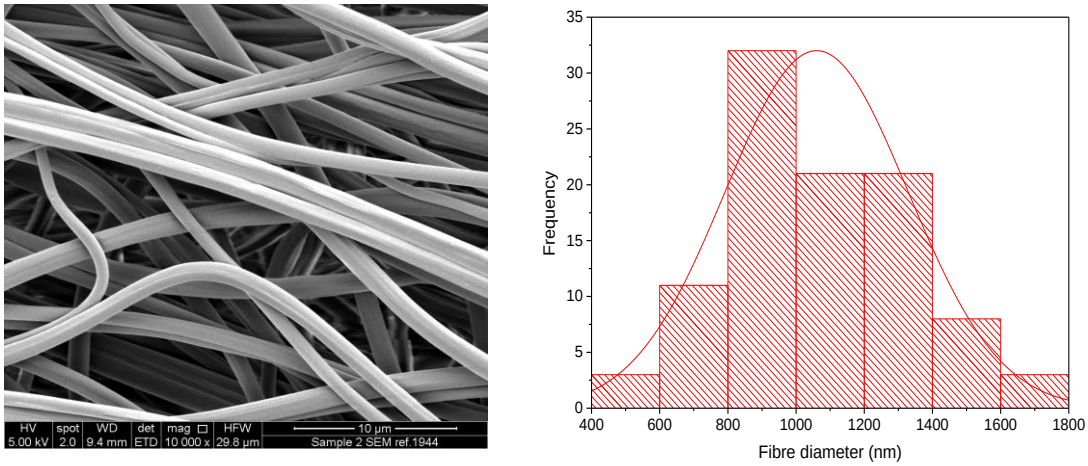

Figure 5.12. SEM and fibre diameter distribution histogram of tri-axially electrospun films containing 7.5 % (w/v) KCT and 3.5 % (w/v) CPM in the core; 40 % (w/v) E-EPO in the middle layer and 10 % (w/v) PVP in the shell.

5.3.2.5 Tetra-axial Electrospinning

Tetra-axial electrospinning of 7.5 % (w/v) KCT with 3.5 % (w/v) CPM in the core, 40 % (w/v) E-EPO in the inner middle layer, absolute ethanol in the outer middle layer and 10 % (w/v) PVP in the shell was completed. The presence of a blank layer of solvent is believed to perform a number of functions such reducing the surface tension or slowing down the evaporation of the other solutions. Those can help reduce formation of solid substances of needle which can cause clogging and subsequently halt the running of the electrospinning process [68,272]. The fibres' SEM and diameter distribution are shown in Figure 5.13. The fibres show a smooth structure and diameter sizes are not skewed, with a mean fibre diameter 742 nm ± 386 nm. The tetra-axial fibres show a reduced fibre diameter compared to the tri-axial fibres, likely due to the increased solvent layer system. As the blank solvent coats the core solutions, the solvent is retained for a longer period as it enters the instability region prolonging its elongation time and therefore resulting in fibres with a smaller diameter [272]. The applied voltage was set at 15 kV and the gap distance at 17.5 cm. The flow rates of all four solutions were set at 0.3 mL/h. This gave rise to a stable Taylor cone and no needle clogging. In addition, at these flow rates, the theoretical drug-loading was determined to be 7.51 % (w/w) CPM, which is comparable to co-axial formulation 2 which

had a drug-loading of 7.60 % (w/w). The film size needed at this theoretical drug-load is 26.67 mg for a 2 mg dose of CPM, which is similar to the film sizes assessed in the human panel. The actual drug-loading of the tri-axial films was determined to be 92.6 % ± 7.1 %, which is a positive indicator of the stability of the electrospinning process and therefore the drug distribution in the fibre mat.

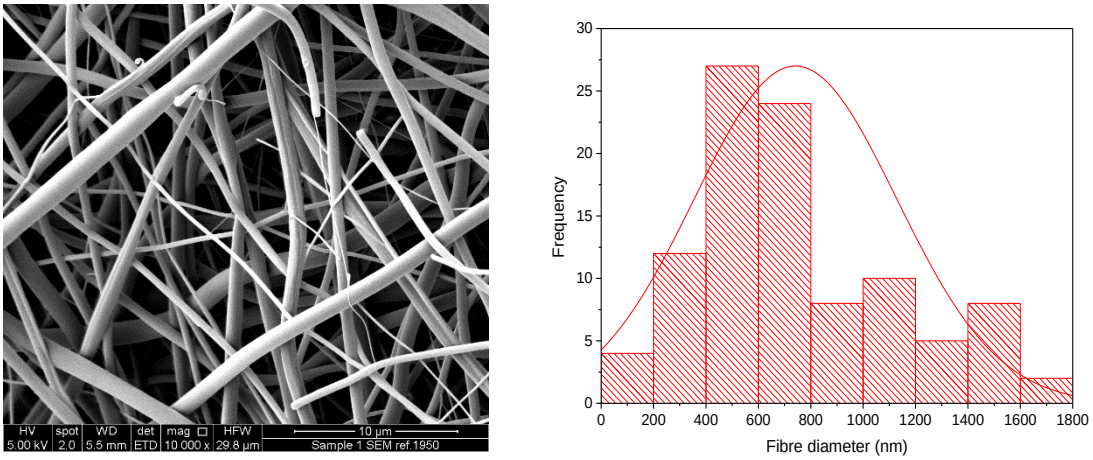

Figure 5.13. SEM and fibre diameter distribution histogram of tetra-axially electrospun films containing 7.5 % (w/v) KCT and 3.5 % (w/v) CPM in the core; 40 % (w/v) E-EPO in the inner middle layer; absolute ethanol in the outer middle layer and 10 % (w/v) PVP in the shell.

5.3.3 Solid State Characterisation

5.3.3.1 Powder X-Ray Diffraction

Figure 5.14 shows the XRD diffraction pattern of all the tri-axial and tetra-axial systems, raw PVP, and the physical mixture. CPM distinctive peaks were seen at 13.19 º, 19.48 º, 20.43 º and 22.06 º, and are clearly observed in the physical mixture but not in the fibres. The electrospun fibre clearly lacks the distinctive diffractions peaks observed in the crystalline CPM pattern indicating amorphous state formation; see Section 4.3.3.1 for the diffraction patterns of CPM, E-EPO and KCT.

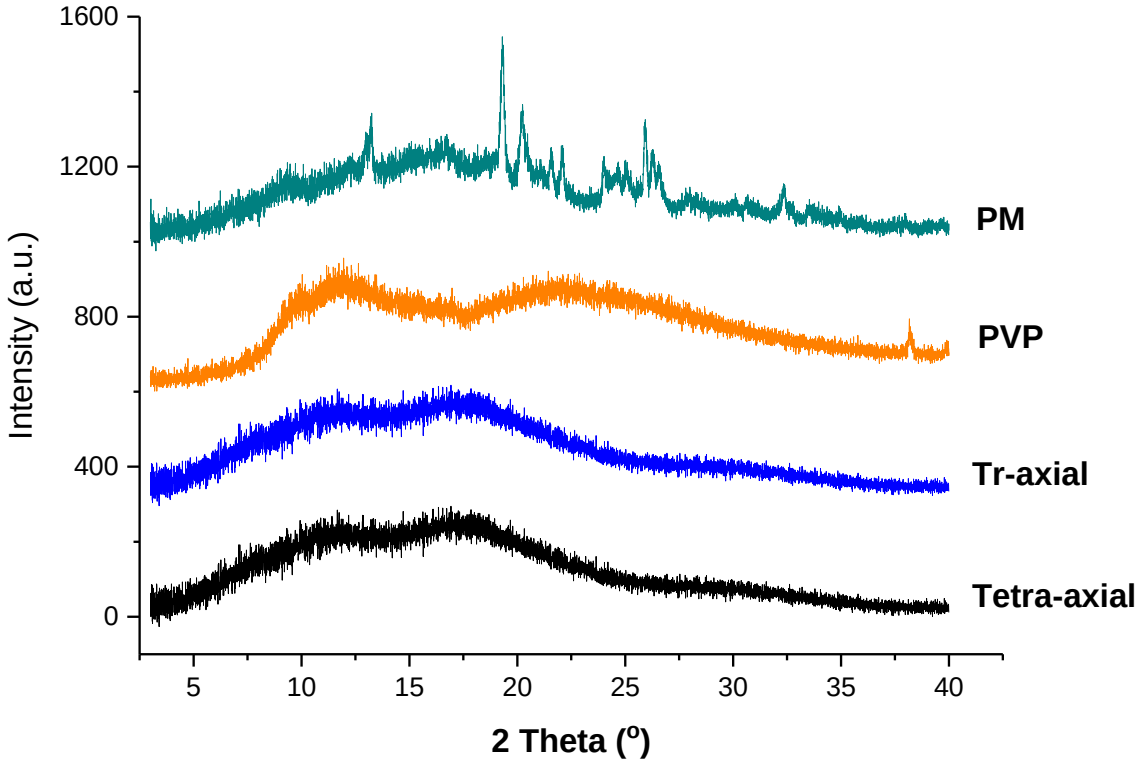

Figure 5.14. XRD diffraction patterns of electrospun drug-loaded tri-axial and tetra-axial films, as well as raw PVP and the physical mixture (PM).

5.3.3.2 Fourier Transform Infra-Red

The FTIR spectra of the tri-axial and tetra-axial films, as well as raw PVP is shown in Figure 5.15. The main peaks observed in the electrospun fibres match those of the raw ingredients discussed in sections 3.3.5.2 and 4.3.3.2. For E-EPO and KCT, these include the characteristic C-O bond peak at 1150 cm^{-1}, as well as 1265 cm^{-1} and 1237 cm^{-1} are also characteristic of this ester group. Other significant peaks noted at 1452 cm^{-1} and 2946 cm^{-1} are characteristic of the hydrocarbon chain vibrations and are in close agreement of literature values of 1450 cm^{-1} and 2950 cm^{-1} [192].

The drug CPM shows characteristic peaks that do not seem to present anymore in the fibres. These results indicate that CPM was amorphously distributed in the polymeric carriers, which was also validated in the XRD data.

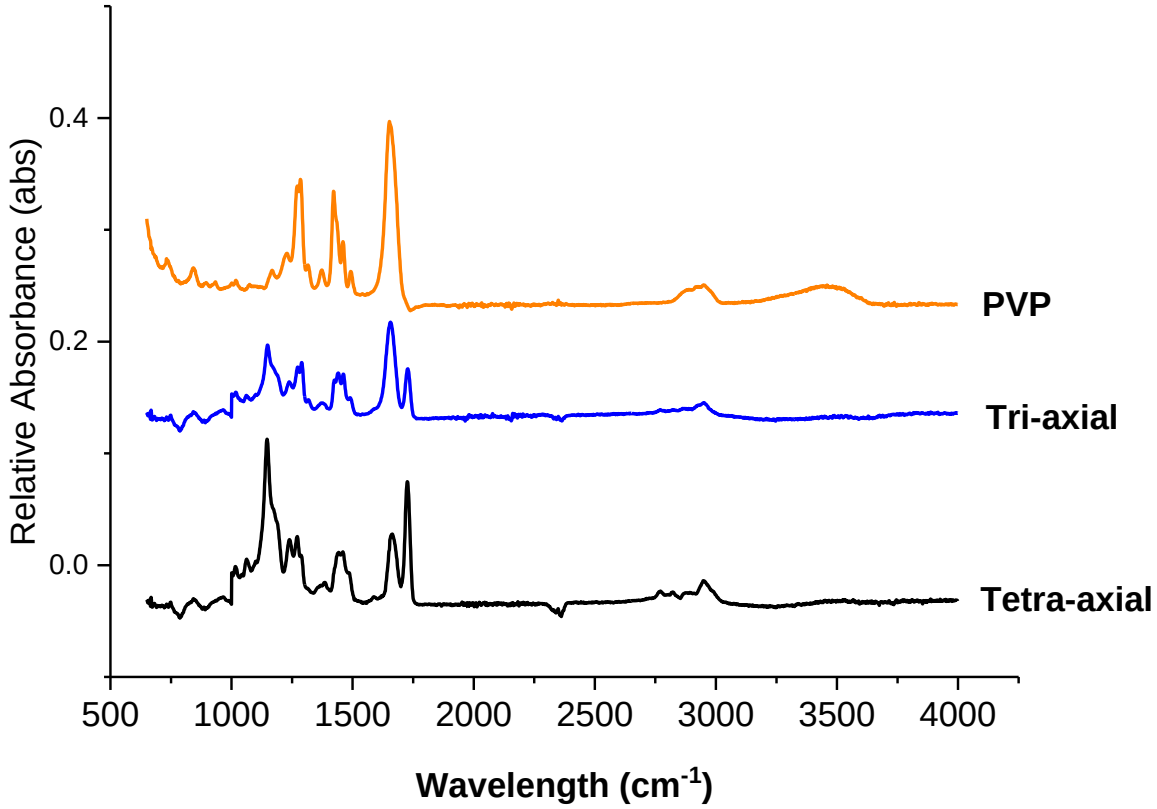

Figure 5.15. FTIR spectra of PVP, the tri-axial and the tetra-axial electrospun films.

PVP shows a significant peak at 1651 cm^{-1} which can be attributed to C=O and N-C stretching vibrations. This is in line close agreement with the literature vale of 1664 cm^{-1} [273]. The polymer shows a 2nd distinctive peak at 1421 cm^{-1}, which represents the scissoring of the CH_2 cyclic groups, also in close agreement of the literature value of 1422 cm^{-1} [273]. In addition, it shows an absorption peak at 1284 cm^{-1} which is indicative of CH_2 wagging; this is in close agreement with the literature value of 1283 cm^{-1} [273]. These three main peaks are present in both the tri-axial and tetra-axial fibres, which indicated the lack of new bond formation between the drug and polymer, and confirms XRD's data that the drug is present in the system as an amorphous solid dispersion.

5.3.4 Thermal Characterisation

5.3.4.1 Thermogravimetric Analysis

A representative thermogram of the tri-axial system and tetra-axial films are shown in Figure 5.16 and Figure 5.17, respectively. For the tri-axial fibres, an analysis between 40 °C and 120 °C showed that a weight loss of 0.22 mg was observed, accounting for 2 % of the total sample weight. This indicates that some residual solvent was present in the representative electrospun fibres. Similarly, for the tetra-axial fibres, between 40 °C and 120 °C a weight loss of 0.18 mg was observed, accounting for 1.94 % of the total sample weight, indicating some residual solvent, likely ethanol and water vapour. In addition, between 160 °C and 190 °C, both the tri-axial and tetra-axial fibres showed 0.03 mg or 0.3 % weight loss around DMSO's and DMAc's boiling points, 189 °C and 168 °C [87], respectively, indicating minimal residual solvent presence for these two solvents. The thermograms display a similar shape to that of E-EPO (mean onset temperature 276 °C), showing that the drug is incorporated in it as a dispersion. The onset point however shifts to a lower temperature, 221 °C for the tri-axial film and 200.2 °C for the tetra-axial film, closely matching that of the drug (mean onset temperature 215 °C).

Similar to the mono-axial and co-axial fibres, the tri-axial and tetra-axial fibres displayed a biphasic degradation profile. For the tri-axial fibres, the first weight loss is seen around 221 °C with approximately 24.30 % of the sample degrading. This is then followed by a larger weight loss at 300.4 °C where approximately 63.96 % of the sample mass degrades. For the tetra-axial fibres, the first weight loss is seen around 200.2 °C with approximately 17.61 % of the sample degrading. This is then followed by a larger weight loss at 352.5 °C where approximately 60.46 % of the sample mass degrades. This is similar to the mono-axial and co-axial fibres' degradation profile, which represent the breakdown of the co-polymers.

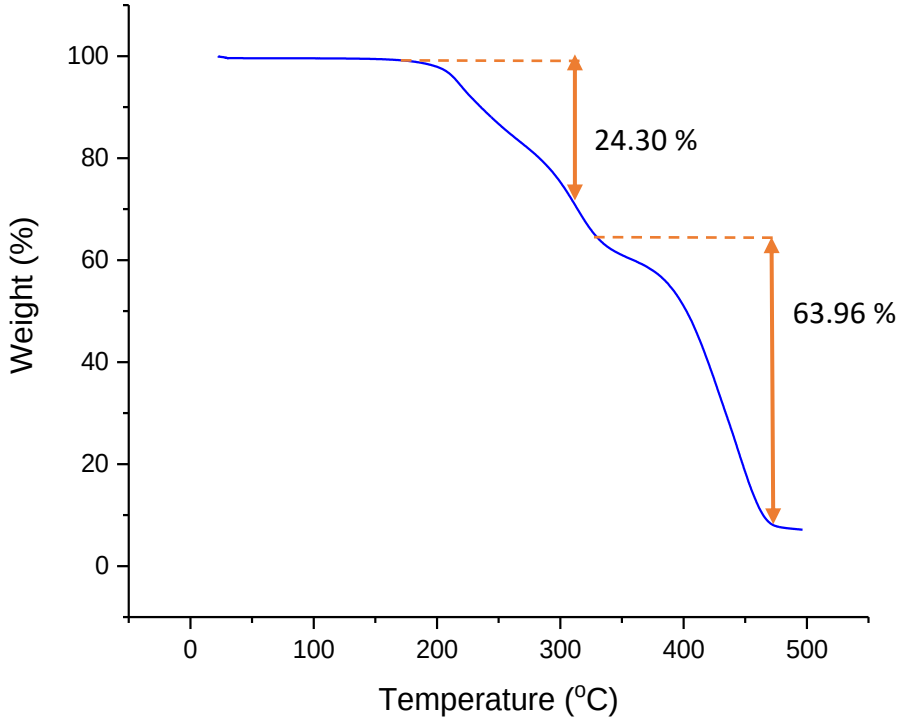

Figure 5.16. TGA thermogram of electrospun drug-loaded tri-axial films showing the % weight loss as temperature increases.

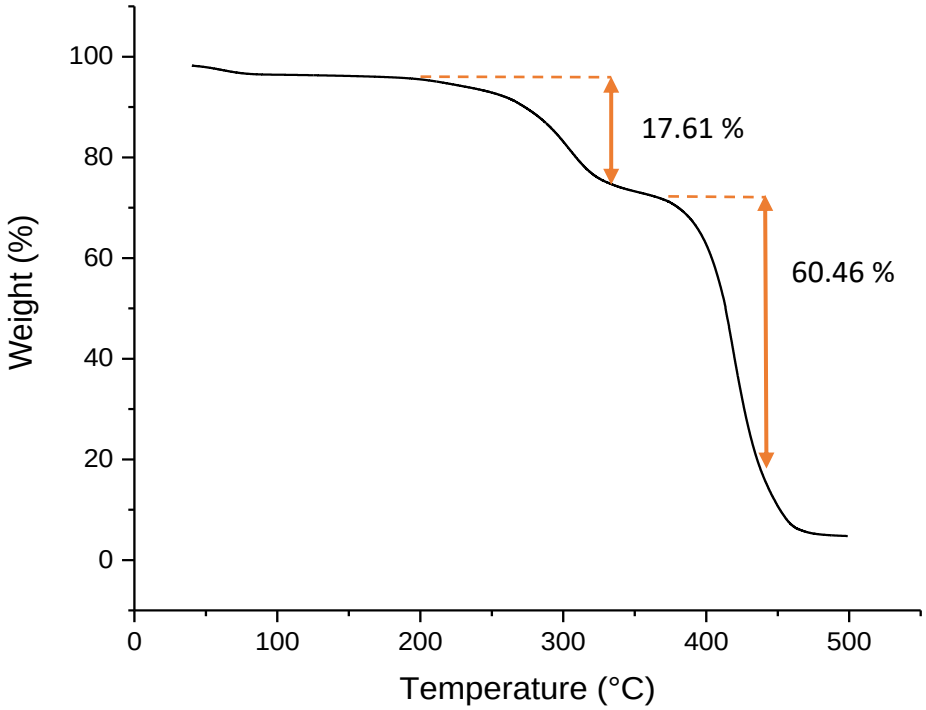

Figure 5.17. TGA thermogram of electrospun drug-loaded tetra-axial films showing the % weight loss as temperature increases.

5.3.4.2 Modulated Temperature Differential Scanning Calorimetry

Figure 5.18 shows representative DSC thermograms of the tri-axial and tetra-axial drug-loaded films. Both systems contained KCT with CPM in the core and PVP in the outermost shell layer. The tri-axial film contained E-EPO in the middle layer, and the tetra-axial film contained E-EPO and ethanol in the middle two layers. From Chapter 3, the data for CPM's melting point was 133.24 °C; E-EPO's glass transition temperature was 50.9 °C, whilst KCT's glass transition temperature was measured around 68 °C. As the measurement range was up to 150 °C, no thermal events were detected for PVP. The literature quoted value of PVP's T_g is 178.5 °C [274,275].

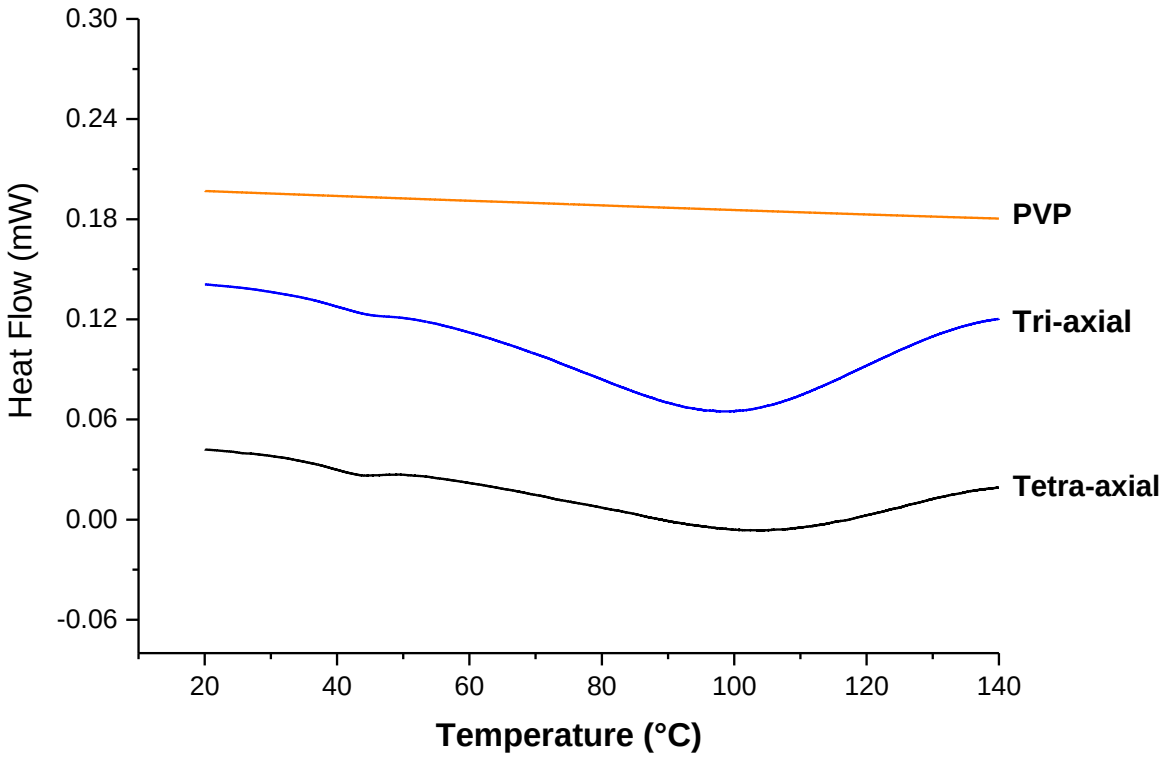

Figure 5.18. A reversing MTDSC heat flow thermogram of the tri-axial and tetra-axial electrospun drug-loaded fibre mats, as well as raw PVP.

The drug-loaded tri-axial and tetra-axial system did not display a melting peak which indicates the conversion of crystalline CPM to the amorphous state in the co-polymer matrix. The addition of the drug lowered the T_g of the system; the tri-axial film showed a T_g of approximately 45.68 °C, whereas the tetra-axial film shows a T_g of 43.70 °C. This reduction can be deduced to be a plasticising effect of the drug. In addition, this can be considered a stable drug-delivery system, as it has been suggested that the formulation's T_g should be between 10 °C to 20 °C higher than the storage temperature [66].

In addition, a water vaporisation peak is seen around 100 °C in both multi-axial formulations. The formulations did not contain water, so it is hypothesised that the water peak is a result of desorption of the sample pan. It can also be due to the PVP in the fibre mats displaying hygroscopic behaviour and absorbing water vapour, which was observed in the TGA thermogram as shown by the detected residual solvent. PVP is highly hygroscopic and it has been recorded that is can absorb up to 40 % of its mass in moisture, which may result in unstable fibre mats [82,256].

5.3.5 Dissolution

The *in-vitro* release profiles of the tri-axial and tetra-axial electrospun fibres are is shown in Figure 5.19. The dissolution experiment was performed in a buffer solution of pH 1.2, mimicking fasted gastric conditions. Children over two have a similar gastric pH to adults, which is generally between 1.0 and 2.5 [133]. It can be seen that the electrospun films release rapidly owing to their high surface area to volume ratio, and therefore a high release rate is expected. This is consistent with the results reported for the monoaxial and co-axial films which released approximately 97 % and 74 % respectively of the drug after 45 minutes. The tri-axial films released approximately 74 % of the drug amount at 45 minutes, while the tetra-axial films released approximately 86 % of the drug amount at 45 minutes, which is in line with an immediate

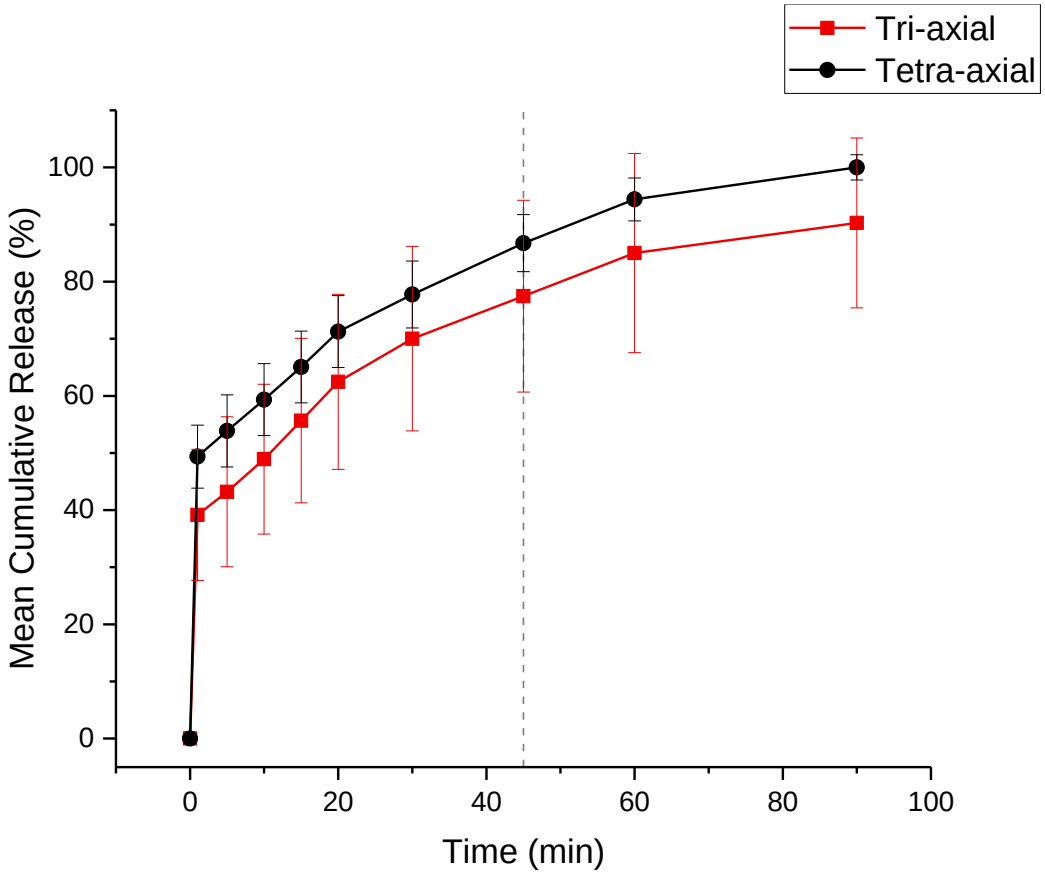

Figure 5.19. Dissolution profile in pH 1.2 of the drug-loaded tri-axial and tetra-axial formulations. The dashed lined represents the 45-minute timepoint.

release formulations' guideline of releasing 70 % of the drug in that timeframe (Ph. Eur. 5.17.1) [199]. It can be noted that when KCT is added to the formulation the release rate is reduced slightly, which is expected due to the increased barrier the polymer creates. However, this is still within the immediate release range; the formulations are expected to release fully in the stomach, where no adverse effect due to the taste-masking on absorption is anticipated. The addition of the PVP layer does not increase the release time if the co-axial and tri-axial films are compared, owing to the polymer's water solubility it is expected the polymer will start to dissolve in the oral cavity.

5.3.6 Film thickness, pH and Folding Endurance

The thickness of the films is of one of the main acceptability parameters for patients. The thickness of a 3 cm x 2 cm triaxial films were taken and the average measurement was found to be 100 µm ± 20 µm. The tetraxial films had an average measurement of 140 µm ± 30 µm. These thickness levels are

in line with literature recommendations, nonetheless, they can easily be altered by increasing the time of electrospinning and therefore the amount fabricated.

In addition to thickness of films, folding endurance is a very important parameter for the formulation to effectively be taken by the patient. The films were folded in the same position, and it was found that after bending them for 30 times they did not break, which is considered high endurance and the experiment was stopped [122,148,149]. The fact that the films have high folding endurance indicates that they will be well handled and easily ingestible.

The pH of the films when dissolved in distilled water was 6.65 ± 0.36, which is approximately neutral pH and within consistent values of saliva's natural pH levels. This indicated that the formulation is not expected to cause any irritation due to its pH levels [103,222].

5.3.7 E-tongue Taste-assessment

Figure 5.20 shows a bar chart of the mean sensor response of the tri-axial and tetra-axial formulations of CPM loaded fibres as well as raw PVP, as determined by the BT0 sensor. Both drug-loaded formulations contained the same amount of CPM; 20 mg/100 mL, which equates to 0.5 mM. This was the same amount added to co-axial and mono-axial films when taste-assessed.

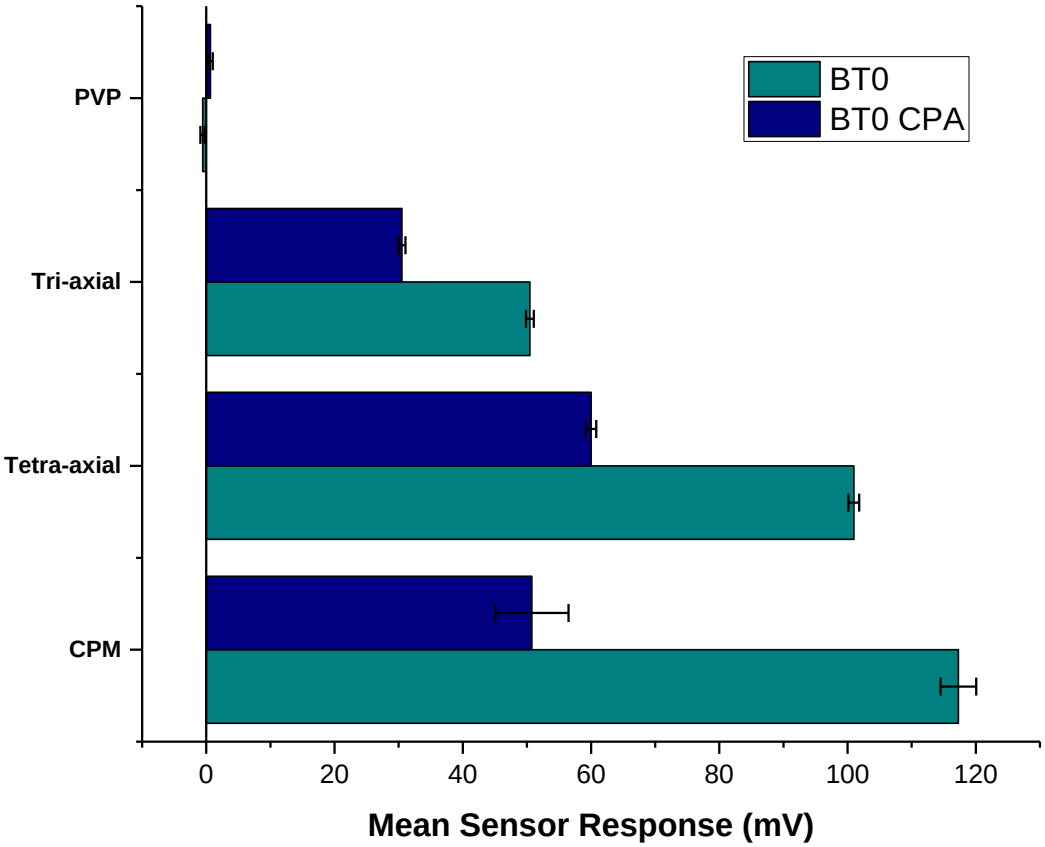

Figure 5.20. A bar chart showing the mean sensor response of the tri-axial and tetra-axial formulations of CPM loaded fibres as well as raw PVP.

It can be seen that the tetra-axial formulation displays a very similar response to the raw drug, indicating little to no taste-masking. This can be attributed to the fact that PVP is a water miscible polymer and upon contact with the aqueous test medium it released trapped drug molecule and therefore a bitter response was recorded. The tetra-axial formulation was more bitter than the tri-axial formulation, likely due to the extra ethanol layer in the tetra-axial system; the ethanol likely facilitated the diffusion of the drug from the core layers to the PVP shell. Nonetheless, the tri-axial formulation also displayed bitterness and therefore was not deemed fully taste-masked. To ensure that the PVP was not contributing to the bitter response recorded by these formulations, it was tested alone; it can be seen that elicits no response to the bitterness sensor. For both the formulations tested aftertaste or CPA is also displayed. CPM's bitterness persists through as an aftertaste, which can be

aversive to patients. In both the formulations tested the aftertaste is less intense than the initial taste. Similar to the findings of the initial taste, the aftertaste of the tri-axial and tetra-axial formulations is not sufficiently reduced for the formulations to be deemed as taste-masked.

PVP was chosen as the shell polymer as it is both ethanol and water soluble; this allowed the electrospinning process to be complete without clogging and in theory would behave similar to PVA and dissolve in an acceptable manner when in contact with saliva. As the multi-axial electrospun solutions were miscible, it is hypothesised that CPM diffused from the core layer into the outermost layers as the solutions approached the nozzle in electrospinning. TEM images of both the tri-axially and tetra-axially electrospun fibre mats are shown in Figure 5.21. It can be seen that defined borders are not seen between the layers, due to the miscible nature of the solvent-systems used. This confirms the hypothesis that the CPM likely diffused from the core to the water-soluble shell of both systems.

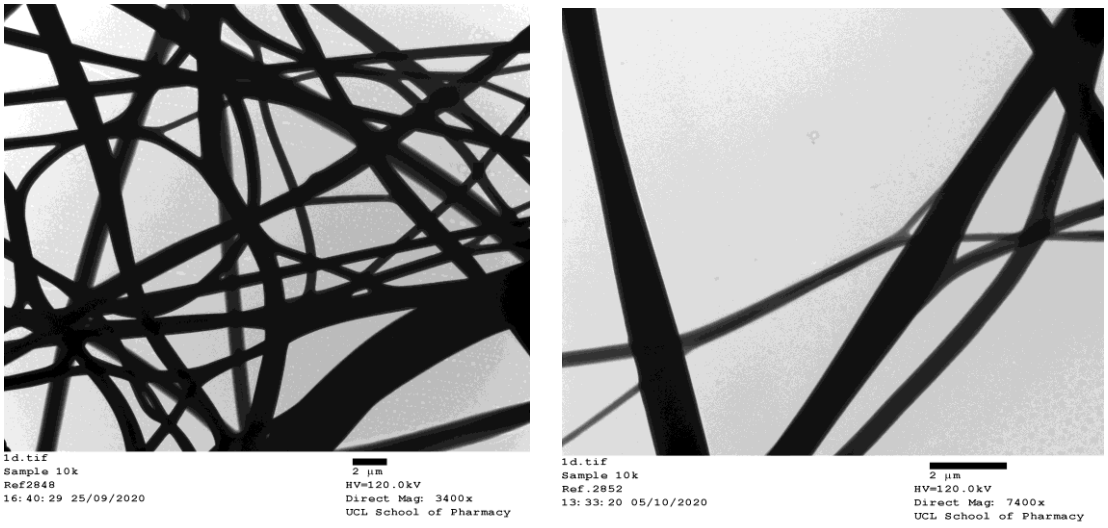

Figure 5.21. TEM images of (left) tri-axially electrospun fibres and (right) tetra-axially electrospun fibres.

5.4 **Conclusions**

A human panel study was performed to investigate the acceptability of orodispersible electrospun and solvent cast films. 50 healthy volunteers took

two drug-free samples of polyvinyl alcohol films prepared by the two methods. On a 5-point hedonic scale, the volunteers assessed the films' perceived size, stickiness, thickness, disintegration time, thickening effect on saliva and handling. The films manufactured by both methods were similar in their end-user acceptability. The modal values of perceived size, thickness, disintegration time, saliva thickening effect and handling were high (4 or 5). However, for both, the stickiness mode was 2 (strongly sticky) and the only negative attribute. Both films were reported to take approximately 30 s to disintegrate completely in the mouth. Electrospun films scored similarly high to solvent cast orodispersible films in most attributes of end-user acceptability. Electrospun films were marginally preferred, with 27 out of 50 participants picking electrospinning when presented with a forced choice test of both fabrication methods. This is one of the first studies to show that electrospinning enables the fabrication of orodispersible films that are acceptable to adult human participants in terms of handling and mouthfeel and suggests that the potential for clinical translation of such formulations is high.

Tri-axial and tetra-axial electrospinning was performed to manufacture a taste-masked oral film based on the human panel results. PVA was unsuitable to be electrospun with ethanol-based E-EPO and KCT; PVP was used instead. PVP coated drug-loaded fibres were prepared and characterised. Tetra and tri-axial films were successfully prepared, despite the limited data in the literature on process optimisation. TGA identified that there was minimal residual solvent left in the fibres, likely due to the hygroscopic nature of PVP or due to incomplete solvent evaporation. XRD and MTDSC confirmed the presence of the drug in the electrospun fibre matrix as an amorphous solid dispersion. In addition, FTIR studies showed that no new bonds were formed, confirming these findings.

Although the fibres showed satisfactory morphology, solid-state and thermal analysis results, the E-tongue taste-assessment indicated that the films were not fully taste-masked due to the hydrophilic nature of the PVP. Co-axial films with the re-optimised solvent system showed comparable satisfactory physical

properties as well as being fully taste-masked, therefore are the primary candidates for the oral film formulation.

Chapter 6

Conclusions and Suggested Future work

6.1 **Conclusions**

Designing and formulating age-appropriate dosage forms is of paramount importance for patient compliance in populations with special needs. More specifically, the paediatric population has suffered from a lack of specifically designed medicines, often leading to the medicine being administered in an off-label or unlicensed fashion. To overcome this problem, the Paediatric Regulation was issued by the EMA in 2007 and mandated that all manufacturers include what is known as a Paediatric Investigation Plan or PIP with the Marketing Authorisation dossier. In addition, an incentive was granted for manufacturers to re-formulate medicines already on the market into a paediatric-friendly dosage form. As well as safety, quality, and efficacy, an age-appropriate paediatric dosage form should be palatable. Palatability comprises the overall acceptability and appreciation of a dosage form which includes taste, mouthfeel, smell, appearance and ease of handling. With all of this in mind, the overarching aim of this thesis was to design an age-appropriate dosage form for a known bitter drug that will result in a palatable and easy to swallow formulation. In addition, the research conducted in this thesis aimed at furthering the understanding of using electrospinning as a taste-masking technology, including co-axial and multi-axial electrospinning. A further aim of the research was to advance the methodology of utilising the E-tongue for taste-assessment of raw bitter drug compounds as well as employing it to rank formulations and aid in the selecting of optimised candidates.

More specifically, the thesis has attempted to develop a prototype electrospun fibre mat formulation from basic principles of developing the electrospinning protocol for the taste-masking polymers, itself a novel contribution to the field, through to examining the taste-masking efficacy of a bitter model drug. This was assessed via a biosensor system which aided in ranking and deselecting formulations. Finally, mouthfeel assessment of electrospun fibre mats in a human panel aided in the development of a mat prototype via multi-axial electrospinning.

Electrospinning combines the advantages of nanotechnology with the taste-masking potential. Electrospun fibres have a high surface area to volume ratio, thus providing improved solubilisation, if needed. In addition, the fibres possess mechanical properties that can be purpose-built depending on the polymer used; these include filtration, biomedical devices, and drug-delivery applications. In terms of taste-masking, an electrospun fibre mat makes a promising candidate for an oral film, an easy to swallow formulation that is suitable for use in paediatrics.

Chapter 3 describes the electrospinning optimisation of Eudragit E PO (E-EPO), a taste-masking polymer. Quality by design principles, namely design of experiment (DoE), were used to identify the most important parameters in producing bead-free fibres that were in the nano-range. As electrospinning can be influenced by process, solution and environmental parameters, a DoE was needed to select the optimum conditions in a reduced number of runs. Applied voltage, gap distance and flow rate, were the process parameters explored. Polymer concentration and solvent content were the solution parameters varied. In addition, conductivity and viscosity measurements were taken to further understand the optimum conditions for E-EPO fibre formation. By increasing the polymer concentration gradually and simultaneously imaging the fibres using scanning electron microscopy, a chain entanglement concentration for the polymer in ethanol was deduced. Once the placebo fibre was optimised, a bitter drug was introduced into the electrospinning process; chlorpheniramine maleate (CPM). CPM has never been electrospun before with E-EPO and thus further optimisation of the drug-loaded polymer was required. Once the fibres were optimised to be bead-free and in the nano-range, solid state characterisation and thermal analysis were utilised to ensure the drug was present as an amorphous solid dispersion, indicating the effective electrospinning of the drug. XRD and DSC indicated that the drug was present as an amorphous solid dispersion whereas FTIR confirmed no new bonds were formed and therefore the drug's performance should not be affected, in theory. TGA confirmed there were no residual solvent which is essential, as for paediatric formulations little to no solvent should be present. Once all the solid state and thermal characterisation were performed, a

functional assessment of the fibre mat was needed. *In-vitro* dissolution studies showed that the formulation releases 75 % or more of the drug within 45 minutes, and thus its immediate release status had not been affected by the coating process. Most importantly, taste needed to be assessed to ensure the palatability of this potential paediatric dosage form. Using an E-tongue, the raw drug was tested initially to ensure that the drug is indeed bitter and can be detected by the instrument. The drug showed high basic bitterness and high detectability by the E-tongue. The taste-masked formulations were assessed and some taste-masking was confirmed. Nonetheless, complete taste-masking was not confirmed using the E-tongue and further taste-masking was required. This chapter, therefore, provided a blue-print for electrospinning of E-EPO with and without CPM, and most specifically highlighted the most important parameters influencing this process.

Chapter 4 aimed at producing a fully taste-masked formulation using electrospinning. For this to be achieved, co-axial electrospinning was utilised. Co-axial electrospinning involves two needles embedded within each other, where two solutions were pumped, subsequently forming a core-shell fibre structure. A second taste-masking polymer was used to fabricate this; Kollicoat Smartseal. To the best of my knowledge, KCT had not been electrospun before and therefore optimisation was initially required. Once parameters were identified for electrospinning placebo KCT, CPM was added. To produce a fully taste-masked co-axial fibre system, both polymers were alternated between the core and shell. The fibres produced were imaged and taste-assessed using a more advanced E-tongue sensor. Initially, the drug's bitterness threshold was calculated. The E-tongue results showed that the formulation with KCT in the core with the drug and E-EPO in shell, yielded a fully taste-masked output. This formulation was now optimised to be bead-free, in the nano-range, and now fully taste-masked. This chapter confirmed the hypothesis that co-axial electrospinning may be a more effective method of taste-masking compared to single-needle electrospinning. In addition, the E-tongue analysis completed in this chapter provides novel information on the bitterness threshold of CPM as well as how E-tongue generated data compares to human data found in the literature. The next challenge was to

make this fibre mat dosage-form ready and ensure its overall potential as an oral film.

In Chapter 5, the aim was to explore the acceptability of electrospun fibre mats as an oral film. A human panel investigated the mouthfeel acceptability of PVA electrospun fibre mats and PVA solvent cast films. It was shown that the electrospun fibre mats performed on par with the solvent cast films in a number of mouthfeel and general acceptability attributes, namely; size, ease of handling, thickness, stickiness, disintegration time and saliva thickening effect. These findings were very promising in the further formulation of the optimised taste-masked CPM electrospun fibre mats. The palatability data produced by this human panel is only one of a couple of reports found in the literature; it confirmed the hypothesis that an electrospun fibre oral film is at least acceptable as the widely available solvent-cast films.

Multi-axial electrospinning was utilised to incorporate the previously optimised co-axial formulation with a water-soluble polymeric outer layer; PVA and PVP were used. It was found that when electrospinning PVA alongside KCT and E-EPO, needle clogging occurred due to PVA's insolubility in ethanol. PVP was used instead to assess the suitability of a water-soluble outer layer of the final taste-masked formulation. PVP was successfully electrospun with drug-loaded KCT and E-EPO using tri-axial and tetra-axial electrospinning. Tetra-axial electrospinning incorporated an extra layer of pure ethanol that aided in reducing needle clogging. Both methods yielded similar electrospun fibres in terms of morphology. In addition, the use of co-solvents that included DMSO and DMAc improved the electrospinnability of E-EPO reducing needle clogging. As per the previous chapters, general solid-state characterisation and thermal analysis were performed to assess the end-product stability and functionality of the formulation. The multi-axial formulations were taste-assessed using the E-tongue where it was found they were not taste-masked. This was likely due to the fact that the electrospinning dopes used were miscible and CPM had diffused from the core of the system to the shell, thereby releasing upon contact with an aqueous medium.

It was therefore concluded that the optimum formulation should incorporate hydrophobic polymers or a hydrophilic outer layer that is not miscible with the drug-loaded layer to prevent drug diffusion.

The co-axial formulation showed complete taste-masking of the bitter drug, as well as reproducible bead-free nanofibres. At the drug-loading used (7.6 % w/w) a film size of 26 mg would be needed to deliver a paediatric clinical dose of 2 mg; this is in line with acceptable literature oral film sizes. Currently, the mat produced has not been taste-assessed in humans and the prolonged stability of the formulation has not been assessed; these aspects would need to be explored further prior to clinical translation. The use of the E-tongue has been very effective in selecting and de-selecting formulations thereby informing the progress of this project. Overall, it was shown that electrospinning offers potential as a taste-masking technology and co-axial electrospinning in particular possess an extra advantage in this area.

6.2 **Suggested Future Work**

In this project, an electrospun taste-masked formulation was successfully designed and manufactured, however, the stability was not assessed. Amorphous states tend to revert to crystalline states and therefore a stability study would be useful to understand the effect of storage on the dissolution profile and subsequent performance. An accelerated stability test would see the films stored in a controlled climate chamber at 40 °C ± 2 °C/75 % RH ± 5% RH for 6 months, as per the WHO guidance [276]. To assess whether the films can be considered stable, morphological and physiochemical changes of the samples can be analysed using SEM, FTIR, XRD and DSC. As oral films are very specialised dosage forms, packaging considerations will need to be explored to ensure the long-term stability as well as the acceptable handling of the dosage form.

Human taste panels are the gold standard of taste-assessment; therefore, the final formulation can be assessed in humans, however, this would require production in GMP facilities and prior ethical approval. In addition, an animal study can be used to also verify the taste data, namely a rodent Brief Access Taste Aversion model or simply known as the BATA model. Furthermore, this work aimed at producing dosage forms suitable for the paediatric population, therefore, a clinical trial in children would provide a more representative view of the films' palatability in their target population.

As well as optimising the multi-axial electrospinning process, solvent-casting can be combined with electrospinning to produce an elegant final formulation. Co-axial electrospinning can be completed on a pre-solvent cast sheet of a hydrophilic polymer such as PVP or PVA, in which case the drug would not have diffused to the surface and thus can be hypothesised the taste-masking would still be intact. Energy dispersive X-ray spectroscopy coupled with SEM can be employed to assess the elemental composition of the sample and identify whether there are residual drug molecules on the surface of the film,

Another route the taste-masked fibre mats can be further formulated into an age-appropriate dosage form is to be formulated into a mini-tablet. Mini-tablets have been shown to be acceptable dosage forms in the paediatric population. Once formulated, taste-assessment can be completed again to ensure the tabletting process did not compromise the taste-masking ability.

To test the hypothesis further that electrospinning can be considered a taste-masking platform technology, different polymers can be processed using the technology. Multi-axial electrospinning was utilised to improve the overall presentation of the fibre mat into a final clinical dosage form. As this affected the taste-masking efficiency of the formulation, an immiscible multi-axial system or one that includes a hydrophobic outer layer can be designed and taste-assessed. In this thesis, taste-masking pH-sensitive polymers were employed in the process. In the future, other hydrophobic polymers can be explored for their taste-masking potential, for example, ethyl cellulose [277]. Multi-axial electrospinning was utilised to improve the overall presentation of the fibre mat into a final clinical dosage form. As this affected the taste-masking efficiency of the formulation, an immiscible multi-axial system or one that includes a hydrophobic outer layer can be designed and taste-assessed. A further study to be included if electrospinning another polymer, is the assessment of drug release in both gastric and intestinal conditions to ensure the drug released is not affected by electrospinning.

A further area of interest is exploring whether specific enantiomers contribute to taste differently. For example, natural L-asparagine is bitter, whereas artificial D-asparagine is sweet [278]. CPM has a chiral centre and is usually given as a racemic mixture; it has not been explored in the literature whether the bitter taste it elicits is associated with the racemate or with one enantiomer only. To test this hypothesis, other chiral drugs can be assessed; 56 % of the drugs currently in use are chiral products and 88 % of those are marketed as racemates consisting of an equimolar mixture of the two enantiomers [279]. Examples of known bitter chiral drugs that can be used in the paediatric population include: guaifenesin [280], an expectorant used in chesty cough over the counter remedies; ketoprofen [281], a non-steroidal anti-inflammatory

drug; and loratadine [266], an anti-histamine. As well as taste-assessing the various enantiomers, it would also be interesting to explore the electrospinning potential of those drug molecules and if they can be taste-masked using the technology.

References

[1] EMA, Reflection paper: Formulation of Choice for the Paediatric Population (EMEA/CHMP/PEG/194810/2005), Guideline. (2006). doi:EMEA/CHMP/PEG/194810/2005.

[2] M.E. Aulton, Aulton's Pharmaceutics, 3rd ed., 2007.

[3] F.L. Lopez, T.B. Ernest, C. Tuleu, M.O. Gul, Formulation approaches to pediatric oral drug delivery: benefits and limitations of current platforms., Expert Opin. Drug Deliv. 12 (2015) 1727–40. doi:10.1517/17425247.2015.1060218.

[4] A.H.A. Mohamed-Ahmed, J. Soto, T. Ernest, C. Tuleu, Non-human tools for the evaluation of bitter taste in the design and development of medicines: A systematic review, Drug Discov. Today. 21 (2016) 1170–1180. doi:10.1016/j.drudis.2016.05.014.

[5] J.A. Mennella, K.M. Roberts, P.S. Mathew, D.R. Reed, Children's perceptions about medicines: individual differences and taste, BMC Pediatr. 15 (2015). doi:10.1186/s12887-015-0447-z.

[6] S. Nordenmalm, E. Kimland, F. Ligas, B. Lehmann, J. Claverol, B. Nafria, A.M. Tötterman, B. Pelle, Children's views on taking medicines and participating in clinical trials, Arch. Dis. Child. (2019) 900–905. doi:10.1136/archdischild-2018-316511.

[7] D. Baguley, E. Lim, A. Bevan, A. Pallet, S.N. Faust, Prescribing for children - Taste and palatability affect adherence to antibiotics: A review, Arch. Dis. Child. 97 (2012) 293–297. doi:10.1136/archdischild-2011-300909.

[8] F. Aljebab, M. Alanazi, I. Choonara, S. Conroy, R. Derby, Observational study on the palatability and tolerability of oral prednisolone and oral dexamethasone in children in Saudi Arabia and the UK, BMJ Open. (2018) 83–88. doi:10.1136/archdischild-2017-312697.

[9] S. Cherian, B.S. Lee, R.M. Tucker, K. Lee, G. Smutzer, Toward Improving Medication Adherence: The Suppression of Bitter Taste in Edible Taste Films, Adv. Pharmacol. Sci. (2018). doi:10.1155/2018/8043837.

[10] L. Bracken, E. McDonough, S. Ashleigh, F. Wilson, J. Shakeshaft, U. Ohia, P. Mistry, H. Jones, N. Kanji, F. Liu, M. Peak, Can children swallow tablets? Outcome data from a feasibility study to assess the acceptability of different-sized placebo tablets in children (creating acceptable tablets (CAT)), BMJ Open. 10 (2020) e036508. doi:10.1136/bmjopen-2019-036508.

[11] E.O. Meltzer, M.J. Welch, N.K. Ostrom, Pill swallowing ability and training in children 6 to 11 years of age, Clin. Pediatr. (Phila). 45 (2006) 725–733. doi:10.1177/0009922806292786.

[12] D. Clarke, F. Pascual, A. Ojoo, Target Product Profiles, WHO. (2018) 126–143.

[13] World Health Organization, Annex 5: Development of paediatric medicines: points to consider in formulation, Forty-Sixth Rep. WHO Expert Comm. Specif. Pharm. Prep. (2012) 235.

[14] J.F. Standing, C. Tuleu, Paediatric formulations - Getting to the heart of the problem, Int. J. Pharm. 300 (2005) 56–66. doi:10.1016/j.ijpharm.2005.05.006.

[15] C. Tuleu, Paediatric formulations in practice, in: Paediatr. Drug Handl., Pharmaceutical Press, London, 2007: pp. 43–75.

[16] J. Mason, M. Pirmohamed, T. Nunn, Off-label and unlicensed medicine use and adverse drug reactions in children: A narrative review of the literature, Eur. J. Clin. Pharmacol. 68 (2012) 21–28. doi:10.1007/s00228-011-1097-1.

[17] F. Liu, S. Ranmal, H.K. Batchelor, M. Orlu-Gul, T.B. Ernest, I.W. Thomas, T. Flanagan, C. Tuleu, Patient-centred pharmaceutical design to improve acceptability of medicines: Similarities and differences in paediatric and geriatric populations, Drugs. 74 (2014) 1871–1889. doi:10.1007/s40265-014-0297-2.

[18] International Conference on Harmonisation (ICH), Clinical Investigation of Medicinal Products in the Pediatric Population (E11), (2000) 1–16. http://www.ich.org/products/guidelines/efficacy/efficacy-single/article/clinical-investigation-of-medicinal-products-in-the-pediatric-population.html.

[19] I. Conference, O.N. Harmonisation, O.F. Technical, R. For, R. Of, P. For, N. Of, I.N. The, International conference on harmonisation of technical requirements for registration of pharmaceuticals for human use: clinical investigation of medicinal products in the pediatric population, (2000).

[20] C. Gale, I. Morris, The UK National Neonatal Research Database: using neonatal data for research, quality improvement and more, Arch. Dis. Child. - Educ. Pract. Ed. 101 (2016) 216–218. doi:10.1136/archdischild-2015-309928.

[21] R. Ternik, F. Liu, J.A. Bartlett, Y. Mei, D. Cheng, T. Tan, T. Dixit, S. Wang, E.A. Galella, Z. Gao, S. Klein, Assessment of swallowability and palatability of oral dosage forms in children : Report from an M-CERSI pediatric formulation workshop, Int. J. Pharm. 536 (2018) 570–581. doi:10.1016/j.ijpharm.2017.08.088.

[22] I. Vieira, J.J. Sousa, C. Vitorino, Paediatric Medicines – Regulatory Drivers, Restraints, Opportunities and Challenges, J. Pharm. Sci. 110 (2021) 1545–1556. doi:10.1016/j.xphs.2020.12.036.

[23] European Medicines Agency, 10-Year Report to the European Commission, 2016.

[24] S.K. Lisa Freerks, Jana Urbaniak, Pia C. Löper, Safe, swallowable and palatable paediatric mini-tablet formulations for a WHO Model List of Essential Medicines for Children compound - a promising starting point for future PUMA applications, 156 (2020) 11–19.

[25] European Comission, Orphan medicinal products, (2020). https://ec.europa.eu/health/human-use/orphan-medicines_en (accessed November 16, 2020).

[26] M.A. Turner, M. Catapano, S. Hirschfeld, C. Giaquinto, Paediatric drug development: The impact of evolving regulations, Adv. Drug Deliv. Rev. 73 (2014) 2–13. doi:10.1016/j.addr.2014.02.003.

[27] J. Mennella, A. Spector, D. Reed, S. Coldwell, The Bad taste of medicines: overview of basic research on bitter taste, Clin. Ther. 35 (2013) 1225–1246. doi:10.1016/j.clinthera.2013.06.007.The.

[28] N. Chaudhari, S.D. Roper, The cell biology of taste, J. Cell Biol. 190 (2010) 285–296. doi:10.1083/jcb.201003144.

[29] M. Momin, Taste masking techniques for bitter drugs - An overview, LAP Lambert, Mumbai, 2013.

[30] S.A. Gravina, G.L. Yep, M. Khan, Human biology of taste, Ann. Saudi Med. 33 (2013) 217–222. doi:10.5144/0256-4947.2013.217.

[31] F.L. Lopez, A. Bowles, M.O. Gul, D. Clapham, T.B. Ernest, C. Tuleu, Effect of formulation variables on oral grittiness and preferences of multiparticulate formulations in adult volunteers, Eur. J. Pharm. Sci. 92 (2016) 156–162. doi:10.1016/j.ejps.2016.07.006.

[32] J.N. Coupland, J.E. Hayes, Physical approaches to masking bitter taste: Lessons from food and pharmaceuticals, Pharm. Res. 31 (2014) 2921–2939. doi:10.1007/s11095-014-1480-6.

[33] D. V Smith, R.F. Margolskee, Making sense of taste., Sci. Am. 284 (2001) 32–39. doi:10.1038/scientificamerican0906-84sp.

[34] S.S. Calvo, J.M. Egan, The endocrinology of taste receptors, Nat Rev Endocrinol. 11 (2015) 213–227. doi:10.1038/nrendo.2015.7.

[35] A. Jaggupilli, R. Howard, J.D. Upadhyaya, R.P. Bhullar, P. Chelikani, Bitter taste receptors: Novel insights into the biochemistry and pharmacology, Int. J. Biochem. Cell Biol. 77 (2016) 184–196. doi:10.1016/j.biocel.2016.03.005.

[36] M.& Reedy, Variations in Human Taste Bud Density and Taste Intensity Perception, Physiol. Behav. 47 (1990) 1213–1219.

[37] L.M. Bartoshuk, V.B. Duffy, I.J. Miller, PTC/PROP tasting: Anatomy, psychophysics, and sex effects, Physiol. Behav. 56 (1994) 1165–1171. doi:10.1016/0031-9384(94)90361-1.

[38] D.E. Chaves, Changes in Taste and Food Intake during the Menstrual Cycle, J. Nutr. Food Sci. 05 (2015). doi:10.4172/2155-9600.1000383.

[39] J. Brown, Taste changes during pregnancy, Am. J. Clin. Nutr. 43 (1986) 414–418.

[40] Z. RD, Oral manifestations of menopause., Compendium. 14 (1993) 1586–1591. https://www.ncbi.nlm.nih.gov/pubmed/8149398.

[41] J. Mojet, E. Christ-Hazelhof, J. Heidema, Taste perception with age: generic or specific losses in threshold sensitivity to the five basic tastes?, Chem. Senses. 26 (2001) 845–860. doi:10.1093/chemse/28.5.397.

[42] J.A. Mennella, D.R. Reed, K.M. Roberts, P.S. Mathew, C.J. Mansfield, Age-related differences in bitter taste and efficacy of bitter blockers, PLoS One. 9 (2014). doi:10.1371/journal.pone.0103107.

[43] P.D.V. De Almeida, A.M.T. Grégio, M.Â.N. Machado, A.A.S. De Lima, L.R. Azevedo, Saliva composition and functions: A comprehensive review, J. Contemp. Dent. Pract. 9 (2008) 072–080. doi:1526-3711-497 [pii].

[44] M. Melis, M.C. Aragoni, M. Arca, T. Cabras, C. Caltagirone, M. Castagnola, R. Crnjar, I. Messana, B.J. Tepper, I.T. Barbarossa, Marked Increase in PROP Taste Responsiveness Following Oral Supplementation with Selected Salivary Proteins or Their Related Free Amino Acids, PLoS One. 8 (2013) 1–8. doi:10.1371/journal.pone.0059810.

[45] D. Trachootham, S. Satoh-Kuriwada, A. Lam-ubol, C. Promkam, N. Chotechuang, T. Sasano, N. Shoji, Differences in taste perception and spicy preference: A thai-japanese cross-cultural study, Chem. Senses. 43 (2018) 65–74. doi:10.1093/chemse/bjx071.

[46] R.G. Strickley, Q. Iwata, S. Wu, T.C. Dahl, Pediatric Drugs—A Review of Commercially Available Oral Formulations, J. Pharm. Sci. 97 (2008) 1731–1774.

[47] J. Abraham, F. Mathew, Reveiw Article TASTE MASKING OF PEADIATRIC FORMULATION : A REVIEW ON TECHNOLOGIES , RECENT TRENDS AND REGULATORY ASPECTS, Int. J. Pharm. Pharm. Sci. 6 (2014).

[48] A. Tripathi, D. Parmar, U. Patel, G. Patel, D. Daslaniya, B. Bhimani, Taste Masking: A Novel Approach for Bitter and Obnoxious Drugs, J. Pharm. Sci. Biosci. Res. 1 (2011) 136–142.

[49] FlavoRX, (2020). https://www.flavorx.com/services-products/ (accessed November 16, 2020).

[50] Senopsys LLC, Senopsys, (2021). https://www.senopsys.com/ (accessed March 30, 2021).

[51] D. Andrews, S. Salunke, A. Cram, J. Bennett, R.S. Ives, A.W. Basit, C. Tuleu, Bitter-blockers as a taste masking strategy: A systematic review towards their utility in pharmaceuticals, Eur. J. Pharm. Biopharm. 158 (2021) 35–51. doi:10.1016/j.ejpb.2020.10.017.

[52] M. Münster, A.H.A. Mohamed-Ahmed, L.I. Immohr, C. Schoch, C. Schmidt, C. Tuleu, J. Breitkreutz, Comparative in vitro and in vivo taste assessment of liquid praziquantel formulations, Int. J. Pharm. 529 (2017) 310–318. doi:10.1016/j.ijpharm.2017.06.084.

[53] T. Liu, X. Wan, Z. Luo, C. Liu, P. Quan, D. Cun, L. Fang, A donepezil/cyclodextrin complexation orodispersible film: Effect of cyclodextrin on taste-masking based on dynamic process and in vivo drug absorption, Asian J. Pharm. Sci. 14 (2019) 183–192. doi:10.1016/j.ajps.2018.05.001.

[54] Z. Hesari, A. Shafiee, S. Hooshfar, N. Mobarra, S.A. Mortazavic, Formulation and taste masking of ranitidine orally disintegrating tablet, Iran. J. Pharm. Res. 15 (2016) 677–686. doi:10.22037/ijpr.2016.1923.

[55] R. Shang, C. Liu, P. Quan, H. Zhao, L. Fang, Effect of drug-ion exchange resin complex in betahistine hydrochloride orodispersible film on sustained release, taste masking and hygroscopicity reduction, Int. J. Pharm. 545 (2018) 163–169. doi:10.1016/j.ijpharm.2018.05.004.

[56] J. Xu, L.L. Bovet, K. Zhao, Taste masking microspheres for orally disintegrating tablets, Int. J. Pharm. 359 (2008) 63–69. doi:10.1016/j.ijpharm.2008.03.019.

[57] A. Amelian, K. Wasilewska, M. Wesoły, P. Ciosek-Skibińska, K. Winnicka, Taste-masking assessment of orally disintegrating tablets and lyophilisates with cetirizine dihydrochloride microparticles, Saudi Pharm. J. 25 (2017) 1144–1150. doi:10.1016/j.jsps.2017.06.001.

[58] O.D. Ogundipe, F.A. Oladimeji, Water-in-Oil-in-Water Multiple Emulsions of Ibuprofen for Paediatrics Using African Walnut Seed Oil, J. Appl. Pharm. Res. 7 (2019) 1–9. doi:10.18231/2348-0335.2018.0014.

[59] N. Verma, A. Tripathi, V. Singh, A brief study on multiple emulsion: a review, Asian J. Phytomedicine Clin. Res. 6 (2018) 133–139.

[60] J. Walsh, A. Cram, K. Woertz, J. Breitkreutz, G. Winzenburg, R. Turner, C. Tuleu, Playing hide and seek with poorly tasting paediatric medicines: Do not forget the excipients, Adv. Drug Deliv. Rev. 73 (2014) 14–33. doi:10.1016/j.addr.2014.02.012.

[61] M. Maniruzzaman, J.S. Boateng, M. Bonnefille, A. Aranyos, J.C. Mitchell, D. Douroumis, Taste masking of paracetamol by hot-melt extrusion: An in vitro and in vivo evaluation, Eur. J. Pharm. Biopharm. 80 (2012) 433–442.

doi:10.1016/j.ejpb.2011.10.019.

[62] I. Speer, M. Preis, J. Breitkreutz, Prolonged drug release properties for orodispersible fi lms by combining hot- melt extrusion and solvent casting methods, Eur. J. Pharm. Biopharm. 129 (2018) 66–73. doi:10.1016/j.ejpb.2018.05.023.

[63] A. V Keating, J. Soto, C. Tuleu, C. Forbes, M. Zhao, D.Q.M. Craig, Solid state characterisation and taste masking efficiency evaluation of polymer based extrudates of isoniazid for paediatric administration, Int. J. Pharm. (2017).

[64] T. Ehtezazi, M. Algellay, Y. Islam, M. Roberts, N.M. Dempster, S.D. Sarker, The Application of 3D Printing in the Formulation of Multilayered Fast Dissolving Oral Films, J. Pharm. Sci. 107 (2018) 1076–1085.

[65] H. Wang, N. Dumpa, S. Bandari, T. Durig, M.A. Repka, Fabrication of Taste-Masked Donut-Shaped Tablets Via Fused Filament Fabrication 3D Printing Paired with Hot-Melt Extrusion Techniques, (2020) 1–11. doi:10.1208/s12249-020-01783-0.

[66] F. Ignatious, L. Sun, C.-P. Lee, J. Baldoni, Electrospun nanofibers in oral drug delivery., Pharm. Res. 27 (2010) 576–588. doi:10.1007/s11095-010-0061-6.

[67] C.L. Ventola, D.J. Bharali, S.A. Mousa, The Nanomedicine Revolution: Part 1: Emerging Concepts. Pharmacy and Therapeutics., Pharmacol. Ther. 128 (2010) 512–525. doi:10.1016/j.pharmthera.2010.07.007.

[68] G.R. Williams, B.T. Raimi-Abraham, C.J. Lou, Nanofibres in drug delivery, 2018.

[69] V. Pillay, C. Dott, Y.E. Choonara, C. Tyagi, L. Tomar, P. Kumar, L.C. Toit, V.M.K. Ndesendo, A Review of the Effect of Processing Variables on the Fabrication of Electrospun Nanofibers for Drug Delivery Applications, J. Nanomater. 2013 (2013) 22. doi:10.1155/2013/789289.

[70] Z.M. Huang, Y.Z. Zhang, M. Kotaki, S. Ramakrishna, A review on polymer nanofibers by electrospinning and their applications in nanocomposites, Compos. Sci. Technol. 63 (2003) 2223–2253. doi:10.1016/S0266-3538(03)00178-7.

[71] W. Zuo, M. Zhu, W. Yang, H. Yu, Y. Chen, Y. Zhang, Experimental study on relationship between jet instability and formation of beaded fibers during

electrospinning, Polym. Eng. Sci. 45 (2005) 704–709. doi:10.1002/pen.20304.

[72] C.J. Thompson, G.G. Chase, A.L. Yarin, D.H. Reneker, Effects of parameters on nanofiber diameter determined from electrospinning model, Polymer (Guildf). 48 (2007) 6913–6922. doi:10.1016/j.polymer.2007.09.017.

[73] J. Stanger, N. Tucker, M. Staiger, Electrospinning, 16 (2005).

[74] S. Bagchi, R. Brar, B. Singh, C. Ghanshyam, Instability controlled synthesis of tin oxide nanofibers and their gas sensing properties, J. Electrostat. 78 (2015) 68–78. doi:10.1016/j.elstat.2015.11.001.

[75] A. Valizadeh, S. Mussa Farkhani, Electrospinning and electrospun nanofibres., IET Nanobiotechnol. 8 (2014) 83–92. doi:10.1049/iet-nbt.2012.0040.

[76] A.L. Yarin, S. Koombhongse, D.H. Reneker, Bending instability in electrospinning of nanofibers, J. Appl. Phys. 89 (2001) 3018–3026. doi:10.1063/1.1333035.

[77] H.M. Khanlou, B.C. Ang, S. Talebian, M.M. Barzani, M. Silakhori, H. Fauzi, Multi-response analysis in the processing of poly (methyl methacrylate) nano-fibres membrane by electrospinning based on response surface methodology: Fibre diameter and bead formation, Meas. J. Int. Meas. Confed. 65 (2015) 193–206. doi:10.1016/j.measurement.2015.01.014.

[78] A. Haider, S. Haider, I.K. Kang, A comprehensive review summarizing the effect of electrospinning parameters and potential applications of nanofibers in biomedical and biotechnology, Arab. J. Chem. (2015). doi:10.1016/j.arabjc.2015.11.015.

[79] B. Poller, C. Strachan, R. Broadbent, G.F. Walker, A minitablet formulation made from electrospun nanofibers, Eur. J. Pharm. Biopharm. 114 (2017) 213–220. doi:10.1016/j.ejpb.2017.01.022.

[80] S.A. Thomson, C. Tuleu, I.C.K. Wong, S. Keady, K.G. Pitt, A.G. Sutcliffe, Minitablets: New modality to deliver medicines to preschool-aged children, Pediatrics. 123 (2009). doi:10.1542/peds.2008-2059.

[81] U.E. Illangakoon, H. Gill, G.C. Shearman, M. Parhizkar, S. Mahalingam, N.P. Chatterton, G.R. Williams, Fast dissolving paracetamol/caffeine nanofibers prepared by electrospinning, Int. J. Pharm. 477 (2014) 369–379. doi:10.1016/j.ijpharm.2014.10.036.

[82] W. Samprasit, P. Akkaramongkolporn, T. Ngawhirunpat, T. Rojanarata, R. Kaomongkolgit, P. Opanasopit, Fast releasing oral electrospun PVP/CD nanofiber mats of taste-masked meloxicam, Int. J. Pharm. 487 (2015) 213–222. doi:10.1016/j.ijpharm.2015.04.044.

[83] W. Samprasit, P. Akkaramongkolporn, R. Kaomongkolgit, P. Opanasopit, Cyclodextrin-based oral dissolving films formulation of taste-masked meloxicam, Pharm. Dev. Technol. 0 (2017) 1–10. doi:10.1080/10837450.2017.1401636.

[84] Y.W.D.Y.X. Li, G.R. Williams, Fast-dissolving sweet sedative nanofiber membranes, (2015) 3604–3613. doi:10.1007/s10853-015-8921-4.

[85] A. Khalf, S. V. Madihally, Recent advances in multiaxial electrospinning for drug delivery, Eur. J. Pharm. Biopharm. 112 (2017) 1–17. doi:10.1016/j.ejpb.2016.11.010.

[86] Y. Lu, J. Huang, G. Yu, R. Cardenas, S. Wei, E.K. Wujcik, Z. Guo, Coaxial electrospun fibers: applications in drug delivery and tissue engineering, Wiley Interdiscip. Rev. Nanomedicine Nanobiotechnology. 8 (2016) 654–677. doi:10.1002/wnan.1391.

[87] Y.H. Wu, D.G. Yu, X.Y. Li, A.H. Diao, U.E. Illangakoon, G.R. Williams, Fast-dissolving sweet sedative nanofiber membranes, J. Mater. Sci. 50 (2015) 3604–3613. doi:10.1007/s10853-015-8921-4.

[88] M. Lallave, J. Bedia, R. Ruiz-Rosas, J. Rodríguez-Mirasol, T. Cordero, J.C. Otero, M. Marquez, A. Barrero, I.G. Loscertales, Filled and hollow carbon nanofibers by coaxial electrospinning of Alcell lignin without binder polymers, Adv. Mater. 19 (2007) 4292–4296. doi:10.1002/adma.200700963.

[89] V. Kalra, J.H. Lee, J.H. Park, M. Marquez, Y.L. Joo, Confined assembly of asymmetric block-copolymer nanofibers via multiaxial jet electrospinning, Small. 5 (2009) 2323–2332. doi:10.1002/smll.200900157.

[90] S. Labbaf, H. Ghanbar, E. Stride, M. Edirisinghe, Preparation of multilayered polymeric structures using a novel four-needle coaxial electrohydrodynamic device, Macromol. Rapid Commun. 35 (2014) 618–623. doi:10.1002/marc.201300777.

[91] Y. Kobayashi, H. Ikezaki, Biochemical sensors: Mimicking gustatory and olfactory senses, Pan Stanford Publishing, 2013.

[92] M. Pein, M. Preis, C. Eckert, F.E. Kiene, Taste-masking assessment of solid oral dosage forms - A critical review, Int. J. Pharm. 465 (2014) 239–254. doi:10.1016/j.ijpharm.2014.01.036.

[93] K. Woertz, C. Tissen, P. Kleinebudde, J. Breitkreutz, Taste sensing systems (electronic tongues) for pharmaceutical applications, Int. J. Pharm. 417 (2011) 256–271. doi:10.1016/j.ijpharm.2010.11.028.

[94] J. Newman, D. O'Riordan, J.C. Jacquier, M. O'Sullivan, Masking of bitterness in dairy protein hydrolysates: Comparison of an electronic tongue and a trained sensory panel as means of directing the masking strategy, LWT - Food Sci. Technol. 63 (2015) 751–757. doi:10.1016/j.lwt.2015.03.019.

[95] Y. Kobayashi, M. Habara, H. Ikezazki, R. Chen, Y. Naito, K. Toko, Advanced taste sensors based on artificial lipids with global selectivity to basic taste qualities and high correlation to sensory scores, Sensors. 10 (2010) 3411–3443. doi:10.3390/s100403411.

[96] S. Gittings, N. Turnbull, C.J. Roberts, P. Gershkovich, Dissolution methodology for taste masked oral dosage forms, J. Control. Release. 173 (2014). doi:10.1016/j.jconrel.2013.10.030.

[97] C. Eckert, M. Pein, J. Reimann, J. Breitkreutz, Taste evaluation of multicomponent mixtures using a human taste panel, electronic taste sensing systems and HPLC, Sensors Actuators, B Chem. 182 (2013). doi:10.1016/j.snb.2013.03.012.

[98] H.E. Abdelhakim, A. Coupe, C. Tuleu, M. Edirisinghe, D.Q.M. Craig, Electrospinning Optimization of Eudragit E PO with and without Chlorpheniramine Maleate Using a Design of Experiment Approach, Mol. Pharm. 16 (2019) 2557–2568. doi:10.1021/acs.molpharmaceut.9b00159.

[99] H.E. Abdelhakim, G.R. Williams, D.Q.M. Craig, M. Orlu, C. Tuleu, Human mouthfeel panel investigating the acceptability of electrospun and solvent cast orodispersible fi lms, Int. J. Pharm. 585 (2020) 119532. doi:10.1016/j.ijpharm.2020.119532.

[100] A. Wiener, M. Shudler, A. Levit, M.Y. Niv, BitterDB: A database of bitter compounds, Nucleic Acids Res. 40 (2012) 413–419. doi:10.1093/nar/gkr755.

[101] A.W.M.S.A.L.M.Y. Niv, BitterDB: a database of bitter compounds., Nucleic Acids Res. 40 (2012) 413–419.

[102] T. Nitanan, P. Akkaramongkolporn, T. Ngawhirunpat, T. Rojanarata, S. Panomsuk, P. Opanasopit, Fabrication and evaluation of cationic exchange nanofibers for controlled drug delivery systems, Int. J. Pharm. 450 (2013) 345–353. doi:10.1016/j.ijpharm.2013.04.031.

[103] R. Bala, S. Khanna, P. Pawar, S. Arora, Orally dissolving strips: A new approach to oral drug delivery system, Int. J. Pharm. Investig. 3 (2013) 67. doi:10.4103/2230-973X.114897.

[104] BNF, BNFc; Erythromycin, 2021. https://bnfc.nice.org.uk/drug/erythromycin.html.

[105] BNFc; Chlorpheniramine maleate, (2017). https://www.medicinescomplete.com/mc/bnfc/current/PHP1934-chlorphenamine-maleate.htm?q=clorpheniramine maleate&t=search&ss=text&tot=33&p=1#_hit (accessed August 15, 2017).

[106] S.S. Gupta, N. Solanki, A.T.M. Serajuddin, Investigation of Thermal and Viscoelastic Properties of Polymers Relevant to Hot Melt Extrusion, IV: Affinisol™ HPMC HME Polymers, AAPS PharmSciTech. 17 (2016) 148–157. doi:10.1208/s12249-015-0426-6.

[107] T. Parikh, S.S. Gupta, A. Meena, A.T.M. Serajuddin, Investigation of Thermal and Viscoelastic Properties of Polymers Relevant to Hot Melt Extrusion - III: Polymethacrylates and polymethacrylic acid based polymers, J. Excipients Food Chem. 5 (2014) 56–64. doi:10.1208/s12249-015-0426-6.

[108] Evonik Industries, EUDRAGIT ® E PO EUDRAGIT ® E 12,5 EUDRAGIT ® E 100, EUDRAGIT ® E PO and EUDRAGIT ® E 12,5 Specification and Test Methods EUDRAGIT ® E PO EUDRAGIT ® E 12,5, (2015) 1–6.

[109] Y.D. Yan, J.S. Woo, J.H. Kang, C.S. Yong, H.G. Choi, Preparation and evaluation of taste-masked donepezil hydrochloride orally disintegrating tablets, Biol. Pharm. Bull. 33 (2010) 1364–1370. doi:10.1248/bpb.33.1364.

[110] A. Balogh, R. Cselkó, B. Démuth, G. Verreck, J. Mensch, G. Marosi, Z.K. Nagy, Alternating current electrospinning for preparation of fibrous drug delivery systems, Int. J. Pharm. 495 (2015) 75–80. doi:10.1016/j.ijpharm.2015.08.069.

[111] A. Balogh, G. Dravavolgyi, K. Farago, A. Farkas, T. Vigh, P.L. Soti, I. Wagner, J. Madarasz, H. Pataki, G. Marosi, Z.K. Nagy, Plasticized drug-loaded melt electrospun polymer mats: Characterization, thermal degradation, and release

kinetics, J. Pharm. Sci. 103 (2014) 1278–1287. doi:10.1002/jps.23904.

[112] Evonik Industries, Acrylic Polymers for Solid Oral Dosage Forms, (2007).

[113] S. Opinion, Scientific Opinion on the use of Basic Methacrylate Copolymer as a food, 8 (2010) 1–23. doi:10.2903/j.efsa.2010.1513.

[114] BASF, Kollicoat Smartseal 30 D, Basf. (2012) 1–8.

[115] A. Keeley, M. Teo, Z. Ali, J. Frost, M. Ghimire, A. Rajabi-siahboomi, M. Orlu, C. Tuleu, In Vitro Dissolution Model Can Predict the in Vivo Taste Masking Performance of Coated Multiparticulates, Mol. Pharm. 16 (2019) 2095–2105. doi:10.1021/acs.molpharmaceut.9b00060.

[116] M. Wesoły, M. Zabadaj, A. Amelian, K. Winnicka, W. Wróblewski, P. Ciosek, Tasting cetirizine-based microspheres with an electronic tongue, Sensors Actuators B Chem. 238 (2016) 1190–1198. doi:10.1016/j.snb.2016.06.147.

[117] SPC, (2017). https://www.medicines.org.uk/emc/medicine/13691 (accessed August 15, 2017).

[118] BCS Classification, (2018). http://www.tsrlinc.net/search.cfm.

[119] BP Chlorphenamine Monograph, (2018). https://www.pharmacopoeia.com/bp-2018/monographs/chlorphenamine-maleate.html?date=2018-01-01&text=chlorphenamine.

[120] PubChem, Chlopheniramine, (2017). https://pubchem.ncbi.nlm.nih.gov/compound/chlorpheniramine#section=Solubility (accessed August 15, 2017).

[121] S.U. Yasuda, P. Zannikos, A.E. Young, K.M. Fried, I.W. Wainer, R.L. Woosley, The roles of CYP2D6 and stereoselectivity in the clinical pharmacokinetics of chlorpheniramine, Br. J. Clin. Pharmacol. 53 (2002) 519–525. doi:10.1046/j.1365-2125.2002.01578.x.

[122] P.R. Vuddanda, A.P. Mathew, S. Velaga, Electrospun nanofiber mats for ultrafast release of ondansetron, React. Funct. Polym. 99 (2016) 65–72. doi:10.1016/j.reactfunctpolym.2015.12.009.

[123] X. Li, M.A. Kanjwal, L. Lin, I.S. Chronakis, Electrospun polyvinyl-alcohol nanofibers as oral fast-dissolving delivery system of caffeine and riboflavin, Colloids Surfaces B Biointerfaces. 103 (2013) 182–188. doi:10.1016/j.colsurfb.2012.10.016.

[124] C. Zhang, X. Yuan, Study on morphology of electrospun poly(vinyl alcohol) mats, Eur. Polym. J. 41 (2005) 423–432. doi:10.1016/j.eurpolymj.2004.10.027.

[125] Keller and Heckman, GRAS Notification for MonoSol's Use of Polyvinyl Alcohol (PVOH) as a Component in Edible Film, Https://Www.Fda.Gov/Food/Generally-Recognized-Safe-Gras/Gras-Notice-Inventory. (2018).

[126] P. Vrbata, P. Berka, D. Stránská, P. Doležal, M. Musilová, L. Čižinská, Electrospun drug loaded membranes for sublingual administration of sumatriptan and naproxen, Int. J. Pharm. 457 (2013) 168–176. doi:10.1016/j.ijpharm.2013.08.085.

[127] L. Hendraningrat, O. Torsæter, Metal oxide-based nanoparticles: revealing their potential to enhance oil recovery in different wettability systems, Appl. Nanosci. 5 (2015) 181–199. doi:10.1007/s13204-014-0305-6.

[128] E.A. Growney Kalaf, K.R. Hixon, P.U. Kadakia, A.J. Dunn, S.A. Sell, Electrospun biomaterials for dermal regeneration, 2017. doi:10.1016/B978-0-08-101022-8.00005-3.

[129] G. Cheng, X. Ma, J. Li, Y. Cheng, Y. Cao, Z. Wang, X. Shi, Y. Du, H. Deng, Z. Li, Incorporating platelet-rich plasma into coaxial electrospun nanofibers for bone tissue engineering, Int. J. Pharm. 547 (2018) 656–666. doi:10.1016/j.ijpharm.2018.06.020.

[130] PubChem, Rhodamine B, (2020). https://pubchem.ncbi.nlm.nih.gov/compound/Rhodamine-B (accessed June 18, 2020).

[131] B. Carter, Review of Op Amp Basics, in: Op Amps Everyone, 4th ed., Elsevier Inc, 2013: pp. 7–17.

[132] P.C. Goodwin, A primer on the fundamental principles of light microscopy: Optimizing magnification, resolution, and contrast, Mol. Reprod. Dev. 82 (2015) 502–507. doi:10.1002/mrd.22385.

[133] K.D. Vernon-Parry, Scanning Electron Microscopy: an introduction, III-Vs Rev. 13 (2000).

[134] H. Kleebe, S. Lauterbach, M.M. Mathis, Transmission Electron Microscopy, in: R. Schafer, P.C. Schmidt (Eds.), Methods Phys. Chem., First, Wiley, 2012: pp.

797–821.

[135] D.B. Williams, C.B. Carter, Transmission electron microscopy: a textbook for materials science, Second, Springer US, New York, 2009.

[136] M.J. Sanderson, I. Smith, I. Parker, M.D. Bootman, Fluorescence Microscopy, Cold Spring Harb. Protoc. (2014) 1–36. doi:10.1101/pdb.top071795.Fluorescence.

[137] T.B. Sil, B. Sahoo, K. Garai, Building, Characterization, and Applications of Cuvette-FCS in Denaturant-Induced Expansion of Globular and Disordered Proteins, Methods Enzymol. 611 (2018) 383–421. doi:10.1016/bs.mie.2018.08.027.

[138] Edmund Optics, Texas Red Cube Specifications, (2021). https://www.edmundoptics.co.uk/p/texas-redtrade-filter-cube-set-nikon/21541/ (accessed January 22, 2021).

[139] S.M. Nilapwar, M. Nardelli, H. V. Westerhoff, M. Verma, Absorption spectroscopy, 1st ed., Elsevier Inc., 2011. doi:10.1016/B978-0-12-385118-5.00004-9.

[140] P. Gabbott, T. Mann, Differntial Scanning Calorimetry, in: S. Gaisford, V. Kett, P. Haines (Eds.), Princ. Therm. Anal. Calorim., Royal Society of Chemistry, 2016.

[141] D.Q.M. Craig, M. Reading, Thermal Analysis of Pharmaceuticals, 1st ed., CRC Press, Boca Raton, USA, 2007.

[142] N.J. Coleman, D.Q.M. Craig, Modulated temperature differential scanning calorimetry: A novel approach to pharmaceutical thermal analysis, Int. J. Pharm. 135 (1996) 13–29. doi:10.1016/0378-5173(95)04463-9.

[143] W.H. Bragg, W.L. Bragg, The reflection of X-rays by crystals, Proc. R. Soc. London. Ser. A, Contain. Pap. a Math. Phys. Character. 88 (1913) 428–438. doi:10.1098/rspa.1913.0040.

[144] C.J. Gilmore, X-Ray Diffraction, in: R.A. Storey, I. Ymen (Eds.), Solid State Charact. Pharm., 1st ed., BlackWell Publishing Ltd., UK, 2011.

[145] A. O'Neil, H. Edwards, Spectroscopic Characterization, in: Solid State Charact. Pharm., 1st ed., BlackWell Publishing Ltd., Oxford, 2011: pp. 71–134.

[146] D. Holbrook, A. Galyean, J. Gorham, A. Herzing, J. Pettibone, Overview of

Nanomaterial Characterization of Metrology, in: Charact. Nanomater. Complex Environ. Biol. Media, 8th ed., Elsevier Ltd., 2015.

[147] J.G. Moffat, AM-FM Viscoelastic Mapping Mode, Santa Barbara, n.d.

[148] K. Bin Liew, Y.T.F. Tan, K.K. Peh, Characterization of oral disintegrating film containing donepezil for Alzheimer disease, AAPS PharmSciTech. 13 (2012) 134–142. doi:10.1208/s12249-011-9729-4.

[149] E.M. Hoffmann, A. Breitenbach, J. Breitkreutz, Advances in orodispersible films for drug delivery., Expert Opin. Drug Deliv. 8 (2011) 299–316. doi:10.1517/17425247.2011.553217.

[150] A.A. Noyes, W.R. Whitney, The rate of solution of solid substances in their own solutions, J. Am. Chem. Soc. 19 (1897) 930–934. doi:10.1021/ja02086a003.

[151] E.A. Tawfik, D.Q.M. Craig, S.A. Barker, Dual drug-loaded coaxial nanofibers for the treatment of corneal abrasion, Int. J. Pharm. 581 (2020). doi:10.1016/j.ijpharm.2020.119296.

[152] M. Guhmann, M. Preis, F. Gerber, N. Pöllinger, J. Breitkreutz, W. Weitschies, Development of oral taste masked diclofenac formulations using a taste sensing system, Int. J. Pharm. 438 (2012) 81–90. doi:10.1016/j.ijpharm.2012.08.047.

[153] U. Siemann, Solvent cast technology – a versatile tool for thin film production, in: Scatt. Methods Prop. Polym. Mater., 2005.

[154] S. Qi, D. Craig, Recent developments in micro- and nanofabrication techniques for the preparation of amorphous pharmaceutical dosage forms, Adv. Drug Deliv. Rev. 100 (2015) 67–84. doi:10.1016/j.addr.2016.01.003.

[155] F. Brako, B. Raimi-Abraham, S. Mahalingam, D.Q.M. Craig, M. Edirisinghe, Making nanofibres of mucoadhesive polymer blends for vaginal therapies, Eur. Polym. J. 70 (2015) 186–196. doi:10.1016/j.eurpolymj.2015.07.006.

[156] A. Balogh, A. Domokos, B. Farkas, A. Farkas, Z. Rapi, D. Kiss, Continuous end-to-end production of solid drug dosage forms : Coupling flow synthesis and formulation by electrospinning, Chem. Eng. J. 350 (2018) 290–299. doi:10.1016/j.cej.2018.05.188.

[157] Z.K. Nagy, A. Balogh, B. Demuth, H. Pataki, T. Vigh, B. Szabo, K. Molnar, B.T. Schmidt, P. Horak, G. Marosi, G. Verreck, I. Van Assche, M.E. Brewster, High

speed electrospinning for scaled-up production of amorphous solid dispersion of itraconazole, Int. J. Pharm. 480 (2015). doi:10.1016/j.ijpharm.2015.01.025.

[158] M. Jelvehgari, L. Barghi, F. Barghi, Preparation of Chlorpheniramine Maleate-loaded Alginate / Chitosan Particulate Systems by the Ionic Gelation Method for Taste Masking, 9 (2014) 39–48.

[159] K. Nollenberger, J. Albers, Poly(meth)acrylate-based coatings, Int. J. Pharm. 457 (2013) 461–469. doi:10.1016/j.ijpharm.2013.09.029.

[160] M. Guhmann, M. Preis, F. Gerber, N. Pöllinger, J. Breitkreutz, W. Weitschies, Design, development and *in-vitro* evaluation of diclofenac taste-masked orodispersible tablet formulations, Drug Dev. Ind. Pharm. 41 (2015) 540–551. doi:10.3109/03639045.2014.884122.

[161] J.F. Cooley, Apparatus for electrically dispersing fluids. US Patent 692,631, US Pat. 692,631. (1900) 1–6. http://www.google.com/patents/US692631.

[162] N. Sarlak, M.A.F. Nejad, S. Shakhesi, K. Shabani, Effects of electrospinning parameters on titanium dioxide nanofibers diameter and morphology: An investigation by Box-Wilson central composite design (CCD), Chem. Eng. J. 210 (2012) 410–416. doi:10.1016/j.cej.2012.08.087.

[163] K. Nasouri, A.M. Shoushtari, M.R.M. Mojtahedi, Evaluation of effective electrospinning parameters controlling polyvinylpyrrolidone nanofibers surface morphology via response surface methodology, Fibers Polym. 16 (2015) 1941–1954. doi:10.1007/s12221-015-5263-4.

[164] M.A. Badawi, L.K. El-Khordagui, A quality by design approach to optimization of emulsions for electrospinning using factorial and D-optimal designs, Eur. J. Pharm. Sci. 58 (2014) 44–54. doi:10.1016/j.ejps.2014.03.004.

[165] S.R. Coles, D.K. Jacobs, M.O. James, G. Barker, A.J. Clark, K. Kirwan, J. Stanger, N. Tucker, A design of experiment approach to material properties optimization of electrospun nanofibres, J. Appl. Polym. Sci. 117 (2010) 2251–2257. doi:10.1002/app.

[166] H. Albetran, Y. Dong, I.M. Low, Characterization and optimization of electrospun TiO2/PVP nanofibers using Taguchi design of experiment method, J. Asian Ceram. Soc. 3 (2015) 292–300. doi:10.1016/j.jascer.2015.05.001.

[167] M. Ranjbar-Mohammadi, S. Kargozar, S.H. Bahrami, M.T. Joghataei,

Fabrication of curcumin-loaded gum tragacanth/poly(vinyl alcohol) nanofibers with optimized electrospinning parameters, J. Ind. Text. 46 (2017) 1170–1192. doi:10.1177/1528083715613631.

[168] F.A.A. Ruiter, C. Alexander, F.R.A.J. Rose, J.I. Segal, A design of experiments approach to identify the influencing parameters that determine poly-D,L-lactic acid (PDLLA) electrospun scaffold morphologies, Biomed. Mater. 12 (2017) 055009. doi:10.1088/1748-605X/aa7b54.

[169] K. Nasouri, H. Bahrambeygi, A. Rabbi, A.M. Shoushtari, A. Kaflou, Modeling and Optimization of Electrospun PAN Nanofiber Diameter Using Response Surface Methodology and Artificial Neural Networks, J. Appl. Polym. Sci. 126 (2012) 127–135.

[170] S. Nista, L. Peres, M.A. D'Avila, F.L. Schmidt, L.H.I. Mei, Nanostructured Membranes Based on Cellulose Acetate Obtained by Electrospinning, Part 1: Study of the Best Solvents and Conditions by Design of Experiments, J. Appl. Polym. Sci. 126 (2012) e70–e78.

[171] International Conference On Harmonisation Of Technical Requirements For Registration Of Pharmaceuticals For Human Uuse, (2009).

[172] L.X. Yu, G. Amidon, M.A. Khan, S.W. Hoag, J. Polli, G.K. Raju, J. Woodcock, Review Article Understanding Pharmaceutical Quality by Design, 16 (2014). doi:10.1208/s12248-014-9598-3.

[173] L. Kong, G.R. Ziegler, Molecular entanglement and electrospinnability of biopolymers., J. Vis. Exp. (2014) e51933. doi:10.3791/51933.

[174] A.J.P. van Heugten, C.L. Braal, M. Versluijs-Helder, H. Vromans, The influence of cetomacrogol ointment processing on structure: A definitive screening design, Eur. J. Pharm. Sci. 99 (2017) 279–284. doi:10.1016/j.ejps.2016.12.029.

[175] H. Abdi, L.J. Williams, Principal component analysis, Wiley Interdiscip. Rev. Comput. Stat. 2 (2010) 433–459. doi:10.1002/wics.101.

[176] K. Woertz, C. Tissen, P. Kleinebudde, J. Breitkreutz, Rational development of taste masked oral liquids guided by an electronic tongue, Int. J. Pharm. 400 (2010) 114–123. doi:10.1016/j.ijpharm.2010.08.042.

[177] R.R. Klossner, H.A. Queen, A.J. Coughlin, W.E. Krause, Correlation of

Chitosan's rheological properties and its ability to electrospin, Biomacromolecules. 9 (2008) 2947–2953. doi:10.1021/bm800738u.

[178] M.G. McKee, G.L. Wilkes, R.H. Colby, T.E. Long, Correlations of Solution Rheology with Electrospun Fiber Formation of Linear and Branched Polyesters, Macromolecules. 37 (2004) 1760–1767. doi:10.1021/ma035689h.

[179] S. Ramakrishna, K. Fujihara, W. Teo, An Introduction to Electrospinning and Nanofibers, London, 2005.

[180] J.H. Song, H.E. Kim, H.W. Kim, Production of electrospun gelatin nanofiber by water-based co-solvent approach, J. Mater. Sci. Mater. Med. 19 (2008) 95–102. doi:10.1007/s10856-007-3169-4.

[181] X. Yan, M. Gevelber, Investigation of electrospun fiber diameter distribution and process variations, J. Electrostat. 68 (2010) 458–464. doi:10.1016/j.elstat.2010.06.009.

[182] J.. Deitzel, J. Kleinmeyer, D. Harris, N.. Beck Tan, The effect of processing variables on the morphology of electrospun nanofibers and textiles, Polymer (Guildf). 42 (2001) 261–272. doi:10.1016/S0032-3861(00)00250-0.

[183] C.J. Luo, E. Stride, M. Edirisinghe, Mapping the influence of solubility and dielectric constant on electrospinning polycaprolactone solutions, Macromolecules. 45 (2012) 4669–4680. doi:10.1021/ma300656u.

[184] R. Nayak, L. Padhye, L. Arnold, Melt-electrospinning of nanofibers, in: Electrospun Nanofibers, 2017: pp. 11–40.

[185] S. De Vrieze, T. Van Camp, A. Nelvig, B. Hagström, P. Westbroek, K. De Clerck, The effect of temperature and humidity on electrospinning, J. Mater. Sci. 44 (2009) 1357–1362. doi:10.1007/s10853-008-3010-6.

[186] G.C. Rutledge, S. V. Fridrikh, Formation of fibers by electrospinning, Adv. Drug Deliv. Rev. 59 (2007) 1384–1391. doi:10.1016/j.addr.2007.04.020.

[187] R. Li, P. Tomasula, A.M.M. de Sousa, S.C. Liu, M. Tunick, K. Liu, L. Liu, Electrospinning pullulan fibers from salt solutions, Polymers (Basel). 9 (2017) 1–12. doi:10.3390/polym9010032.

[188] J. Du, X. Zhang, Role of Polymer–Salt–Solvent Interactions in the Electrospinning of Polyacrylonitrile/Iron Acetylacetonate, J. Appl. Polym. Sci. 109 (2008) 2935–2941. doi:10.1002/app.28396.

[189] G.R. Williams, N.P. Chatterton, T. Nazir, D.-G. Yu, L.-M. Zhu, C.J. Branford-White, Electrospun nanofibers in drug delivery: recent developments and perspectives, Ther. Deliv. 3 (2012) 515–533. doi:10.4155/tde.12.17.

[190] SAS Institute Inc., JMP, (2021). https://community.jmp.com/ (accessed March 31, 2021).

[191] D.H. Reneker, A.L. Yarin, Electrospinning jets and polymer nanofibers, Polymer (Guildf). 49 (2008) 2387–2425. doi:10.1016/j.polymer.2008.02.002.

[192] V. Linares, C.J. Yarce, J.D. Echeverri, E. Galeano, C.H. Salamanca, Relationship between degree of polymeric ionisation and hydrolytic degradation of Eudragit® E polymers under extreme acid conditions, Polymers (Basel). 11 (2019). doi:10.3390/polym11061010.

[193] H. Wang, Step size, scanning speed and shape of X-ray diffraction peak, J. Appl. Crystallogr. 27 (1994) 716–722. doi:10.1107/s002188989400186x.

[194] National Center for Biotechnology Information. PubChem Compound Database; CID=702, https://pubchem.ncbi.nlm.nih.gov/compound/702 (accessed Dec 6, 2017)., (2017).

[195] S. Payab, N. Jafari-Aghdam, M. Barzegar-Jalali, G. Mohammadi, F. Lotfipour, T. Gholikhani, K. Adibkia, Preparation and physicochemical characterization of the azithromycin-Eudragit RS 100 nanobeads and nanofibers using electrospinning method, J. Drug Deliv. Sci. Technol. 24 (2014) 585–590. doi:10.1016/S1773-2247(14)50123-2.

[196] Y. Matveev, V. Grinberg, V. Tolstoguzov, The plasticizing effect of water on proteins, polysaccharides and theirmixtures. Glassy state of biopolymers, food and seeds, Food Hydrocoll. 12 (2000) 425–437.

[197] K. Ghosal, A. Chandra, G. Praveen, S. Snigdha, S. Roy, C. Agatemor, S. Thomas, I. Provaznik, Electrospinning over Solvent Casting : Tuning of Mechanical Properties of Membranes, Sci. Rep. (2018) 1–9. doi:10.1038/s41598-018-23378-3.

[198] A. Bowles, J. Keane, T. Ernest, D. Clapham, C. Tuleu, Specific aspects of gastro-intestinal transit in children for drug delivery design, Int. J. Pharm. 395 (2010) 37–43. doi:10.1016/j.ijpharm.2010.04.048.

[199] EMA, Reflection paper on the dissolution specification for generic solid oral

immediate release products with systemic action, 44 (2017). www.ema.europa.eu/contact.

[200] Y. Tahara, K. Toko, Electronic tongues-a review, IEEE Sens. J. 13 (2013) 3001–3011. doi:10.1109/JSEN.2013.2263125.

[201] N.T. Hansen, I. Kouskoumvekaki, F.S. Jørgensen, S. Brunak, S.Ó. Jónsdóttir, Prediction of pH-dependent aqueous solubility of druglike molecules, J. Chem. Inf. Model. 46 (2006) 2601–2609. doi:10.1021/ci600292q.

[202] Z. Rahman, A.S. Zidan, S.R. Khan, I.K. Reddy, M.A. Khan, Cholorpheniramine tannate complexes: Physicochemical, chemometric, and taste masking evaluation, Int. J. Pharm. 436 (2012) 582–592. doi:10.1016/j.ijpharm.2012.07.037.

[203] S.M.S. Shahriar, J. Mondal, M.N. Hasan, V. Revuri, D.Y. Lee, Y.K. Lee, Electrospinning nanofibers for therapeutics delivery, Nanomaterials. 9 (2019). doi:10.3390/nano9040532.

[204] D. Jia, Y. Gao, G.R. Williams, Core/shell poly(ethylene oxide)/Eudragit fibers for site-specific release, Int. J. Pharm. 523 (2017) 376–385. doi:10.1016/j.ijpharm.2017.03.038.

[205] D.G. Yu, J.H. Yu, L. Chen, G.R. Williams, X. Wang, Modified coaxial electrospinning for the preparation of high-quality ketoprofen-loaded cellulose acetate nanofibers, Carbohydr. Polym. 90 (2012) 1016–1023. doi:10.1016/j.carbpol.2012.06.036.

[206] A. Greiner, J.H. Wendorff, A.L. Yarin, E. Zussman, Biohybrid nanosystems with polymer nanofibers and nanotubes, Appl. Microbiol. Biotechnol. 71 (2006) 387–393. doi:10.1007/s00253-006-0356-z.

[207] D.G. Yu, L.M. Zhu, C.J. Branford-White, J.H. Yang, X. Wang, Y. Li, W. Qian, Solid dispersions in the form of electrospun core-sheath nanofibers., Int. J. Nanomedicine. 6 (2011) 3271–3280. doi:10.2147/ijn.s27468.

[208] X.Y. Li, Y.C. Li, D.G. Yu, Y.Z. Liao, X. Wang, Fast disintegrating quercetin-loaded drug delivery systems fabricated using coaxial electrospinning, Int. J. Mol. Sci. 14 (2013) 21647–21659. doi:10.3390/ijms141121647.

[209] M. Slavkova, J. Breitkreutz, Orodispersible drug formulations for children and elderly, Eur. J. Pharm. Sci. 75 (2015). doi:10.1016/j.ejps.2015.02.015.

[210] R. Krampe, J.C. Visser, H.W. Frijlink, J. Breitkreutz, H.J. Woerdenbag, M. Preis, Oromucosal film preparations: points to consider for patient centricity and manufacturing processes., Expert Opin. Drug Deliv. 13 (2016) 493–506. doi:10.1517/17425247.2016.1118048.

[211] J. Soto, A. Keeley, A. V Keating, A.H.A. Mohamed-ahmed, Y. Sheng, G. Winzenburg, R. Turner, S. Desset-brèthes, M. Orlu, C. Tuleu, Rats can predict aversiveness of Active Pharmaceutical Ingredients, Eur. J. Pharm. Biopharm. 133 (2018) 77–84. doi:10.1016/j.ejpb.2018.09.027.

[212] K. Woertz, C. Tissen, P. Kleinebudde, J. Breitkreutz, Performance qualification of an electronic tongue based on ICH guideline Q2, J. Pharm. Biomedc. 51 (2010) 497–506. doi:10.1016/j.jpba.2009.09.029.

[213] S. Chang, M. Wang, F. Zhang, Y. Liu, X. Liu, D.G. Yu, H. Shen, Sheath-separate-core nanocomposites fabricated using a trifluid electrospinning, Mater. Des. 192 (2020) 108782. doi:10.1016/j.matdes.2020.108782.

[214] F.L. Lopez, G.C. Shearman, S. Gaisford, G.R. Williams, Amorphous formulations of indomethacin and griseofulvin prepared by electrospinning, Mol. Pharm. 11 (2014) 4327–4338. doi:10.1021/mp500391y.

[215] T.J. Sill, H.A. von Recum, Electrospinning: Applications in drug delivery and tissue engineering, Biomaterials. 29 (2008) 1989–2006. doi:10.1016/j.biomaterials.2008.01.011.

[216] M. Wang, T. Hai, Z. Feng, D.G. Yu, Y. Yang, S.W.A. Bligh, The relationships between the working fluids, process characteristics and products from the modified coaxial electrospinning of zein, Polymers (Basel). 11 (2019). doi:10.3390/polym11081287.

[217] Y. Haru, A. Tomioka, Luminescent electrospun nanofibers doped with organic dye: Toward a disentangled deposition, Phys. Status Solidi Basic Res. 254 (2017). doi:10.1002/pssb.201600721.

[218] Sigma Aldrich, FTIR table, (2021). https://www.sigmaaldrich.com/technical-documents/articles/biology/ir-spectrum-table.html (accessed April 1, 2021).

[219] E.H. IMMERGUT, H.F. MARK, Principles of Plasticization, (1965) 1–26. doi:10.1021/ba-1965-0048.ch001.

[220] V.D. Prajapati, A.M. Chaudhari, A.K. Gandhi, P. Maheriya, Pullulan based oral

thin film formulation of zolmitriptan : Development and optimization using factorial design, Int. J. Biol. Macromol. 107 (2018) 2075–2085. doi:10.1016/j.ijbiomac.2017.10.082.

[221] Y. Tian, M. Orlu, H.J. Woerdenbag, M. Scarpa, D. Kottke, E. Sjöholm, H. Öblom, N. Sandler, L.J. Wouter, H.W. Frijlink, J. Breitkreutz, J.C. Visser, Y. Tian, M. Orlu, H.J. Woerdenbag, M. Scarpa, W. Frijlink, J. Breitkreutz, J.C. Visser, Oromucosal films : from patient centricity to production by printing techniques, Expert Opin. Drug Deliv. 16 (2019) 981–993. doi:10.1080/17425247.2019.1652595.

[222] M. Irfan, S. Rabel, Q. Bukhtar, M.I. Qadir, F. Jabeen, A. Khan, Orally disintegrating films: A modern expansion in drug delivery system, Saudi Pharm. J. 24 (2016). doi:10.1016/j.jsps.2015.02.024.

[223] A. V Keating, J. Soto, C. Forbes, M. Zhao, D.Q.M. Craig, C. Tuleu, Multi-Methodological Quantitative Taste Assessment of Anti-Tuberculosis Drugs to Support the Development of Palatable Paediatric Dosage Forms, Pharmaceutics. (2020).

[224] Y. Takeuchi, R. Usui, H. Ikezaki, K. Tahara, H. Takeuchi, An advanced technique using an electronic taste-sensing system to evaluate the bitterness of orally disintegrating films and the evaluation of model films, Int. J. Pharm. 531 (2017) 179–190. doi:10.1016/j.ijpharm.2017.07.073.

[225] OriginLab Corporation, Origin Pro, (2019).

[226] K. Izawa, Y. Amino, M. Kohmura, Y. Ueda, M. Kuroda, Human-environment interactions - taste, Compr. Nat. Prod. II Chem. Biol. 4 (2010) 631–671.

[227] J. Ali, A. Zgair, G.S. Hameed, M.C. Garnett, C.J. Roberts, J.C. Burley, P. Gershkovich, Application of biorelevant saliva-based dissolution for optimisation of orally disintegrating formulations of felodipine, Int. J. Pharm. 555 (2019) 228–236. doi:10.1016/j.ijpharm.2018.11.051.

[228] M. Pein, X.D. Gondongwe, M. Habara, G. Winzenburg, Interlaboratory testing of Insent e-tongues, Int. J. Pharm. 469 (2014) 228–237. doi:10.1016/j.ijpharm.2014.02.036.

[229] European Medicines Agency, ICH Q2, Definitions. 2 (2020) 1–15. doi:10.32388/yokp53.

[230] S.K. Chay, A. V Keating, C. James, A.E. Aliev, S. Haider, D.Q.M. Craig, Evaluation of the taste-masking effects of (2- hydroxypropyl)-b-cyclodextrin on ranitidine hydrochloride; a combined biosensor, spectroscopic and molecular modelling assessment, RSC Adv. (2018) 3564–3573. doi:10.1039/c7ra11015d.

[231] K. Centkowska, E. Ławrecka, M. Sznitowska, Technology of orodispersible polymer films with micronized loratadine—influence of different drug loadings on film properties, Pharmaceutics. 12 (2020). doi:10.3390/pharmaceutics12030250.

[232] S. Lade Milind, A. Payghan Santosh, J. Tamboli Zaki, I. Disouza John, Polymer Based Wafer Technology : A Review Polymer Based Wafer Technology : A Review, Int. J. Pharm. Biol. Arch. 4 (2013) 1060–1074.

[233] V. Garsuch, J. Breitkreutz, Comparative investigations on different polymers for the preparation of fast-dissolving oral films., J. Pharm. Pharmacol. 62 (2010) 539–45. doi:10.1211/jpp/62.04.0018.

[234] EMEA, Guideline on Pharmaceutical Development of Medicines for Paediatric Use Guideline on Pharmaceutical Development of Medicines for Paediatric Use, EMEA. 44 (2013) 1–23. doi:EMA/CHMP/QWP/805880/2012 Rev. 2.

[235] R.G. Strickley, Pediatric Oral Formulations : An Updated Review of Commercially Available Pediatric Oral Formulations Since 2007, J. Pharm. Sci. 108 (2019) 1335–1365. doi:10.1016/j.xphs.2018.11.013.

[236] T. Casian, E. Borbás, K. Ilyés, B. Démuth, A. Farkas, Z. Rapi, C. Bogdan, S. Iurian, V. Toma, R. Știufiuc, B. Farkas, A. Balogh, G. Marosi, I. Tomuță, Z.K. Nagy, Electrospun amorphous solid dispersions of meloxicam: Influence of polymer type and downstream processing to orodispersible dosage forms, Int. J. Pharm. 569 (2019). doi:10.1016/j.ijpharm.2019.118593.

[237] S.M. Hanning, F.L. Lopez, I.C.K. Wong, T.B. Ernest, C. Tuleu, M. Orlu Gul, Patient centric formulations for paediatrics and geriatrics: Similarities and differences, Int. J. Pharm. 512 (2016) 355–359. doi:10.1016/j.ijpharm.2016.03.017.

[238] M. Scarpa, S. Stegemann, W. Hsiao, H. Pichler, S. Gaisford, M. Bresciani, A. Paudel, M. Orlu, Orodispersible fi lms : Towards drug delivery in special populations, Int. J. Pharm. 523 (2017) 327–335.

doi:10.1016/j.ijpharm.2017.03.018.

[239] J.C. Visser, L. Wibier, O. Kiefer, M. Orlu, J. Breitkreutz, H.J. Woerdenbag, K. Taxis, A pediatrics utilization study in the Netherlands to identify active pharmaceutical ingredients suitable for inkjet printing on orodispersible films, Pharmaceutics. 12 (2020) 1–10. doi:10.3390/pharmaceutics12020164.

[240] A.F. Borges, C. Silva, J.F.J. Coelho, S. Simões, Oralfilms: Current status and future perspectives II—Intellectual property, technologies and market needs, J. Control. Release. 206 (2015) 108–121. http://library1.nida.ac.th/termpaper6/sd/2554/19755.pdf.

[241] V. Klingmann, C.E. Pohly, T. Meissner, E. Mayatepek, A. Möltner, K. Flunkert, J. Breitkreutz, H.M. Bosse, Acceptability of an orodispersiblefilm compared to syrup in neonates and infants: A randomized controlled trial, Eur. J. Pharm. Biopharm. 151 (2020) 239–245. http://library1.nida.ac.th/termpaper6/sd/2554/19755.pdf.

[242] M. Orlu, S.R. Ranmal, Y. Sheng, C. Tuleu, P. Seddon, Acceptability of orodispersible films for delivery of medicines to infants and preschool children, Drug Deliv. 24 (2017) 1243–1248. doi:10.1080/10717544.2017.1370512.

[243] J.M.L. Sergio Torres-Giner, Rocio Perez-Masia, A Review on Electrospun Polymer Nanostructures as Advanced Bioactive Platforms, Polym. Eng. Sci. 56 (2016) 500–527. doi:10.1002/pen.

[244] P. Vass, E. Szabó, A. Domokos, G. Marosi, Scale-up of electrospinning technology : Applications in the pharmaceutical industry, (2019) 1–24. doi:10.1002/wnan.1611.

[245] Z.K. Nagy, K. Nyúl, I. Wagner, K. Molnár, G. Marosi, Electrospun water soluble polymer mat for ultrafast release of donepezil HCL, Express Polym. Lett. 4 (2010) 763–772. doi:10.3144/expresspolymlett.2010.92.

[246] K. Nazari, E. Kontogiannidou, R.H. Ahmad, A. Gratsani, M. Rasekh, M.S. Arshad, B.S. Sunar, D. Armitage, N. Bouropoulos, M.W. Chang, X. Li, D.G. Fatouros, Z. Ahmad, Development and characterisation of cellulose based electrospun mats for buccal delivery of non-steroidal anti-inflammatory drug (NSAID), Eur. J. Pharm. Sci. 102 (2017) 147–155. doi:10.1016/j.ejps.2017.02.033.

[247] A. Domokos, A. Balogh, D. Dénes, G. Nyerges, Z. Levente, B. Farkas, G.

Marosi, Z. Kristóf, Continuous manufacturing of orally dissolving webs containing a poorly soluble drug via electrospinning, Eur. J. Pharm. Sci. 130 (2019) 91–99. doi:10.1016/j.ejps.2019.01.026.

[248] K. Ghosal, R. Augustine, A. Zaszczynska, A. Jain, A. Hasan, N. Kalarikkal, Novel drug delivery systems based on triaxial electrospinning based nanofibers, React. Funct. Polym. (2021) 104895. doi:10.1016/j.reactfunctpolym.2021.104895.

[249] S. Labbaf, H. Ghanbar, E. Stride, M. Edirisinghe, Preparation of Multilayered Polymeric Structures Using a Novel Four-Needle Coaxial Electrohydrodynamic Device, (2014) 618–623.

[250] FDA, Guidance for Industry Sterile Drug Products Produced by Aseptic Processing — Current Good Manufacturing Practice, 2004.

[251] M. Scarpa, A. Paudel, F. Kloprogge, W.K. Hsiao, M. Bresciani, Key acceptability attributes of orodispersible films, 125 (2018) 131–140. doi:10.1016/j.ejpb.2018.01.003.

[252] C.J. Smith, H.M. Sammons, A. Fakis, S. Conroy, A prospective study to assess the palatability of analgesic medicines in children, J. Adv. Nurs. 69 (2013). doi:10.1111/j.1365-2648.2012.06050.x.

[253] S. Manikandan, Measures of central tendency : Median and mode, Postgrad. Corner. 2 (2011) 214–216. doi:10.4103/0976-500X.83300.

[254] A. Villa, C.L. Connell, S. Abati, Diagnosis and management of xerostomia and hyposalivation, (2015) 45–51.

[255] P. Patil, S.K. Shrivastava, Fast Dissolving Oral Films : a Novel Drug Delivery System, Int. J. Sci. Res. 3 (2014) 2088–2093.

[256] X. Guo, D. Cun, F. Wan, H. Bera, Q. Song, X. Tian, Y. Chen, J. Rantanen, M. Yang, Comparative assessment of in vitro/in vivo performances of orodispersible electrospun and casting films containing rizatriptan benzoate, Eur. J. Pharm. Biopharm. 154 (2020) 283–289. doi:10.1016/j.ejpb.2020.06.023.

[257] F. Ruiz, A. Keeley, L. Patrick, C. Tuleu, C. Lachuer, J. Rwabihama, N. Bachalat, I. Boulaich, F. Abdallah, M. Rabus, Sex Diff erences in Medicine Acceptability : A New Factor to Be Considered in Medicine Formulation,

Pharmaceutics. 11 (2019) 1–12. doi:10.3390/pharmaceutics11080368.

[258] E. Sipos, A. Kazsoki, Formulation and Characterization of Aceclofenac-Loaded Nanofiber Based Orally Dissolving Webs, 2 (2019) 1–11.

[259] S. Tort, A. Yıldız, F. Tuğcu-demiröz, G. Akca, F. Acartürk, Development and characterization of rapid dissolving ornidazole loaded PVP electrospun fibers electrospun fibers, Pharm. Dev. Technol. 24 (2019) 864–873. doi:10.1080/10837450.2019.1615088.

[260] Z. Irem, T. Uyar, Applied Surface Science Fast-dissolving electrospun nano fi brous fi lms of paracetamol / cyclodextrin inclusion complexes, 492 (2019) 626–633. doi:10.1016/j.apsusc.2019.06.220.

[261] S. Thakkar, N. More, D. Sharma, G. Kapusetti, K. Kalia, M. Misra, Fast dissolving electrospun polymeric films of anti-diabetic drug repaglinide : formulation and evaluation, Drug Dev. Ind. Pharm. 45 (2019) 1921–1930. doi:10.1080/03639045.2019.1680994.

[262] K. Göke, T. Lorenz, A. Repanas, F. Schneider, D. Steiner, K. Baumann, H. Bunjes, A. Dietzel, J.H. Finke, B. Glasmacher, A. Kwade, European Journal of Pharmaceutics and Biopharmaceutics Novel strategies for the formulation and processing of poorly water- soluble drugs, Eur. J. Pharm. Biopharm. 126 (2018) 40–56. doi:10.1016/j.ejpb.2017.05.008.

[263] Z. Qin, X. Jia, Q. Liu, B. Kong, H. Wang, Fast dissolving oral films for drug delivery prepared from chitosan / pullulan electrospinning nanofibers, Int. J. Biol. Macromol. 137 (2019) 224–231. doi:10.1016/j.ijbiomac.2019.06.224.

[264] C. Rustemkyzy, P. Belton, S. Qi, Preparation and Characterization of Ultrarapidly Dissolving Orodispersible Films for Treating and Preventing Iodine Deficiency in the Pediatric Population, J. Agric. Food Chem. 63 (2015) 9831–9838. doi:10.1021/acs.jafc.5b03953.

[265] Q. Song, X. Guo, Y. Sun, M. Yang, Anti-solvent Precipitation Method Coupled Electrospinning Process to Produce Poorly Water-Soluble Drug-Loaded Orodispersible Films, AAPS PharmSciTech. (2019) 1–11. doi:10.1208/s12249-019-1464-2.

[266] P.N. Raju, M.S. Kumar, C.M. Reddy, K. Ravishankar, Formulation and Evaluation of Fast Dissolving Films of Loratidine by Solvent Casting Method, 2 (2013).

[267] Rivelin, (2019). https://afyxtx.com/ (accessed March 5, 2020).

[268] X. Li, M.A. Kanjwal, L. Lin, I.S. Chronakis, Electrospun polyvinyl-alcohol nanofibers as oral fast-dissolving delivery system of caffeine and riboflavin, Colloids Surfaces B Biointerfaces. 103 (2013) 182–188. doi:10.1016/j.colsurfb.2012.10.016.

[269] H. Bukhary, G.R. Williams, M. Orlu, Electrospun fi xed dose formulations of amlodipine besylate and valsartan, Int. J. Pharm. 549 (2018) 446–455. doi:10.1016/j.ijpharm.2018.08.008.

[270] L. Hardelin, J. Thunberg, E. Perzon, G. Westman, P. Walkenstrom, P. Gatenholm, Electrospinning of Cellulose Nanofibers from Ionic Liquids: The Effect of Different Cosolvents Linda, J. Appl. Polym. Sci. 125 (2012) 1901–1909. doi:10.1002/app.

[271] B. Tarus, N. Fadel, A. Al-Oufy, M. El-Messiry, Effect of polymer concentration on the morphology and mechanical characteristics of electrospun cellulose acetate and poly (vinyl chloride) nanofiber mats, Alexandria Eng. J. 55 (2016) 2975–2984. doi:10.1016/j.aej.2016.04.025.

[272] D.G. Yu, C. Branford-White, S.W.A. Bligh, K. White, N.P. Chatterton, L.M. Zhu, Improving polymer nanofiber quality using a modified co-axial electrospinning process, Macromol. Rapid Commun. 32 (2011) 744–750. doi:10.1002/marc.201100049.

[273] B.T. Raimi-Abraham, S. Mahalingam, M. Edirisinghe, D.Q.M. Craig, Generation of poly(N-vinylpyrrolidone) nanofibres using pressurised gyration, Mater. Sci. Eng. C. 39 (2014) 168–176. doi:10.1016/j.msec.2014.02.016.

[274] C. Asgreen, M.M. Knopp, J. Skytte, K. Löbmann, Influence of the polymer glass transition temperature and molecular weight on drug amorphization kinetics using ball milling, Pharmaceutics. 12 (2020). doi:10.3390/pharmaceutics12060483.

[275] S. Biswal, J. Sahoo, P.N. Murthy, Physicochemical properties of solid dispersions of gliclazide in polyvinylpyrrolidone K90, AAPS PharmSciTech. 10 (2009) 329–334. doi:10.1208/s12249-009-9212-7.

[276] WHO, Stability testing of active pharmaceutical ingredients and finished pharmaceutical products Introduction, WHO Expert Comm. Specif. Pharm. Prep. Fifty-Second. 52 (2018) 309–352.

https://database.ich.org/sites/default/files/Q1F_Stability_Guideline_WHO_2018.pdf.

[277] L.A. Felton, Use of polymers for taste-masking pediatric drug products, Drug Dev. Ind. Pharm. 44 (2018) 1049–1055. doi:10.1080/03639045.2018.1430822.

[278] H.U. Blaser, Chirality and its implications for the pharmaceutical industry, Rend. Lincei. 24 (2013) 213–216. doi:10.1007/s12210-012-0220-2.

[279] L.A. Nguyen, H. He, C. Pham-Huy, Chiral Drugs: An Overview, Int. J. Biomed. Sci. 6 (2006) 85–100. doi:10.1111/deci.12302.

[280] P. Dabhi, N. Jivani, Design and Evaluation of Guaifenesin Medicated Chewing Gum for Cough Relief, Int. J. Eng. Sci. Comput. 9 (2019) 22668–22677. http://ijesc.org/.

[281] A.S. Alshetaili, B.K. Almutairy, M.A. Repka, Preparation and Evaluation of Hot-Melt Extruded Patient-Centric Ketoprofen Mini-Tablets, Curr. Drug Deliv. 13 (2015) 1–10.

[282] Spraybase, Spraybase, (2017). https://www.spraybase.com/electrospinning/ (accessed December 8, 2017).

Appendix A

Table showing 42 experiments of drug-loaded E-EPO used for predictive modelling of optimum conditions.

CPM (%w/w)	E-EPO (%w/v)	Water (%v/v)	Voltage (kV)	Rate (mL/h)	Distance (cm)
14.3	25	20	20	1	15
16.7	25	20	20	1	15
20	25	20	20	1	15
25	25	20	20	1	15
33.3	25	20	20	1	15
33.3	25	20	25	1	15
20	45	20	10	0.5	15
20	45	0	10	0.5	15
20	45	0	20	0.5	15
25	45	20	10	0.5	15
25	45	0	10	0.5	15
25	45	0	14	0.5	15
14.3	45	0	10	0.5	15
14.3	45	0	12	1	20
14.3	45	0	20	1	20
14.3	45	0	10	1	20
14.3	45	0	10	1	20
50	25	20	25	1	20
16.7	25	20	25	1	20
16.7	25	0	25	1	20
16.7	35	20	20	1	20
16.7	35	0	20	1	20
16.7	40	0	10	1	20
16.7	40	0	20	1	20
16.7	40	0	15	1	20
16.7	40	20	20	1	20
20	40	0	20	1	20
20	40	0	15	1	20
16.7	37.5	0	20	1	20
16.7	37.5	0	12	1	25
16.7	30	0	20	1	20
16.7	30	0	20	1	20
14.3	30	0	18.5	1	17.5
14.3	35	0	15	1	17.5
14.3	40	0	15	1	17.5
12.5	35	0	15	1	17.5

11.1	35	0	15	1	17.5
14.3	35	0	15	1	17.5
11.1	35	0	25	0.5	17.5
10	35	0	25	0.5	17.5
9.1	35	0	25	0.5	17.5
9.1	35	25	25	0.5	17.5

Appendix B: REC Application

NOTE TO APPLICANTS: IT IS IMPORTANT FOR YOU TO INCLUDE ALL RELEVANT INFORMATION ABOUT YOUR RESEARCH IN THIS APPLICATION FORM AS YOUR ETHICAL APPROVAL WILL BE BASED ON THIS FORM. THEREFORE ANYTHING NOT INCLUDED WILL NOT BE PART OF ANY ETHICAL APPROVAL.

YOU SHOULD READ THE ETHICS APPLICATION GUIDELINES AND HAVE THEM AVAILABLE AS YOU COMPLETE THIS FORM.

APPLICATION FORM

SECTION A APPLICATION FOR ETHICAL REVIEW: HIGH RISK

A1

Project Title:

Mouthfeel evaluation comparison between orally administered fibre mats and fast dissolving films.

Date of Submission: 07 June 2019	Proposed Data Collection Start Date: 01 July 2019
UCL Ethics Project ID Number: 15975/001	Proposed Data Collection End Date: 01 July 2020

Is this application for continuation of a research project that already has ethical approval? ***For example, a preliminary/pilot study has been completed and this is an application for a follow-up project? If yes, please provide the information requested below.***

Project ID for the previous study: N/A

A2

Principal Researcher

Please note that a student – undergraduate, postgraduate or research postgraduate cannot be the Principal Researcher for Ethics purposes.

Full Name: Prof. Catherine Tuleu	Position Held: Professor in paediatric pharmaceutics
Name and Address of Department: UCL School of Pharmacy, 29-39 Brunswick Square, WC1N 1AX, London, UK.	Email: c.tuleu@ucl.ac.uk
	Telephone: 0044 20 7753 5857
	Fax: N/A

Declaration To be Signed by the Principal Researcher

- I have met with and advised the student on the ethical aspects of this project design *(applicable only if the Principal Researcher is not also the Applicant).*
- I understand that it is a UCL requirement for both students & staff researchers to undergo Disclosure and Barring Service (DBS) Checks when working in controlled or regulated activity with children, young people or vulnerable adults. The required DBS Check Disclosure Number(s) is: N/A
- I have obtained approval from the UCL Data Protection Officer stating that the research project is compliant with the General Data Protection Regulation 2018. My Data Protection Registration Number is: **Z6364106/2019/06/10**

- I am satisfied that the research complies with current professional, departmental and university guidelines including UCL's Risk Assessment Procedures and insurance arrangements.
- I undertake to complete and submit the 'Continuing Review Approval Form' on an annual basis to the UCL Research Ethics Committee.
- I will ensure that changes in approved research protocols are reported promptly and are not initiated without approval by the UCL Research Ethics Committee, except when necessary to eliminate apparent immediate hazards to the participant.
- I will ensure that all adverse or unforeseen problems arising from the research project are reported in a timely fashion to the UCL Research Ethics Committee.
- I will undertake to provide notification when the study is complete and if it fails to start or is abandoned.

SIGNATURE: [redacted] **DATE:** 06/06/2019

A3 **Applicant(s) Details** *(if Applicant is not the Principal Researcher e.g. student details):*

Full Name: Hend Abdelhakim	
Position Held: PhD student	
Name and Address of Department: UCL School of Pharmacy 29-39 Brunswick Square WC1N 1AX London UK	Email: hend.abdelhakim.16@ucl.ac.uk Telephone: 07701342165 Fax: N/A
Full Name: N/A	
Position Held: N/A	
Name and Address of Department: N/A	Email: N/A Telephone: N/A Fax: N/A

A4 **Sponsor/ Other Organisations Involved and Funding**

a) Sponsor: ☒ **UCL** ☐ **Other institution**
If your project is sponsored by an institution other than UCL please provide details:

b) Other Organisations: If your study involves another organisation, please provide details. *Evidence that the relevant authority has given permission should be attached or confirmation provided that this will be available upon request.*

Bioinicia electrospraying and electrospinning solutions, Valencia, Spain, will be providing the drug-free samples. They will prepare them in a controlled environment, label them, and ship them to UCL.

c) Funding: What are the sources of funding for this study and will the study result in financial payment or payment in kind to the department or College? *If study is funded solely by UCL this should be stated, the section should not be left blank.*

A5 **Signature of Head of Department [or Chair of your Departmental Research Ethics Committee/Departmental Ethics Lead]**
(This must not be the same signature as the Principal Researcher)

A. I have discussed this project with the principal researcher who is suitably qualified to carry out this research and I approve it.

I am satisfied that *[please highlight as appropriate]:*

(1) Data Protection registration:

- **has been satisfactorily completed**
- **has been initiated**
- **is not required**

(2) a risk assessment:

- **has been satisfactorily completed**
- **has been initiated**

(3) appropriate insurance arrangements are in place and appropriate sponsorship [funding] has been approved and is in place to complete the study. ☒ Yes ☐ No

(4) a Disclosure and Barring Service check(s):

- **has been satisfactorily completed**
- **has been initiated**
- **is not required**

Links to details of UCL's policies on the above can be found at: http://ethics.grad.ucl.ac.uk/procedures.php

****If any of the above checks are not required please clarify why below.**

N/A

PRINT NAME: Duncan Craig

SIGNATURE: [redacted] **DATE:** 6 June 2019

SECTION B DETAILS OF THE PROJECT

****It is essential that Sections B1 and B2 are completed in simple understandable lay language that a non-expert could understand or you risk your project being rejected**

B1 **Please provide a brief summary of the project in simple lay person's prose outlining the intended value of the project, giving necessary scientific background.** *(max 500 words)*.

Dysphagia is remarkably common in the general population and oral medicine administration often comprises a major obstacle for people with swallowing difficulties. The investigation of promising medicine forms in human panel studies enables the effective screening of easy-to swallow formulations with potential to improve therapeutic outcome and patient adherence. UCL School of Pharmacy has ongoing research on patient centric medicine design with the overall goal of optimizing medicine use. Among these novel patient centric formulations, orodispersible films (ODF) and nanofibre mats (NM) can be administered without the need of water as they melt in the oral cavity with the aid of saliva. NM and ODF have been prepared by electrospinning and manual solvent casting respectively. Although different fabrication methods are used, NM and ODF can have the same composition for comparison purposes.

In this study we aim to assess the ability and willingness of healthy young volunteers to swallow

placebo nanofibre mat and placebo orodispersible film formulations. Specifically we aim to learn:

• the acceptability of size, thickness, disintegration time, mouthfeel and ease of swallowing of ODF and NM solid dosage forms

• the impact of the fabrication method on the mouthfeel perception of ODF and NM in comparison

A single blind, crossover, single centre pilot human panel will be conducted on healthy adult volunteers. The assessment of swallowability consists in one questionnaire. Healthy adult volunteers will be required to take two drug-free samples and rate their satisfaction after picking and swallowing on a 5 point hedonic facial scale. This study will be randomized based on two sequences of AB and BA, each of the letters corresponding to one of the two samples. The ratio of AB : BA tested will be 1:1. On this type of 5 point hedonic scale our significance level would be a 1 face difference at least in between A and B. We also intend to recruit half male and half female participants.

N

Briefly characterise in simple lay person's prose the research protocol, type of procedure and/or research methodology (e.g. observational, survey research, experimental). Give details of any samples or measurements to be taken *(max 500 words).*

This study titled **mouthfeel evaluation comparison between orally administered fibre mats and fast dissolving films** will aim to compare two formulations, a nanofibre mat (NM) produced by electrospinning, and a fast dissolving film known as an orally dispersible film (ODF) prepared using solvent casting. It is aimed that 50 participants are to be recruited, presenting only two drug-free sampled to each of them, one prepared by each manufacturing method. Flow diagram of the study design is shown in Appendix 6. This is in line with the findings by Scarpa *et al.* [251], where the administration of the formulations on 3 different occasions did not change the findings. Therefore, it was decided to recruit a larger number of participants and only ask them to attend one 15 minute session, to try both drug-free samples once only. This will also reduce the burden on the participants.

The polymer used is going to be Parteck MXP (Polyvinyl alcohol), CAS number 9002-89-5, a Merck Polymer at 32kDa – Safety Data Sheet attached.

The films will be cast into 3 x 2 cm with 65 – 100 micrometre thickness. The electrospun fibre mats will have the same % polymer mass to allow for 1:1 comparison.

Once recruited, participants will be assigned individual, anonymous codes only accessible by the researchers. The final results of the study may be anonymously reported and disseminated in peer reviewed scientific journals, internal reports and conference presentations. A statement is included in the participant information sheet inviting participants to contact the research team should they wish to know the results of the study. In such cases, an abstract of the overall outcomes will be shared with participants.

Personal data (age, gender and randomisation code) is written down in paper, collected in a folder and safely stored in the Principal Researcher's office, which is kept locked at all times.

Access to consent forms and paper-based data recording templates will be restricted to the research team and stored in designated folders in a locked office at the UCL School of Pharmacy.

All information collected via data collection form will be kept confidentially. The answers will be available on web application called 'Qualtrics'. This is application used to design and perform the online surveys/data collection forms. The data will be stored in a password protected electronic format. Qualtrics does not collect identifying information such as name, email address, or IP address. Therefore, participant's responses will remain anonymous. Apart from research team, no one will be able to identify the participant or their answers, and no one will know whether or not the participant took part in the study, this will reduce the risk in terms of data protection. The data on the Qualtrics web application are actually stored in Germany and thus adhere to the EU's GDPR regulations. Qualtrics' Security White Paper as confirmation is attached.

Access to consent forms will be restricted to the research team. All information transferred on to the designated study encrypted laptop will have restricted password-protected access to only the immediate research team. Data transfer on to laptop will be done in a secure office at the UCL School of Pharmacy.

Confidentiality will be maintained when results are disseminated. As the outcomes of the research do not lead to direct benefit to the participants involved, collecting and storing personal contact information has not been deemed justifiable simply for the purposes of disseminating the end results. Instead participants will be able to request and obtain the results themselves, if they wish to do so.

Plans for analysis:
The 'Qualtrics® [Version 6.2, © 2018 Qualtrics, LLC, Provo, UT, USA]' application (automated web-based) will be used to collect the data. All answers will be compiled in an Excel sheet for further analysis. It is planned to use the coding or thematic method to analyse qualitative data drawn from the responses. The data will be anonymous and results will be kept confidential.

Details of partners:
Bioinicia e-spinning and e-spraying services company will be providing the drug-free samples. These will be prepared in a controlled environment and labelled with appropriate batch numbers and expiry dates.

Duration – participants will be asked to attend one session of approximately 15 minutes.

Inclusion criteria: Healthy male or female adults, able to understand and speak English. We will attempt to recruit an equal number of male and female subjects.

Exclusion criteria: Recent dental care up to 15 days before the tests and any known excipient allergies. Medicinal treatments altering saliva production. Sensory disorders affecting the mouth or local anaesthetics into the mouth within 24 hours of the study.

Experimental protocol:
Participants will be asked to place the whole sample in their mouth, start the stopwatch, allow the sample to dissolve completely, stop the stopwatch, and swallow the sample. Participants will be alerted of the possibility to reject one or more samples if they don't feel confident to swallow the sample safely. Immediately after sample ingestion, they will rate the sample properties using a computerised questionnaire (Qualtrics) with categorical scales and multiple choice questions (Appendix 3 - data collection form). Participants will have free access to water to aid swallowing and/or rinse their palate.

In each session, participants will receive a total of two placebo ODF (3 x 2 cm – 60 to 100 μm thick) film samples. An interval of 5 minutes will be respected between samples. Film samples will be numbered with a random codes.

Attach any questionnaires, psychological tests, etc. (a standardised questionnaire does not need to be attached, but please provide the name and details of the questionnaire together with a published reference to its prior usage).

B3

Where will the study take place (please provide name of institution/department)?
If the study is to be carried out overseas, what steps have been taken to secure research and ethical permission in the study country? Is the research compliant with Data Protection legislation in the country concerned or is it compliant with the General Data Protection Regulation 2018?

UCL School of Pharmacy, in the pharmacy practice dispensary. Participants will be seated at individual computer stations and screened off from other volunteers.

Environment: Calm, daylight, aired and odourless (to avoid any influence on the sensory part of the test).

The research is GDPR compliant.

B4

Have collaborating departments whose resources will be needed been informed and agreed to participate?
Attach any relevant correspondence.

Bioinicia e-spinning and e-spraying services company will be providing the drug-free samples. These will be prepared in a controlled environment and labelled with appropriate batch numbers and expiry dates.

B5

How will the results be disseminated, including communication of results with research participants?

Upon recruitment, participants will be assigned an individual, anonymous code only accessible by the researchers. If they wish so, participants can request to visualise the results of their performance after the study. Once completed, the results of the study may be anonymously reported and disseminated in peer reviewed scientific journals, internal reports and conference presentations.

A statement is included in the participant information sheet inviting participants to contact the research team should they wish to know the results of the study. As the results are collected anonymously, participant confidentiality will be maintained when results are disseminated.

B6

Please outline any ethical issues that might arise from the proposed study and how they are be addressed. *Please note that all research projects have some ethical considerations so do not leave this section blank.*

Confidentiality: This study will not be very intrusive since minimum personal details (contact details, age and gender) will be recorded. Confidentiality will not be breeched as once participants will be recruited, they will be assigned a code only accessible by the researchers. Once completed, the results of the study may be reported and disseminated in anonymous form.

Participant burden: The study will require each participant to attend sensory evaluation sessions for approximately 15 on one occasion only. There is a potential for participants to suffer from temporary oral discomfort if the taste, aftertaste or mouthfeel of the sample is aversive. In some cases, sample size or misplacement may cause the film to accidentally trigger chocking reflex though this is rare. This does not represent any hazard as the film samples are very thin, soft and flexible, and their maximum disintegration time is 60 seconds. Even in case of aspiration, the film will keep dissolving as previously wet by the participant's saliva and will turn into a completely liquid form.

Furthermore, the small size of the films prevents any risk of airway obstruction. If any participant shows high discomfort, the assessment will be immediately stopped.

Adverse effects: The time of contact with the sample depends on the disintegration time and film forming polymer. In any case, this will not exceed 90 seconds. The formulation in dissolved form will be swallowed by the participant. All the formulations are placebos (no drug content), and excipients are selected on the basis of their safety and only when already in use in authorised dosage forms. Participants who are aware of any allergic reaction to any of the components will be excluded from the study.

Concentrations for Polyvinyl alcohol PVA Parteck MXP (32 kDa)

Poly(vinyl) alcohol (PVA) (CAS no. 9002-89-5) is a synthetic polymer used in a wide range of industrial, commercial, medical and food applications. The acute oral toxicity of PVA is very low, with LD50s in the range of 15-20 g/kg. Orally administered PVA is very poorly absorbed from the gastrointestinal tract. PVA does not accumulate in the body when administered orally. PVA is not mutagenic or clastogenic. No-Observed-Adverse-Effect-Level (NOAELs) of orally administered PVA in male and female rats were 5000 mg/kg body weight/day in the 90-day dietary study and 5000 mg/kg body weight/day in the two generation reproduction study (DeMerlis and Schoneker, 2003). In 2003, PVA received notification as Generally Recognised As Safe (GRAS) by the Food and Drug Administration (FDA). The assignment of a permanent Acceptable Daily Intake (ADI) of **50 mg/kg** body weight/day by the Joint FAO/WHO Expert Committee on Food Additives was conferred in June 2003 (FDA-WHO).

Considering the average weight of participants (young adults) to be around 68 kg (males) and 58 kg (females) (Source: British National Formulary), the ADI would correspond to 3,500 mg/day (**3.5 g/day**).

Each orodispersible film (area 6 cm^2), will contain no more than 100mg of PVA. Each participant receives maximum 2 samples. Therefore, the total daily intake of PVA would be 200 mg/day (Males: 2.94 mg/kg/day; Females: 3.45 mg/kg/day), way below the ADI values stated by FDA.

In the case of any adverse events, first aid will be sought as necessary and the study will be stopped. For complaints, the supervisor or a third party (not directly involved in research team) Ms. Joanna O'Brien (Institute Manager) can be contacted for further advice.

The research team has previous experience in taste-assessment studies using the "swirl and spit" method. The principal investigator has considerable experience of conducting and supervising such studies using volunteer panels including the following published/presented research:

Scarpa, M.; Paudel, A.; Kloprogge, F.; Hsiao, W. K.; Bresciani, M. Key Acceptability Attributes of Orodispersible Fi Lms. ***2018****, 125 (August 2017), 131–140. https://doi.org/10.1016/j.ejpb.2018.01.003.*

School of Pharmacy REC/A/09/68 - Orlu-Gul M, Fisco G, Parmar D, Gill H, Tuleu C. A new reconstitutable oral paediatric hydrocortisone solution containing hydroxypropyl-β-cyclodextrin. Drug Dev Ind Pharm. 2013;39(7):1028-36;

UCL REC 4612/003 - Soto J, Ranmal S, Gondongwe X, Olanipekun F, Marbay J, Orlu Gul M and Tuleu C. Amlodipine in Paediatrics and Geriatrics: palatability issues. 5th European Paediatric Formulation Initiative Conference-Formulating Better Medicines for Children, 18-19 September 2013, Barcelona, Spain.

SECTION C DETAILS OF PARTICIPANTS

C1 **Participants to be studied**

C1a. Number of volunteers:	50
Upper age limit:	65
Lower age limit:	18

C1b. Please justify the age range and sample size:

Any healthy adults (staff and students) working at UCL. Age range should exclude any vulnerable groups. We will attempt to recruit an equal number of male and female subjects. This sample size is within the range used in previous human taste panel pilot palatability studies and large enough to apply appropriate statistical analysis.

C2 **Accessing/Using Pre-Collected Data:**
If you are using data or information held by a third party, please explain how you will obtain this. You should confirm that the information has been obtained in accordance with the General Data Protection Regulation 2018.

N/A

C3 **Will the research include children or vulnerable adults such as individuals with a learning disability or cognitive impairment or individuals in a dependent or unequal relationship?** ☐ **Yes** ☒ **No**

How will you ensure that participants in these groups are competent to give consent to take part in this study? *If you have relevant correspondence, please attach it.*

N/A

C4

Will payment or any other incentive, such as gift service or free services, be made to any research participant?

☒ **Yes** ☐ **No**

If yes, please specify the level of payment to be made and/or the source of the funds/gift/free service to be used.

Participants will be paid £5 in cash for volunteering. This will be paid from the GL account of the applicant. Before and during any part of the study, participants will have the option to withdraw if they wish.

Please justify the payment/other incentive you intend to offer.

This is a thank you gesture for the time committed to the project.

C5

Recruitment

(i) Describe how potential participants will be identified:

Potential participants will be students and staff members of UCL School of Pharmacy (healthy adults aged 18 to 65 years), and these will be the only persons invited to participate in this study.

(ii) Describe how potential participants will be approached:

An email (Appendix 4) will be circulated using the UCL School of Pharmacy Staff and Students mailing lists to advertise the study. Potential participants interested in taking part in the study will be invited to contact the research team directly using the contact details included in the email. Members of the research team who will be responsible for recruitment will be postgraduate students only. Staff members in the position of influencing in any way the decision of participants in taking part to the study will not be involved in the recruitment process.

(iii) Describe how participants will be recruited:

Potential participants who contact the research team will be provided with the information sheet. They will until one week before the study to evaluate whether to take part, and will be invited to ask questions or obtain further information if they wish. Once decision has been made, participants will contact the research team to confirm their participation and select suitable dates and times. Prior to the session, a member of the research team will verbally explain the study and take informed consent from the participant.

Attach recruitment emails/adverts/webpages. A data protection disclaimer should be included in the text of such literature.

C6

Will the participants participate on a fully voluntary basis? ☒ **Yes** ☐ **No**

Will UCL students be involved as participants in the research project? ☒ **Yes** ☐ **No**

If yes, care must be taken to ensure that they are recruited in such a way that they do not feel any obligation to a teacher or member of staff to participate.

Please state how you will bring to the attention of the participants their right to withdraw from the study without penalty?

Granting this information will be included in the invitation email, information sheet and consent form, all participants will be reminded in any suitable occasion that their participation is completely optional and will not affect in any way their studies/ relationships with the academic environment

C7 **CONSENT**

Please describe the process you will use when seeking and obtaining consent.

The attached form will be used to obtain written informed consent from the recruited participants on the day of the study. Participants are expected to sign the consent form only after having read and understood the information sheet previously provided, and after having asked any questions they may have to the research team. On the day of the study, members of the research team will be available to further provide information before the consent form will be signed. The form will be provided in two copies to be signed.

One will be kept by the participant and another will be retained by the research team.

A copy of your participant information sheet(s) and consent form(s) must be attached to this application. For your convenience proformas are provided in Appendix I. These should be filled in and modified as necessary.

In cases where it is not proposed to obtain the participants informed consent, please explain why below.

N/A

C8 **Will any form of deception be used that raises ethical issues? If so, please explain.**

N/A

C9 **Will you provide a full debriefing at the end of the data collection phase?** ☒ **Yes** ☐ **No**

If 'No', please explain why below.

N/A

C10 **Information Sheets And Consent Forms: Appendix I**

A poorly written Information Sheet(s) and Consent Form(s) that lack clarity and simplicity frequently delay ethics approval of research projects. The wording and content of the Information Sheet and Consent Form must be appropriate to the age and educational level of the research participants and clearly state in simple non-technical language what the participant is agreeing to. Use the active voice e.g. "we will book" rather than "bookings will be made". Refer to participants as "you" and yourself as "I" or "we". An appropriate translation of the Forms should be provided where the first language of the participants is not English. If you have different participant groups you should provide Information Sheets and Consent Forms as appropriate (e.g. one for children and one for parents/guardians) using the templates provided in Appendix I. Where children are of a reading age, a written Information Sheet should be provided. When participants cannot read or the use of forms would be inappropriate, a description of the verbal information to be provided should be given. Where possible please ensure that you trial the forms on an age-appropriate person before you submit your application.

Appendix added at end of document.

RISKS

THE ESEARCHER AND THE RESEARCHED

SECTION D: APPROPRIATE SAFEGUARDS, DATA STORAGE AND SECURITY

SECTIO

D1 **Will the research involve the collection and/or use of personal data?**
☐ **Yes** ☒ **No**

Personal data *is data which relates to a living individual who can be identified from that data OR from the data and other information that is either currently held, or will be held by the data controller (the researcher).*

This includes:

- *any expression of opinion about the individual and any intentions of the data controller or any other person toward the individual.*
- *sensor, location or visual data which may reveal information that enables the identification of a face, address, etc (some postcodes cover only one property).*
- *combinations of data which may reveal identifiable data, such as names, email/postal addresses, date of birth, ethnicity, descriptions of health diagnosis or conditions, computer IP address (if relating to a device with a single user).*

If yes, is the research collecting or using special category data as defined by the GDPR 2018, for example participants' :

- sexual behaviour or orientation
- political opinions or philosophical beliefs
- violence towards them
- abuse or exploitation
- mental or physical health
- gender or ethnic status
- trade union membership

- **data which might be considered sensitive in some countries, cultures or contexts?**

If yes, state whether explicit consent will be sought for its use and what data management measures are in place to adequately manage and protect the data.

N/A

D2

<u>During the Project</u> (including the write up and dissemination period)

State what types of data will be generated from this project (i.e. transcripts, videos, photos, audio tapes, field notes, etc).
Personal data (age, gender and randomisation code) is written down in paper, collected in a folder and safely stored in the Principal Researcher's office, which is kept locked at all times.

Access to consent forms and paper-based data recording templates will be restricted to the research team and stored in designated folders in a locked office at the UCL School of Pharmacy.

Participants answers (anonymised) are recorded on an online survey web application Qualtrics.

Data will be used to write up peer-reviewed articles, be presented at conferences, or be written up in a thesis.

How will data be stored, including where and for how long? This includes all hard copy and electronic data on laptops, share drives, usb/mobile devices.

Access to consent forms and paper-based data recording templates will be restricted to the research team and stored in designated folders in a locked office at the UCL School of Pharmacy

All information collected via data collection form will be kept confidentially. The answers will be available on web application called 'Qualtrics'. This is application used to design and perform the online surveys/data collection forms. The data will be stored in a password protected electronic format. Qualtrics does not collect identifying information such as name, email address, or IP address. Therefore, participant's responses will remain anonymous.

Apart from research team, no one will be able to identify the participant or their answers, and no one will know whether or not the participant took part in the study, this will reduce the risk in terms of data protection.

The data on the Qualtrics web application are actually stored in Germany and thus adhere to the EU's GDPR regulations. Qualtrics' Security White Paper as confirmation is attached.

Who will have access to the data, including advisory groups and during transcription?

D3	**Will personal data be processed or be sent outside of the European Economic Area (EEA)*?** **No** **If yes,** please confirm that there are adequate levels of protection in compliance with the General Data Protection Regulation 2018 and state what these arrangements are below. N/A

D4	**After the Project** **What data will be stored and how will you keep it secure?** The answers (data) and completed consent/assent forms will available on Qualtrics application for as long as is required for the research study. The data will be stored in a password protected electronic format within this application. Access to this information will be restricted to the research team. **Where will the data be stored and who will have access?** All answers will be compiled in an Excel spreadsheet for further analysis and will be kept in a designated study encrypted UCL laptop with restricted password-protected access only to the immediate research team. All information transferred on to the designated study encrypted UCL laptop will have restricted password-protected access to only the immediate research team and will be kept as long as it is required for the research study. Data transfer on to laptop will be done in a secure office at the UCL School of Pharmacy. **Will the data be securely deleted?** **If yes,** please state when will this occur: Yes, on completion of the research study and appropriate publications, the responses, consent/assent forms will be deleted.

D5	**Will the data be archived for use by other researchers?** ☐ **Yes** ☒ **No** If **Yes**, please describe provide further details including whether researchers outside the EEA will be given access. N/A

SECTION E: DETAILS OF RISKS AND BENEFITS TO THE RESEARCHER AND THE RESEARCHED

E1	**Please state briefly any precautions being taken to protect the health and safety of researchers and others associated with the project (as distinct from the research participants).** This project hold little risk to the research which has been risk assessed (Appendix 3).

E2	**Will these participants participate in any activities that may be potentially stressful or harmful in connection with this research?** ☒ **Yes** ☐ **No** If **Yes**, please describe the nature of the risk or stress and how you will minimise and monitor it. The procedures may cause temporary physical discomfort (exposure to unpleasant taste or general mouthfeel) during assessment if the test samples texture, taste or aftertaste is aversive. The potential discomfort is minimal and not greater than that ordinarily encountered in daily life. In order to minimise the discomfort, a delay of at least 10 minutes will be respected between each tested sample. Before and after each test sample, subjects can rinse their mouth with water until they can no longer perceive the previous sample. The participants will be provided with necessary instruction on properly testing the samples. Risk will be continuously monitored by asking participants how they feel between sample administrations. If

	participant report any distress, they will be excluded from the study. If some participants show high discomfort to texture or taste, the study will be immediately stopped.

E3	**Will group or individual interviews/questionnaires raise any topics or issues that might be sensitive, embarrassing or upsetting for participants?** **No** If **Yes,** please explain how you will deal with this. N/A
E4	**Please describe any expected benefits to the participant.** Participants will receive no direct benefits by taking part to this study. They may receive indirect benefit through contribution to patient care improvement regarding the acceptability of patient-centric formulations.

E5	**Specify whether the following procedures are involved:** **Any invasive procedure(s)** ☐ **Yes** ☒ **No** **Physical contact** ☐ **Yes** ☒ **No** **Any procedure(s) that may cause mental distress** ☐ **Yes** ☒ **No** Please state briefly any precautions being taken to protect the health and safety of the research participants. The study is only one session and the number of samples is kept to a minimum (2 films) to minimise fatigue and discomfort. Before and after each test sample, subjects will rinse their mouth with water and will have free access to water during the study. Risk will be continuously monitored by asking participants how they feel between samples. If participant report any distress, the study will be immediately stopped.

E6	**Does the research involve the use of drugs?** ☐ **Yes** ☒ **No** If **Yes**, please name the drug/product and its intended use in the research and then complete Appendix II N/A **Does the project involve the use of genetically modified materials?** ☐ **Yes** ☒ **No** If **Yes**, has approval from the Genetic Modification Safety Committee been obtained for work? ☐ Yes ☐ No If **Yes**, please quote the Genetic Modification Reference Number: N/A

E7	**Will any non-ionising radiation be used on the research participant(s)?** ☐ **Yes** ☒ **No** If **Yes**, please complete Appendix III.

E8	**Are you using a medical device in the UK that is CE-marked and is being used within its product indication?** ☐ **Yes** ☒ **No** If **Yes**, please complete Appendix IV.

CHECKLIST

Documents to be Attached to Application Form (if applicable)	**Tick if attached**
Section B: Details of the Project	
• Questionnaire(s) / Psychological Tests **(Appendix 5)**	☒
• Relevant correspondence relating to involvement of collaborating department/s and agreed participation in the research i.e. approval letters to gatekeepers seeking permission to do research on their premises/ in their company etc.	☐
Section C: Details of Participants	
• Parental/guardian consent form for research involving participants under 18	☐
• Participant/s information sheet	☒
• Participant/s consent form/s	☒
• Advertisement	☒
Appendix I: Information Sheet(s) and Consent Form(s) ☒	
Appendix II: Research Involving the Use of Drugs	
• Relevant correspondence relating to agreed arrangements for dispensing with the pharmacy	☐
• Written confirmation from the manufacturer that the drug/substance has has been manufactured to GMP **(Appendix 2)**	☒
• Proposed volunteer contract	☐
• Full declaration of financial or direct interest	☐
• Copies of certificates: CTA etc…	☐
Appendix III: Use of Non-Ionising Radiation ☐	
Appendix IV: Use of Medical Devices ☐	

Consent Form / Participant information sheet

CONSENT FORM FOR *Healthy Adults* IN RESEARCH STUDIES

Please complete this form after you have read the Information Sheet and/or listened to an explanation about the research.

Title of Study: Mouthfeel evaluation comparison between orally administered fibre mats and fast dissolving films.

Department: UCL School of Pharmacy, Department of Pharmaceutics

Name and Contact Details of the Researcher(s): Hend Abdelhakim, UCL School of Pharmacy, 29-39 Brunswick Square, WC1N 1AX, London, UK. T: 07701342165, E: hend.abdelhakim.16@ucl.ac.uk

Name and Contact Details of the Principal Researcher: Prof Catherine Tuleu, UCL School of Pharmacy, 29-39 Brunswick Square, WC1N 1AX, London, UK. T: 00 44 20 7753 5857. E: c.tuleu@ucl.ac.uk

Name and Contact Details of the UCL Data Protection Officer: Lee Shailer, Data Protection & Freedom of Information Officer (x58726) l.shailer@ucl.ac.uk responsible for Data Protection and FOI queries.

This study has been approved by the UCL Research Ethics Committee: Project ID number: 15975/001

Thank you for considering taking part in this research. The person organising the research must explain the project to you before you agree to take part. If you have any questions arising from the Information Sheet or explanation already given to you, please ask the researcher before you decide whether to join in. You will be given a copy of this Consent Form to keep and refer to at any time.

I confirm that I understand that by ticking/initialling each box below I am consenting to this element of the study. I understand that it will be assumed that unticked/initialled boxes means that I DO NOT consent to that part of the study. I understand that by not giving consent for any one element that I may be deemed ineligible for the study.

		Tick Box
1.	***I confirm that I have read and understood the Information Sheet for the above study**. I have had an opportunity to consider the information and what will be expected of me. I have also had the opportunity to ask questions which have been answered to my satisfaction.	
2.	***I consent to participate in the study.** I understand that my personal information *(age and gender only)* will be used for the purposes explained to me. I understand that according to data protection legislation, 'public task' will be the lawful basis for processing.	
3.	**Use of the information for this project only** *I understand that all personal information will remain confidential and that all efforts will be made to ensure I cannot be identified.	

	I understand that my data gathered in this study will be stored anonymously and securely. It will not be possible to identify me in any publications.	
4.	*I understand that my information may be subject to review by responsible individuals from the University and sponsors for monitoring and audit purposes.	
5.	*I understand that my participation is voluntary and that I am free to withdraw at any time without giving a reason, *without the care I receive or my legal rights being affected*.	
6.	I understand the potential risks of participating and the support that will be available to me should I become distressed during the course of the research.	
7.	I understand the direct/indirect benefits of participating.	
8.	I understand that the data will not be made available to any commercial organisations but is solely the responsibility of the researcher(s) undertaking this study.	
9.	I understand that I will not benefit financially from this study or from any possible outcome it may result in in the future.	
10.	I understand that I will be compensated for the portion of time spent in the study (if applicable) or fully compensated if I choose to withdraw.	
11.	I agree that my anonymized research data may be used by others for future research. No one will be able to identify you when this data is shared.	
12.	I hereby confirm that I understand the inclusion criteria as detailed in the Information Sheet and explained to me by the researcher.	
13.	I hereby confirm that: (a) I understand the exclusion criteria as detailed in the Information Sheet and explained to me by the researcher; and (b) I do not fall under the exclusion criteria.	
14.	I agree that my GP may be contacted if any unexpected results are found in relation to my health.	
15.	I have informed the researcher of any other research in which I am currently involved or have been involved in during the past 12 months.	
16.	I am aware of who I should contact if I wish to lodge a complaint.	
17.	I voluntarily agree to take part in this study.	
18.	Use of information for this project and beyond I would be happy for the data I provide to be archived at designated study encrypted laptop and Qualtrics® application for as long as it is required by the research project. I understand that other authenticated researchers will have access to my anonymised data.	

If you would like your contact details to be retained so that you can be contacted in the future by UCL researchers who would like to invite you to participate in follow up studies to this project, or in future studies of a similar nature, please tick the appropriate box below.

	Yes, I would be happy to be contacted in this way	
	No, I would not like to be contacted	

_____	_____	_____
Name of participant	Date	Signature
_____	_____	_____
Researcher	Date	Signature

Participant Information Sheet for Healthy Adults
UCL Research Ethics Committee Approval ID Number: _____

YOU WILL BE GIVEN A COPY OF THIS INFORMATION SHEET

Title of Study: Mouthfeel evaluation comparison between orally administered fibre mats and fast dissolving films.

Department: UCL School of Pharmacy, Department of Pharmaceutics

Name and Contact Details of the Researcher(s): Hend Abdelhakim, UCL School of Pharmacy, 29-39 Brunswick Square, WC1N 1AX, London, UK. T: 07701342165, E: hend.abdelhakim.16@ucl.ac.uk

Name and Contact Details of the Principal Researcher: Prof Catherine Tuleu, UCL School of Pharmacy, 29-39 Brunswick Square, WC1N 1AX, London, UK. T: 00 44 20 7753 5857. E: c.tuleu@ucl.ac.uk

1. Invitation Paragraph

Explain that the potential participant is being asked to take part in a research project.

We would like to invite you to participate in this PhD research project. Taking part is voluntary; it is up to you to decide whether or not to take part, and choosing not to will not disadvantage you in any way. If you do decide to take part, you will still be free to withdraw at any time without the need to give a reason.

Before you decide whether you want to take part, it is important for you to read the following information carefully and discuss it with others if you wish. Please feel free to ask us if there is anything that is not clear or you would like more information.

2. What is the project's purpose?

The ability to take medicines according to their instructions is key to the success of a medical treatment. Orodispersible films are considered "more acceptable" dosage forms, especially to certain patient groups (E.g. children, older patients, etc…). However, some characteristics of orodispersible films may affect the ability or willingness to take them as recommended. There is a great need to understand which characteristics of orodispersible films make them preferable or unpleasant/unacceptable. In addition, this study aims to compare films prepared by two different manufacturing methods to evaluate their mouthfeel and overall acceptability. This study is expected to provide us with valuable information to develop more acceptable orodispersible films.

Drug-free films will be given to you to test. These are thin transparent films that quickly dissolve with saliva. The ingredients (Polyvinyl alcohol) is a pharmaceutical excipient that is widely used in orodispersible films, tablets and food.

Why have I been chosen?

We are looking for healthy adults aged between 18 and 65 years that can understand and speak English to take part. We aim to recruit an equal number of male and female subjects.

Exclusion criteria: Recent dental care up to 15 days before the tests and any known excipient allergies.

Medicinal treatments altering saliva production. Sensory disorders affecting the mouth or local anaesthetics into the mouth within 24 hours of the study.

Medications preventing your eligibility to participate to the study (Scully CBE, 2003):

Medicinal treatments altering saliva production such as:

Anticholinergic drugs
Tricyclics antidepressants
Muscarinic receptor antagonists for treatment
of overactive bladder
Alpha receptor antagonists for treatment of urinary retention
Antipsychotics such as phenothiazines
Diuretics
Antihistamines
Sympathomimetic drugs
Antihypertensive agents
Antidepressants (serotonin agonists, or noradrenaline
and/or serotonin re-uptake blockers)
Appetite suppressants
Decongestants and cold cures'
Bronchodilators
Skeletal muscle relaxants
Antimigraine agents
Benzodiazepines, hypnotics, opioids and drugs of abuse
H 2 antagonists and proton pump inhibitors
Cytotoxic drugs
Retinoids
Anti-HIV drugs such as dideoxyinosine (DDI)
and protease inhibitors
Cytokines

You should detail what the inclusion and exclusion criteria are. You should explain how the participant was chosen and how many other participants will be recruited to the study.

3. Do I have to take part?

It is up to you to decide whether or not to take part. If you do decide to take part you will be given this information sheet to keep and be asked to sign a consent form. You can withdraw at any time without giving a reason and without it affecting any benefits that you are entitled to. if you decide to withdraw you will be asked what you wish to happen to the data you have provided up that point.

4. What will happen to me if I take part?

The study will take place in the consultation rooms of the pharmacy practice dispensary at UCL. You will be asked to commit to 15 minutes only. If you decide to take part, you will be asked to take two drug-free orodispersible films. We will ask you to place them in your mouth, wait until they dissolve completely and then swallow. Meanwhile, you will be asked to take the time in which films dissolve in your mouth using a stopwatch. We will then ask you to rate various sensory aspects each time on a scale (size, thickness, etc.).

You will be allowed to reject ANY of the samples at any point of the study if you don't feel comfortable to take it.

5. Will I be recorded and how will the recorded media be used?

You will not be recorded.

6. What are the possible disadvantages and risks of taking part?

The films being tested only contain polyvinyl alcohol (PVA).

This is a perfectly safe pharmaceutical excipient already used in many marketed formulations, for example you might have seen it in eye drops as a lubricant to prevent irritation or to relieve dryness of the eye.
If you experience any unpleasant reaction, you must alert a member of the team and we will stop the study immediately. The researchers are trained in First Aid and a registered pharmacist will be

present to assess the situation. If necessary, we will also contact emergency services. PVA is a very safe compound, so we do not anticipate that you will experience any side effects.

If the samples you are given have a poor texture, there is potential to suffer from temporary oral discomfort. Some sensitive participants may gag in response to the samples and vomit, however this is extremely rare. Nevertheless, films dissolve rapidly, which minimises the potential for adverse effects, and can be spit out at any time. Further, a minimum delay of 5 minutes will be respected between each test film.

7. What are the possible benefits of taking part?

Whilst there are no immediate benefits for those people participating in the project, it is hoped that this work will aid in the future production of easier to swallow medications for various patient opulations.

8. What if something goes wrong?

If you have questions at any time about the study or the procedures, you may contact Prof Catherine Tuleu via phone 020 7753 5857 or via email c.tuleu@ucl.ac.uk. If you feel you have not been treated according to the descriptions in this form, or that your rights as a participant in research have not been honored during the course of this study or you have any questions, concerns, or complaints that you wish to address to someone other than the principal researcher, you may contact Dr Mine Orlu at m.orlu@ucl.ac.uk.

If you would like to discuss it with someone outside of the research team, please contact Ms Joanna O'Brien, Institute Manager, UCL School of Pharmacy, 29/39 Brunswick Square, London, WC1N 1AX, Tel: 020 7753 5814, Email: joanna.o'brien@ucl.ac.uk. Should you feel your complaint has not been handled to your satisfaction by the researchers you can contact the Chair of the UCL Research Ethics Committee – ethics@ucl.ac.uk.

In the first instance you should inform the participants which member of the research project they should contact should they wish to raise a complaint (this is most likely to be the Principal Researcher or Supervisor). However the participants should also be informed that should they feel their complaint has not been handled to their satisfaction (e.g. by the PR or the supervisor) that they can contact the Chair of the UCL Research Ethics Committee – ethics@ucl.ac.uk

9. Will my taking part in this project be kept confidential?

Only members of the research team will know that you took part and have access to the results. Confidentiality will be maintained during the study and after it has finished. If the study is published or presented to a wider audience, your anonymity will be respected through anonymization procedures. All data will be collected and stored in accordance with GDPR.

No one (except the researchers) will be able to identify the participant or their answers, and no one will know whether or not the participant participated in the study. However, as participation is anonymous it will not be possible for us to withdraw your data once you have submitted your questionnaire. If the study is published or presented to a wider audience, your anonymity will be respected through anonymisation procedures.

10. Limits to confidentiality

Please note that confidentiality will be maintained throughout the study and when results are disseminated.

11. What will happen to the results of the research project?

The final results of the study may be anonymously reported and disseminated in peer reviewed scientific journals, internal reports and conference presentations. A statement is included in the participant information sheet inviting participants to contact the research team should they wish to know the results of the study. In such cases, an abstract of the overall outcomes will be shared with participants. All information transferred on to the designated study encrypted laptop will have restricted password-protected access to only the immediate research team. Data transfer on to

laptop will be done in a secure office at the UCL School of Pharmacy and data will be kept as long it is required for the research project.

12. Local Data Protection Privacy Notice

Notice:
The controller for this project will be University College London (UCL). The UCL Data Protection Officer provides oversight of UCL activities involving the processing of personal data, and can be contacted at data-protection@ucl.ac.uk

This 'local' privacy notice sets out the information that applies to this particular study. Further information on how UCL uses participant information can be found in our 'general' privacy notice:

For participants in health and care research studies, click here

The information that is required to be provided to participants under data protection legislation (GDPR and DPA 2018) is provided across both the 'local' and 'general' privacy notices.

The categories of personal data used will be as follows:

Gender and age.

The lawful basis that would be used to process your *personal data* will be performance of a task in the public interest.

Your personal data will be processed so long as it is required for the research project. Your data will be anonymised and will endeavour to minimise the processing of personal data wherever possible.

If you are concerned about how your personal data is being processed, or if you would like to contact us about your rights, please contact UCL in the first instance at data-protection@ucl.ac.uk.

13. Who is organising and funding the research?

UCL

16. Contact for further information

Please contact the research team, using the details overleaf, if you would like to take part, or have any questions about the study.

If you would like to discuss it with someone outside of the research team, please contact:

Ms Joanna O'Brien
Institute Manager
UCL School of Pharmacy
29/39 Brunswick Square
London, WC1N 1AX
Tel: 020 7753 5814
Email: joanna.o'brien@ucl.ac.uk

The participant will be given a copy of the information sheet and a signed consent form to keep.

Thank you for reading this information sheet and for considering to take part in this research study.

Letter from Bioinicia

Bioinici

c'.-11gepsel; 65 -- Nave 3
Porcine Empresarial Tactica
46980-Pah:ma (1alencia) -
Spain www.bioinicia.com

Dear Customer,

According to your requirements, the samples for human panel study will be manufactured in an ISO 7 clean room according to cGMP standards, which include cleaning procedures to ensure no contamination of samples.

All supplied human panel study samples will be composed entirely of material appropriate for human use and will be individually packaged into clean packaging and labelled.

Each human panel study sample will contain no more than 100mg of pharmaceutical grade polyvinyl alcohol.

Signed by:

Javier Gregori Puertas

Qualified Person

BIOINICIA, S.L.

Appendix 3: Risk assessment

Risk Assessment

Summary

Reference: RA026693/1 **Sign-off Status: Authorised**

Date Created:	09/05/2019	**Confidential?**	No
Assessment Title:	Mouthfeel evaluation comparison between orally administered fibre mats and fast dissolving films		
Assessment Outline:	This is a new activity risk assessment with regards to the overall mouthfeel evaluation of orodispersible film preparations to be carried out with adult human volunteers. The aim of this study is to assess the overall mouthfeel of placebo poly(vinyl) alcohol orodispersible films prepared externally by solvent casting and electrospinning. This risk assessment covers the human panel for sensory evaluation. Placebo formulations will be given to subjects in a dry form .For the mouthfeel evaluation, volunteers will be asked to take a small number of samples (2). The intensity of the test stimuli is assessed using categorical measurement scales. Individual COSHH assessment will be carried out for each of the excipients included in the formulation before sensory evaluation.		
Area Responsible (for management of risks)		**Location of Risks**	On-Site
Division, School, Faculty, Institute:	Faculty of Life Sciences	**Building:**	School of Pharmacy
Department:	UCL School of Pharmacy	**Area:**	Ground and Above
Group/Unit:	All Groups/Units	**Sub Area:**	All Sub Areas
Further Location Information:	Sensory evaluation - Pharmacy Dispensary (First floor) Sample preparation - Bioinicia electrospinning and electrospraying solutions		
Assessment Start Date:	01/07/2019	**Review or End Date:**	01/07/2020

Relevant Attachments:

Description of attachments:

Location of non-electronic documents:

All documentation will be kept in Lab B21 in a dedicated folder placed into a transparent wall mounted document holder next to the entrance door.

Assessor(s):	ABDELHAKIM, HEND
Approver(s):	CATHERINE TULEU
Signed Off:	CATHERINE TULEU (05/06/2019 12:27)
Distribution List:	ISABEL GONCALVES (i.goncalves@ucl.ac.uk) - 26/08/2016

PEOPLE AT RISK (from the Activities covered by this Risk Assessment)

Risk Assessment **Activities, Hazards, Controls**

Reference: RA026693/1 **Sign-off Status: Authorised**

1. Mouthfeel evaluation	
Description of Activity:	Volunteers will be asked to take, allow to dissolve, and swallow a small number of samples (2). The mouthfeel is assessed using categorical measurement scales. Measurement of sample dissolution time will be asked from participants using a stopwatch.

Hazard 1. Chocking hazard	
There is a potential for chocking while swallowing of the formulations tested by the adults volunteers.	**Existing Control Measures** Participants can refuse ingestion of any of the samples at any point during the study if they feel not capable or not comfortable swallowing the sample. Moreover, subjects have free access to water to aid swallowing and rinse their mouth at all times. Films are expected to completely dissolve in max 90 seconds from intake. If accidentally aspirated, films will keep dissolving as wet by the participant's saliva. Films are very thin and flexible. Therefore the risk of airway occlusion is remote. If something should go wrong, first aid will be sought as necessary and the experiment will be stopped. We can seek for medical help on the premises (Dr Kirsten Harvey, MD). If someone complains, the supervisor or a third party (not directly involved in research team) Ms Joanna O'Brien (Institute Manager) can be contacted for further advice.
Hazard 2. Chemical agent	
Dose intake must not surpass maximum daily intake of the substance.	**Existing Control Measures** MSDS for all substances must be read and understood and COSHH assessment carried out before sample preparation and dispensing. Based on the composition of the formulation, the number of samples received and the amount per sample, the maximum dose of each substance that will be received by the volunteers must be calculated. The obtained value must be well below the maximum daily intake stated in the MSDS of that particular excipient.

Risk Level

With Existing Controls:

A -

Risk **Very**

Level **Low/ Trivial**

Risk Assessment

2. Poly(vinyl) alcohol **Description of**	**chemical hazard** Poly(vinyl) alcohol (PVOH)-based polymeric thin films will be prepared and administered to volunteers for overall mouthfeel assessment. Hazards related to handling and intake of PVOH are assessed.

Hazard 1. Risk of dust explosion	
Development of hazardous combustion gases or vapours possible in the event of fire.	**Existing Control Measures** All activities involving the handling of free powder or granules will be performed under safety cabinet and away from any source of free flames.
Hazard 2. Dust inhalation	
In case of accidental release dust inhalation may occur	**Existing Control Measures** All activities involving the handling of free powder or granules will be performed under safety cabinet.
Hazard 3. Oral toxicity	

The acute oral toxicity is very low, with LD50s between 15 and 20 g/kg (>2,000 mg/kg in rats). Orally administered PVA is very poorly absorbed from the gastrointestinal tract. PVA does not accumulate in the body when administered orally. PVA is not mutagenic or clastogenic. No-Observed-Adverse-Effect-Level (NOAELs) of orally administered PVA in male and female rats were 5000 mg/kg body weight/day in the 90-day dietary study and 5000 mg/kg body weight/day in the two-generation reproduction study, which was the highest dose tested (DeMerlis and Schoneker, 2003). In 2003, PVA received notification as Generally Recognised As Safe (GRAS) by the Foods and Drugs Administration (FDA). The assignment of a permanent Acceptable Daily Intake (ADI) of 50 mg/kg body weight/day by the Joint FAO/WHO Expert Committee on Food Additives was conferred in June 2003 (FDA-WHO).	**Existing Control Measures** Considering the average weight of participants (young adults) to be around 68 kg (males) and 58 kg (females) (Source: British National Formulary), the ADI would correspond to 3,500 mg/day (3.5 g/day). Each orodispersible film (area 6 cm2), contains 31 mg of PVA. Each participant receives maximum 2 samples. Therefore, the total daily intake of PVA would be 62 mg/day (Males: 0.91 mg/kg/day; Females: 1.06 mg/kg/day), way below the ADI values stated by FDA.

Risk Level

05/0

UCL

Risk Assessment

With Existing Controls:

Risk Level **A - Very Low / Trivial**

LONDON'S GLOBAL UNIVERSITY

Email advertisement

VOLUNTEERS NEEDED

We are carrying out a study looking at **Mouthfeel evaluation comparison between orally administered fibre mats and fast-dissolving films.**

Orodispersible films and nanofibre mats are oral dosage forms that dissolve in the mouth.

You will be asked to **place a sample into your mouth, allow it to dissolve, and then rate how it felt using scales and questions**. Only two samples will be assessed.

The results of this study will help formulation scientists use the best strategies to develop acceptable oral films, especially for special patient populations. The samples you will be given are placebos and **do not** contain any drugs.

If you're a healthy adult aged 18-65 years you are eligible to take part in our study.

The study will take place at UCL School of Pharmacy. You will be asked to attend one session only which will last approximately 15 minutes.

You will be paid £5 as compensation for your time.

Click here to receive a detailed information sheet and to register your interest in the study.

Thank you!

If you have any questions and to request more information, please contact:

Prof. Catherine Tuleu
Department of Pharmaceutics, UCL School of Pharmacy
29-39 Brunswick Square, WC1N 1AX
Email: c.tuleu@ucl.ac.uk
Tel. 02077535857

This study has been approved by the UCL Research Ethics Committee - ID Number: 15975/001

All data will be collected and stored in accordance with the General Data Protection Regulation 2018.

Data collection form (Qualtrics)

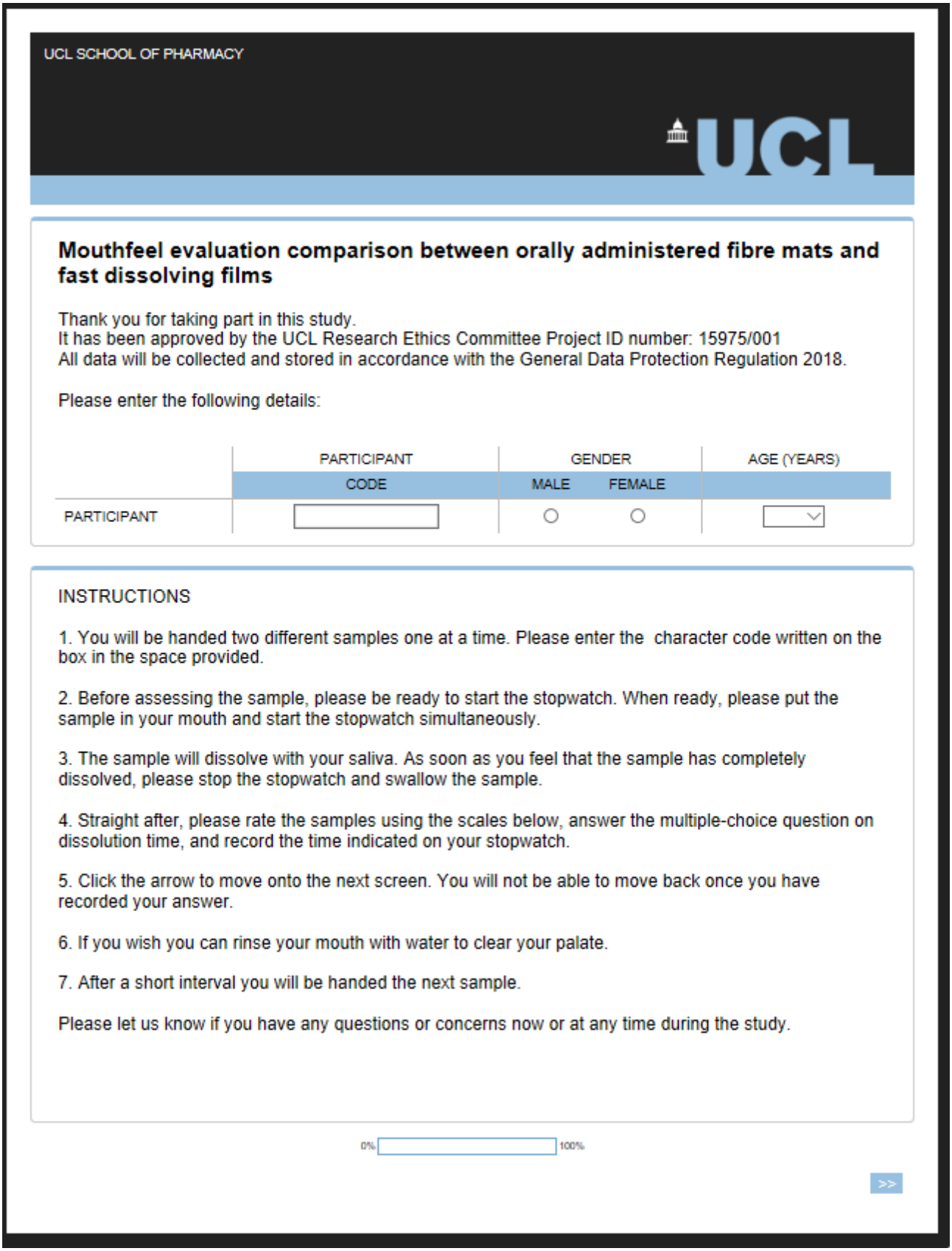

UCL SCHOOL OF PHARMACY

UCL

Mouthfeel evaluation comparison between orally administered fibre mats and fast dissolving films

Thank you for taking part in this study.
It has been approved by the UCL Research Ethics Committee Project ID number: 15975/001
All data will be collected and stored in accordance with the General Data Protection Regulation 2018.

Please enter the following details:

	PARTICIPANT	GENDER		AGE (YEARS)
	CODE	MALE	FEMALE	
PARTICIPANT		○	○	

INSTRUCTIONS

1. You will be handed two different samples one at a time. Please enter the character code written on the box in the space provided.

2. Before assessing the sample, please be ready to start the stopwatch. When ready, please put the sample in your mouth and start the stopwatch simultaneously.

3. The sample will dissolve with your saliva. As soon as you feel that the sample has completely dissolved, please stop the stopwatch and swallow the sample.

4. Straight after, please rate the samples using the scales below, answer the multiple-choice question on dissolution time, and record the time indicated on your stopwatch.

5. Click the arrow to move onto the next screen. You will not be able to move back once you have recorded your answer.

6. If you wish you can rinse your mouth with water to clear your palate.

7. After a short interval you will be handed the next sample.

Please let us know if you have any questions or concerns now or at any time during the study.

0% 100%

>>

UCL SCHOOL OF PHARMACY

Please enter the sample code below:

SAMPLE CODE

Please rate each of the sample characteristics on the left using the face scale:

	Extremely comfortable	Somewhat comfortable	Neither comfortable nor uncomfortable	Somewhat uncomfortable	Extremely uncomfortable
					
Film size perceived in the mouth	○	○	○	○	○
Film thickness perceived in the mouth	○	○	○	○	○
Film stickiness perceived in the mouth	○	○	○	○	○
Disintegration time	○	○	○	○	○
Film thickening effect perceived on saliva	○	○	○	○	○
Handling of sample	○	○	○	○	○

While the film was melting away, did it turn sticky?

	Not sticky	Slightly sticky	Moderately sticky	Strongly sticky	Extremely sticky
Stickiness intensity	○	○	○	○	○

After the film had melted away, could you feel your saliva thickened?

	Not thickened	Slightly thickened	Moderately thickened	Strongly thickened	Extremely thickened
Thickening intensity	○	○	○	○	○

How long did the sample take to dissolve?
(Please refer to the time displayed on the stopwatch to answer this question)

- ○ Less than 1 minute
- ○ Between 1 and 3 minutes
- ○ More than 3 minutes

Please write here the dissolution time as it appears on the stopwatch display

Please rate whether the film has been swallowed:

- ○ Film was swallowed without loss
- ○ Film was spat out with partial loss
- ○ Film was spat out completely

Overall, how would you rate the acceptability of this formulation?

Extremely good	Somewhat good	Neither good nor bad	Somewhat bad	Extremely bad
○	○	○	○	○

Do you have any comments about this sample?

0% 100%

>>

UCL SCHOOL OF PHARMACY

UCL

Do you prefer sample A or B?

A	B	Neither
○	○	○

0% 100%

>>

Flow diagram

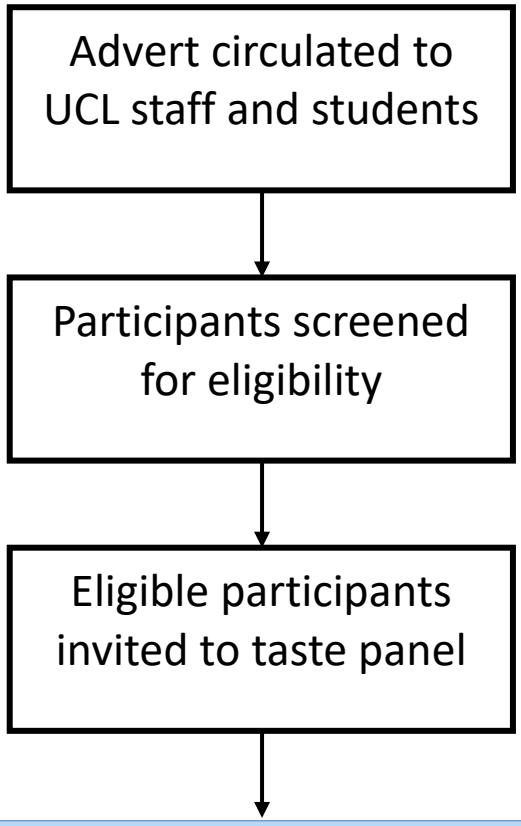

Tasting protocol: 15 min sessions per participant

- Volunteers: n=50
- Design: 2 films – cross-over design
- Samples: in randomised sequences

A = Electrospun fibre mats

B = Solvent cast Orodispersible films

5 minutes will be observed between samples. During this interval participants can consume a plain cracker or water to neutralise their palate if they wish.

Computerised data collection:

Each sample will be rated once immediately upon ingestion on a hedonic scale (5 points). *See data collection form.*